

การจัดในเตรตด้วยระบบผสมผสานของการรื้ดักซ้ันด้วยเหล็กประจุนย์/คาร์บอนไดออกไซด์  
การตตะกอนผลึกเหล็ก และการไล้แอมโมเนีย



นายเฉลิมชัย เรืองชัยนิคม

สถาบันวิทยบริการ  
จุฬาลงกรณ์มหาวิทยาลัย  
วิทยานิพนธ์นี้เป็นส่วนหนึ่งของการศึกษาหลักสูตรปริญญาวิทยาศาสตรดุษฎีบัณฑิต

สาขาวิชาการจัดการสิ่งแวดล้อม (สหสาขาวิชา)

บัณฑิตวิทยาลัย จุฬาลงกรณ์มหาวิทยาลัย

ปีการศึกษา 2548

ISBN 974-53-2608-9

ลิขสิทธิ์ของจุฬาลงกรณ์มหาวิทยาลัย

INTEGRATED SYSTEM FOR AQUEOUS NITRATE REMOVAL USING  $\text{Fe}^0/\text{CO}_2$   
REDUCTION, IRON PRECIPITATION, AND AMMONIA STRIPPING



Mr. Chalermchai Ruangchainikom

A Dissertation Submitted in Partial Fulfillment of the Requirements  
for the Degree of Doctor of Philosophy Program in Environmental Management  
(Inter-Department)

Graduate School

Chulalongkorn University

Academic Year 2005


ISBN 974-53-2608-9

Copyright of Chulalongkorn University


Thesis Title                    INTEGRATED SYSTEM FOR AQUEOUS NITRATE  
REMOVAL USING Fe<sup>0</sup>/CO<sub>2</sub> REDUCTION, IRON  
PRECIPITATION, AND AMMONIA STRIPPING  
By                                    Mr. Chalermchai Ruangchainikom  
Field of Study                    Environmental Management  
Thesis Advisor                   Associate Professor Jin Anotai, Ph.D.  
Thesis Co-advisor               Professor Chih-Hsiang Liao, Ph.D.


---

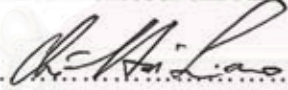
Accepted by the Graduate School, Chulalongkorn University in Partial  
Fulfillment of the Requirements for the Doctor's Degree

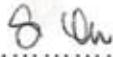
 ..... Dean of the Graduate School  
(Assistant Professor M.R. Kalaya Tingsabadh, Ph.D.)


THESIS COMMITTEE

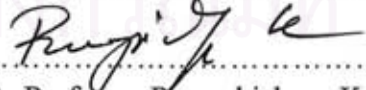
 ..... Chairman  
(Manaskorn Kachakornkij, Ph.D.)

 ..... Thesis Advisor  
(Associate Professor Jin Anotai, Ph.D.)

 ..... Thesis Co-advisor  
(Professor Chih-Hsiang Liao, Ph.D.)

 ..... Member  
(Assistant Professor Sutha Khaodhien, Ph.D.)

 ..... Member  
(Associate Professor Wanpen Wirojanagud, Ph.D.)

 ..... Member  
(Associate Professor Proesphichaya Kanatharana, Ph.D.)

 ..... Member  
(Associate Professor Chart Chiemchaisri, Ph.D.)

เฉลิมชัย เรื่องชัชนิคม : การกำจัดไนเตรดด้วยระบบผสมผสานของการรีดักชันด้วยเหล็ก  
 ประจุศูนย์/คาร์บอนไดออกไซด์ การตกตะกอนผลึกเหล็ก และการไล่แอมโมเนีย  
 (INTEGRATED SYSTEM FOR AQUEOUS NITRATE REMOVAL USING  
 $\text{Fe}^0/\text{CO}_2$  REDUCTION, IRON PRECIPITATION, AND AMMONIA  
 STRIPPING) อ. ที่ปรึกษา : รศ. ดร. จินต์ อโชนัย, อ. ที่ปรึกษาร่วม: PROF. CHIH-  
 HSIANG LIAO, Ph.D. 209 หน้า. ISBN 974-53-2608-9

งานวิจัยนี้เน้นถึงการศึกษาการกำจัดไนเตรดด้วยระบบผสมผสานของการรีดักชันด้วยเหล็กประจุศูนย์/  
 คาร์บอนไดออกไซด์ การตกตะกอนผลึกเหล็ก และการไล่แอมโมเนีย ผลการทดลองแสดงให้เห็นว่าอัตราการ  
 กำจัดคาร์บอนไดออกไซด์ที่ 200 มิลลิลิตรต่อนาที เพียงพอต่อการทำให้สารละลายมีสถานะที่เป็นกรดซึ่งก่อให้เกิด  
 ปฏิกิริยาการกำจัดไนเตรดได้ดี สมการจลนศาสตร์ของโมเดลสามารถอธิบายพฤติกรรมของการกำจัดไนเตรด การสะสม  
 ของเฟอร์รัส และแอมโมเนียมที่เกิดขึ้นในระบบ อีกทั้ง  $\mu_{\text{Fe}}$  จากสมการจลนศาสตร์ของโมเดลสามารถเป็นเครื่องมือใน  
 การเปรียบเทียบอัตราการกำจัดไนเตรดได้เป็นอย่างดี จากระบบการทดลองของคุณภาพของน้ำเสียแสดงให้เห็น  
 เห็นว่าการกำจัดไนเตรดจะลดลงเมื่อมีสารฮิวมิกและแคลเซียมในน้ำเสีย ในทางตรงกันข้ามสารคลอไรด์นั้น  
 สามารถช่วยในการกำจัดไนเตรดได้ดีขึ้น ผลของการศึกษาการกำจัดเฟอร์รัสที่เกิดขึ้นจากกระบวนการกักกร่อน  
 เหล็กประจุศูนย์โดยใช้การตกตะกอนผลึกเหล็กในถังปฏิกรณ์แบบฟลูอิด ไบซ์เฟสแสดงให้เห็นว่าให้  
 อัตราการใช้อากาศที่ 20 มิลลิลิตรต่อนาทีสามารถกำจัดเหล็กได้มากถึง 95% ซึ่งมีประสิทธิภาพสูงกว่าอัตราการ  
 ใช้อากาศที่สูงกว่า ภายใต้การศึกษาเห็นได้ว่าอัตราการใช้อากาศและพื้นที่ผิวของทรายนั้นเป็นสิ่งสำคัญในการ  
 กำหนดกระบวนการตกผลึกของเหล็กบนผิวทราย แอมโมเนียมเป็นผลผลิตที่เกิดขึ้นจากการกำจัดไนเตรดโดยใช้  
 กระบวนการรีดักชันด้วยเหล็กประจุศูนย์/คาร์บอนไดออกไซด์ การกำจัดแอมโมเนียมสามารถถูกกำจัดโดยใช้การ  
 ใช้อากาศไล่แอมโมเนียและใช้พีเอชที่เหมาะสมคือ 12 การกำจัดแอมโมเนียมสามารถเพิ่มขึ้นโดยการเพิ่มอัตราการ  
 ใช้อากาศให้สูงขึ้น จากการทดลองแบบต่อเนื่องแสดงให้เห็นว่าไนเตรดที่ความเข้มข้น 23 มิลลิกรัมไนโตรเจน  
 ต่อลิตรสามารถถูกกำจัดให้ลดลงถึง 2.9 มิลลิกรัมไนโตรเจนต่อลิตร ที่สภาวะการทดลอง สารละลายเข้าระบบ  
 เท่ากับ 3 ลิตรต่อชั่วโมง เหล็กประจุศูนย์เท่ากับ 60 กรัม และอัตราการใช้อากาศคาร์บอนไดออกไซด์ที่ 200 มิลลิลิตร  
 ต่อนาที การเพิ่มเหล็กประจุศูนย์เท่ากับ 40 กรัมทุกๆช่วงเวลา 27 ชั่วโมงสามารถช่วยรักษาความเข้มข้นไนเตรดให้  
 ต่ำกว่าระดับมาตรฐานน้ำดื่ม จากการทดลองโดยใช้น้ำบาดาลแสดงให้เห็นว่าสารละลายอินทรีย์และแคลเซียมมี  
 ผลต่อการลดลงในการกำจัดไนเตรดอย่างมาก อย่างไรก็ตามการกำจัดไนเตรดเกิดขึ้นได้มากกว่า 70% ซึ่งมีผลจาก  
 การพบคลอไรด์ในน้ำใต้ดินที่สามารถช่วยในการกำจัดไนเตรดได้ดีขึ้น

สาขาวิชาการจัดการสิ่งแวดล้อม (สหสาขาวิชา)  
 ปีการศึกษา 2548

ลายมือชื่อนิติ..... Chalangkrai.....  
 ลายมือชื่ออาจารย์ที่ปรึกษา.....  
 ลายมือชื่ออาจารย์ที่ปรึกษาร่วม.....

## 4689662920 : MAJOR ENVIRONMENTAL MANAGEMENT

KEY WORD: NITRATE REDUCTION /  $\text{Fe}^0/\text{CO}_2$  / IRON PRECIPITATION/  
AMMONIA STRIPPING

CHALERMCHAI RUANGCHAINIKOM: INTEGRATED SYSTEM FOR  
AQUEOUS NITRATE REMOVAL USING  $\text{Fe}^0/\text{CO}_2$  REDUCTION, IRON  
PRECIPITATION, AND AMMONIA STRIPPING. THESIS ADVISOR:  
ASSOC. PROF. JIN ANOTAI, Ph.D., THESIS CO-ADVISOR: PROF. CHIH-  
HSIANG LIAO, Ph.D., 209 pp. ISBN 974-53-2608-9.

This research focuses on investigation of integrated system for aqueous nitrate removal using  $\text{Fe}^0/\text{CO}_2$  reduction, iron precipitation, and ammonia stripping. Results show that the bubbling of  $\text{CO}_2$  flow rate at 200 mL/min was sufficient for supplying  $\text{H}^+$  into solution to create an acidic environment favorable to nitrate reduction by  $\text{Fe}^0$ . Sigmoidal model equation satisfactorily describes the S-curve behaviors of nitrate reduction, ferrous accumulation and ammonium formation. The  $t_{1/2}$  obtained from the sigmoidal model can serve as a powerful tool for the comparison of nitrate reduction rate. In the system with various water characteristics, it found that humic acid significantly inhibited the reduction of nitrate. Calcium ions also strongly retarded nitrate removal, whereas chloride ion promoted the nitrate removal. Removal of ferrous from  $\text{Fe}^0$  corrosion was investigated using the fluidized sand bed reactor. The results show that the lower air flow rate of 20 mL/min could achieve up to 95% removal which provided a better performance than at higher flow rate. Under the studied conditions, air flow rate and surface area of sand were found to play an important role for iron pelletization onto the sand. Ammonia was the dominating end product from nitrate reduction by  $\text{Fe}^0/\text{CO}_2$  processes. The optimum pH at 12 is recommended for ammonia stripping and the removal efficiency increased with increasing air flow rate. Considering continuous operation, nitrate of 23 mg-N/L was reduced to 2.9 mg-N/L within 2.5 hours of stripping under influent feeding rate,  $\text{Fe}^0$  dosage, and  $\text{CO}_2$  gas flow rate of 3 L/hr, 60 g, and 200 mL/min, respectively. However, to maintain effluent nitrate to comply with drinking water quality standard of nitrate, supplement of 40g of  $\text{Fe}^0$  at every 27 hrs of operation was needed. According to field test, dissolved organic carbons and calcium ion existing in groundwater strongly inhibited nitrate removal similar to the batch study. Nonetheless, 70% removal of nitrate was still achieved due to enhancement effect from high chloride content of the tested groundwater.

จุฬาลงกรณ์มหาวิทยาลัย

Field of study Environmental Management

(Inter-Department)

Academic year 2005

Student's signature

Advisor's signature

Co-advisor's signature

*Chalermchai*

*Jin Anotai*

*Chih-Hsiang Liao*

## ACKNOWLEDGEMENTS

I would like to express my sincere appreciation to my thesis advisors, Assoc. Prof. Dr. Jin Anotai and Prof. Dr. Chih-Hsiang Liao, for their encouragement, invaluable support, and guidance. Their comments and suggestions not merely provide valuable knowledge but broaden perspective in practical applications as well. Special gratitude goes to the chairman of the committee, Dr. Manaskorn Rachakornkij for providing invaluable advice. I would also like to thank other committee members, Assoc. Prof. Dr. Wanpen Wirojanagud, Asst. Prof. Dr. Sutha Khaodhiar, Assoc. Prof. Proesphichaya Kanatharana, and Assoc. Prof. Chart Chiemchaisri for many valuable comments and their insightful suggestions.

I would like to extend my sincere appreciation to all staffs and students especially generation 2 and 4 at the National Research Center for Environmental and Hazardous Waste Management (NRC-EHWM) Program. Special thanks should go to Department of Environmental Resources Management, Chia Nan University of Pharmacy and Science, Department of Environmental Engineering, National Chen Kung University in Taiwan and Department of Environmental Engineering, King Mongkut's University of Technology Thonburi in Thailand for their supporting and their helps.

This research was granted by the National Science Council of Taiwan (Project No. NSC 93-2211-E-041-001) and by the National Research Center for Environmental and Hazardous Waste Management (NRC-EHWM) Program, Thailand. Without these financial supports, my achievement should not become true.

Special thanks are also made to all my friends, especially Mr. Nara Toyam, Mr. Worawit Wongniramaikul, Mr. Setawat Hormanee, Mr. Somboon Chintitana, Miss Pasoota Sakulkittimasak, Miss Ladaporn Khunikakorn, Miss Massakul Kitmongkonsak, member of Redox-ANN group which are Ming-Tang Lee, Jui-Yuan Huang, Chen-Wen Hsiao, Hsin-Yi Tu, Pei-Yu Lin, Chiung-Yuan Hsu, and Gin-Yee Lee, Prof. Chien-Jung Lin's and Prof. Ming-Chun Lu's group from Chia Nan University of Pharmacy and Science in Taiwan, Prof. Chitsan Lin's group from Department of Marine Environmental Engineering, National Kaoshung Marine University in Taiwan and Prof. Yao-Hui Huang's group from Department of Chemical Engineering, National Cheng Kung University in Taiwan and acrylic manufacturing for their assistance and encouragement during period of staying in Taiwan.

Finally, I feel proud to dedicate this dissertation with due respect to my beloved parents, brothers and Miss Nilpatra Wongpen for their wholehearted understanding, encouragement, and patient support throughout my entire study.

# CONTENTS

	Page
ABSTRACT IN THAI.....	iv
ABSTRACT IN ENGLISH.....	v
ACKNOWLEDGEMENTS.....	vi
CONTENTS.....	vii
LIST OF TABLES.....	x
LIST OF FIGURES .....	xi
NOMENCLATURES.....	xiv
CHAPTER I INTRODUCTION.....	1
1.1 Research rationale.....	1
1.2 Objectives.....	5
1.3 Hypotheses.....	5
1.4 Scopes of work.....	6
1.5 Advantages of this work.....	6
CHAPTER II BACKGROUNDS AND LITERATURE REVIEW.....	7
2.1 Nitrate in the environment .....	7
2.1.1 Source of nitrate.....	7
2.1.2 Effect of nitrate .....	8
2.1.3 Solution of nitrate contaminant in groundwater.....	9
2.2 Zero-valent iron process (Fe <sup>0</sup> )... ..	9
2.2.1 Zero-valent iron corrosion mechanism .....	9
2.2.2 Application of zero-valent iron process .....	11
2.2.3 Nitrate reduction by zero-valent iron (Fe <sup>0</sup> ) process.....	12
2.2.4 Pathways and mechanism of nitrate reduction by Fe <sup>0</sup> .....	18
2.2.5 Nitrate reduction by Fe <sup>0</sup> /CO <sub>2</sub> process.....	18
2.3 Iron precipitation process by fluidized bed process .....	23

	Page
2.3.1 Iron precipitation.....	23
2.3.2 Fluidized bed process.....	24
2.4 Ammonia removal by air stripping .....	26
<b>CHAPTER III METHODOLOGY.....</b>	<b>28</b>
3.1 Material and reagents.....	28
3.2 Experimental procedure.....	29
3.2.1 Laboratory test.....	29
3.2.2 Field test.....	42
3.4 Analytical methods.....	44
<b>CHAPTER IV RESULTS AND DISCUSSION.....</b>	<b>46</b>
4.1 Batch mode study.....	46
4.1.1 CO <sub>2</sub> /H <sub>2</sub> O system.....	46
4.1.2 Fe <sup>0</sup> /CO <sub>2</sub> system.....	47
4.1.3 Fe <sup>0</sup> /CO <sub>2</sub> /NO <sub>3</sub> <sup>-</sup> system.....	49
4.1.3.1 Effect of CO <sub>2</sub> bubbling rate.....	49
4.1.3.2 Effect of Fe <sup>0</sup> dosage.....	52
4.1.3.3 Correlation between nitrate reduction and ferrous ion accumulation.....	56
4.1.4 Effect of operating mode.....	58
4.1.5 Supplement of fresh Fe <sup>0</sup> .....	60
4.1.6 Effect of water quality.....	62
4.1.6.1 Effect of humic acid.....	62
4.1.6.2 Effects of cations and anions.....	64
4.1.7 Iron precipitation by fluidized bed process.....	70
4.1.7.1 Effect of air flow rate .....	70
4.1.7.2 Effect of sand dosage.....	72
4.1.7.3 Effect of initial iron concentration.....	73
4.1.8 Ammonia removal by air stripping process.....	76
4.1.8.1 Effect of pH .....	76



	Page
4.1.8.2 Effect of air flow rate.....	78
4.1.8.3 Effect of initial ammonia concentration.....	79
4.2 Continuous mode study.....	80
4.2.1 Nitrate removal by Fe <sup>0</sup> /CO <sub>2</sub> process.....	80
4.2.1.1 Effect of CO <sub>2</sub> flow rate.....	80
4.2.1.2 Effect of Fe <sup>0</sup> dosage .....	82
4.2.1.3 Effect of NO <sub>3</sub> <sup>-</sup> concentration.....	84
4.2.1.4 Effect of feeding solution rate.....	85
4.2.1.5 Effect of process operation.....	86
4.2.2 Ferrous removal by iron precipitation process.....	89
4.2.3 Ammonia removal by air stripping process.....	92
4.3 Field testing study.....	93
4.3.1 Nitrate reduction by Fe <sup>0</sup> /CO <sub>2</sub> process.....	93
4.3.2 Ferrous removal by iron precipitation process.....	97
4.3.3 Ammonia removal by air stripping process.....	100
 CHAPTER V CONCLUSIONS AND SUGGESTIONS FOR FUTURE WORKS	 103
5.1 Conclusions.....	103
5.1.1 Batch mode study.....	103
5.1.2 Continuous mode study.....	105
5.1.3 Field testing study.....	105
5.2 Suggestions for future works.....	106
 REFERENCES.....	 108
APPENDICES.....	114
APPENDIX A. Experimental raw data .....	115
APPENDIX B. Standard calibration curves .....	198
APPENDIX C. List of accepted journal papers and conference papers.....	207
BIOGRAPHY.....	209

## LIST OF TABLES

Table	Page
1.1 Group of similar frequency of wells subjected to nitrate and chloride contamination .....	2
1.2 Levels of nitrate monitored in the wells located at Min-Jen, Nan Tou, Taiwan.....	4
2.1 Equilibrium constants for redox half-cell reactions.....	18
2.2 Proposed pathways for nitrate reduction by Fe <sup>0</sup> shown in chronological order .....	19
3.1 Preparation of ferrous ion at different Fe <sup>0</sup> dosages.....	34
3.2 Classification of sand size from commercial sand.....	41
3.3 Hydrochemistry of groundwater at Chia Nan University of Pharmacy and Science, Tainan, Taiwan.....	43
4.1 Values of constants in the proposed sigmoidal model equation for nitrate reduction (Y).....	55
4.2 Values of constants in the proposed sigmoidal model equation for ferrous accumulation (Y).....	55
4.3 Values of constants in the proposed sigmoidal model equation for ammonium formation (Y).....	56
4.4 Composition of iron coated sand by SEM-EDS.....	76

สถาบันวิทยบริการ  
 จุฬาลงกรณ์มหาวิทยาลัย

## LIST OF FIGURES

Figure	Page
1.1 Topography of Northeast Thailand .....	2
1.2 Schematic diagram of integrated system work.....	6
2.1 The nitrogen cycle.....	8
2.2 Corrosion of iron immersed in acid solution.....	10
2.3 Disribution of aqueous carbonate species as a function of pH .....	22
2.4 pC-pH diagram for hydrolysis products of Fe <sup>3+</sup> .....	24
2.5 Schematic of representation of three phase fluidized bed.....	25
3.1 Configuration of reactor for the Fe <sup>0</sup> /CO <sub>2</sub> system.....	29
3.2 Schematic diagram for nitrate reduction by Fe <sup>0</sup> /CO <sub>2</sub> in the first phase.....	29
3.3 Schematic diagram for nitrate reduction by Fe <sup>0</sup> /CO <sub>2</sub> process in the second phase.....	32
3.4 Configuration of reactor for the iron precipitation by fluidized bed process.....	29
3.5 Three-phase fluidized bed operation procedure: 1. ferrous preparation by Fe <sup>0</sup> /CO <sub>2</sub> , 2. settling Fe <sup>0</sup> , 3. iron precipitation by fluidized bed process.....	33
3.6 Schematic diagram for ferrous removal by iron precipitation.....	35
3.7 Configuration of reactor for the ammonia stripping process.....	36
3.8 Schematic diagram for ammonia removal by air stripping.....	36
3.9 Configuration of reactor for the Fe <sup>0</sup> /CO <sub>2</sub> system in continuous process.....	37
3.10 Schematic diagram for nitrate reduction by Fe <sup>0</sup> /CO <sub>2</sub> in continuous process.....	39
3.11 Configuration of reactor for the iron precipitation by fluidized bed system in continuous process.....	40
3.12 Schematic diagram for ferrous removal by iron precipitation in continuous process.....	40
3.13 Configuration of reactor for the ammonia stripping system in continuous process.....	42

Figure	Page
3.14 Schematic diagram for ammonia removal by air stripping in continuous process.....	42
3.15 Configuration of reactor for integrated system for aqueous nitrate removal using Fe <sup>0</sup> /CO <sub>2</sub> reduction, iron precipitation, and ammonia stripping.....	43
3.16 Schematic diagram for integrated system for aqueous nitrate removal using Fe <sup>0</sup> /CO <sub>2</sub> reduction, iron precipitation, and ammonia stripping.....	44
4.1 Effect of CO <sub>2</sub> bubbling rate on aqueous solution.....	47
4.2 Effect of Fe <sup>0</sup> dosage on aqueous solution .....	48
4.3 Effect of CO <sub>2</sub> bubbling rate in the Fe <sup>0</sup> /CO <sub>2</sub> /NO <sub>3</sub> <sup>-</sup> system.....	50
4.4 Effect of Fe <sup>0</sup> dosage on nitrate reduction under initial nitrate concentration in the Fe <sup>0</sup> /CO <sub>2</sub> /NO <sub>3</sub> <sup>-</sup> system.....	53
4.5 Effect of Fe <sup>0</sup> dosage on t <sub>1/2</sub> under various initial nitrate concentrations.....	54
4.6 Correlation between nitrate removal and ferrous ion accumulation.....	57
4.7 Profiles of different operating modes.....	58
4.8 Effect of Fe <sup>0</sup> supplement on (a) nitrate residue, and (b) ferrous accumulation.....	61
4.9 Effect of humic acid concentration.....	63
4.10 SEM photograph (a) Fresh Fe <sup>0</sup> (b) Fe <sup>0</sup> under the condition of Fe <sup>0</sup> = 2g/L with 30 mg/L NO <sub>3</sub> <sup>-</sup> at 60 min (c) Fe <sup>0</sup> under the condition with 0.55 mg/L humic acid at 90 min.....	64
4.11 Nitrate removal with various concentrations of sodium carbonate.....	65
4.12 Nitrate removal with various concentrations of sodium chloride.....	66
4.13 Effect of cation and anion on nitrate reduction.....	67
4.14 Nitrate removal with various concentrations of calcium chloride without other background species.....	67
4.15 Nitrate removal with various concentrations of calcium chloride.....	68
4.16 Effect of air flow rate on iron removal.....	71
4.17 Effect of sand dosage on iron removal by fluidized bed process.....	73
4.18 Effect of initial ferrous concentration on iron removal.....	74

Figure	Page
4.19 Morphology of iron pellets.....	75
4.20 The distribution of fresh sand properties by SEM-EDS.....	76
4.21 Effect of pH on ammonia removal by air stripping.....	77
4.22 Effect of air flow rate on ammonia removal by air stripping.....	78
4.23 Effect of initial ammonium concentration on ammonia removal by air stripping.....	79
4.24 Effect of CO <sub>2</sub> bubbling rate on nitrate reduction.....	81
4.25 Effect of Fe <sup>0</sup> on nitrate reduction.....	83
4.26 Effect of initial nitrate concentration on nitrate reduction .....	84
4.27 Effect of feeding solution rate on nitrate reduction.....	86
4.28 Effect of Fe <sup>0</sup> supplement on nitrate reduction .....	88
4.29 Effect of sand dosage on iron removal.....	90
4.30 Effect of air flow rate on ammonia removal.....	93
4.31 Comparison system performance between NO <sub>3</sub> <sup>-</sup> spiked groundwater and NO <sub>3</sub> <sup>-</sup> spiked RO water.....	95
4.32 Performance comparison of nitrate reduction by Fe <sup>0</sup> /CO <sub>2</sub> in integrated system between NO <sub>3</sub> <sup>-</sup> spiked groundwater and NO <sub>3</sub> <sup>-</sup> spiked RO water....	98
4.33 Performance comparison of iron precipitation in integrated system between NO <sub>3</sub> <sup>-</sup> spiked groundwater and NO <sub>3</sub> <sup>-</sup> -spiked RO water.....	99
4.34 Performance comparison of ammonia stripping in integrated system between NO <sub>3</sub> <sup>-</sup> spiked groundwater and NO <sub>3</sub> <sup>-</sup> -spiked RO water.....	101

**NOMENCLATURES**

$\text{NO}_3^-$	=	nitrate
$\text{NO}_2^-$	=	nitrite
$\text{NH}_4^+$	=	ammonium
$\text{NH}_3$	=	ammonia
$\text{N}_2$	=	nitrogen gas
$\text{Fe}^{2+}$	=	ferrous ion
$\text{Fe}^{3+}$	=	ferric ion
$\text{Na}^+$	=	sodium ion
$\text{Ca}^{2+}$	=	calcium ion
$\text{Cl}^-$	=	chloride ion
TOC	=	total organic carbon
$\text{H}_2\text{O}_2$	=	hydrogen peroxide
$\text{CO}_2$	=	carbon dioxide gas
$\text{H}_2\text{CO}_3$	=	carbonic acid
$\text{HCO}_3^-$	=	bicarbonate
$\text{CO}_3^{2-}$	=	carbonate
$\text{H}^+$	=	hydrogen ions
$\text{OH}^-$	=	hydroxide ion
Hr	=	hour
min	=	minute
M	=	molar
k	=	rate constant

# CHAPTER I

## INTRODUCTION

### 1.1 Research rationale

In recent years, nitrate contamination in groundwater has become a serious problem because of public health concern and ecological concern. (Banens and Devis, 1998). The health effect of nitrate in drinking water is really related to nitrite because nitrate can be microbially reduced to nitrite, which can cause methemoglobinemia in newborn infant by oxidizing the heme  $\text{Fe}^{2+}$  of hemoglobin or known as “blue baby syndrome” (Walton, 1951). Additionally, cancers and damages to liver and other organs by nitrite are convinced to be referred to formation of nitrosamines, group of carcinogens produced from reaction of nitrate with amines, amides, and other nitrogenous compounds (Menzer, 1991). Therefore, the regulatory health limit of 44 mg nitrate/L (~10 mg-N/L) is applied as a safe drinking water quality standard in the most of developed countries (Westerhoff et al., 2003). Moreover, nitrate discharged into surface water bodies especially lake and reservoir, can cause an abnormal algae bloom, which will result in the difficulty and complexity in water purification processes. In general, nitrate contamination arises from such sources as agricultural fertilizers, high strength stock waste, and defected sanitary sewer system. Many groundwater sites in Thailand have nitrate content beyond the standard especially those in Khorat Plateau of northeast region as shown in Fig. 1.1. Intensive utilization of fertilizer in this area for greater cultivation is believed to cause nitrate contamination in groundwater. Not only high nitrate but also high chloride was found in this area. Table 1.1 summarizes the portion of groundwater wells which have high nitrate and chloride contents. Top three nitrate contamination areas are Mahasarakham, Khonkaen, and Nakorn Ratchasima, respectively. In Taiwan, the use of poultry excrete as fertilizer for the tea trees plantation located at Nan-Tou, Taiwan has caused significant increase of nitrate content in groundwater over the years (Chang et al., 2002).

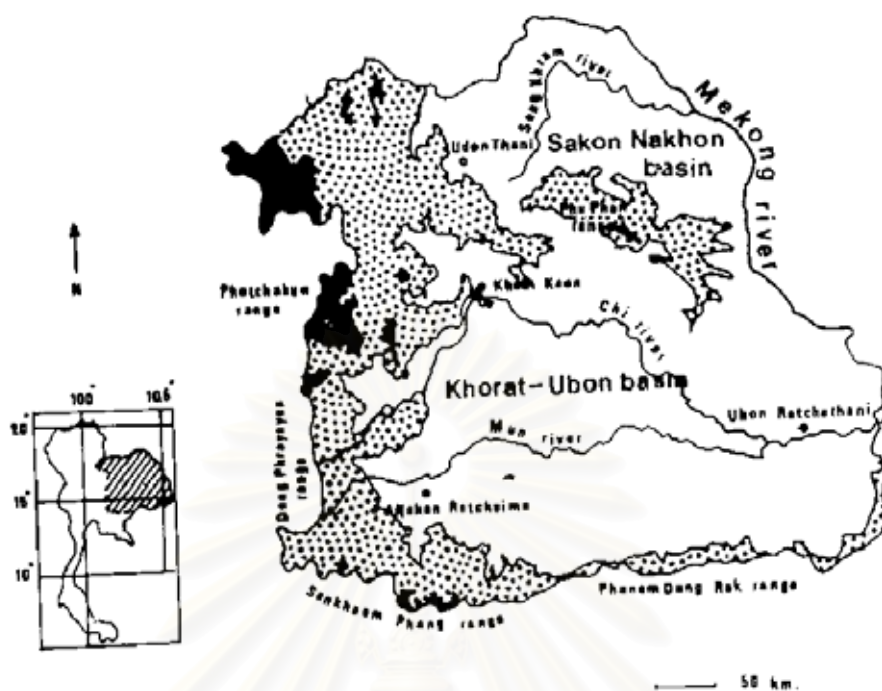


Fig. 1.1 Topography of northeast Thailand (Piromlert S., 1995).

Table 1.1 Group of similar frequency of wells subjected to nitrate and chloride contamination (Piromlert S., 1995).

Province	Total NO. of wells	NO <sub>3</sub> <sup>-</sup> > 10 mg N/L (% of total)	Cl <sup>-</sup> > 600 mg/L (% of total)
BURIRUM	646	9.9	14.0
CHAIYAPHUM	905	12.0	8.0
KALASIN	600	11.4	7.4
KHON KAEN	1218	15.5	17.9
MAHASARAKHAM	592	25.5	22.3
NAKHON PHANOM	1249	3.1	3.1
NAKHON RATCHASIMA	1090	14.0	23.0
ROI ET	1278	7.8	10.7
SRISAKET	1137	3.7	9.2
SURIN	1047	6.1	9.1
UBON RATCHATHANI	1740	2.0	5.1



Table 1.2 demonstrates that nitrate concentrations monitored in several wells in Taiwan in November 2001 have risen far beyond its criteria for drinking water quality. Therefore, certain actions need to be taken for numerous sites where the nitrate in groundwater exceeds the drinking water standard. Many technologies are capable of removing nitrate from contaminated water including ion exchange, reverse osmosis, biological denitrification, and chemical reduction. Reverse osmosis and ion exchange are not selective for nitrate and requires frequent regeneration of the media. Both processes do not destroy nitrate and generate secondary brine wastes. Biological denitrification is unfavorable because it requires intensive maintenance and constant supply of organic substrates. Additional drawbacks include biomass sludge disposal and treatment (aeration and disinfection) of denitrified water. Moreover, these microbial processes are generally slow and sometimes incomplete, compared to chemical reduction (Huang et al., 1998). Additionally, groundwaters in northeast Thailand contain not only high nitrate but also high chloride content as shown in Table 1.1 which can interfere with biological nitrate removal process. This is because most denitrification bacteria are not well developed in saline condition (Piromlert S., 1995). Therefore, biological process was not suitable for treating groundwater in northeast Thailand. To deal with nitrate contamination problem in groundwater, the chemical process is selected as an alternative treatment process. Zero-valent iron ( $\text{Fe}^0$ ) has been selected for nitrate reduction in the past decade (Cheng et al., 1997; Huang et al., 1998; Choe et al., 2000; Huang and Zheng, 2002; Alowitz and Scherer, 2002; Westerhoff and James, 2003; Liao et al., 2003; Choe et al., 2004; Huang and Zheng, 2004).  $\text{Fe}^0$ , serving as an electron donor to nitrate reduction, represents the most common metallic reducing agent since zero-valent iron is readily available at low cost and non-toxic. The reductive removal of nitrate can be seen as a result of metallic iron corrosion, especially significant in acidic solution (Piron, 1991). The application of acids such as  $\text{H}_2\text{SO}_4$  (Huang et al. 1998),  $\text{HCl}$ , and acetic acid (Cheng et al. 1997) might be considered to speed up the rate of nitrate removal; however, in so doing, this will risk the drinking quality of treated water due to the presence of species of sulfate, chloride, and acetate. To avoid this, bubbling  $\text{CO}_2$  into water was attempted as a major source of supplying hydrogen ions. The application of  $\text{CO}_2$ , called either carbonation or re-carbonation, is also a safe and common practice in water purification industries.

**Table 1.2 Levels of nitrate monitored in the wells located at Min-Jen, Nan Tou, Taiwan.**

Well No.	Date of Well Construction	Initial NO <sub>3</sub> <sup>-</sup> -N (mg/L)	NO <sub>3</sub> <sup>-</sup> -N in Nov. 2001 (mg/L)	Well Depth (m)	Designed Pumping Rate (m <sup>3</sup> /d)
Hsin-Je #1	Nov. 1979	-	<b>21.00</b>	120	4500
Hsin-Je #2	Mar. 1998	3.00	5.30	200	3000
Jen-Ho #1	Dec. 1998	0.64	5.60	150	3000
Jen-Ho #2	Jul. 2001	4.20	5.8 (Apr. 2002)	200	3000
Sha-Hsin #1	Apr. 1989	0.06	<b>22.0</b>	250	3000
Sha-Hsin #2	Aug. 1996	3.80	<b>10.00</b>	220	3500
Hsin-Min #1	Apr. 1997	0.96	1.10	300	4000
Hsin-Min #2	Apr. 1997	0.92	1.20	250	4000
Tan-Liaw	Feb. 1995	4.50	<b>18.00</b>	250	2000
Kam-Ka	Feb. 1997	4.60	7.70	200	3500
Hsin-Kwang	Mar. 1993	0.20	<b>23.0</b> (Sep. 1996)	-	2000
I-Tsan #1	Aug. 1990	0.04	<b>11.00</b>	200	2000
I-Tsan #2	Feb. 1998	1.80	-	-	2000
Er-Tsan	Jan. 1993	3.00	<b>28.00</b>	-	2000

In addition, as the hydrogen ions are consumed in the reaction system, the resulting bicarbonate alkalinity can help remove background hardness and ferrous species through the formation of precipitates such as CaCO<sub>3</sub> and FeCO<sub>3</sub>. In considering the nitrate reduction by Fe<sup>0</sup>, ammonium (NH<sub>4</sub><sup>+</sup>) is found as the dominating reaction product of nitrate reduction reported by several researchers (Cheng et al, 1997, Huang et al, 1998, and Choe et al., 2004). To get rid of ammonium from solution, air-stripping process is recommended as one of the methods (US.EPA, 2000). Ammonium can be stripped out of aqueous phase to ammonia gas under alkaline solution. Addition of alkaline species to raise the pH is a simple and common practice in water purification. Not only ammonium, ferrous ion (Fe<sup>2+</sup>) is one of reaction products from Fe<sup>0</sup> corrosion also. Normally, the conventional process that is used for ferrous treatment is chemical precipitation method. Fe<sup>2+</sup> in soluble species will be changed to solid species such as iron oxide or hydroxide to settle out of solution as solid precipitate. Theoretical speaking, suitable pH for iron precipitation was around neutral pH. However, the settling process is often accelerated by addition of a polymer coagulant, which gathers

the insoluble metal compound particles into a coarse floc that can settle rapidly by gravity. Regarding the disadvantage of precipitation process, a setting and a sludge dewatering facilities are needed which increase the treatment expense. Therefore, the iron pelletization onto media in a fluidized-bed reactor is selected as an alternative process. A great amount of surface area of fluidized media can serve as a large zone for iron pelletization. When high iron was precipitated on sand surface, the iron coated sand size become larger and heavier. Therefore, it will be hard to become fluidized and will tend to settle at the bottom of reactor. Then, iron-coated sand will be drained out of reactor and new seeding sands are replenished. Normally, this method is applied to remove hardness from drinking water softening (Van Der Veen and Graveland, 1988; Chen et al., 2000) and heavy metal from wastewater (Zhou et al., 1999).

## 1.2 Objectives

1. To evaluate the effects of water characteristic and process operation on nitrate reduction by  $\text{Fe}^0/\text{CO}_2$  process;
2. To optimize ferrous ion removal by iron pelletization in fluidized-bed reactor;
3. To optimize ammonia removal by air stripping process;
4. To design integrated system in continuous mode for complete nitrate removal in groundwater.

## 1.3 Hypotheses

1. Nitrate-contaminated groundwater can be treated by the integrated system effectively
2. Ferrous can be removed by iron coating process under fluidized bed reactor.
3. Ammonia can be eliminated completely in shorten time by using air stripping process.

## 1.4 Scopes of work

This research investigated the nitrate removal by  $\text{Fe}^0/\text{CO}_2$  reduction and the follow-up strippers of ferrous and ammonia. The experiments focused on apply in system for treating nitrate-contaminated groundwater. The synthetic wastewater is prepared to simulate the process conditions for laboratory test (batch and continuous modes). In addition, real groundwater was also used in the continuous treatment mode. The scope of this study is illustrated in Fig. 1.2, including laboratory and field tests.

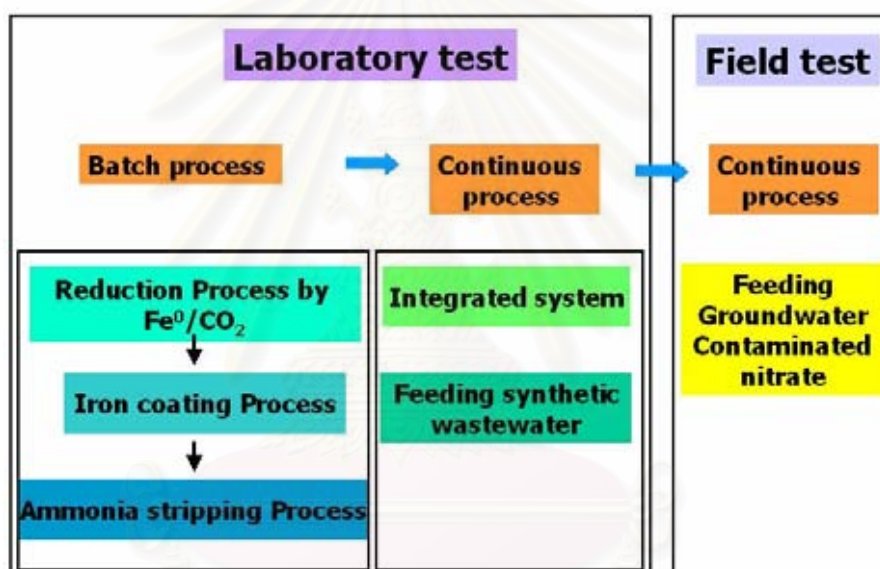


Fig. 1.2 Schematic diagram of integrated system work.

## 1.5 Advantages of this work

1. This technique can be applied in groundwater purification or in some industrial wastewater treatment associated with nitrate species.
2. The problem of alien species of sulfate, chloride and acetate from application of acids that risk the drinking quality of treated water is mitigated by bubbling  $\text{CO}_2$  to provide hydrogen ion ( $\text{H}^+$ ).
3. The iron pellets reclaimed from iron coating process may be reutilized for environmental contaminant treatment purpose through Fenton-like process.

## CHAPTER II

### BACKGROUND AND LITERATURE REVIEWS

#### 2.1 Nitrate in the environment

##### 2.1.1 Source of nitrate

Nitrate is an inorganic compound that occurs under a variety of conditions in the environment, both naturally and synthetically. Nitrate is composed of one atom of nitrogen (N) and three atoms of oxygen (O); the chemical symbol for nitrate is  $\text{NO}_3^-$ . The nitrogen cycle that explains the relationship between the various forms of nitrogen compounds and the change that can occur in nature is illustrated in Figure 2.1. The most common sources of nitrate are municipal and industrial wastewaters, refuse dumps, animal feed lots, and septic systems. Other sources are runoff or leachate from manured or fertilized agricultural lands and urban drainage. However, high level nitrate in groundwater usually results from human activities such as overuse of chemical fertilizers. Fertilizer nitrogen that is not taken up by plants leaches into the groundwater in the form of nitrate. Additionally, manure and sewage contain both ammonia and organic forms of nitrogen, organic nitrogen may be converted to ammonia in the soil. This ammonia, along with any ammonia fertilizer applied, is converted to nitrate by soil bacteria. This process is called *nitrification* as shown in reaction (2.1).



Nitrification is important because plants can only use nitrogen in the nitrate form. However, when more ammonia is nitrified than plants can use, the unused nitrate will accumulate in the soil or seepage into groundwater. Some plants, soybeans and alfalfa in particular, can take nitrogen out of the air and put it into the ground through their root nodules by using the specialized bacteria.

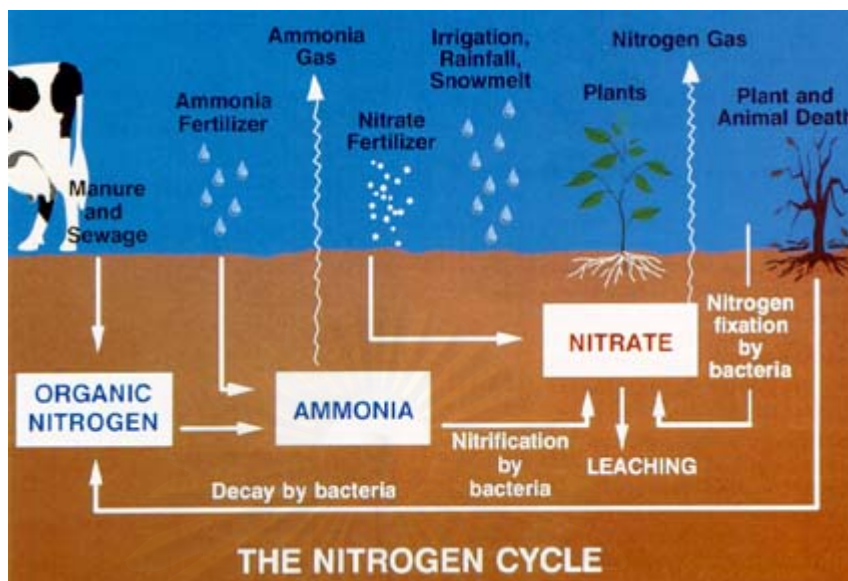
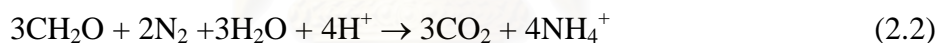


**Fig. 2.1** The nitrogen cycle (Karen M.M., 1987).

These bacteria have the ability to transform atmospheric nitrogen into ammonium. This process is called *nitrogen fixation* as shown in reaction (2.2).



### 2.1.2 Effect of Nitrate

Contamination of nitrate in natural waters has drawn widespread attention due to the public health and ecological concerns. The health effect of nitrate in drinking water is really related to nitrite because nitrate can be microbially reduced to nitrite, which can cause methemoglobinemia in newborn infant by oxidizing the heme  $\text{Fe}^{2+}$  of hemoglobin or known as “blue baby syndrome” (Walton, 1951). Additionally, cancers and damages to liver and other organs by nitrite are convinced to be referred to formation of nitrosamines, group of carcinogens produced from reaction of nitrate with amines, amides, and other nitrogenous compounds (Menzer, 1993). Therefore, the regulatory health limit of  $45 \text{ mg NO}_3^-/\text{L}$  ( $10 \text{ mg-N/L}$ ) is applied as a safe drinking water quality standard in the most of developed countries (Waterhoff et al., 2003). In ecological concerns, nitrate discharged into surface water bodies especially lake and reservoir, can cause an abnormal algae bloom, which will result in the difficulty and

complexity in water purification processes.

### **2.1.3 Solution of nitrate contaminant in groundwater**

A number of treatment technologies have been used to remove nitrate from groundwater including ion exchange, reverse osmosis, biological denitrification, and chemical reduction (Kapoor and Viraraghavan, 1997; Huang et al., 1998). The first three technologies have been applied in full scale (Fanning, 2000). Recently, Chew and Zhang (1998) employed electrokinetic process and a combined electrokinetic/iron wall process for In Situ remediation of nitrate-contaminated groundwater. In view of disadvantage of treatment technologies, reverse osmosis and ion exchange are not selective for nitrate and requires frequent regeneration of the media. Both processes do not destroy nitrate and generate secondary brine wastes. Therefore, these methods may require additional treatment processes. Biological denitrification is unfavorable because it requires intensive maintenance and constant supply of organic substrates. Additional drawbacks include biomass sludge disposal and treatment (aeration and disinfection) of denitrified water. Moreover, these microbial processes are generally slow and sometimes incomplete, compared to chemical reduction (Huang et al., 1998).

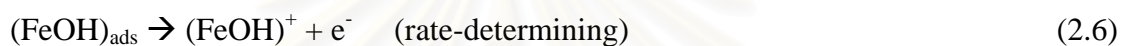
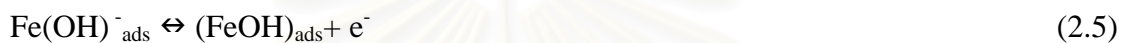
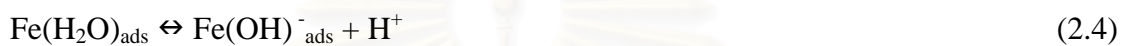
## **2.2 Zero-valent iron ( $\text{Fe}^0$ ) process**

### **2.2.1. Zero-valent iron corrosion mechanism**

Zero-valent iron represents the most common metallic reducing agent used for the treatment of environmental contaminants since it is available at low cost and nontoxic. In general, the key factor of zero-valent iron corrosion depends considerably on the solution pH level.

According to the mechanism of electron releasing from iron metal presented in Reactions (2.3)-(2.7) (Kelly, 1965), the release of two electrons from  $\text{Fe}^0$  begins from the adsorption of water molecule on its surface, and ends up with the dissolution of ferrous ion ( $\text{Fe}^{2+}$ ) in the presence of hydrogen ions ( $\text{H}^+$ ). Reaction (2.5) and (2.6) depict that the electrons are released from iron metal in two stages, with Reaction (2.6)

as a rate-determining step. In addition, the ejection of  $\text{Fe}^{2+}$  from the iron metal surface is extremely dependent on solution pH (Reaction (2.7)). In contrast, lowering the pH accelerates the forward reaction in Reaction (2.7), and this in turn enhances the rate of electron releasing, as shown in Reaction (2.7). Another important role of the hydrogen ions is its function in the breakdown of protective films formed on the surface of metal (Coehn, 1979).



Due to tendency of corrosion, charge separation will occur to form an electrical double layer on the iron metal surface, as illustrated in Fig. 2.2 (Piron, 1991). In the initial stage, the concentration of  $\text{Fe}^{2+}$  in the bulk solution is much smaller than in the metal surface. This creates a concentration gradient, leading to a tendency to expel  $\text{Fe}^{2+}$  from the metal and thus leaving an excess of electrons. However, this chemical driving force will be opposed increasingly as the electrical double layer, an electrical force of attraction, build up, and ultimately an electrochemical equilibrium will result.

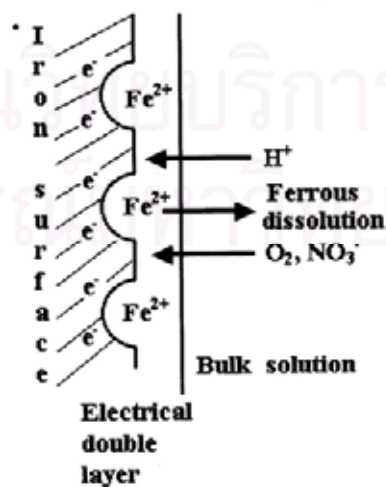


**Fig. 2.2 Corrosion of iron immersed in acid solution** (Liao et al., 2003a).



In the electro-chemical process, oxidation of  $\text{Fe}^0$  is readily oxidized into  $\text{Fe}^{2+}$  in the anodic half reaction.  $\text{Fe}^0$  is called reductant. The available electron acceptors or oxidant (e.g.,  $\text{H}^+$  and dissolved oxygen) in the same system will be involved in the associated cathodic half reaction. Therefore, the overall process of corrosion in anaerobic  $\text{Fe}^0$ - $\text{H}_2\text{O}$  system is described by Reaction (2.8).



Under aerobic conditions dissolved oxygen would play a role of the electron acceptor in the preferred cathodic half reaction. In this case, the primary reaction yields only  $\text{OH}^-$  and not  $\text{H}_2$  (Huang and Zhang, 2004). The reaction was illustrated in reaction (2.9).



### 2.2.2 Application of Zero-valent iron process

In recent year, Zero-valent iron has received considerable attention from various research groups for nitrate removal (Flis, 1991; Siantar et al., 1996; Chew and Zhang, 1998; Huang et al., 1998; Till, 1998; Choe et al., 2000; Kielemoes et al., 2000; Alowitz and Scherer, 2002; Liao et al., 2003; Huang and Zhang, 2002, 2004), reduction of azo dye (Cao et al., 1999), remediation of explosive compounds (Singh et al., 1998), and heavy metal (Ponder et al., 2000) as well as for dechlorination of chlorinated solvents (Cheng et al., 2000; Gillham et al., 1994; Orth et al., 1996; Gotpagar et al., 1997), polychlorinated biphenyls (Chuang et al., 1995), pentachlorophenol (Kim and Carraway, 2000), DDT, DDD, and DDE (Sayles et al., 1997). At the present time, zero-valent iron process can be applied to simulate in In-Situ groundwater treatment as reactive barrier wall (Furukawa et al., 2002; Wilkin et al., 2003) or Ex-Situ groundwater treatment as pack bed column treatment process (Westerhoff, 2003; Westerhoff and James, 2003) or very recently, fluidized bed treatment (Chen et al., 2005).

### 2.2.3 Nitrate reduction by zero-valent iron process

Nitrate reduction by  $\text{Fe}^0$  has been known to occur; however, only a few studies were done in the past (Young et al., 1964). Recently, various research groups have demonstrated that  $\text{Fe}^0$  is an effective reductant used for reducing nitrate. In the past two decades, several researches related to chemical reduction of nitrate by  $\text{Fe}^0$  have been reported.

Flis (1991) reported that iron might reduce nitrate to nitrite, nitrogen, and ammonia depending on the reaction conditions.

Siantar et al. (1996) reported that under anaerobic conditions, nitrate (56.6 mg/L) in 0.1M HEPES-buffered Milli-Q<sup>TM</sup> water (pH 7) was reduced by 100–200 mesh  $\text{Fe}^0$  (36.4 g/L) in 14 min with nitrite as an intermediate. The reaction was pseudo-first-order in nitrate with a rate constant of  $0.208 \pm 0.04 \text{ min}^{-1}$ .

Cheng et al. (1997) studied the effect of pH on nitrate reduction by  $\text{Fe}^0$  (97%, 325 mesh, Aldrich). When pH was controlled at 5, 6 and 7, reduction of nitrate in various pH buffers under aerobic conditions was found to be a pseudo-first-order reaction with rate constants of 0.053, 0.0408, and  $0.0143 \text{ min}^{-1}$ , respectively. However, in unbuffered solutions with an initial pH of 5.5, there was no loss in nitrate and no production of ammonia.

Huang et al. (1998) reported that pH 4 is favorable for the reduction of nitrate to ammonia by hydrogen-reduced  $\text{Fe}^0$  (6–10 mm, specific surface area of  $0.3125 \text{ m}^2 \text{ g}^{-1}$ ) with a ratio of 120  $\text{m}^2 \text{ Fe}^0$ -to-mol  $\text{NO}_3^-$  or higher. In their study, the reduction rate of nitrate by stoichiometric excess of  $\text{Fe}^0$  could be empirically expressed as  $d[A]/dt = k_{\text{obs}}[A]^{1.7}$ . It appeared to be a 1.7 order reaction. The  $k_{\text{obs}}$  value was determined to be  $0.035 \text{ L}^{0.7} \text{ mg}^{-0.7} \text{ min}^{-1}$  when initial  $[\text{NO}_3^-]$  was 50 mg/L and 0.05 M sulfate was present.

Chew and Zhang (1998) conducted a research of In-Situ remediation of nitrate-contaminated groundwater by electrokinetic processing and a combined electrokinetic/iron wall process. Experimental results have shown that the nitrate removal was only 25–37% for the cases without iron wall near the anode. When the iron wall (80 mesh, 20 g) was present, the nitrate-to-nitrogen transformation increased to 54–87% at various constant voltages. Apparently, the presence of  $\text{Fe}^0$  in the

neighborhood of the anode would enhance the removal efficiency of the nitrate from contaminated groundwater.

Zawaideh and Zhang (1998) reported that  $\text{Fe}^0$  would increase the removal efficiency of nitrate at lower pHs. At normal pH range of 6–8, nitrate removal was usually lower than 50% without buffer treatment. An organic buffer (HEPES) was found to greatly enhance the nitrate transformation in a wide pH range (e.g., pH 2–11). At low pH (e.g., pH < 2), the nitrate removal was fast and efficient (95–100%). However, at high pH (e.g., pH > 11), the transformation of nitrate was fast and efficient only for low concentration of nitrate in the  $\text{Fe}^0$ - $\text{H}_2\text{O}$  system.

Choe et al. (2000) conducted a study on kinetics of reductive denitrification by stoichiometric excess of nanoscale zero-valent iron. Under the condition without pH control, micro-scale iron particles having a Brunauer–Emmet–Teller (BET) surface area of  $0.063 \text{ m}^2 \text{ g}^{-1}$  would convert nitrate to ammonia. In contrast, nanoscale iron (1–100 nm) having a BET surface area of  $31.4 \text{ m}^2 \text{ g}^{-1}$  would convert nitrate to nitrogen gas. The reduction of nitrate was found to be a pseudo-first-order reaction with rate constants ranging from 0.1489 to  $0.1565 \text{ min}^{-1}$ . Evidently, iron particles at the nanoscale and the resulting large surface area had a marked effect on the degradation mechanism of nitrate and the related treatment efficiency.

Alowitz and Scherer (2002) studied the effects of pH and surface area concentration on removal of nitrate, nitrite, and Cr (VI) using micro-scale  $\text{Fe}^0$ .  $\text{Fe}^0$  obtained from different suppliers (i.e., 18–35 mesh for Peerless  $\text{Fe}^0$  and Connelly  $\text{Fe}^0$ ; and 40 mesh for Fisher  $\text{Fe}^0$ ). The surface area concentration is defined as the product of the iron concentration and the surface area of iron particles. The results showed that a lower pH condition would be favorable for nitrate removal, but the effect of the surface area concentration on nitrate removal would be negligible, except for Connelly  $\text{Fe}^0$ . A pseudo-first-order reaction was observed for nitrate reduction by Fisher  $\text{Fe}^0$  in different buffers with average rate constants ranging from  $(9.57 \pm 0.27) \times 10^{-1} \text{ h}^{-1}$  at pH 5.5 to  $(7.7 \pm 0.13) \times 10^{-3} \text{ h}^{-1}$  at pH 9. Apparently, the reaction rate constant increased when the system pH decreased.

Based on the results of batch experiments of nitrate reduction in an iron/water/nitrate system under anoxic conditions, Huang and Zhang (2002) proposed the following hypothetical reaction:



In all kinetic tests,  $\text{Fe}^0$  was pre-coated with magnetite. The granular iron powder employed has a diameter of 0.5 mm and a specific surface area of  $0.04 \text{ m}^2 \text{ g}^{-1}$ . No initial pH adjustment was made in these tests. In their study, a kinetic model with a double-Langmuir-adsorption formulation was developed to represent site saturation effects of aqueous  $\text{Fe}^{2+}$  and  $\text{NO}_3^-$  on nitrate reduction in a  $\text{Fe}^0$  system at near neutral pH. In their study, a two-layer semiconductor model, with the inner layer a semiconductor with good (metallic) conductivity (e.g., magnetite) and the outer one a semiconductor with poorer-than-metallic conductivity (e.g.,  $\gamma\text{-Fe}_2\text{O}_3$ , maghemite), was employed to tie all the experimental observations together.

Liao et al. (2003a) explored the impact of parameters on nitrate removal by iron metal powder such as pH (3-5), particle size (10 and 150  $\mu\text{m}$ ),  $\text{N}_2$  purging, and the presence of  $\text{H}_2\text{O}_2$ . Results show that a pH value  $\geq 5$  will inactivate iron corrosion completely, leaving no removal of nitrate. At lower pH, the iron particle size played important role for nitrate reduction. The use of large size of 150  $\mu\text{m}$  caused no removal of nitrate throughout the whole reaction period, as the solution was purged with  $\text{N}_2$ , while 30% removal was observed at 50 min, without  $\text{N}_2$  purging. Results also show that the behavior of ferrous accumulation can be described by S-curve, involving initial lag phase, exponential growth, rate declining and zero rate phases. As ORP dropped all the way down to -400 mV, the nitrate disappeared completely from the solution. As the particle size of 10  $\mu\text{m}$  was used, the presence of  $\text{H}_2\text{O}_2$  terminated all reactions in the acid solution; nitrate removal or ferrous accumulation was no longer observed, and the initial  $\text{H}_2\text{O}_2$  remained intact. Surprisingly, the use of 150  $\mu\text{m}$  led to a rapid decomposition of  $\text{H}_2\text{O}_2$  and  $\text{H}_2\text{O}_2$  has been completely consumed in 50 min. Ferrous ions started to accumulate significantly after 50 min and, nitrate removal was started accordingly.

Liao et al. (2003b) investigated zero-valent reduction of nitrate in the presence of ultraviolet light, organic matter and hydrogen peroxide. The results show that the nitrate removal increases with increasing  $\text{Fe}^0$  dosage; however, the removal makes no difference as the  $\text{Fe}^0$  dosage is greater than 2 g/L. UV radiation retards the dissolution of ferrous ion and the removal of nitrate. The species of propanol, which has a

functional group of  $-OH$ , plays a role of organic inhibitor for  $Fe^0$  corrosion. The presence of  $H_2O_2$  appears to inactivate all reactions as the  $Fe^0$  of  $10\ \mu m$  was used; the final  $H_2O_2$  remains intact throughout the entire reaction period, and there were no removal of nitrate and no dissolution of ferrous ion. Surprisingly, with the use of a larger  $Fe^0$  particle size of  $150\ \mu m$ , the  $H_2O_2$  was seen to decompose rapidly through Fenton reaction. Nevertheless, the rate of ferrous accumulation as well as nitrate removal is still slow.

Westerhoff and James (2003) investigated nitrate removal by laboratory and field continuous-flow zero-valent iron ( $Fe^0$ ) packed bed column. They reported that nitrate was stoichiometrically converted to ammonium, only 70% of the applied nitrogen was recovered as nitrate, ammonium, or nitrite ( $<0.1\ mg/L$ ) during shorter-term column tests (2–20 BVs) and less than 25% of the applied nitrogen was recovered during longer-term field testing (500–1000 BVs) at elevated nitrate levels ( $\sim 25\ mg\ N/L$ ). It was possible that ammonium ion ( $NH_4^+$ ) sorbed to freshly precipitated iron oxides.

Choe et al. (2004) investigated nitrate reduction by zero-valent iron under different pH regimes. The anaerobic reduction of  $NO_3^-$  was carried out using  $Fe^0$  powder in unbuffered solutions from pH 2 to greater than 10. The initial pH of the solution was adjusted to 2, 3, or 4 by addition of HCl,  $H_2SO_4$ , or  $CH_3COOH$ , because the Fe oxidation and  $NO_3^-$  reduction reactions consume acidity. The initial pH values of 2 and 3 with HCl and  $CH_3COOH$ , respectively, provided sufficient acidity to preserve the activity of the  $Fe^0$  powder throughout the reaction. The  $NO_3^-$  can be reduced completely with initial pH setting with acids. The rise of pH was stabilized and the  $NO_3^-$  reduction was carried out continuously and completely with the appearance of green rusts at pH 6.5. The pH was buffered by the consumption of hydroxyl ions through the formation of green rusts. The surface area normalized pseudo-first order reaction rates for  $NO_3^-$  reduction at pH  $>6.5$  or after the formation of green rusts are consistent with those reported for buffered solutions.

Su and Puls (2004) investigated nitrate reduction by zero-valent iron on the effect of formate, oxalate, citrate, chloride, sulfate, borate, and phosphate. The results show that nitrate reduction rates (pseudo-first order) increased in the order of  $HPO_3 <$

citric acid < H<sub>3</sub>BO<sub>3</sub> < oxalic acid < H<sub>2</sub>SO<sub>4</sub> < formic acid < HCl, ranging from 0.00278 to 0.0913 h<sup>-1</sup>, or 0.126 to 4.15 h<sup>-1</sup> m<sup>-2</sup> mL in term of surface area normalized rate. Correlation analysis showed a negative linear relationship between the nitrate reduction rates for the soluble complexes of the ligands with Fe<sup>2+</sup> (R<sup>2</sup> = 0.701) or Fe<sup>3+</sup> (R<sup>2</sup> = 0.918) ions. This sequence of reactivity corresponds also to surface adsorption and complexation of the three organic ligands to iron oxides, which increase in the order: formate < oxalate < citrate. The results are also consistent with the sequence of strength of surface complexation of the inorganic ligands to iron oxides, which increases in the order: chloride < sulfate < borate < phosphate. The blockage of reactive sites on the surface of Fe<sup>0</sup> and its corrosion products by specific adsorption of the inner-sphere complex forming ligands (oxalate, citrate, sulfate, borate, and phosphate) may be responsible for the decreased nitrate reduction by Fe<sup>0</sup> relative to the chloride system.

Huang and Zhang (2004) further studied the effects of low pH (2–4.5) on nitrate reduction by iron grains (approximately 0.5 mm in diameter with a BET surface area of 0.04m<sup>2</sup> g<sup>-1</sup>). As compared with that of the iron/nitrate/water system at near neutral pH, a modified kinetic model was used to describe the experimental findings. The proposed kinetic model incorporated the effects of pH on nitrate reduction and Langmuir adsorption. The kinetic parameters were estimated by nonlinear curve fitting. An analysis of experimental results has indicated that nitrate reaction in an iron/nitrate/water system at low pH might follow first-order kinetics with respect to [H<sup>+</sup>].

Hsu et al. (2004) investigated treatment of aqueous nitrate by zero-valent iron powder in the presence of CO<sub>2</sub> bubbling. The results show that the bubbling of CO<sub>2</sub> effectively creates an acidic environment favorable to Fe<sup>0</sup> corrosion, which results in nitrate reduction. In 10 min, the solution pH dropped to 3.2 with CO<sub>2</sub> inflow rate of 500 mL/min. In the presence of Fe<sup>0</sup> (2 g/L), the CO<sub>2</sub> bubbling (500 mL/min) induced conversion of nitrate-N (~7 mg/L) by 85% in 40 min. In addition, the end product in the reaction mixture was ammonium, which accounts for 90% to 104% of nitrate conversion with the presence of various iron dosages (0.5 to 2 g/L). Though the formation of ammonium is a drawback, the ammonium was eliminated from aqueous phase by a follow-up treatment of settling (30 min) and air aeration (50 min).

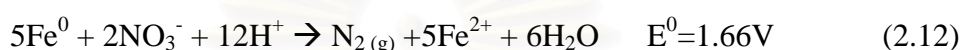
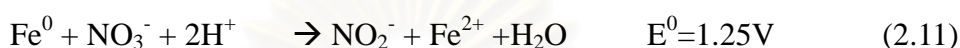
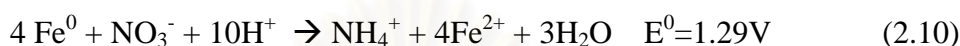
Yang and Lee (2005) investigated chemical reduction of nitrate by nanoscale zero-valent iron ( $\text{Fe}^0$ ) in aqueous solution. In the last decade, employment of micro-scale  $\text{Fe}^0$  has gained its popularity in nitrate solution and related kinetics and pathways. Nano-sized iron was synthesized and tested in this work. It has a size in the range of 50-80 nm and BET surface area of  $37.83 \text{ m}^2\text{g}^{-1}$ . Nitrate reduction by nano-sized  $\text{Fe}^0$  primarily is an acid-driven surface-mediated process. A stronger acidic condition is more favorable for nitrate reduction. Results of the kinetics study have indicated that a higher initial nitrate concentration would yield a greater reaction rate constant. Additional test results also showed that the reduction rate of nitrate increased as the dose of nano-sized  $\text{Fe}^0$  increased. In all tests, reaction rate equations developed do not obey the first- or pseudo-first order reaction kinetics with respect to the nitrate concentration. Two possible reaction pathways for nitrate reduction by nano-scale iron particles have been proposed. Based on the Pourbaix diagram and experimental results obtained, however the following reaction pathway dominates:

$$\text{NO}_3^- + 4\text{Fe}^0 + 10\text{H}^+ \rightarrow 4\text{Fe}^{2+} + \text{NH}_4^+ + 3\text{H}_2\text{O}$$

Chen et al. (2005) investigated nitrate reduction by a fluidized bed zero valent iron ( $\text{Fe}^0$ ).  $\text{Fe}^0$  powder with nominal particle size of 325 mesh ( $40 \mu\text{m}$ ) from Acros Organics Co., USA was used. The results showed that the pH solution can be maintained at optimal conditions for rapid nitrate reduction. For hydraulic retention times of 15 min, the nitrate reduction efficiency increased with increasing  $\text{Fe}^0$  dosage. At  $\text{Fe}^0$  loadings of 33 g/l, results indicate that the nitrate removal efficiency increased from less than 13% for systems without pH control to more than 92% for systems operated at pH 4. By maintaining pH at 4, nitrate reduction still achieves more than 87% when the hydraulic retention time decreases. The recovery of total nitrogen added as nitrate, ammonium, and nitrite was less than 50% for system operated at pH 4, and was close to 100% for a system without control. The possibility of nitrate and ammonium adsorption onto iron corrosion products was ruled out by studying the behavior of their adsorption onto freshly hydrous ferric oxide at variable pH. Results indicated that the probable formation of nitrogen gas species during reaction in pH 4.

### 2.2.4 Pathways and mechanism of nitrate reduction by Fe<sup>0</sup>

In considering the reaction process, the possible reactions of zero-valent iron for removing nitrate in solution based on redox half-cell reactions in Table 2.1, are expressed in Reactions 2.10 -2.12



Several studies have indicated the final products of chemical reduction of nitrate by Fe<sup>0</sup> could be N<sub>2</sub> or NH<sub>4</sub><sup>+</sup>, depending on the experimental conditions (Flis, 1991; Agrawal and Tratnyek, 1996; Huang et al., 1998; Hu et al., 1999; Choe et al., 2000).

Based on a literature survey, pathways for nitrate reduction by Fe<sup>0</sup> proposed by various researchers are presented in Table 2.2.

### 2.2.5 Nitrate reduction by Fe<sup>0</sup>/CO<sub>2</sub> process

Nitrate reduction by Fe<sup>0</sup> is a rapid reaction if the solution pH remains at an acidic range. The CO<sub>2</sub> bubbling in the Fe<sup>0</sup> system for nitrate removal was used as hydrogen ion supplying source since the CO<sub>2</sub> is able to create an acidic environment efficiently (Hsu et al., 2004). The application of CO<sub>2</sub>, called either carbonation or re-carbonation, is a safe and common practice in water purification industries.

**Table 2.1 Equilibrium constants for redox half-cell reactions.**

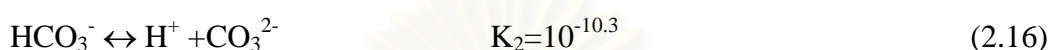
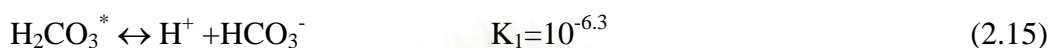
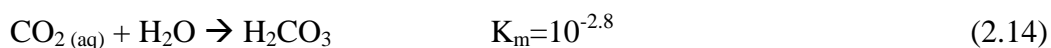
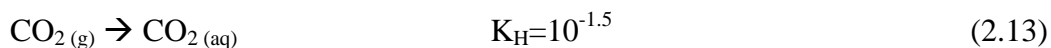
Reaction half-Reactions	Log K	pe <sup>0</sup>	E <sub>H</sub> <sup>0</sup> , V
$\text{NO}_3^- + 2\text{e}^- + 2\text{H}^+ \rightleftharpoons \text{NO}_2^- + \text{H}_2\text{O}$	28.3	14.15	0.84
$\text{NO}_3^- + 5\text{e}^- + 6\text{H}^+ \rightleftharpoons 1/2\text{N}_2(\text{g}) + 3\text{H}_2\text{O}$	105.3	21.05	1.25
$\text{NO}_3^- + 8\text{e}^- + 10\text{H}^+ \rightleftharpoons \text{NH}_4^+ + 3\text{H}_2\text{O}$	119.2	14.9	0.88
$\text{NO}_2^- + 6\text{e}^- + 8\text{H}^+ \rightleftharpoons \text{NH}_4^+ + 2\text{H}_2\text{O}$	90.8	15.14	0.9
$\text{Fe}^{2+} + 2\text{e}^- \rightleftharpoons \text{Fe}(\text{s})$	-13.8	-6.92	-0.409



**Table 2.2 Proposed pathways for nitrate reduction by Fe<sup>0</sup> shown in chronological order.**

Proposed pathway (s)		Author(s) (Year)
(1)	$10\text{Fe}^0 + 6\text{NO}_3^- + 3\text{H}_2\text{O} \rightarrow 5\text{Fe}_2\text{O}_3 + 6\text{OH}^- + 3\text{N}_2(\text{g})$	Flis (1991)
(2)	$\text{Fe}^0 + \text{NO}_3^- + 2\text{H}^+ \rightarrow \text{Fe}^{2+} + \text{H}_2\text{O} + \text{NO}_2^-$	
(1)	$10\text{Fe}^0 + 6\text{NO}_3^- + 3\text{H}_2\text{O} \rightarrow 5\text{Fe}_2\text{O}_3 + 6\text{OH}^- + 3\text{N}_2(\text{g})$	Siantar et al. (1995, 1996)
(2)	$\text{Fe}^0 + \text{NO}_3^- + 2\text{H}^+ \rightarrow \text{Fe}^{2+} + \text{H}_2\text{O} + \text{NO}_2^-$	
	$5\text{Fe}^0 + 2\text{NO}_3^- + 6\text{H}_2\text{O} \rightarrow 5\text{Fe}^{2+} + \text{N}_2(\text{g}) + 12\text{OH}^-$	Chew and Zhang (1998)
(1)	$\text{NO}_3^- + \text{Fe}^0 + 2\text{H}_3\text{O}^+ \rightarrow \text{Fe}^{2+} + \text{NO}_2^- + 3\text{H}_2\text{O}$	Huang et al. (1998)
(2)	$\text{NO}_3^- + 4\text{Fe}^0 + 10\text{H}_3\text{O}^+ \rightarrow 4\text{Fe}^{2+} + \text{NH}_4^+ + 13\text{H}_2\text{O}$	
(1)	$5\text{Fe}^0 + 2\text{NO}_3^- + 6\text{H}_2\text{O} \rightarrow 5\text{Fe}^{2+} + \text{N}_2(\text{g}) + 12\text{OH}^-$	Till et al. (1998)
(2)	$4\text{Fe}^0 + \text{NO}_3^- + 7\text{H}_2\text{O} \rightarrow 4\text{Fe}^{2+} + \text{NH}_4^+ + 10\text{H}_2\text{O}$	
(1)	$\text{Fe}^0 + \text{NO}_3^- + 2\text{H}^+ \rightarrow \text{Fe}^{2+} + \text{H}_2\text{O} + \text{NO}_2^-$	Choe et al. (2000)
(2)	$5\text{Fe}^0 + 2\text{NO}_3^- + 6\text{H}_2\text{O} \rightarrow 5\text{Fe}^{2+} + \text{N}_2(\text{g}) + 12\text{OH}^-$	
(1)	$5\text{Fe}^0 + 2\text{NO}_3^- + 6\text{H}_2\text{O} \rightarrow 5\text{Fe}^{2+} + \text{N}_2(\text{g}) + 12\text{OH}^-$	Kielemoes et al. (2000)
(2)	$4\text{Fe}^0 + \text{NO}_3^- + 7\text{H}_2\text{O} \rightarrow 4\text{Fe}^{2+} + \text{NH}_4^+ + 10\text{H}_2\text{O}$	
(1)	$\text{NO}_3^- + 4\text{Fe}^0 + 10\text{H}^+ \rightarrow 4\text{Fe}^{2+} + \text{NH}_4^+ + 3\text{H}_2\text{O}$	Alowitz and Schere (2002)
(2)	$\text{NO}_2^- + 3\text{Fe}^0 + 8\text{H}^+ \rightarrow 3\text{Fe}^{2+} + \text{NH}_4^+ + 2\text{H}_2\text{O}$	
	$\text{NO}_3^- + 2.82\text{Fe}^0 + 0.75\text{Fe}^{2+} + 2.25\text{H}_2\text{O} \rightarrow \text{NH}_4^+ + 1.19\text{Fe}_3\text{O}_4 + 0.5\text{OH}^-$	Huang and Zhang (2002)
(1)	$\text{NO}_3^- + 4\text{Fe}^0$ (coated with an iron oxide) $+ 10\text{H}^+ \rightarrow 4\text{Fe}^{2+} + \text{NH}_4^+ + 3\text{H}_2\text{O}$	Huang and Zhang (2004)
(2)	$8\text{Fe}^0 + \text{NO}_3^- + 10\text{H}^+ \rightarrow 8\text{Fe}^{3+} + \text{NH}_4^+ + 3\text{H}_2\text{O}$	

According to the water chemistry (Snoeyink and Jenkins, 1982), carbonated system can be described by Reactions (2.13) – (2.17).



The equilibrium pH in the above carbonated system is dependent on the partial pressure of  $\text{CO}_2$  gas and the speciation of carbonic acid and bicarbonate ion (Girard, 2005). With the sufficient exposure time, equilibrium will occur between  $\text{CO}_2(\text{aq})$  and  $\text{CO}_2(\text{g})$ , as described by Henry's law:

$$[\text{CO}_2(\text{aq})] = K_{\text{H}} P_{\text{CO}_2} \quad (2.18)$$

The Henry's constant for carbon dioxide,  $K_{\text{H}}$ , is  $0.034 \text{ M atm}^{-1}$ . Regarding composition of air, percent of carbon dioxide ( $\text{CO}_2$ ) in dry air was 0.035. Therefore, the atmosphere contains a mole fraction of 350 ppm of  $\text{CO}_2$ . The equilibrium molar concentration of aqueous  $\text{CO}_2$  exposed to clean air at a pressure of 1 atm is  $0.034 \times 350 \times 10^{-6} \text{ M} = 12 \text{ }\mu\text{M}$ . The dissolved  $\text{CO}_2$  reacts rapidly with water to form carbonic acid according to Reaction (2.14). The equilibrium relationship is described by the following expression, with the water concentration incorporated into the equilibrium constant:

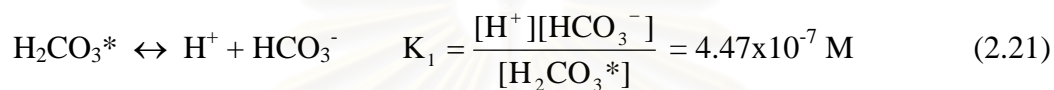
$$\frac{[\text{H}_2\text{CO}_3]}{[\text{CO}_2(\text{aq})]} = K_{\text{m}} = 1.58 \times 10^{-3} \quad (2.19)$$

It is to differentiate experimentally between  $\text{CO}_2(\text{aq})$  and  $\text{H}_2\text{CO}_3$ . Therefore,  $\text{CO}_2(\text{aq})$  and  $\text{H}_2\text{CO}_3$  can combine into  $\text{H}_2\text{CO}_3^*$  and referred as "carbonic acid":

$$[\text{H}_2\text{CO}_3^*] = [\text{CO}_2(\text{aq})] + [\text{H}_2\text{CO}_3] = [\text{CO}_2(\text{aq})](1+K_m) \quad (2.20)$$

Since  $K_m \ll 1$ ,  $[\text{H}_2\text{CO}_3^*]$  is approximately equal to  $[\text{CO}_2(\text{aq})]$ . At equilibrium, with exposure to a  $\text{CO}_2$  partial pressure of  $350 \times 10^{-6}$  atm,  $[\text{H}_2\text{CO}_3^*] = 12 \mu\text{M}$ .

Carbonic acid is a weak acid, and its conjugate base, bicarbonate, is an even weaker acid. The acid dissociation reactions of these species are described at equilibrium as follows:



The carbonate system contains three aqueous-phase species,  $\text{H}_2\text{CO}_3^*$ ,  $\text{HCO}_3^-$ , and  $\text{CO}_3^{2-}$ . Therefore, the total concentration of aqueous carbonate species can be defined by

$$C_{\text{carbonate}} = [\text{H}_2\text{CO}_3^*] + [\text{HCO}_3^-] + [\text{CO}_3^{2-}] \quad (2.23)$$

The distribution of  $C_{\text{carbonate}}$  among the three species can be expressed by the following relationships, derived from equation (2.23) combined with the equilibrium relationship (2.21) and (2.22). The left-hand portion of each expression defines  $\alpha_i$  as the fraction that species  $i$  comprises of the total concentration  $C_{\text{carbonate}}$ .

$$\alpha_{\text{H}_2\text{CO}_3^*} = \frac{[\text{H}_2\text{CO}_3^*]}{C_{\text{carbonate}}} = \frac{[\text{H}^+]^2}{[\text{H}^+]^2 + K_1[\text{H}^+] + K_1K_2} \quad (2.24)$$

$$\alpha_{\text{HCO}_3^-} = \frac{[\text{HCO}_3^-]}{C_{\text{carbonate}}} = \frac{K_1[\text{H}^+]}{[\text{H}^+]^2 + K_1[\text{H}^+] + K_1K_2} \quad (2.25)$$

$$\alpha_{\text{CO}_3^{2-}} = \frac{[\text{CO}_3^{2-}]}{C_{\text{carbonate}}} = \frac{K_1K_2}{[\text{H}^+]^2 + K_1[\text{H}^+] + K_1K_2} \quad (2.26)$$

Fig. 2.3 plots the three fractions versus pH. Note that when  $\text{pH} = \text{pK}_1 = 6.35$ ,  $[\text{H}_2\text{CO}_3^*] = [\text{HCO}_3^-]$ , and when  $\text{pH} = \text{pK}_2, 10.33$ ,  $[\text{HCO}_3^-] = [\text{CO}_3^{2-}]$ . This figure also generates the partitioning of aqueous carbonate among the three species:

When the pH is 6.5 to 10,  $\text{HCO}_3^-$  is the predominant ion in natural waters.

When  $\text{pH} = \text{pK}_{a1}$ ,  $\alpha_{\text{H}_2\text{CO}_3^*} = \alpha_{\text{HCO}_3^-}$

When  $\text{pH} = \text{pK}_{a2}$ ,  $\alpha_{\text{H}_2\text{CO}_3^*} = \alpha_{\text{HCO}_3^-}$

When the pH is low (less than 5.5),  $\text{H}_2\text{CO}_3^*$  is the predominant species.

When pH is high (more than 10.5),  $\text{CO}_3^{2-}$  is the predominant species.

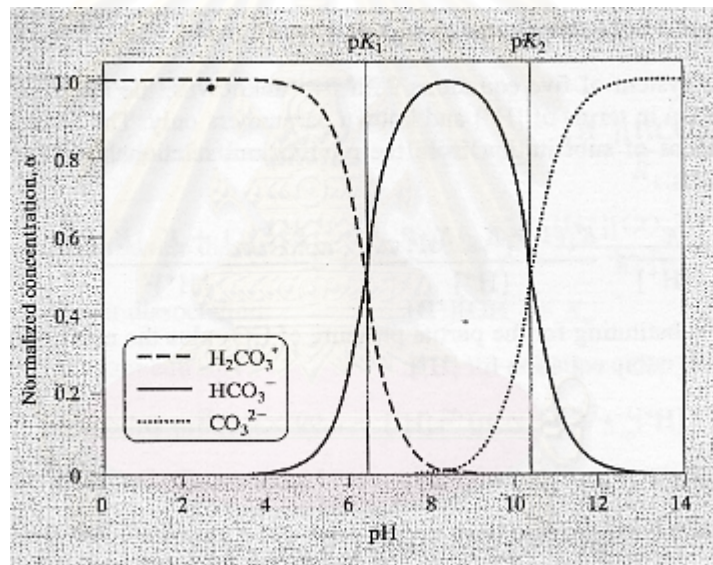


**Fig. 2.3 Distribution of aqueous carbonate species as a function of pH.** The vertical axis gives  $\alpha$ , the concentration of each species divided by the total concentration of aqueous carbonate ( $C_{\text{carbonate}}$ ).

## 2.3 Iron precipitation process by fluidized bed process

### 2.3.1 Iron precipitation

According to  $\text{Fe}^0/\text{CO}_2$  process, a great amount of ferrous ion generated from zero-valent iron. In general, iron does not present a danger to human health or the environment, but it brings unpleasantness of an aesthetic. Indeed, iron gives a rust colour to the water, which can stain linen, sanitary facilities or even food industry products. Therefore, ferrous removal should be concerned for water quality. The US EPA has established a secondary drinking water regulation of 0.3 ppm of water. This is not federally enforceable, since it is not considered a health risk. However, it may be enforced at the state or county level. Normally, the conventional process that is used for ferrous ion treatment is chemical precipitation. The elimination of the ferrous iron is obtained by raising the water redox potential by oxidation related to oxygen of the air. Air is bubbled up through the water. The iron will precipitate, since the air has oxygen contained within it, as long as there is adequate time. The ferrous iron can be oxidized to ferric iron ( $\text{Fe}^{3+}$ ) in equation (2.27). Ferric iron ( $\text{Fe}^{3+}$ ) is not expected to remain soluble. Therefore, magetite ( $\text{Fe}_3\text{O}_4$ ), ferrous hydroxide ( $\text{Fe}(\text{OH})_2$ ), and ferric hydroxide ( $\text{Fe}(\text{OH})_3$ ) can be predominant for insoluble form depending upon redox conditions and pH as shown in equations (2.28) – (2.30)



Generally, most of precipitation form is the ferric hydroxide. The suitable pH for precipitation of ferric hydroxide was around neutral pH and slightly basic as shown in Fig. 2.4. Following the aeration reactor, a settling tank and /or filter should be utilized

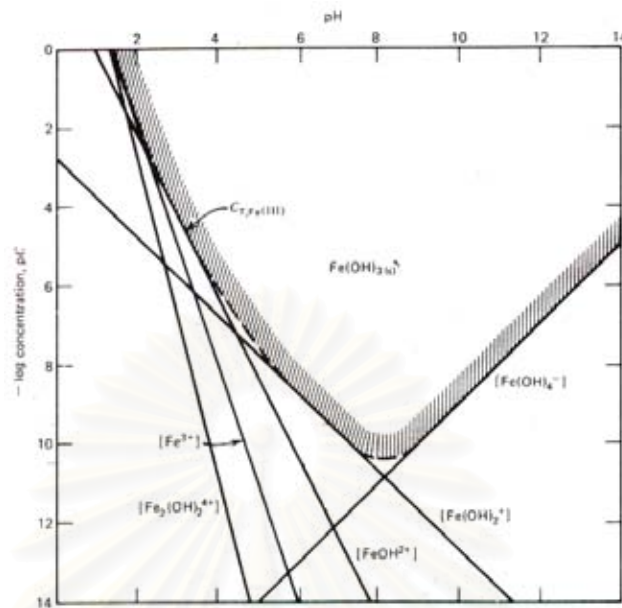


**Fig. 2.4 pC-pH diagram for hydrolysis products of Fe<sup>3+</sup>** (Snoeyink and Jenkins, 1982).

to remove the precipitation iron. The settling process is often accelerated by addition of a polymer coagulant, which gathers the insoluble metal compound particles into a coarse floc for effective settling and/or filtration. Regarding the disadvantage of precipitation process, it requires a large volume of sedimentation tank and a sludge dewatering facility for the removal of moisture content. Therefore, the iron precipitation onto media in a fluidized-bed reactor is selected as an alternative process in this study.

### 2.3.2 Fluidized bed process

Fluidized bed system has been widely utilized in industry, such as facilitating catalytic and non-catalytic reactions, drying, and other forms of mass transfer. It is especially useful in the precipitation process. Fluidization involves the passing of fluid upwards through a bed of particles and expanding it. The minimum fluidization velocity is reached when the pressure drop over the column is equal to the weight of the bed divided by its cross-sectional area. The minimum fluidization velocity is

important parameter for operation to determine the water flow that is required to expand the bed of particles. The media in fluidized bed reactor provides a great amount of specific area. Generally, this method is applied to remove hardness in drinking water softening (Van Der Veen and Graveland, 1988; Chen et al., 2000) and heavy metal (Zhou et al., 1999).

According ferrous removal from  $\text{Fe}^0/\text{CO}_2$  process, three-phase fluidized bed was selected as a novel process. Three phases consist of gas-solid-liquid phases. Sand is served as media in solid phase for iron precipitation in the fluidized bed reactor. The recirculated solution is liquid phase. Air is selected as gas phase. Sand can be lifted upward by air by the recirculated flow. A schematic of three-phase fluidized bed operation is shown in Fig. 2.5. Regarding on the reaction mechanism in fluidized bed reactor, the ferrous iron is oxidized into ferric iron by oxygen provided from air. Therefore, the insoluble iron forms such as iron hydroxide  $\text{Fe}(\text{OH})_3$  or others can be generated as mentioned earlier in iron precipitation issue. Then, a great amount of specific area of sand can be utilized for pelletization. When iron precipitates on sand surface, the iron coated sands become larger and heavier. Therefore, it will be hard to become fluidized and will settle to bottom of reactor easily. Then, iron seeding materials will be drained out of reactor and replaced by new seeding materials.

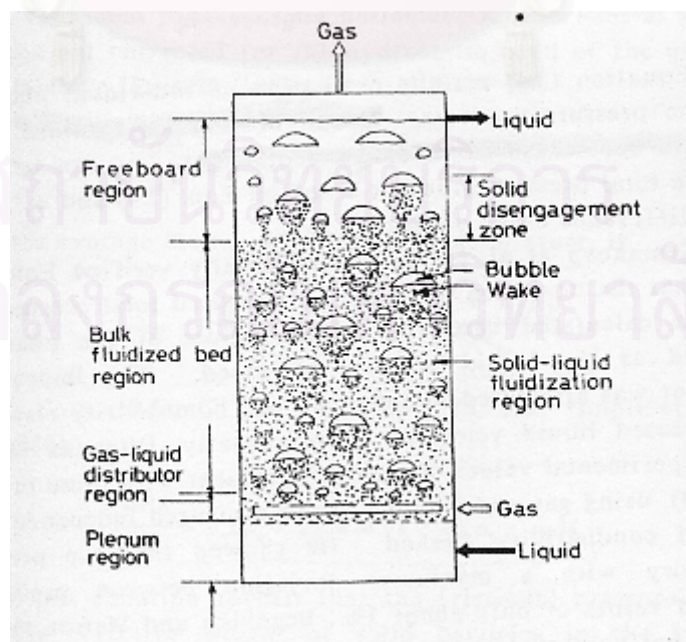
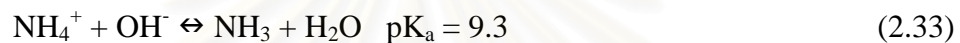


**Fig. 2.5 Schematic of representation of three phase fluidized bed (Fan, 1989).**

## 2.4 Ammonia removal by air stripping

Air-stripping process is recommended as one of the methods to get rid of ammonium from solution (US.EPA, 2000). Generally, ammonia nitrogen can be removed from water by the volatilization of gaseous ammonia into the air by forcing air through the water in stripping towers. According to reaction 2.33 (Benjamin, 2002), ammonium can be stripped out of aqueous phase and become ammonia gas under alkaline solution. Addition of alkaline species to raise the pH is a simple and common practice in water purification.



Ammonium equilibrium in aqueous solution depends on pH and temperature and free ammonia concentration expressed with the following equation,

$$[\text{NH}_3] = \frac{[\text{NH}_3 + \text{NH}_4^+]}{1 + \frac{[\text{H}^+]}{\text{K}_a}} = \frac{[\text{NH}_3 + \text{NH}_4^+]}{1 + 10^{\text{pK}_a - \text{pH}}} \quad (2.34)$$

where  $[\text{NH}_3]$  is the free ammonia concentration,  $[\text{NH}_3] + [\text{NH}_4^+]$  is total ammonia concentration,  $[\text{H}^+]$  is the hydrogen ion concentration, and  $\text{K}_a$  is acid ionization constant for ammonia (Bonmati and Flotats, 2003). The  $\text{pK}_a$  can be expressed as function of temperature  $T$  obtained by polynomial regression of data from Lide (1993) as the following equation,

$$\text{pK}_a = 4 \times 10^{-8} \times T^3 + 9 \times 10^{-5} \times T^2 - 0.0356 \times T + 10.072 \quad (2.35)$$

The higher the pH and temperature, the higher the free ammonia fraction was found. Another parameter related to ammonia stripping is its Henry's law constant. The molar Henry's law constant ( $\text{K}_H$ ) of  $\text{NH}_3$  at  $25^\circ\text{C}$  is  $56.9 \text{ atm}/(\text{mol}/\text{litre})$ , according to equation (2.36) (Plambeck, 1996).



$$C_{\text{equil}} = K_{\text{H}} P_{\text{gas}} \quad (2.36)$$

where  $C_{\text{equil}}$  is the concentration of gas dissolved in the liquid at equilibrium,  $P_{\text{gas}}$  is the partial pressure of the gas above the liquid, and  $K_{\text{H}}$  is the Henry's law constant for the gas at the given temperature.

Ammonia air stripping has been considered a good option when treating different types of waste: liquid fraction of dewatered sewage sludge (Janus and van der Roest, 1997; Thron Dahl, 1992; Watergroup, 1990), urea fertilizer plant wastes (Minocha and Prabhakar, 1988; Kabdasli et al., 2000), landfill leachate (Cheung et al., 1997) and condensates from a sugar beet factory (Schiweck and Nahle, 1990; Gonzalez and Garcia, 1996). In all these cases, the process was performed at high pH values.

Liao et al., (1995) investigated ammonia air stripping from pig slurry at room temperature (22°C). At this temperature, a high pH (10.5-11.5) was required to obtain high ammonia removal efficiency, and the excess lime caused problems of calcium carbonate scaling and, as a result, the efficiency of the system decreased and severe maintenance problem arose. However, if air stripping is performed at high temperature, high buffering capacity of the pig slurry could probably maintain pH at the needed value, and the amount of alkali could be reduced.

Bonmati and Flotats (2003) investigated the effect of pig slurry waste type, fresh or anaerobically digested, and the effect of initial pH on ammonia air stripping from pig slurry waste at high temperature (80°C). Stripping process as pre- or post treatment to anaerobic digestion has been also evaluated. Treatment performances differed according to pig slurry type. When fresh pig slurry was used, despite working at 80°C, a high initial pH (11.5) is required for complete ammonia removal. On the other hand, for digested pig slurry, complete ammonia removal without pH modification is possible and organic matter significantly less contaminates recovered ammonia salt. Batch anaerobic tests showed that ammonia air stripping was not an advisable pre-treatment to pig slurry anaerobic digestion.

## CHAPTER III

### METHODOLOGY

#### 3.1 Material and reagents

All chemicals used in this work were analytical reagent grade. Solutions were prepared using deionized water treated by a Millipore-Q system (Millipore Simplicity, France). Zero-valent iron ( $\text{Fe}^0$ ) of 10  $\mu\text{m}$  size (specific surface area  $\approx 1 \text{ m}^2/\text{g}$ ) purchased from Merck KGaA, Darmstadt, Germany was used without any pretreatment. The  $\text{CO}_2$  gas with purity greater than 99.5% was purchased from a local supplier. Sodium nitrate ( $\text{NaNO}_3$ ) and potassium nitrate ( $\text{KNO}_3$ ) (Merck KGaA, Darmstadt, Germany) was used to prepare the nitrate solution. Humic acid (Sigma-Aldrich, St. Louis, USA) was prepared as organics in solution.  $\text{CaCl}_2 \cdot 2\text{H}_2\text{O}$ ,  $\text{Na}_2\text{CO}_3$  and  $\text{NaCl}$  were purchased from Merck KGaA, Darmstadt, Germany. In analysis of ferrous ion ( $\text{Fe}^{2+}$ ), the reagents used include ammonium acetate, 1,10-phenanthroline (Merck KGaA, Darmstadt, Germany), and 35%  $\text{HCl}$  (Merck KGaA, Darmstadt, Germany).

Regarding iron precipitation process, two different sand sizes with the diameters of 40 to 30 mesh sieves (0.42 to 0.59 mm in diameter) and of 160 to 70 mesh sieves (0.096 to 0.21 mm in diameter) were investigated for their effects on iron removals. Air pump connected with air flow meter was used for supplying air in the system.

In ammonia stripping process, ammonium chlorite ( $\text{NH}_4\text{Cl}$ ) purchased from Merck KGaA, Darmstadt, Germany was used to prepare stock solution. Sodium hydroxide ( $\text{NaOH}$ ) purchased from Merck KGaA, Darmstadt, Germany was used for pH control. Air pump connected with air flow meter was used for supplying air into the system. In analysis of ammonium ion ( $\text{NH}_4^+$ ), the reagents used include phenol solution, sodium nitroprusside, alkaline citrate and sodium hypochlorite (Merck KGaA, Darmstadt, Germany). The solution pH was adjusted by using pH controller (Hotec, Taiwan) connected with feeding pump (Tacima, Osaka, Japan).

### 3.2 Experimental procedure

The overall study was divided into two phases: Laboratory and field test, as described in the following:

#### 3.2.1. Laboratory test

Laboratory test involved batch and continuous operation, as detailed below:

##### 1. Batch operation

- 1.1. Nitrate reduction by  $\text{Fe}^0/\text{CO}_2$  process.
- 1.2. Iron precipitation by fluidized bed process
- 1.3. Ammonia removal by air stripping process

According to batch process of nitrate reduction by  $\text{Fe}^0/\text{CO}_2$  process, a schematic setup of the experimental system was shown in Fig. 3.1. A glass column with diameter of 5.5 cm and length of 55 cm was employed as reactor. The liquid volume was 1 L. Internal recirculated flow by a peristaltic pump was used to achieve homogeneous mixing of solution. The  $\text{CO}_2$  gas was introduced by passing through a disk diffuser of silicate material installed at the bottom of reactor. Nitrate reduction by  $\text{Fe}^0/\text{CO}_2$  process was investigated into two aspects. In the first aspect, the experiment was set for understanding operation process. The diagram of experiment was shown in Fig. 3.2.

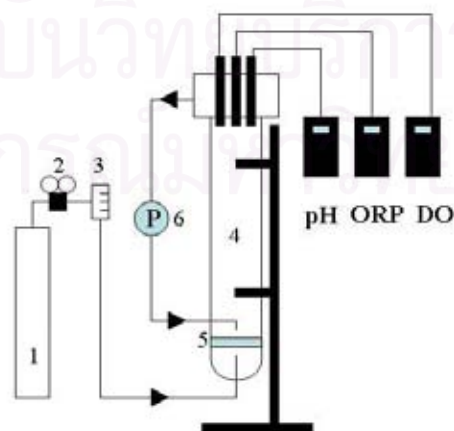


**Fig. 3.1 Configuration of reactor for the  $\text{Fe}^0/\text{CO}_2$  system.** (1:  $\text{CO}_2$  cylinder; 2: Pressure gauge; 3: Flow meter; 4: Reactor; 5: Disk diffuser; 6: Recirculated water pump).

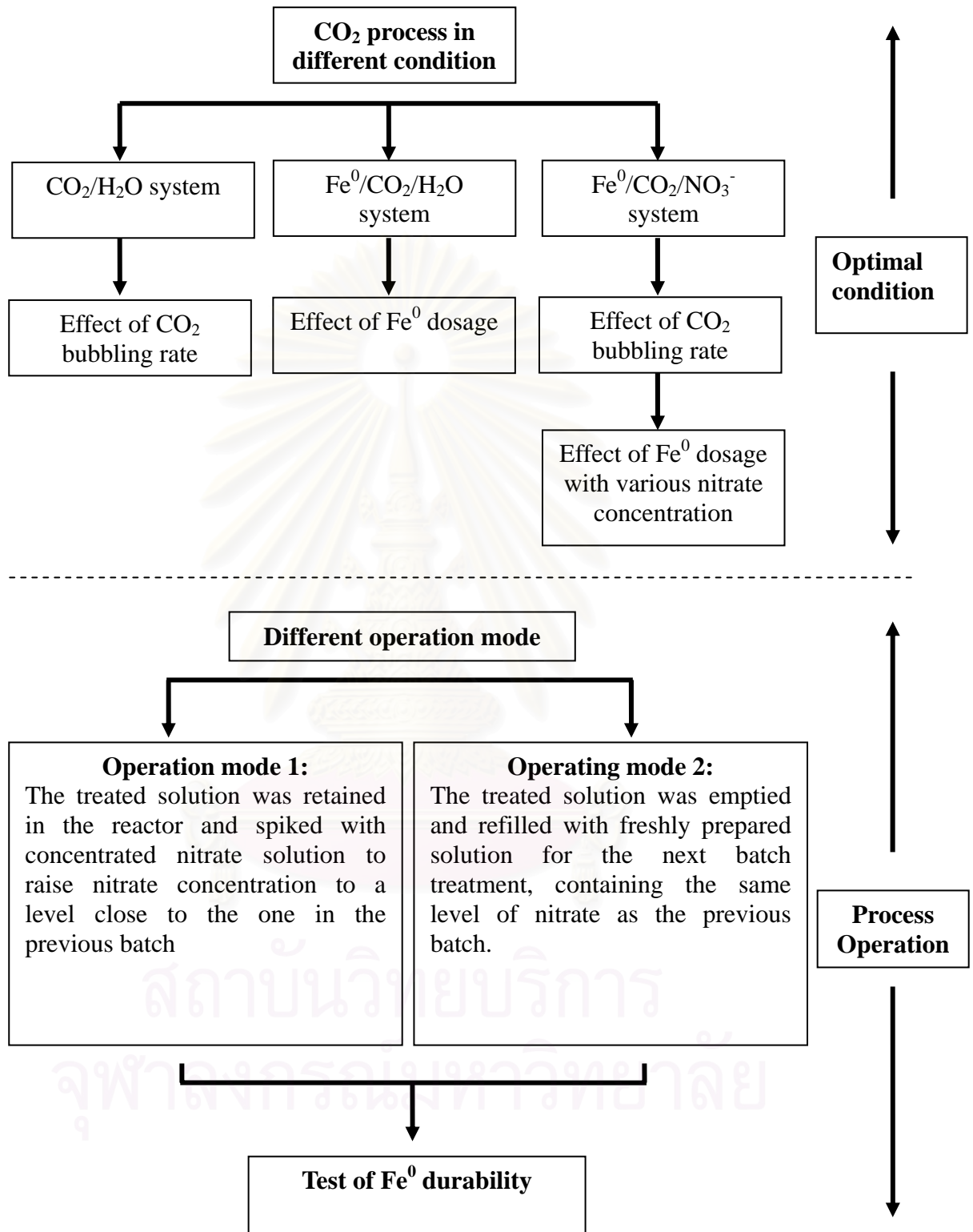


**Fig. 3.2 Schematic diagram for nitrate reduction by Fe<sup>0</sup>/CO<sub>2</sub> in the first phase.**

The optimal condition in the different system of CO<sub>2</sub>/H<sub>2</sub>O, Fe<sup>0</sup>/CO<sub>2</sub> and

$\text{Fe}^0/\text{CO}_2/\text{NO}_3^-$  was investigated. To understand characteristic aspects of  $\text{CO}_2$  bubbling in  $\text{CO}_2/\text{H}_2\text{O}$  system, deionized water was first used to fulfill this purpose. The bubbling time period was controlled at 40 min, the recirculated flow rate was 1000 mL/min, and the  $\text{CO}_2$  inflow rate varied from 100 to 400 mL/min.

Regarding  $\text{Fe}^0/\text{CO}_2$  system, the corrosion behavior of  $\text{Fe}^0$  in  $\text{CO}_2$ -bubbled solution was investigated. The  $\text{Fe}^0$  dosages ranging from 1 to 4 g were tested, while the rate of  $\text{CO}_2$  bubbling remained at 200 mL/min. Deionized water was used as a liquid medium.

According to  $\text{Fe}^0/\text{CO}_2/\text{NO}_3^-$  system, the experiment was divided into 2 conditions. First, the effect of  $\text{CO}_2$  inflow rate on nitrate solution was investigated. The initial  $\text{NO}_3^-$  concentration was 30 mg/L (6.8 mg N/L). The inflow rates of  $\text{CO}_2$  varied from 100 to 400 mL/min. The experiment was conducted by using 2 g/L of  $\text{Fe}^0$ . A recirculated flow of 1000 mL/min was selected for completely mixing solution. Second, the experiment was set to optimize the  $\text{Fe}^0$  dosage for treating different initial nitrate concentrations. The initial nitrate concentration was varied from 30 to 100 mg/L (6.8 -23.4 mg N/L). The experiments were conducted by using various  $\text{Fe}^0$  dosages as well as an  $\text{CO}_2$  inflow rate selected from the effect of  $\text{CO}_2$  inflow rate experiment and a recirculated flow of 1000 mL/min.

In view of process operation, two operating modes were designed, including (1) Mode 1: treated solution was retained in the reactor and spiked with concentrated nitrate solution to raise nitrate concentration to a level close to the initial concentration of the previous batch; (2) Mode 2: treated solution was emptied and refilled with freshly prepared solution for the next batch treatment, containing the same level of nitrate as the previous batch.

As understood from the above operation modes, mass of zero-valent iron will decrease due to corrosion process during operation. Therefore, the supplement of fresh zero-valent iron is required to maintain a satisfactory efficiency of nitrate reduction when the process is operated in a longer time period.

In the second phases of nitrate reduction by  $\text{Fe}^0/\text{CO}_2$  process, the experiment was set for determining the effect of water quality on nitrate reduction by  $\text{Fe}^0/\text{CO}_2$  process; this serves to simulate the field test.

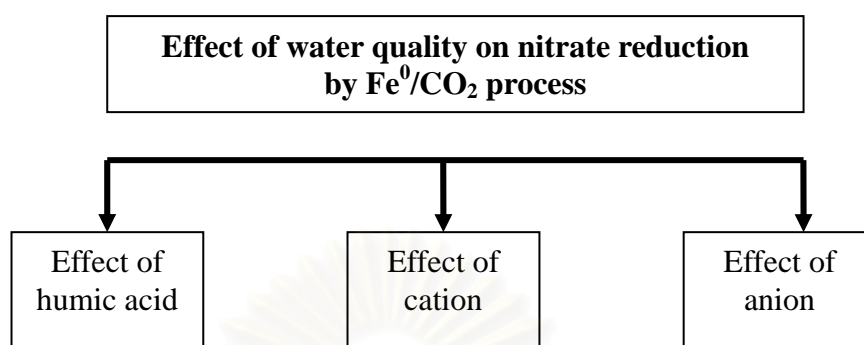


**Fig. 3.3 Schematic diagram for nitrate reduction by Fe<sup>0</sup>/CO<sub>2</sub> process in the second phase.**

The diagram of experiment was shown in Fig. 3.3. Of the natural organic matters, the humic substances represent a major fraction in diverse water and soil environments. Therefore, humic acid was selected as one of studied conditions. Moreover, water quality parameters such as alkalinity, hardness, and saltiness are concerned when applying the proposed Fe<sup>0</sup>/CO<sub>2</sub> process for the field treatment of nitrate-contaminated water. In general, these parameters commonly found in groundwater contain cations and anions such as Na<sup>+</sup>, CO<sub>3</sub><sup>2-</sup>, Ca<sup>2+</sup> and Cl<sup>-</sup>. In running the relevant experiments, chemical reagents of sodium carbonate, calcium chloride, and sodium chloride were employed to investigate their impacts on the process performance.

According to iron precipitation by fluidized bed process, a schematic setup of the experimental system was shown in Fig. 3.4. The experimental method was divided in two steps as follows: (1). ferrous ion preparation and (2). fluidized bed process operation. Fig. 3.5 shows the operation procedure. Regarding on ferrous preparation, Fe<sup>0</sup>/CO<sub>2</sub> process was used to prepare ferrous solution in a cylindrical reactor with a 5.5 cm diameter and 55 cm height. The liquid volume of working solution prepared by deionized water was 1 L. The 1000 mL/min of internal recirculated flow was used to achieve complete mixing of solution using a peristaltic pump. The CO<sub>2</sub> gas with a flowrate of 200 mL/min was introduced by passing through a disk diffuser of silicate material installed at the bottom of reactor.

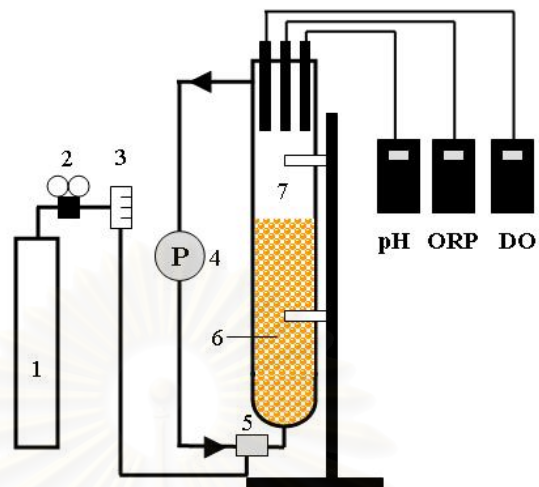


**Fig. 3.4 Configuration of reactor for the iron precipitation by fluidized bed process.** (1: air tank; 2: Pressure gauge; 3: Flow meter; 4: Recirculated water pump; 5: air dissolver; 6: sand; 7: fluidized bed reactor).

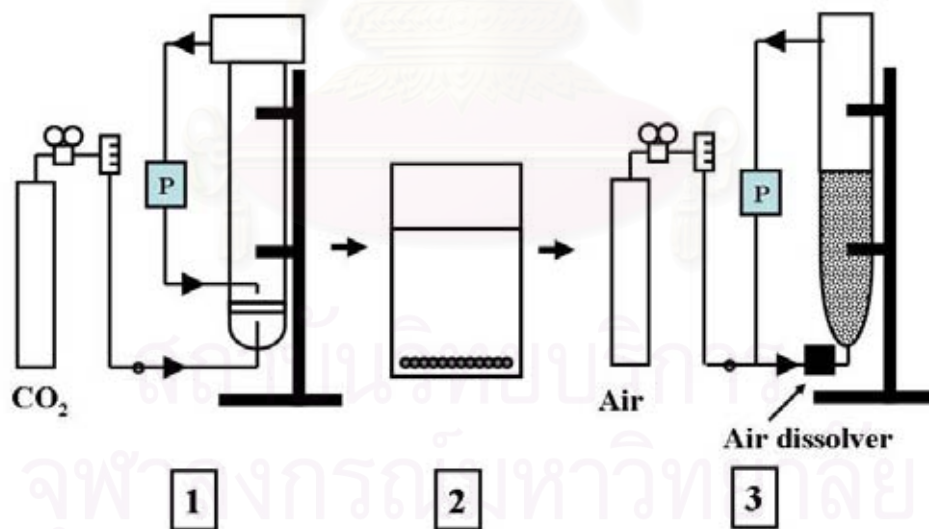


**Fig. 3.5 Three-phase fluidized bed operation procedure:** 1. ferrous preparation by  $\text{Fe}^0/\text{CO}_2$ , 2. settling  $\text{Fe}^0$ , 3. iron precipitation by fluidized bed process.

**Table 3.1 Preparation of ferrous ion at different Fe<sup>0</sup> dosages.**

<b>Fe<sup>0</sup> dosage (g/L)</b>	<b>Fe<sup>2+</sup> concentration (mg/L)</b>
1	121
2	189
4	275
6	350

The reaction time of ferrous preparation was 60 min. Then, Fe<sup>0</sup> in the solution was settled for 30 min in a container covered by a piece of paraffilm to keep ambient oxygen away. The supernatant with ferrous ions separated from Fe<sup>0</sup> was used as working solution. The initial ferrous concentration was varied by changing Fe<sup>0</sup> dosage as shown in Table 3.1.

In fluidized bed process, sand media were added into the reactor for the iron precipitation as shown in Fig. 3.5. Then, the working solution was introduced into the cylindrical reactor. The diameter and height of reactor was 5 and 70 cm respectively. The recirculated pump was used for sand bed fluidization. The flow rate was adjusted to provide the bed expansion ratio at 0.5, relative to the original sand bed depth. In this study, the experiment was performed under 3 conditions as shown in Fig. 3.6. First, the effect of air flow rate on iron removal by fluidized bed was investigated. The initial Fe<sup>2+</sup> concentration was prepared from 2g Fe<sup>0</sup>/L dosage. The experiment was conducted by varying air inflow rate from 20 to 500 mL/min and sand dosage of 400 g/L. Second, the effect of air flow rate on iron removal by fluidized bed process was investigated. The experiment was conducted by varying sand dosages from 100 to 400 g/L and the same air inflow rate which was selected from the first condition. In this part, two sizes of sand, 0.42 - 0.59 mm in diameter and 0.096 - 0.21 mm in diameter, were used and compared for their iron removal performance. Third, the effect of initial ferrous concentration was investigated. The various initial Fe<sup>2+</sup> concentrations were prepared from 1 g to 6 g Fe<sup>0</sup>/L dosages. The experiment was conducted by using sand dosage determined from the second condition, and air inflow rate which was selected from the first condition. Water sample were taken at desired time intervals



and pretreated with solution pH dropped down below 2 by  $\text{HNO}_3$  for total iron analysis.

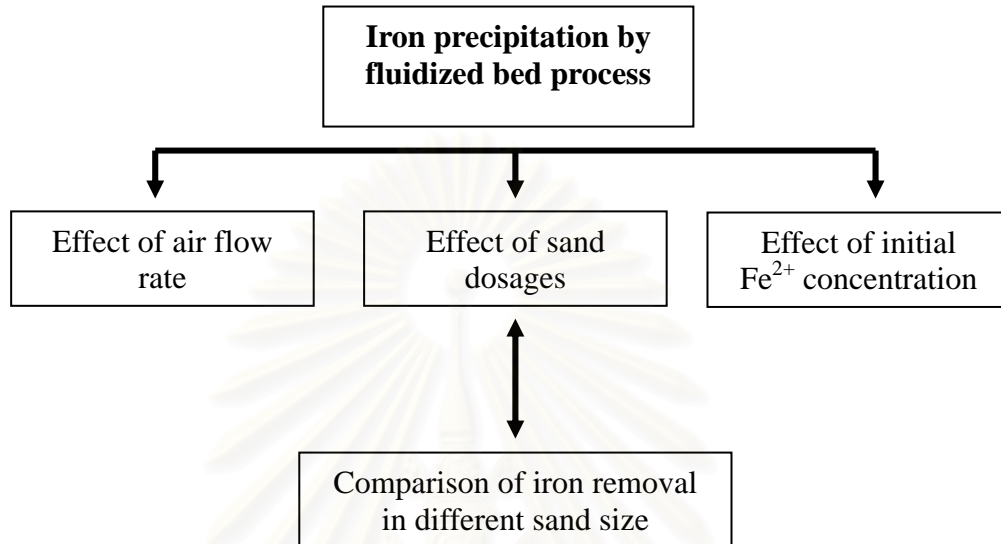


**Fig. 3.6 Schematic diagram for ferrous removal by iron precipitation.**

According to ammonia removal by air stripping process, a schematic setup of the experimental system was shown in Fig. 3.7. The alkaline solution is used to raise the pH above  $\text{pK}_a$  of ammonia. The experiment was set for investigating optimal conditions by dividing into 3 scenarios as shown in Fig.3.8. First, the effect of solution pH on ammonia stripping was investigated. The initial  $\text{NH}_4^+$  concentration was prepared at 6.8 mg N/L. The experiment was conducted by varying pH from 10 to 14 by using pH controller and air flow rate of 30 L/min. Second, the effect of air flow rate on ammonia stripping performance was investigated. The initial  $\text{NH}_4^+$  concentration was prepared at 6.8 mg N/L. The experiment was conducted by varying air flow rate from 10 to 50 L/min and maintained at the optimum pH obtained from the previous experiment. Third, the effect of initial concentration was investigated. Initial  $\text{NH}_4^+$  concentration was prepared at 6.8 to 23.5 mg N/L. The experiment was conducted by using air flow rate obtained from the second scenario and the pH from the first scenario.

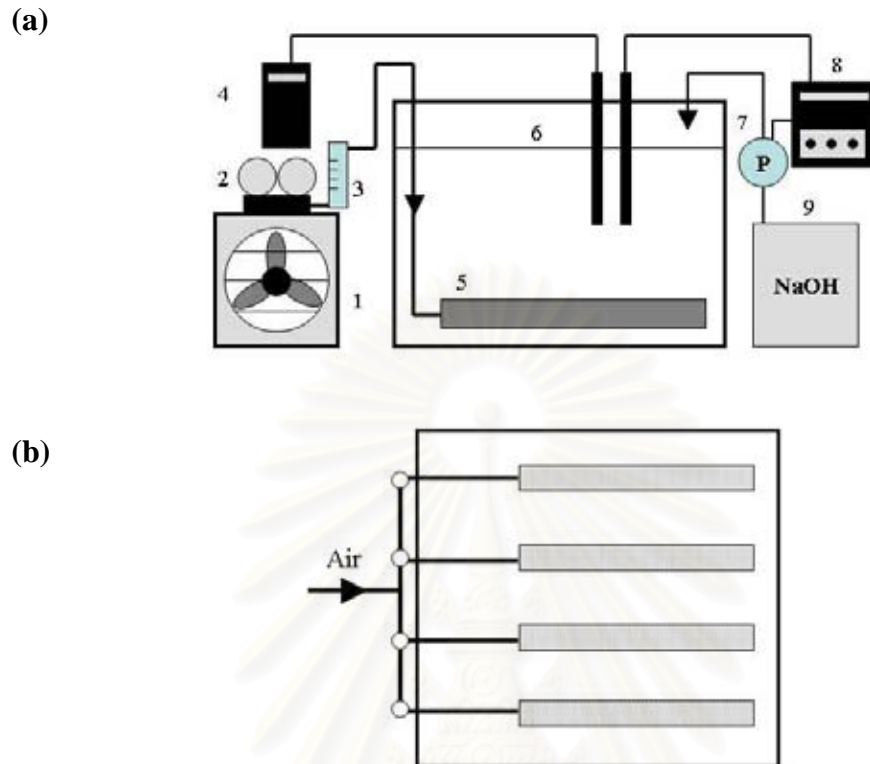


**Fig. 3.7 Configuration of reactor for the ammonia stripping process (a) side view and (b) top view. (1: air pump; 2: Pressure gauge; 3: Flow meter; 4: DO meter; 5: cylindrical diffuser; 6: reactor; 7: pump; 8: pH controller; 9: solution container).**

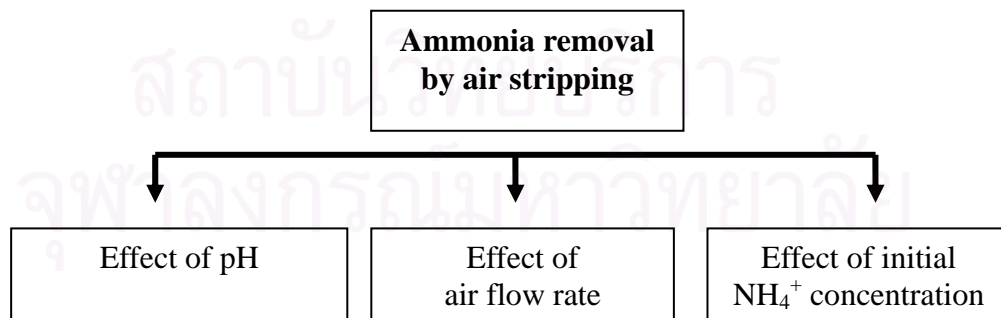


**Fig. 3.8 Schematic diagram for ammonia removal by air stripping.**

## 2. Continuous process

2.1 Nitrate removal by  $\text{Fe}^0/\text{CO}_2$  process.

2.2 Iron precipitation by fluidized bed process

2.3 Ammonia removal by air stripping process

To be able to continuously reduce nitrate by using  $\text{Fe}^0/\text{CO}_2$  process, a schematic setup of the experimental system was developed as shown in Fig. 3.9.

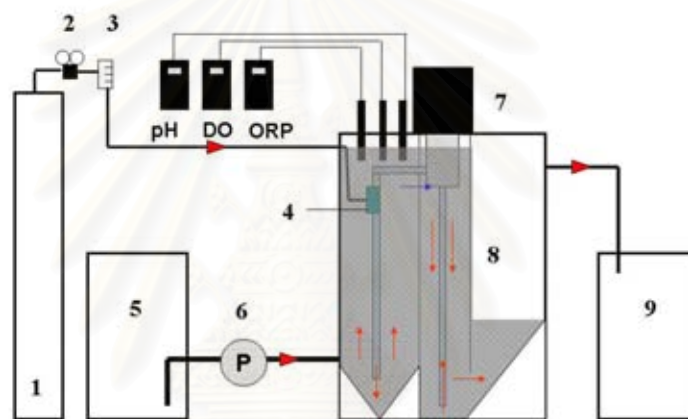


**Fig. 3.9 Configuration of reactor for the  $\text{Fe}^0/\text{CO}_2$  system in continuous process. (1:  $\text{CO}_2$  cylinder; 2: Pressure gauge; 3: Flow meter; 4: Air/liquid valve; 5: Storage tank; 6: pump; 7: Recirculated water pump; 8: Reactor; 9: Effluent tank).**

The reactor volume was 12 L. The bottom slope of the first compartment was 75 degree in cone shape to avoid dead-zone settling of  $\text{Fe}^0$ . With such design, the discharge of recirculated flow at the cone-shape bottom can cause complete mixing of  $\text{Fe}^0$  powder and  $\text{CO}_2$  bubbles. The discharge moved upward and passed over a weir into the second compartment. The second compartment is divided into recirculated and settling zones. The  $\text{Fe}^0$  powder from the first compartment is sucked into a perpendicular tube by the recirculated pump and discharged back to the first compartment. This settling zone separates upward supernatant from the  $\text{Fe}^0$  powder, which is recycled back to the reaction system through a cone-shape bottom design. The nitrate solution feeding was introduced into the system by using a peristaltic

pump. The recirculated flow of 90 L/min was used to provide a complete mixing of reaction solution. The CO<sub>2</sub> gas was introduced into the first compartment through the venturi tube valve with gas pressure controlled at 3 atm. As the reaction of all the experiments was carried on, water samples were taken from the reactor at different time intervals for subsequent analyses of water quality parameters. In this study, the experiment was divided to 2 phases as shown in Fig. 3.10.

The first phase of this experimental part was conducted for investigating the optimal condition. First, the effect of CO<sub>2</sub> inflow rate on nitrate solution was investigated. The initial NO<sub>3</sub><sup>-</sup> concentration was 100 mg/L (23.4 mg N/L). The experiment was conducted by using various CO<sub>2</sub> bubbling rates, 100 - 800 mL/min, while maintaining a constant Fe<sup>0</sup> dosage at 40 g. The feeding rate of NO<sub>3</sub><sup>-</sup> solution was 50 mL/min. Second, the experiment was set to optimize the Fe<sup>0</sup> dosage for treating nitrate concentrations. The experiment was conducted by using various Fe<sup>0</sup> dosages of 40 - 80 g, with the optimum CO<sub>2</sub> inflow rate obtained from the previous part. The feeding rate of NO<sub>3</sub><sup>-</sup> solution was 50 mL/min. Third, The initial NO<sub>3</sub><sup>-</sup> concentration was 23.4 mg N/L. The experiment was conducted by using the optimum Fe<sup>0</sup> dosage as well as bubbling CO<sub>2</sub> at an inflow rate of 200 mL/min. The feeding rate of NO<sub>3</sub><sup>-</sup> solution was varied from 50 to 200 mL/min. Last, the effect of initial NO<sub>3</sub><sup>-</sup> concentration was investigated. The initial NO<sub>3</sub><sup>-</sup> concentration varied from 30 to 200 mg/L (6.8 to 45.16 mg N/L). The experiment was conducted by using the optimum conditions from previous tests.

The second phase of experiment was conducted to gain understanding of process operation from which continuous process of nitrate reduction by Fe<sup>0</sup>/CO<sub>2</sub> process can be maintained properly. The operating mode was divided into 2 steps. Step 1: the initial Fe<sup>0</sup> was tested until its exhaustion without any supplement of Fe<sup>0</sup>. Step 2: the supplement of Fe<sup>0</sup> was introduced in the system at suitable time interval. The conditions of the experiments were based on optimal conditions obtained from previous scenario.

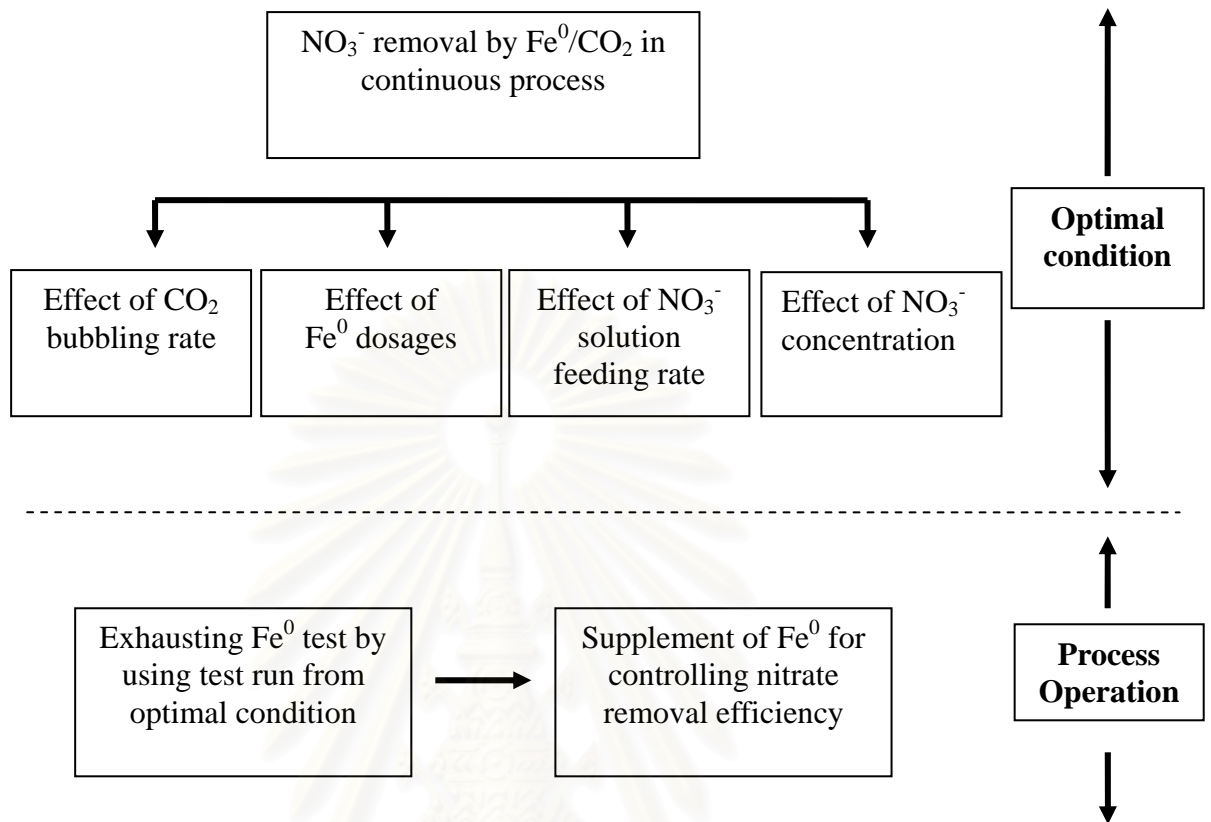


**Fig. 3.10 Schematic diagram for nitrate reduction by  $\text{Fe}^0/\text{CO}_2$  in continuous process.**

To study the iron precipitation using fluidized bed process, a schematic setup of the experimental system was shown in Fig. 3.11. The dimension of reactor system was 15 cm x 15 cm x 180 cm (H). The reactor volume was 40.5 L. The recirculated pump was used for creating fluidized bed expansion. The air bubbles were created through venturi valve to create a large amount of bubbles.

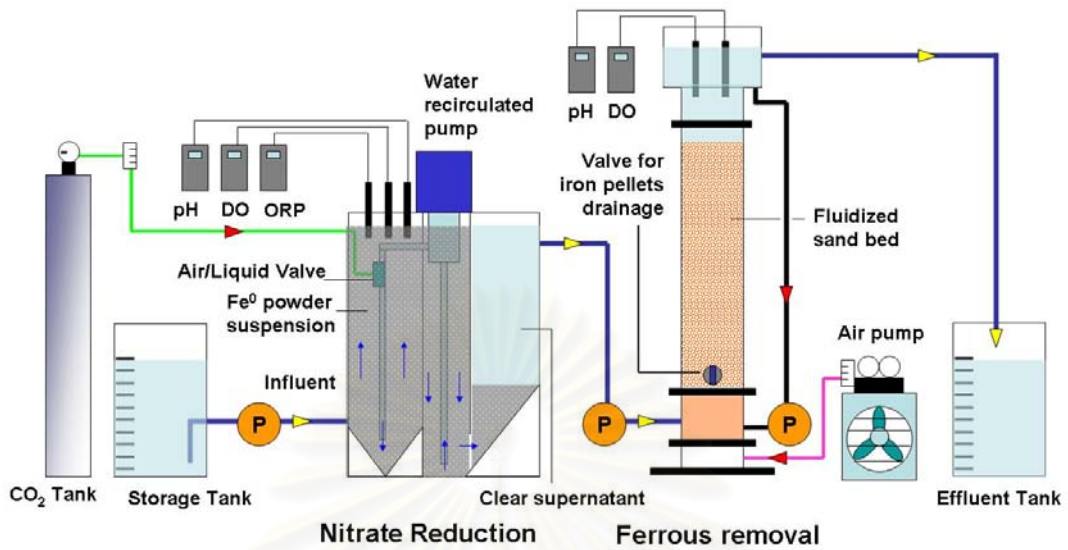


**Fig. 3.11 Configuration of reactor for the iron precipitation by fluidized bed system in continuous process.**

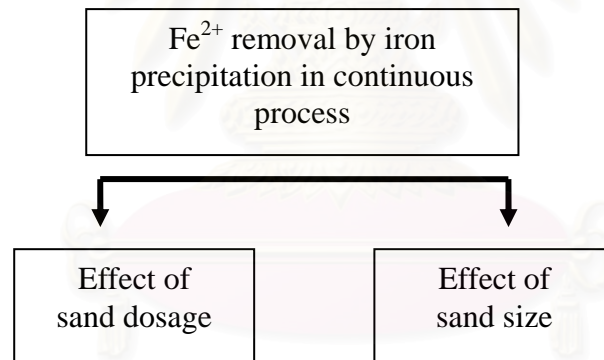


**Fig. 3.12 Schematic diagram for ferrous removal by iron precipitation in continuous process.**

The air flow rate was set at 5 L/min to completely convert ferrous to ferric ion. The feeding solution rate was 50 mL/min. Commercial sand was selected for this experiment. In this study, the preliminary experiment was divided into 2 conditions as shown in Fig. 3.12. First, the effect of sand dosage on iron removal by fluidized bed was investigated. The initial Fe<sup>2+</sup> concentration was prepared from 2g Fe<sup>0</sup>/L dosages. The experiment was conducted by varying sand dosage (0.42-0.59 mm in diameter) from 10 to 20 kg.

**Table 3.2 Classification of sand size from commercial sand.**

<b>Sand size (mm)</b>	<b>Percent (%)</b>
<0.297	0.6
0.297-0.42	2.6
0.42-0.59	25.4
0.59-0.84	66.6
>0.84	4.8
<b>Total</b>	<b>100</b>

Second, the commercial sand without classification was tested for comparison with the category falling within the range of 0.42-0.59 mm diameter, in terms of ferrous removal efficiency. The size distribution of sand size from commercial sand was shown in Table 3.2.

According to continuous process of ammonia removal by air stripping process, a schematic setup of the experimental system was shown in Fig. 3.13. The dimension of rectangular reactor was 20.5 cm (W) x 22 cm (L) x 23 cm (H). The height of water level was 8.5 cm. The headspace inside in the reactor chamber was designed for ventilation of  $\text{NH}_3$  gas in the reactor. The cascade ammonia strippers and recarbonation were installed at 6 different trays from top to the bottom. the top five were for ammonia stripping and the bottom one was for recarbonation. The reactor volume for each tray was 3.8 L; therefore, total reactor volume was 22.8 L. The pH controller was used for adjusting pH at 12 by using alkaline solution of 6 N NaOH. The controlled valve was used for supplying NaOH solution in each of ammonia stripping trays. The air bubbles were created through diffuser made of ceramic material. The  $\text{CO}_2$  was selected for controlling the pH to comply with the effluent standard of 5.5 to 9. The  $\text{NH}_4^+$  prepared from  $\text{NH}_4\text{Cl}$  feeding rate was 50 mL/min. In this study, the preliminary experiment was shown in Fig. 3.14. The effect of air flow rate on ammonia stripping was investigated. Depending on desired conditions, the air inflow rate was controlled through a gas flow meter.

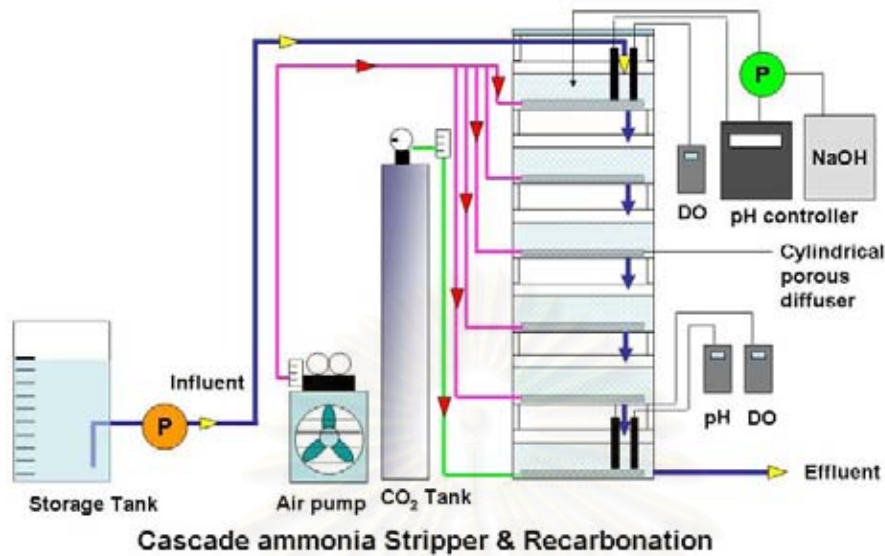


**Fig. 3.13 Configuration of reactor for the ammonia stripping system in continuous process.**

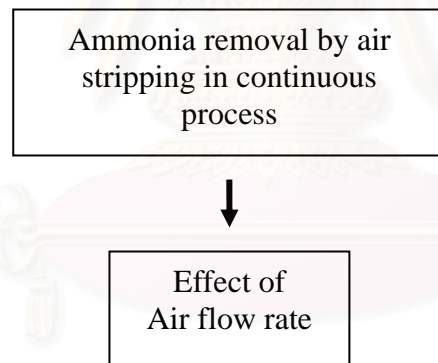


**Fig. 3.14 Schematic diagram for ammonia removal by air stripping in continuous process.**

### 3.2.2 Field test

After the preliminary test of each continuous process, the integrated system for aqueous nitrate removal using  $\text{Fe}^0/\text{CO}_2$  reduction, iron precipitation, and ammonia stripping was performed. A schematic setup of the experimental system was shown in Fig. 3.15. This field test was set up at Chia Nan University of Pharmacy and Science, Tainan, Taiwan by using groundwater pumped from the nearby monitoring well. The



hydrochemistry of the groundwater was shown in Table 3.3. This experiment was set to compare the process efficiency between nitrate spiked groundwater and RO water, as shown in Fig. 3.16.

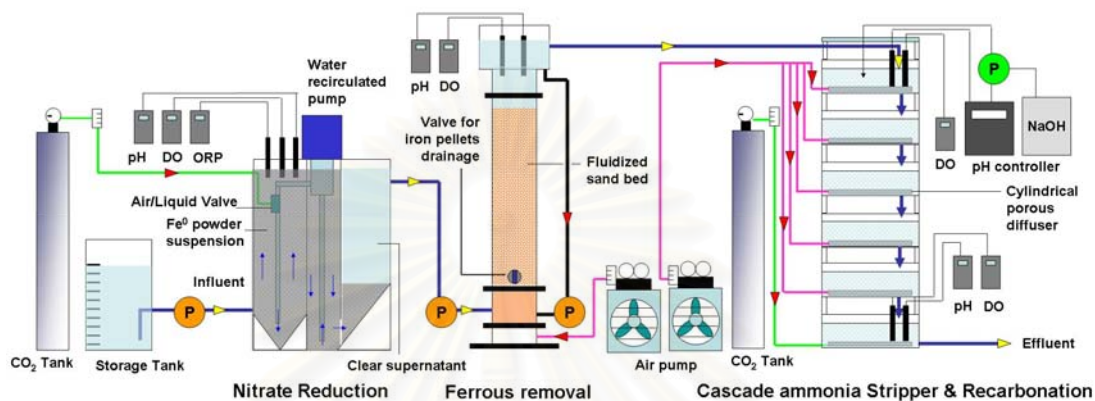


**Fig. 3.15 Configuration of reactor for integrated system for aqueous nitrate removal using  $\text{Fe}^0/\text{CO}_2$  reduction, iron precipitation, and ammonia stripping.**

**Table 3.3 Hydrochemistry of groundwater at Chia Nan University of pharmacy and science, Tainan, Taiwan (5-12-2005).**

Parameter	Parameter value
pH	6.86
Conductivity ( $\mu\text{S}/\text{cm}$ )	2700 (groundwater) 47 (RO)
Eh (mV)	235
Dissolved oxygen (mg/L)	1.63
Dissolved organic carbon (mg/L)	2.09
TS (ppm) = TDS (ppm) + SS (ppm)	660 = 294 + 366
Major anions	
Chloride (ppm)	513
Sulfate (ppm)	51.36
Nitrate (ppm)	0.95
Nitrite (ppm)	0
Fluoride (ppm)	0
Phosphate (ppm)	0
Major cations	
Sodium (ppm)	539.5
Potassium (ppm)	15.8
Calcium (ppm)	42.8
Magnesium (ppm)	26.7
Total iron (ppm)	0.24
Alkalinity (ppm as $\text{CaCO}_3$ )	300
Hardness (ppm as $\text{CaCO}_3$ )	331.96

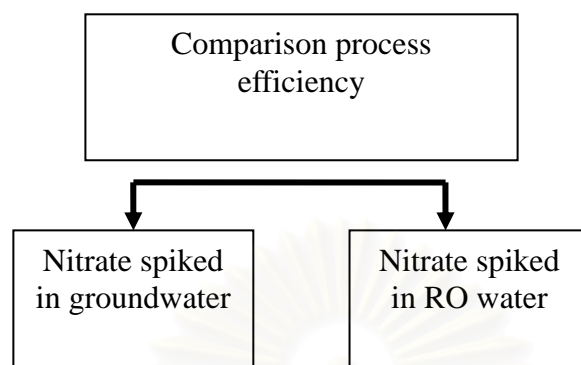


**Fig. 3.16 Schematic diagram for integrated system for aqueous nitrate removal using  $\text{Fe}^0/\text{CO}_2$  reduction, iron precipitation, and ammonia stripping.**

### 3.3 Analytical methods

In the  $\text{Fe}^0/\text{CO}_2$  system, the residual nitrate, nitrite, and end product ammonium were analyzed by using ion chromatography (IC) (DIONEX-120, USA). The triplicate analysis was done for precision of the instrument for standardized sample before sample test was analyzed. In IC analyses, 4 drops of 15,000 mg/L  $\text{H}_2\text{O}_2$  were spiked into the above filtrate to convert  $\text{Fe}^{2+}$  into ferric precipitate (Fenton's reaction product), and then the water sample was furthered filtered using a 0.45  $\mu\text{m}$  membrane filter to remove the iron precipitate from solution. The stock  $\text{H}_2\text{O}_2$  solution was quantified by using a potassium permanganate titration method (Vogel, 1978). The residual  $\text{H}_2\text{O}_2$  concentration in the reaction solution was determined by using the potassium titanium (IV) oxalate method (Sellers, 1980). Under an acidic condition, the  $\text{H}_2\text{O}_2$  reacts with  $\text{Ti}^{4+}$  to form a yellowish complex. Through the measurement of light absorption at 400 nm (SHIMADZU, UV-1201, Japan), the absorbance can be converted into equivalent  $\text{H}_2\text{O}_2$  by reading the  $\text{H}_2\text{O}_2$  value from a pre-determined linear calibration curve. Similarly, the ferrous ion ( $\text{Fe}^{2+}$ ) is able to form a colored complex with 1,10-phenanthroline (Standard Methods, 1995), and its concentration can be determined through the measurement of light absorption at 510 nm (SHIMADZU, UV-1201, Japan), which is equivalent to a certain ferrous quantity. Humic acid was analyzed by TOC analyzer (Elementar-liqui TOC, Germany). In

addition, the pH was monitored continuously by using a pH meter (Suntex, TS-1, Taiwan).

Regarding iron precipitation process, Ferrous ion ( $\text{Fe}^{2+}$ ) was analyzed by standard method as mentioned in  $\text{Fe}^0/\text{CO}_2$  process. Total iron was analyzed by ICP-AES (JY2300, MLS-1200, Milestone, Italy). Micro-morphology and the surface composition of the iron coated sand (ICS) were measured by a scanning electron microscopy coupled with energy-dispersive spectrometry (SEM-EDS, Hitachi S-3000N, Japan, EDS detector: HORIBA MOBEL 7021-H). In addition, the solution pH was monitored continuously by using a pH meter (Suntex, TS-1, Taiwan).

In ammonia stripping process, the phenate method was selected for the measurement of residual ammonium ion ( $\text{NH}_4^+$ ). An intensely blue compound, indophenol, is formed through the reaction among ammonia, hypochlorite, and phenol using sodium nitroprusside as catalyst (Standard methods, 1995).



สถาบันวิทยบริการ  
จุฬาลงกรณ์มหาวิทยาลัย

## CHAPTER IV

### RESULTS AND DISCUSSION

#### 4.1 Batch operation

##### 4.1.1 CO<sub>2</sub>/H<sub>2</sub>O system

To understand different characteristic aspects of carbonated water system (CO<sub>2</sub>/H<sub>2</sub>O), deionized water without any other background species was used to fulfill this purpose. Different profiles of pH, DO, ORP are presented in Fig. 4.1. The bubbling time period was controlled within 40 min, and the CO<sub>2</sub> bubbling rate varied from 100 to 400 mL/min. In Fig. 4.1 (a), it can be seen that all solution pH drop rapidly from the neutral to acidic range and remain unchanged after 10 min. The pH profile indicates that the pH decreases with increasing CO<sub>2</sub> bubbling rate. According to Reactions (2.13)-(2.17), the source of hydrogen ion in the reaction system was the dissociation of H<sub>2</sub>CO<sub>3</sub>, and the ultimate equilibrium pH depends on the absorption rate of CO<sub>2</sub> in water. Fig. 4.1 (a) shows that continuous CO<sub>2</sub> bubbling is efficient for providing hydrogen ion to create acidic conditions in the pH range of 3-4. In summary, the bubbling of CO<sub>2</sub> was an effective alternative to create a desired acidic environment for nitrate reduction by Fe<sup>0</sup>. For example, Whitman et al. (1924) observed that the iron corrosion rate at room temperature was greatly enhanced by lowering the pH down to less than 4.

As illustrated in Fig. 4.1 (b), the solution DO decreased rapidly to nearly zero in all cases, though, it took longer time for lower bubbling rate of CO<sub>2</sub>. The dissolved oxygen was stripped out of the aqueous system by the CO<sub>2</sub> gas. As a result, the solution became anaerobic which was favorable for the corrosion of zero-valent iron according to Bigg and Judd (2000). As shown in Fig. 4.1 (c), the ORP value in solution increased slightly when the CO<sub>2</sub> gas was bubbled into solution continuously. In general, the higher the CO<sub>2</sub> bubbling rate, the lower the ORP profile. Additionally,

the ORP's under different CO<sub>2</sub> bubbling rates were all positive values, indicating that the solution conditions were an oxidizing environment.

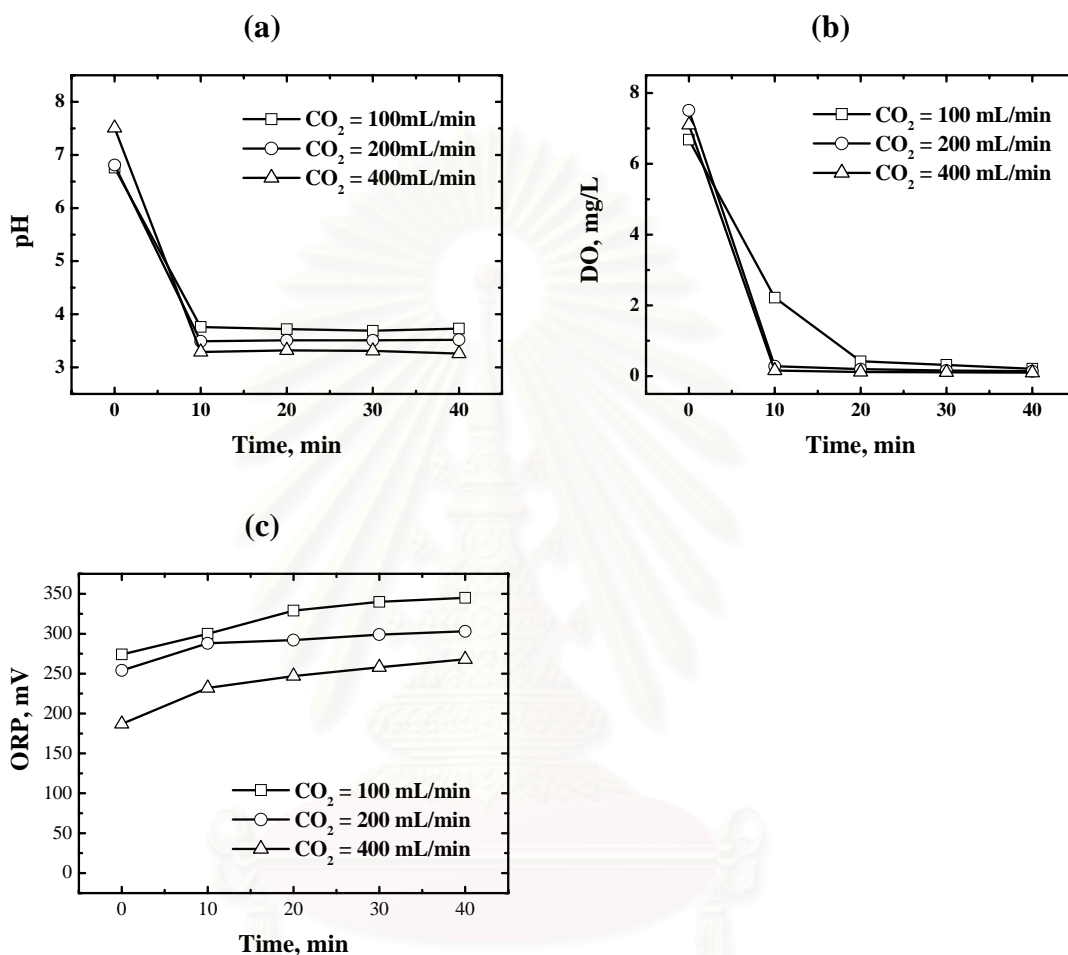


**Fig. 4.1 Effect of CO<sub>2</sub> bubbling rate on aqueous solution (a) pH, (b) DO and (c) ORP.**

#### 4.1.2. Fe<sup>0</sup>/CO<sub>2</sub> system

In the presence of Fe<sup>0</sup> (1-4 g/L), Fig. 4.2 shows the resulted profiles of pH, DO, and ORP in the CO<sub>2</sub>-bubbled solution. The CO<sub>2</sub> bubbling was controlled at a constant flow rate of 200 mL/min. In comparison, Fig. 4.2(a) shows a rapid drop of pH from the neutral value to around 4.5 at the time of 10 min in the presence of Fe<sup>0</sup>, and to around 3.5 in the absence of Fe<sup>0</sup>.

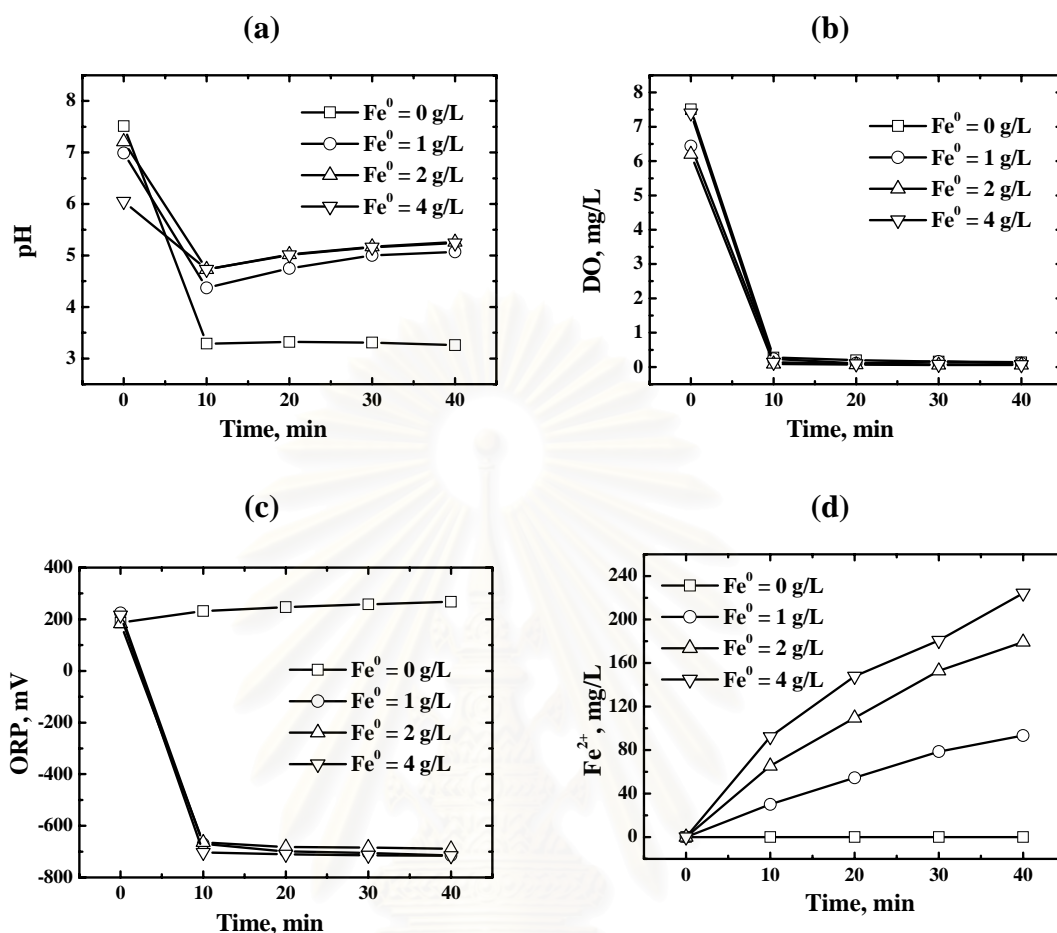
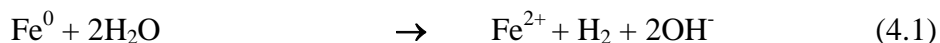


**Fig. 4.2** Effect of  $\text{Fe}^0$  dosage on aqueous solution (a) pH, (b) DO, (c) ORP, and (d)  $\text{Fe}^{2+}$  accumulation. (The  $\text{CO}_2$  bubbling rate = 200 mL/min; internal water recirculated flow = 1000 mL/min).

After 10 min, the pH rebounds in the presence of  $\text{Fe}^0$ , whereas remained unchanged in the absence of  $\text{Fe}^0$ . The reason that the final pH with  $\text{Fe}^0$  was higher than that without  $\text{Fe}^0$  can be explained through Reactions (4.1) and (4.2), where the hydroxide ions are generated when  $\text{Fe}^0$  becomes corroded. Thus, it is implied that, if the  $\text{Fe}^0$  dosage increased, the solution pH should increased correspondingly, as evidenced in Fig. 4.2(a). However, the solution pH with dosage of 2 g  $\text{Fe}^0$ /L was nearly the same as that with 4 g  $\text{Fe}^0$ /L, indicating that the  $\text{Fe}^0$  in excess has been applied.



Furthermore, Fig. 4.2 (b) shows that the DO value in solution decreased to nearly zero in all cases. As mentioned earlier, the DO was stripped out of the aqueous system as CO<sub>2</sub> gas was bubbled into the reactor continuously. In addition to this, the dissolved oxygen can be also reduced directly by Fe<sup>0</sup> at the initial reaction stage as depicted in Reaction (4.2). Fig. 4.2(c) shows that the ORP value swiftly decreased from positive values to negative ones and remained unchanged at around -650 mV in the presence of 1-4 g Fe<sup>0</sup>/L. This indicates that the reducing environment has occurred in the Fe<sup>0</sup>/CO<sub>2</sub> system. In contrast, without Fe<sup>0</sup>, the ORP hangs up in the region of positive values. In Fig. 4.2(d), it was observed that ferrous ion accumulation increased with increasing Fe<sup>0</sup> dosages, the highest one of which can reach up to around 235 mg/L. It is obvious that the appearance of Fe<sup>2+</sup> brings the ORP from a positive value down to a negative one, the latter of which is favorable to trigger the occurrence of nitrate reduction reaction.

### 4.1.3 Fe<sup>0</sup>/CO<sub>2</sub>/NO<sub>3</sub><sup>-</sup> system

#### 4.1.3.1 Effect of CO<sub>2</sub> bubbling rate

In the Fe<sup>0</sup>/CO<sub>2</sub>/NO<sub>3</sub><sup>-</sup> system, the experiments were carried out with various CO<sub>2</sub> bubbling rates of 0-400 mL/min as well as Fe<sup>0</sup> dosages of 0-4 g/L, whereas the initial nitrate concentration was kept at a constant value of 6.8 mg N/L. As can be seen in Fig. 4.3(a), the pH in all CO<sub>2</sub> bubbling rates fell rapidly from the neutral pH to around 3.5 in less than 5 min. Then, the pH gradually rebounded in all cases except the one without CO<sub>2</sub> bubbling. As depicted in Reactions (4.3)-(4.5), the reason of pH rebounding after their initial drop is due to the reduction of nitrate by Fe<sup>0</sup>, in addition to water and oxygen-induced corrosion of Fe<sup>0</sup> (Reactions (4.1) and (4.2)). Fig. 4.3 (b) shows that the DO value in solution decreased to nearly zero within 10 min under different CO<sub>2</sub> bubbling rates. As understood, the DO disappeared because of CO<sub>2</sub> stripping and its reaction with Fe<sup>0</sup> (Reaction (4.2)).

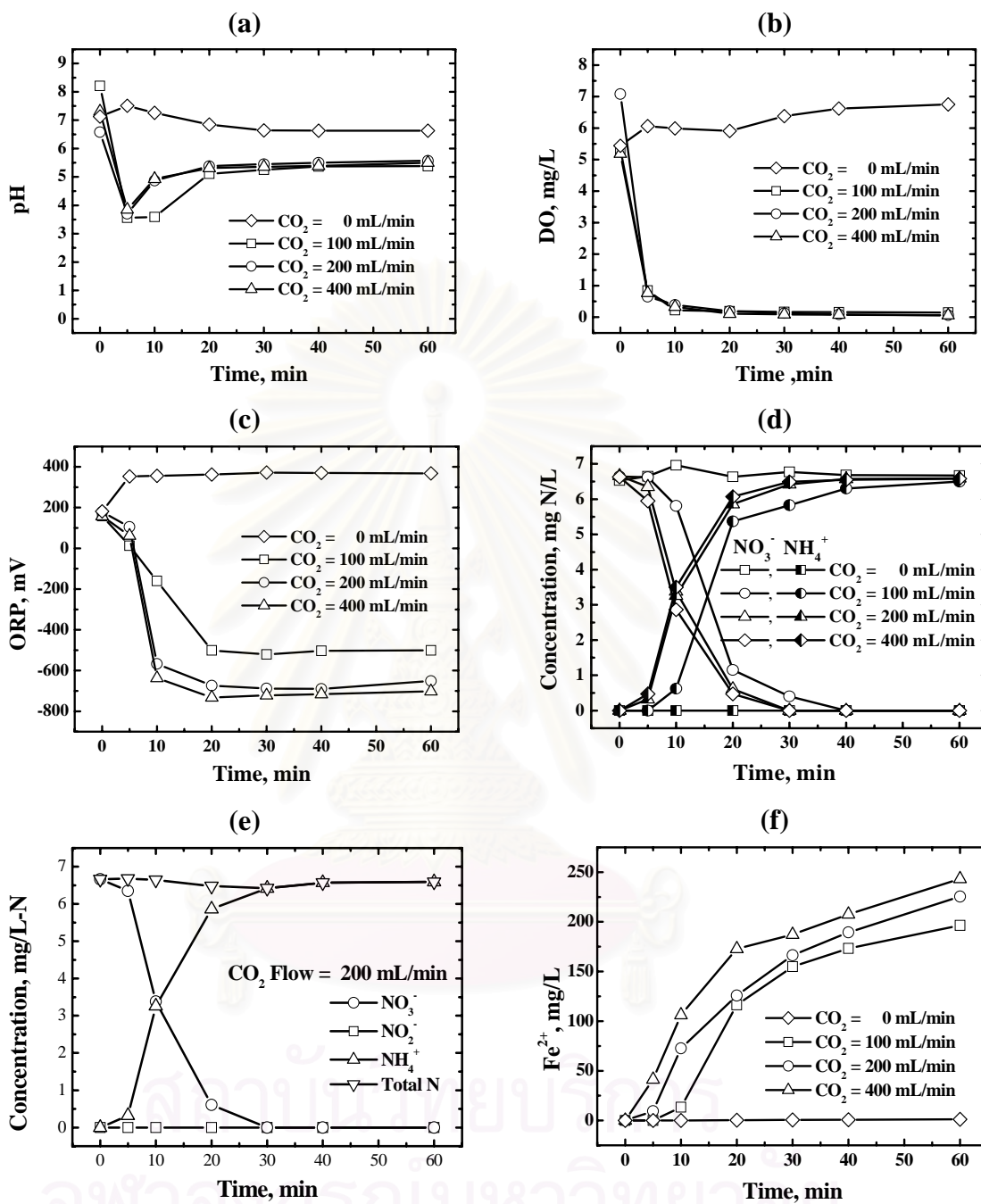
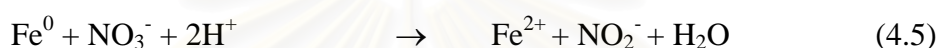


**Fig. 4.3** Effect of CO<sub>2</sub> bubbling rate in the Fe<sup>0</sup>/CO<sub>2</sub>/NO<sub>3</sub><sup>-</sup> system (a) pH, (b) DO, (c) ORP, (d) nitrate residue and ammonium concentration, (e) nitrogen balance and (f) ferrous (Fe<sup>2+</sup>) accumulation. ( $[\text{NO}_3^-]_{\text{initial}} = 6.8 \text{ mg N/L}$ ;  $[\text{Fe}^0]_{\text{initial}} = 2 \text{ g/L}$ ; internal water recirculated flow = 1000 mL/min).



Similar to  $\text{NO}_3^-$ , the dissolved oxygen can act an electron acceptor; hence competing with nitrate for electrons. In regard to the ORP, Fig. 4.3(c) shows that the initial positive ORP values for  $\text{CO}_2$  at 100, 200 and 400 mL/min were 158, 179 and 158 mV, respectively. After 20 min, the ORP values dropped down to the negative ones of -501, -651, and -702 mV, respectively. Furthermore, the final ORP values were lower as the bubbling rate increased.



As shown in Fig. 4.3(d), nitrate decreased slightly during the initial time period and dropped down swiftly after 5 min for all different  $\text{CO}_2$  bubbling rates. Slow nitrate removal in the initial phase may be due to impurities and iron surface activation as will be illustrated later in the iron reutilization experiments. With  $\text{CO}_2$  inflow at 100 mL/min, the nitrate was removed by 94% at 30 min, and complete nitrate removal occurred at 60 min. In contrast, as the  $\text{CO}_2$  bubbling rates of 200 and 400 mL/min were used, the nitrate was completely removed at only 30 min in both cases. In addition, the residual profiles of nitrate show no difference for these two  $\text{CO}_2$  bubbling rates. Therefore, it can be implied that the  $\text{CO}_2$  bubbling rate at 200 mL/min was the optimum condition in this reaction system. According to Fig. 4.3(e), the results show that nitrite ( $\text{NO}_2^-$ ) was not detected in the treated solution throughout the whole reaction period, whereas ammonium was the predominant products. The ammonium occurred rapidly when the nitrate reduction began, and its formation rate was reduced as the nitrate reduction rate became slowing down. The ammonia yield at the end of reaction was 95-105% of initial supplied nitrate. This can be implied that rate of adsorption and redox between  $\text{Fe}^0$  and nitrate was very fast. Therefore, the ammonium was detected immediately. Cheng et al. (1997) and Huang et al. (1998) reported that ammonium dominates the reaction products in the  $\text{Fe}^0$  process under their conditions. Under such a setting, a post treatment of separating ammonium from treated water is needed if the reduction process of  $\text{Fe}^0$  is employed for the treatment of nitrate-contaminated waters. As shown in Fig. 4.3 (f), ferrous accumulation increased

with increasing CO<sub>2</sub> bubbling rate. It is interesting to point out that the initial lag phase for ferrous accumulation was observed for each CO<sub>2</sub> bubbling rate. In addition, the accumulation rate of ferrous (Fig. 4.3 (f)) appears to be in consistence with the rate of nitrate removal (Fig. 4.3(d)). It can be said that nitrate removal is highly correlated with the ferrous accumulation in the bulk solution. Thus, monitoring of ferrous ion can provide a reasonable prediction of the degree of nitrate being removed in the reaction system.

#### 4.1.3.2 Effect of Fe<sup>0</sup> dosage

To optimize the Fe<sup>0</sup> dosages for treating different initial nitrate concentrations, several experiments were conducted to fulfill this purpose and the results were shown in Fig. 4.4(a)-(c). In Fig. 4.4(a), the average initial nitrate concentration was 6.95 mg N/L. The nitrate removal with dosage of 1 g Fe<sup>0</sup>/L was 91% at 30 min, and 96% at 60 min. On the other hand, as the dosages increased to 2 and 4 g/L, the nitrate was completely removed within 30 min in both cases. In addition, the residual profiles of NO<sub>3</sub><sup>-</sup> show no difference for the two dosages of 2 and 4 g/L, but the difference becomes quite significant as the iron dosage was reduced from 2 to 1 g/L. Hence, the optimum Fe<sup>0</sup> dosage of 2 g/L is recommended for the case of initial nitrate of 6.95 mg N/L. As presented in Fig. 4.4(b) and 4.4(c), with the average initial nitrate concentrations of 10.25 and 23.14 mg N/L, the profiles of nitrate were similar to that of the previous case. By using the Fe<sup>0</sup> dosage of 2 g/L, it appears that there's no way to achieve complete removal of nitrate at the end of 60 min for both initial nitrate concentrations. Complete removal can be achieved for both initial nitrate concentrations only when the Fe<sup>0</sup> dosages were increased up to 3 and 4 g/L, respectively. However, the marginal benefit in nitrate removal is limited as the Fe<sup>0</sup> dosage is applied in excess. Based on the above results, it is concluded here that the optimum Fe<sup>0</sup> dosages to remove nitrate with initial concentrations of 6.95, 10.24 and 23.14 mg N/L were 2, 3, and 4, respectively, given a CO<sub>2</sub> bubbling rate of 200 mL/min.

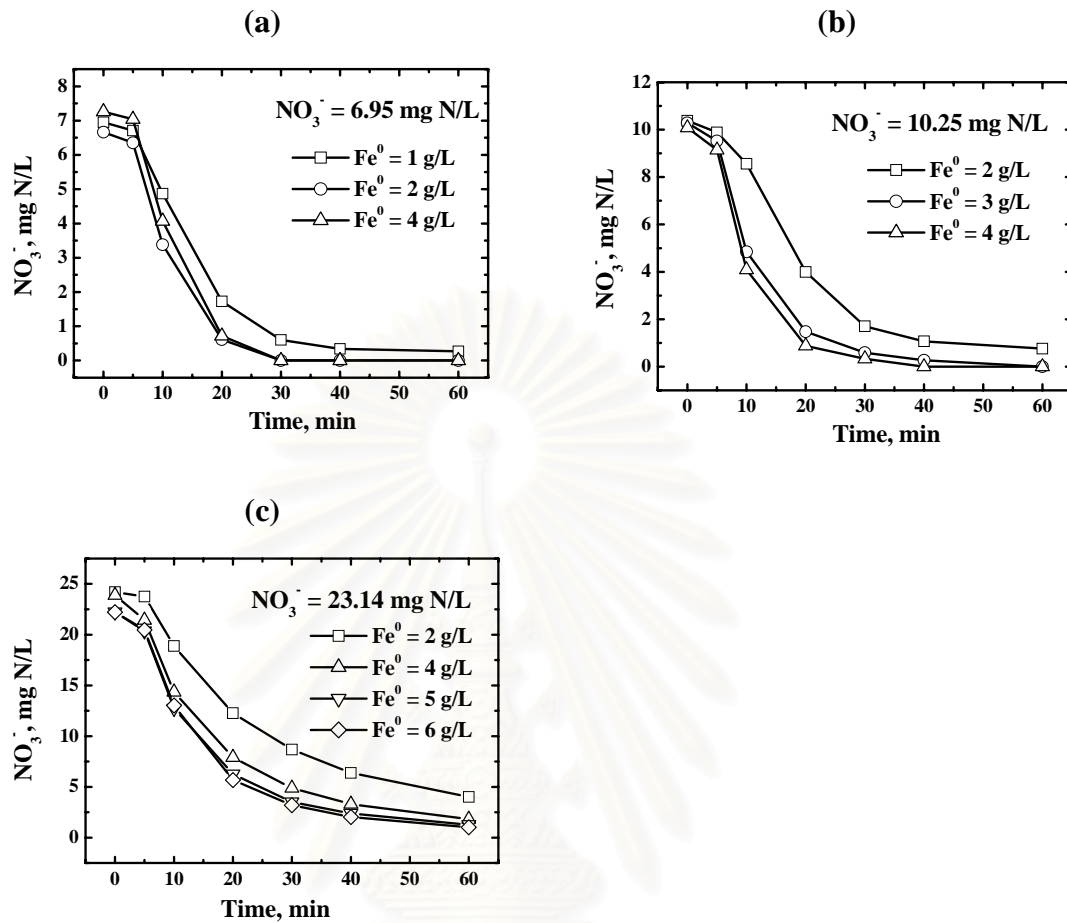


**Fig. 4.4** Effect of  $\text{Fe}^0$  dosage on nitrate reduction under initial nitrate concentration in the  $\text{Fe}^0/\text{CO}_2/\text{NO}_3^-$  system (a) 6.95 mg N/L; (b) 10.25 mg N/L; and (c) 23.14 mg N/L. (The  $\text{CO}_2$  bubbling rate = 200 mL/min; internal water recirculated flow = 1000 mL/min).

As observed from Fig. 4.4, all the nitrate profiles exhibit a 5-min period of lag phase. To understand the reaction behavior of nitrate reduction throughout the whole reaction period, a sigmoidal model equation describing an S curve is proposed as follows:

$$Y = A_1 - \frac{(A_1 - A_2)}{1 + \exp(-(t - t_{1/2})/W)} \quad (4.6)$$

where

$Y$  (mg-N/L) = concentration at time  $t$ ;

$A_1$  (mg-N/L) = the initial value;

$A_2$  (mg-N/L) = the final value;

$t_{1/2}$  (min) = time at which the Y value is average between the two limiting values  $A_1$  and  $A_2$

W (min) = time from lag phase to zero reaction rate phase.

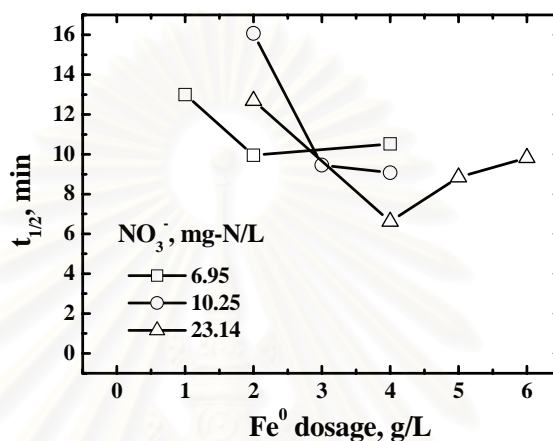


**Fig. 4.5 Effect of Fe<sup>0</sup> dosage on  $t_{1/2}$  under various initial nitrate concentrations**

Based on the data taken from Fig. 4.4, all the  $R^2$  values, the indicator of fitness of this equation, are larger than 0.99 under different Fe<sup>0</sup> dosages as well as different initial nitrate concentrations (Table 4.1). The high  $R^2$  value indicates that this S-curve equation can be used as a tool for nitrate residue prediction purposed in the studied system. In addition, the parameter  $t_{1/2}$  in Equation (4.6) can be used for the comparison of nitrate reduction rate; its calculated values were further plotted against Fe<sup>0</sup> dosages under different initial nitrate concentrations as shown in Fig. 4.5. It is clear to see that the least times of  $t_{1/2}$  occur when the Fe<sup>0</sup> dosages are optimized at 2, 3, and 4 g/L or equivalent to specific surface area of 2, 3, and 4 m<sup>2</sup>/L, respectively, for the average initial nitrate concentrations of 6.95, 10.24, and 23.14 mg N/L. In all optimum cases, it takes less than 10 min to remove nitrate by 50%. Similar to nitrate profile, an S-curve trend was also observed in ammonium formation and ferrous accumulation. Therefore, the same sigmoidal model equation was employed to simulate the reaction kinetics of these two species. By using the experimental data of ferrous and ammonium ions, Tables 4.2 and 4.3 present those constants described in Equation (4.6) under various Fe<sup>0</sup> dosages and various initial nitrate concentrations.

**Table 4.1 Values of constants in the proposed sigmoidal model equation for nitrate reduction (Y).**

Initial $\text{NO}_3^-$ (mg N/L)	$\text{Fe}^0$ (g/L)	$\text{Fe}^0$ ( $\text{m}^2/\text{L}$ )	$A_1$ (mg N/L)	$A_2$ (mg N/L)	$t_{1/2}$ (min)	W (min)	$R^2$
<b>6.95</b>	1	1	7.54	0.33	13.00	4.76	0.997
	2	2	6.77	0.13	9.95	2.01	0.995
	4	4	7.59	0.11	10.51	2.66	0.994
<b>10.25</b>	2	2	10.88	0.91	16.06	5.18	0.999
	3	3	10.55	0.55	9.46	2.24	0.990
	4	4	10.22	0.28	9.07	1.98	0.996
<b>23.14</b>	2	2	30.86	4.20	12.69	10.12	0.991
	4	4	34.73	2.30	6.61	8.68	0.991
	5	5	28.23	1.95	8.84	6.56	0.989
	6	6	26.69	1.76	9.82	5.82	0.991

**Table 4.2 Values of constants in the proposed sigmoidal model equation for ferrous accumulation (Y).**

Initial $\text{NO}_3^-$ (mg N/L)	$\text{Fe}^0$ (g/L)	$\text{Fe}^0$ ( $\text{m}^2/\text{L}$ )	$A_1$ (mg /L)	$A_2$ (mg /L)	$t_{1/2}$ (min)	W (min)	$R^2$
<b>6.95</b>	1	1	0	159.69	13.89	3.83	0.984
	2	2	0	211.39	18.17	7.32	0.965
	4	4	0	261.13	17.26	6.13	0.965
<b>10.25</b>	2	2	0	229.54	20.38	4.99	0.989
	3	3	0	271.36	13.69	5.32	0.960
	4	4	0	273.39	10.07	3.46	0.966
<b>23.14</b>	2	2	0	338.71	18.26	6.84	0.974
	4	4	0	405.01	14.80	5.78	0.975
	5	5	0	428.82	14.16	5.51	0.980
	6	6	0	438.79	12.95	5.19	0.978

**Table 4.3 Values of constants in the proposed sigmoidal model equation for ammonium formation (Y).**

Initial NO <sub>3</sub> <sup>-</sup> (mg N/L)	Fe <sup>0</sup> (g/L)	Fe <sup>0</sup> (m <sup>2</sup> /L)	A <sub>1</sub> (mg N/L)	A <sub>2</sub> (mg N/L)	t <sub>1/2</sub> (min)	W (min)	R <sup>2</sup>
<b>6.95</b>	1	1	0	6.44	15.07	4.09	0.992
	2	2	0	6.36	9.93	1.78	0.994
	4	4	0	6.85	10.56	2.08	0.993
<b>10.25</b>	2	2	0	9.29	17.12	4.64	0.998
	3	3	0	10.71	9.29	2.06	0.992
	4	4	0	11.35	8.46	2.07	0.998
<b>23.14</b>	2	2	0	18.02	15.25	5.54	0.973
	4	4	0	20.40	12.87	4.29	0.983
	5	5	0	20.40	9.81	2.75	0.983
	6	6	0	18.72	9.80	2.87	0.977

Again, all R<sup>2</sup> values (> 0.97) are significantly high; hence, it is concluded here that the profiles of ferrous accumulation and ammonium formation can be expressed satisfactorily by the proposed model equation.

#### 4.1.3.3 Correlation between nitrate reduction and ferrous ion accumulation

According to the results of this study, the residual nitrate profile is strongly correlated with ferrous ion accumulation. Hence, an effort was also made to figure out the relationship between nitrate removal and ferrous ion concentration by using all experimental data in Fig. 4.4. As illustrated in Fig. 4.6, strong linear relationship between nitrate removal and ferrous ion accumulation was obtained; the value of correlation coefficient “R<sup>2</sup>” is 0.947. The slope indicated in Fig. 4.6 represents that 0.0473 mg NO<sub>3</sub><sup>-</sup>-N was removed when 1 mg of ferrous ion was accumulated, the molar ratio of which is 1 to 5.42. Based on the result of this study, the ferrous ion that occurs in the system come mainly from the reduction of both nitrate (Reaction (4.3))

and water molecule (Reaction (4.1)). In other words, the presence of one mol of nitrate leads to the oxidation of 4 mol of  $\text{Fe}^0$  as well as the formation of 4 mol of ferrous ions, while 2 mol of water molecules result in 1 mol  $\text{Fe}^0$  oxidation and 1 mol ferrous ion formation. Hence, it is expected that 5 mol of ferrous ions will accumulate in the presence of one mol of aqueous nitrate. By comparing this ratio with 5.42, it is concluded that both Reactions (4.1) and (4.3) are responsible for 92% of overall ferrous ion accumulation in the studied system. In addition, based on such result, the nitrate removal can be predicted well by indirect measurement of ferrous ion accumulation in the  $\text{Fe}^0/\text{CO}_2$  process. According to treatment cost analysis, 1 g of  $\text{NO}_3^-$  have to use 4.8 g of  $\text{Fe}^0$  derived from the molar ratio of 5.42: 1 ( $\text{NO}_3^-$ :  $\text{Fe}^0$ ). A 500 g package of  $\text{Fe}^0$  in pure grade is 3700 baht. Therefore, the price of  $\text{Fe}^0$  from Merck KGaA, Darmstadt, Germany for removing 1 g of  $\text{NO}_3^-$  equals to 35.52 baht. Comparing with resin applied for ion exchange process, 1 L of resin for series of Dowex Marathon A, strongly basic anion exchange, Dow chemical company, USA, has an exchange capacity of 1.2 eq. with 250 baht. Hence, the cost of resin for removing 1 g (0.016 eq) of  $\text{NO}_3^-$  is 3.33 baht which is much cheaper than  $\text{Fe}^0$  scenario. However, the use of  $\text{Fe}^0$  is aimed for the reactive barrier wall application for in-situ treatment of nitrate which cannot be achieved by ion-exchange resin. In addition,  $\text{Fe}^0$  technology can remove targeting nitrate specifically whereas exchange resin is a non-specific treatment.

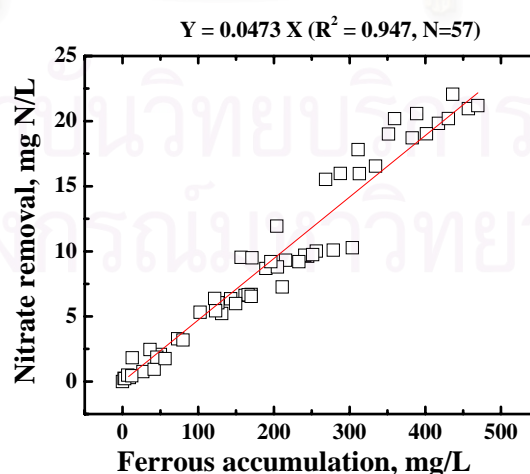


**Fig. 4.6 Correlation between nitrate removal and ferrous ion accumulation.**

#### 4.1.4 Effect of operating mode

In view of process operation, two operating modes were designed and tested. In Mode 1, treated solution was retained in the reactor and spiked with concentrated nitrate solution to raise nitrate concentration to a level close to the one in the previous batch; and in Mode 2: treated solution was emptied and refilled with freshly prepared solution for the next batch treatment which, containing the same level of nitrate as the previous batch.

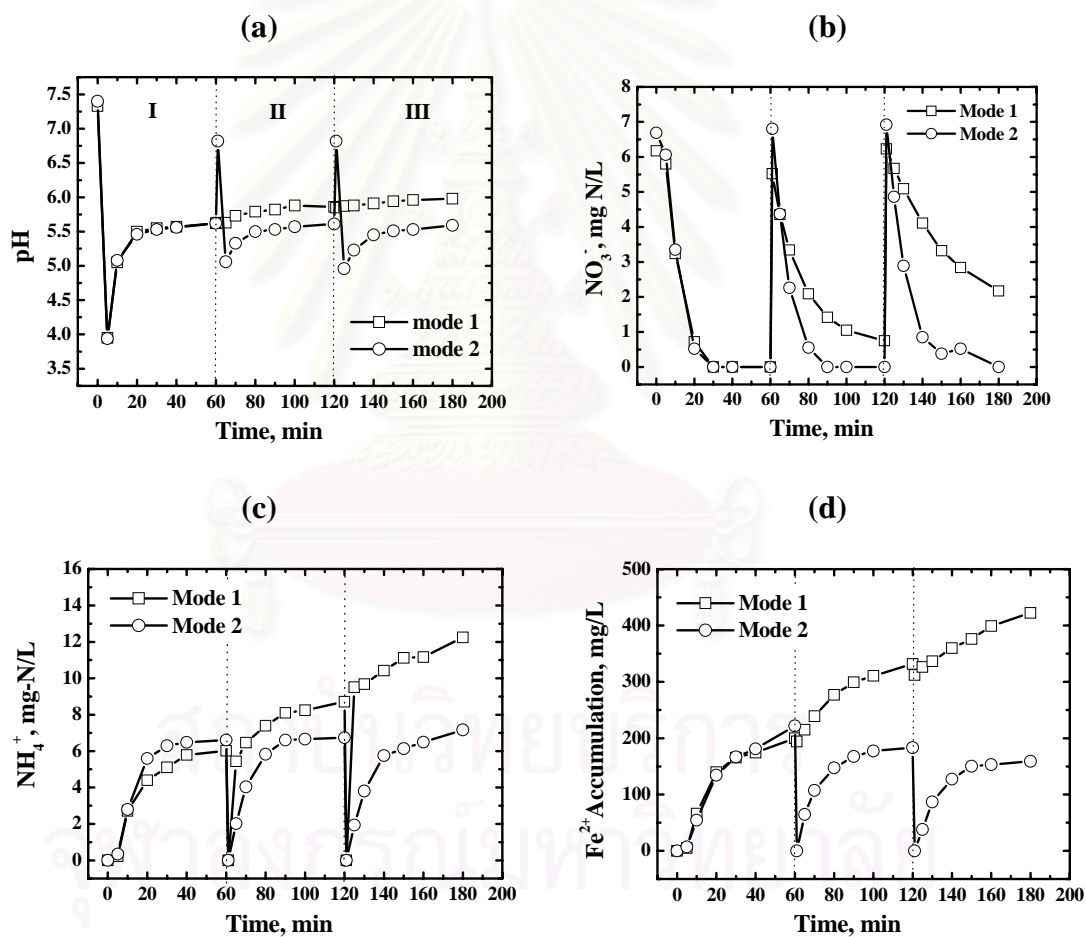


**Fig. 4.7 Profiles of different operating modes (a) pH, (b) nitrate residue, (c) ammonium formation, and (d) ferrous accumulation.** The experiment was conducted under the conditions of CO<sub>2</sub> bubbling rate of 200 mL/min and a recirculated flow of 1000 mL/min. The first phase (0-60 min) was conducted by using



2 g Fe<sup>0</sup>/L and initial NO<sub>3</sub><sup>-</sup> of 6.8 mg N/L. In the second (60- 120 min) and third phases (120-180 min), 3 mL of 10,000 mg/L nitrate solution was spiked into the reactor at 60 min and 120 min, respectively (operating mode 1). In Operating mode 2, the treated solutions from the first phase were emptied and filled in with fresh nitrate-contained solution at times of 60 and 120 min, respectively.

With Modes 1 and 2, Fig. 4.7 presents the comparison between the paired profiles of pH, nitrate, ammonium, and ferrous accumulation. All paired profiles were almost the same in the first batch treatment because the experiments were conducted under identical conditions. Nitrate in the first batch was removed completely from solution within 30 min, and the ammonium formation and ferrous accumulation at 60 min in both modes were around 6.8 mg N/L and 225 mg/L, respectively. However, in the 2<sup>nd</sup> and 3<sup>rd</sup> batches, significant difference between the two modes began to appear. With Mode 1, the efficiency of nitrate reduction decreased with increasing number of batch treatment. For example, the efficiency of nitrate reduction was 100, 86.4, and 65.2% for the 1<sup>st</sup>, 2<sup>nd</sup>, and 3<sup>rd</sup> batches, respectively. The decreasing of nitrate reduction efficiency might be due to the following three reasons. First, the deterioration of nitrate reduction is caused by pH in Mode 1 increasing from the lowest pH value at 5.62 (1<sup>st</sup> batch), to 5.86 (2<sup>nd</sup> batch) and to 5.98 (3<sup>rd</sup> batch), at which becomes unfavorable to trigger the nitrate reduction. As described earlier, the gradually increasing pH was due to reduction of nitrate and water by Fe<sup>0</sup>. Second, the continuous accumulation of NH<sub>4</sub><sup>+</sup> and Fe<sup>2+</sup> might be another reason that the nitrate reduction is deteriorating. For example, the ammonium concentrations were 6.0 mg N/L, 8.7 mg N/L and 12.3 mg N/L, respectively, at the end of 1<sup>st</sup>, 2<sup>nd</sup>, and 3<sup>rd</sup> batches, while the ferrous ions were 200, 332 and 422 mg/L, respectively. These cations tend to suppress Fe<sup>2+</sup> dissolution from Fe<sup>0</sup> surface, leading to lesser capacity of nitrate removal. Third, the available amount of reactive surface sites of Fe<sup>0</sup> for nitrate reduction. In fact, this third reason relates strongly with the pH variation as well. As the pH continues to increase, precipitation of iron corrosion product is accelerated and may coat and occupy on the reactive sites of Fe<sup>0</sup> available to nitrate reduction.

With Mode 2, the nitrate was completely removed from solution within 60 min in all three batches. However, the nitrate reduction performance decreased

slightly with increasing number of batch treatment. For example, nitrate was removed by 100% in 30 min in the first and second batch treatment, while the nitrate was removed by 100% in a longer reaction time of 60 min for the third batch. As mentioned above, the pH and cations accumulation imposing their inhibiting effect on nitrate removal in Mode 2 are not as strong as in Mode 1 because the treated solution was discharged and refilled with fresh nitrate solution for the next batch treatment. Yet, the activity of  $\text{Fe}^0$  was degrading as the number of batch treatment increased. For example, ferrous accumulations were 222, 183, and 159 mg/L in the chronological order of batch treatment; the difference of ferrous accumulation between the first and the third batches is quite significant. In addition, no lag phase was observed in the second and third batches because the  $\text{Fe}^0$  surface has been activated from the previous batch. Based on the above results, it is concluded that parameters such as the pH, background ferrous concentration, and the operating mode should be concerned, if this process is applied to the groundwater treatment.

#### 4.1.5 Supplement of fresh $\text{Fe}^0$

As understood from the above operating mode, the reduction efficiency of nitrate by zero-valent iron decreases with increasing number of batch treatment, and the process operation using Mode 2 outperformed Mode 1 on nitrate removal. With such understanding in mind, it appears that supplement of fresh zero-valent iron is required to maintain a satisfactory efficiency of nitrate reduction when the process is operated simultaneously. Hence, additional experiment with Mode 2 operation was further tested by stepwise supplement of fresh  $\text{Fe}^0$  during each batch operation. As shown in Fig. 4.8(a), nitrate can be removed by 100% in all cases. However, supplement of 1 g  $\text{Fe}^0$  imposed the most rapid removal of nitrate in the third batch. Without  $\text{Fe}^0$  supplement, the nitrate can be removed completely from solution in 60 min for the third batch, as compared to 30 and 20 min of with  $\text{Fe}^0$  supplements of 0.25 and 1.0 g, respectively. As mentioned earlier, Fig. 4.8(b) shows that, without  $\text{Fe}^0$  supplement, ferrous accumulations were 222, 183, and 159 mg/L, respectively, in the chronological order of batch treatment; the activity of  $\text{Fe}^0$  corrosion was decreasing with increasing number of batch treatment.

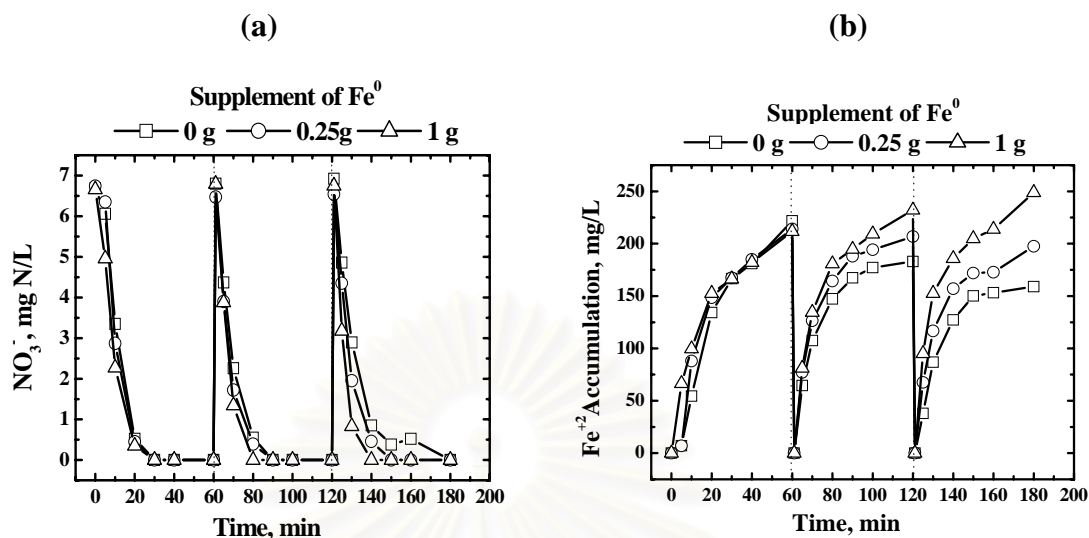


**Fig. 4.8 Effect of  $\text{Fe}^0$  supplement on (a) nitrate residue, and (b) ferrous accumulation.** Three batches were conducted under the conditions of  $\text{CO}_2$  bubbling rate of 200 mL/min and a recirculated flow of 1000 mL/min. The time for each batch was 60 min. The first batch was conducted by using 2 g  $\text{Fe}^0/\text{L}$  and 6.8 mg  $\text{NO}_3^-/\text{N/L}$ . In the second batch (60- 120 min) and third batch (120-180 min), the treated solution of previous batch was removed from reactor, the iron residue from previous batch was reclaimed and then  $\text{Fe}^0$  was supplemented at various dosages. In the meantime, fresh solution of 6.8 mg  $\text{NO}_3^-/\text{N/L}$  was filled into reactor for the next batch operation.

With  $\text{Fe}^0$  supplement of 0.25 g, ferrous accumulations were 213, 206, and 197 mg/L, respectively. As the  $\text{Fe}^0$  supplement was 1 g, ferrous accumulations were 211, 232 and 248 mg/L, respectively. Based on these ferrous accumulation data, it was demonstrated that appropriate amount of the  $\text{Fe}^0$  supplement applied can meet the requirement of nitrate removal efficiency in the studied batch operation. Knowing of the ferrous accumulation, post treatment of ferrous is also required to ensure safe drinking water quality.

#### 4.1.6 Effect of water quality

##### 4.1.6.1 Effect of humic acid

Of the natural organic matter, humic substances represent a major fraction in diverse water and soil environments. In this study, humic acid concentrations used were in the range of 0.36-2.29 mg/L as TOC. The effect of humic acid on nitrate reduction was shown in Fig. 4.9. The pH profiles with humic acid (Fig. 4.9(a)) are quite similar to the previous cases without humic acid, except that the rebounding of pH was much slower. It is interesting to observe that the ORP in the solution with humic acid decreased slowly and reached to a negative value after quite a long reaction time of 60 min (Fig. 4.9(b)). On the other hand, the DO disappeared nearly completely within 20 min (Fig. 4.9(c)). Regarding nitrate removal (Fig. 4.9(d)), it decreased remarkably with increasing humic acid content; this implies that humic acid was an important factor adversely affecting nitrate removal in the  $\text{Fe}^0/\text{CO}_2$  process. Retardation on nitrate reduction might derive from the strong competition of humic acid with nitrate for the available reactive surface sites of  $\text{Fe}^0$ . Humic acid appears to be a much stronger adsorbate than nitrate for adsorption onto iron surface. For example, humic acid of only 0.36 mg TOC/L could prolong the reaction time for complete nitrate removal from 30 to 90 min. This result is in agreement with the study of Tratnyek et al. (2001), who reported that carbon tetrachloride reduction rate by zero-valent iron decreased in the presence of three aquatic and soil humic acids. The results from SEM show some differences of iron surface among these conditions. Normally, the shape of fresh zero-valent iron was round and the surface of zero-valent iron was smooth as illustrated in Fig. 4.10(a). When the zero-valent iron reacted with nitrate alone, it can be seen that the surface of zero-valent iron was changed due to corrosion from nitrate reduction as shown in Fig. 4.10(b). From Fig. 4.10(c), the characteristic of zero-valent iron at 90 min in the condition with humic acid showed something which might be humic acid adsorbed on iron surface as well as some corrosion due to nitrate reduction. Thus, it can be concluded that the rate of nitrate reduction depended largely on the availability of the reactive site on zero-valent iron surface.

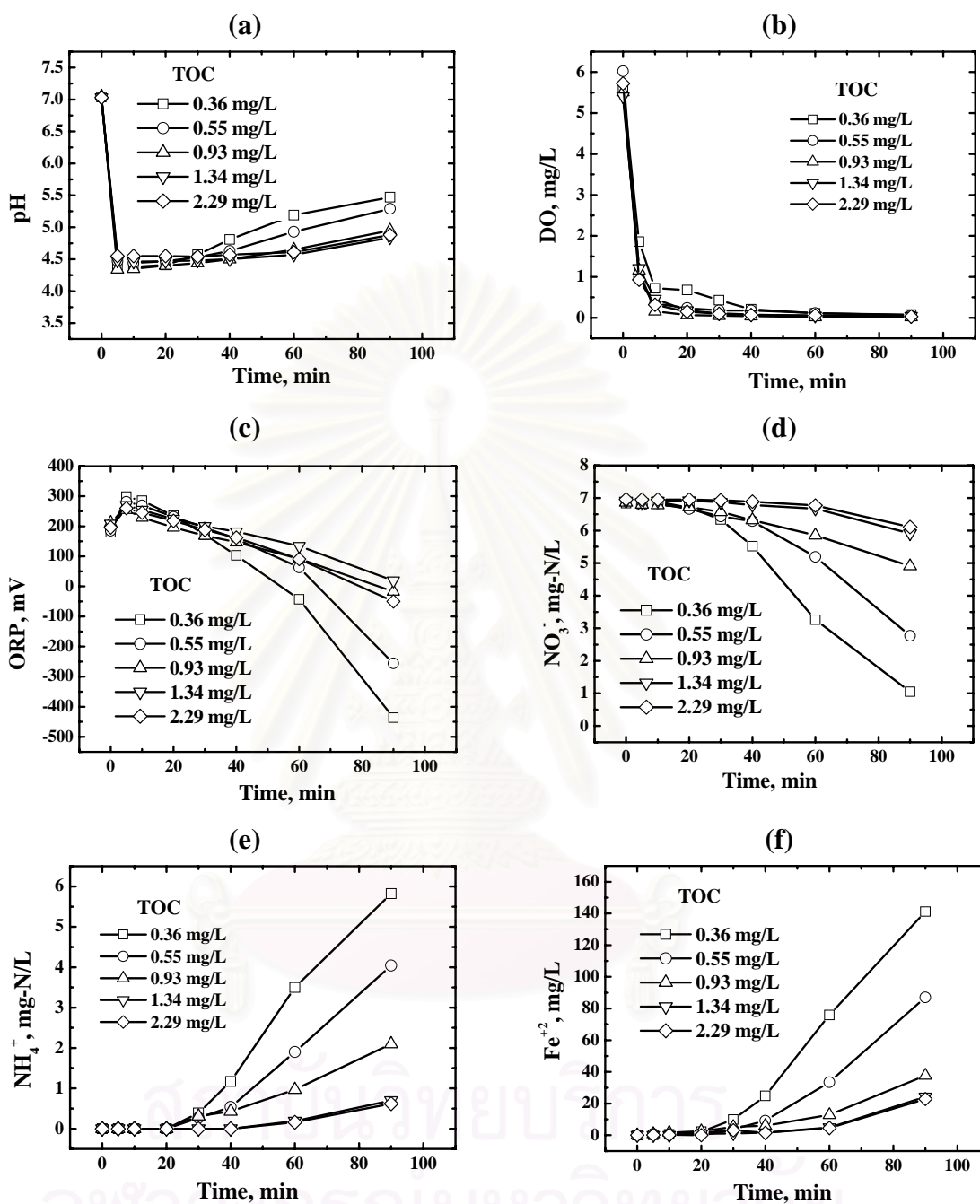


**Fig. 4.9** Effect of humic acid concentration on (a) pH, (b) DO, (c) ORP, (d) nitrate residue, (e) ammonium formation and (f) ferrous ion accumulation. The experiment was conducted by using various humic acid concentrations such as 0.36, 0.55, 0.93, 1.34, 2.29 mg/L with  $\text{CO}_2$  bubbling at an inflow rate of 200 mL/min, 2g  $\text{Fe}^0/\text{L}$  and a recirculated flow of 1000 mL/min. The initial nitrate concentration was 30 mg/L (6.88 mg-N/L). The  $\text{Na}_2\text{CO}_3$  and  $\text{CaCl}_2 \cdot 2\text{H}_2\text{O}$  used as background species were 94 mg/L as  $\text{CaCO}_3$  and 150 mg/L as  $\text{CaCO}_3$ , respectively.

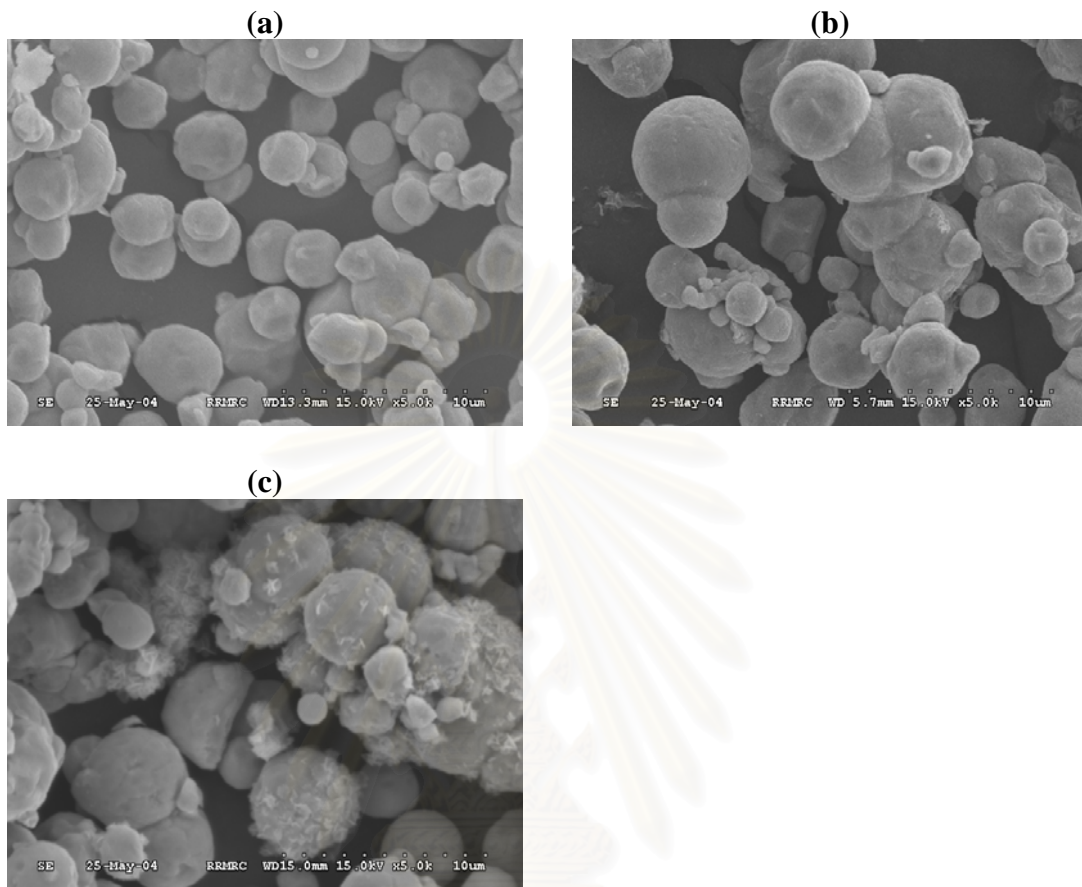


**Fig. 4.10 SEM photograph (a) Fresh Fe<sup>0</sup> (b) Fe<sup>0</sup> under the condition of Fe<sup>0</sup> = 2g/L with 30 mg/L NO<sub>3</sub><sup>-</sup> at 60 min (c) Fe<sup>0</sup> under the condition with 0.55 mg/L humic acid at 90 min.**

Similar to the previous one, the principal product from nitrate reduction remains the same which was ammonia. As shown in Fig. 4.9(e), the ferrous ion released from Fe<sup>0</sup> surface begins to accumulate only when the nitrate reduction reaction starts to occur. It was found that the rate of ferrous ion accumulation decreased with increasing humic acid concentration, due to the hindrance by humic acid.

#### *4.1.6.2 Effects of cations and anions*

Water characteristic parameters such as alkalinity, hardness, and salinity are concerned when applying the proposed Fe<sup>0</sup>/CO<sub>2</sub> process for the field treatment of

nitrate-contaminated water. In general, these parameters involve several cations and anions such as  $\text{Na}^+$ ,  $\text{CO}_3^{2-}$ ,  $\text{Ca}^{2+}$  and  $\text{Cl}^-$ . In running the relevant experiments, chemical reagents of sodium carbonate, calcium chloride, and sodium chloride were employed to investigate their impacts on the process performance. In most cases, unless specified, background species involve (1) organic humic acids and (2) inorganic sodium chloride, calcium chloride, and sodium carbonate. In addition, when alkalinity species of sodium carbonate was added into the solution, the initial pH for each experiment in this Section was adjusted at around 7. To investigate the effect of alkalinity on nitrate reduction by the  $\text{Fe}^0/\text{CO}_2$  process, the sodium carbonate was prepared and added into the solutions at various concentrations of 47, 94, and 141 mg/L as  $\text{CaCO}_3$ . Fig. 4.11 presents the effect of sodium carbonate on nitrate reduction in the presence of other background species. It can be seen that the nitrate removal profiles were close to one another. For example, nitrate removal at 90 min was 48% with the lowest  $\text{Na}_2\text{CO}_3$  concentration of 47 mg/L as  $\text{CaCO}_3$ , and it was 54% with the highest  $\text{Na}_2\text{CO}_3$  concentration of 141 mg/L.

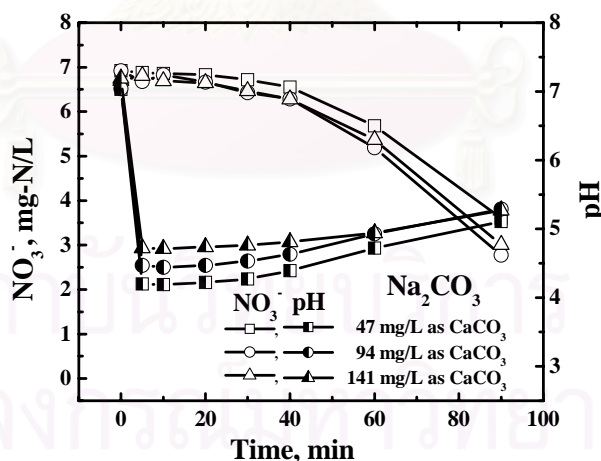


**Fig. 4.11 Nitrate removal with various concentrations of sodium carbonate.** The humic acid and  $\text{CaCl}_2 \cdot 2\text{H}_2\text{O}$  used as background species were 0.55 mg/L as TOC and 150 mg/L as  $\text{CaCO}_3$ , respectively. Unless specified, some other conditions remain the same as those described in Fig. 4.9.

As a result, it appears that the presence of sodium and carbonate ions have no significant effect on nitrate removal under the studied background condition. As presented in Fig. 4.11, the pH values all fell within 4-5 for the three different sodium carbonate concentrations at the time of 5 min, and remained unchanged for a certain time interval; however raised up slightly in the final reaction period. As is understood, carbonate will shift toward the formation of bicarbonate or carbonic acid under the acidic condition, which was created by bubbling CO<sub>2</sub> into the solution continuously. Hence, it seems that carbonate species can be assimilated into the carbonated water system without causing any significant impact on the Fe<sup>0</sup>/CO<sub>2</sub> process performance. Under such setting, sodium ions with single positive valence impose only slightly inhibiting effect on the nitrate removal.

As for the calcium and chloride ions, their individual effect was illustrated in Figs. 4.12-4.15. Chloride is frequently found in the groundwater intruded by the neighboring seawater, while the calcium is one of the major species present in the solution which normally quantified as hardness.

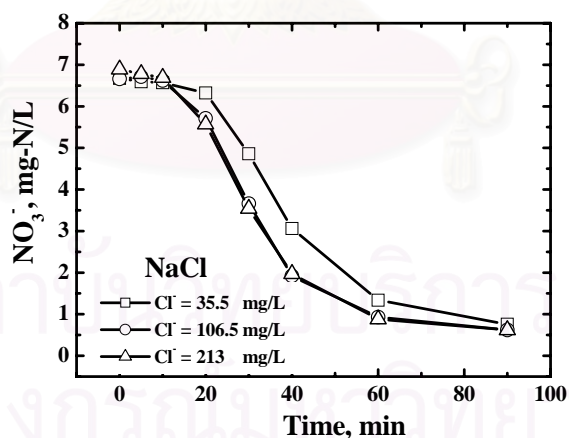


**Fig. 4.12 Nitrate removal with various concentrations of sodium chloride.** The humic acid and Na<sub>2</sub>CO<sub>3</sub> used as background species were 0.55 mg/L and 94 mg/L as CaCO<sub>3</sub>, respectively. Unless specified, some other conditions remain the same as those described in Fig. 4.9.



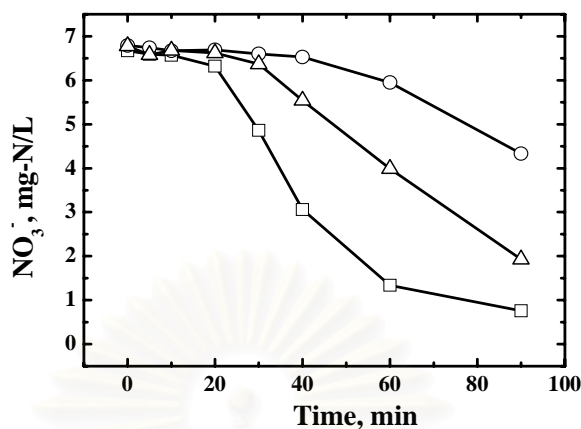


**Fig. 4.13 Effect of cation and anion on nitrate reduction.** ((-□-) With species of  $\text{NaNO}_3$  (30 mg /L as  $\text{NO}_3^-$ ),  $\text{Na}_2\text{CO}_3$  (94 mg/L as  $\text{CaCO}_3$ ), and  $\text{NaCl}$  (106.5 mg/L as  $\text{Cl}^-$ ) and humic acid (0.55 mg/L), which contain  $\text{Cl}^- = 106.5$  mg/L,  $\text{Ca}^{2+} = 0$  mg/L, and  $\text{Na}^+ = 123$  mg/L; (-○-) With species of  $\text{CaCl}_2 \cdot 2\text{H}_2\text{O}$  (150 mg/L as  $\text{CaCO}_3$ ),  $\text{NaNO}_3$  (30 mg /L as  $\text{NO}_3^-$ ),  $\text{Na}_2\text{CO}_3$  (94 mg/L as  $\text{CaCO}_3$ ) and humic acid (0.55 mg/L), which contain  $\text{Cl}^- = 106.5$  mg/L  $\text{Ca}^{2+} = 60$  mg/L, and  $\text{Na}^+ = 54$  mg/L; (-Δ-) With species of  $\text{NaNO}_3$  (30 mg /L as  $\text{NO}_3^-$ ) and humic acid (0.55 mg/L), which contains  $\text{Cl}^- = 0$  mg/L,  $\text{Ca}^{2+} = 0$  mg/L, and  $\text{Na}^+ = 11$  mg/L).

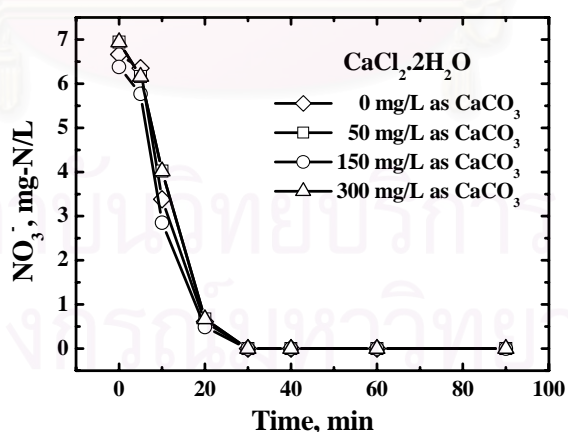


**Fig. 4.14 Nitrate removal with various concentrations of calcium chloride without other background species.** The experiments were conducted by using various calcium chloride concentrations from 0 to 300 mg/L as  $\text{CaCO}_3$  with  $\text{CO}_2$  bubbling at an inflow rate of 200 mL/min, 2 g  $\text{Fe}^0$ /L and a recirculated flow of 1000 mL/min. The initial nitrate concentration was 30 mg/L (6.8 mg-N/L).

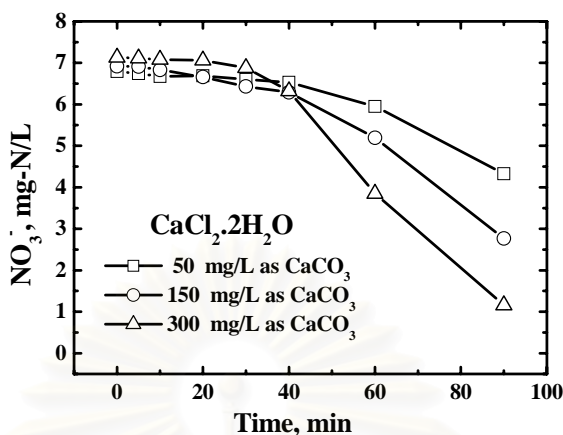


**Fig. 4.15 Nitrate removal with various concentrations of calcium chloride.** The humic acid and  $\text{Na}_2\text{CO}_3$  used as background species were 0.55 mg/L and 94 mg/L as  $\text{CaCO}_3$ , respectively. Unless specified, some other conditions remain the same as those described in Fig. 4.9.

To further single out the effect of chloride ion alone on nitrate reduction, various concentrations of sodium chloride was used in this study, including 35.5, 106.5, 213 mg/L as  $\text{Cl}^-$ . As shown in Fig. 4.12, the nitrate removal significantly increased with increasing  $\text{NaCl}$  concentration. However, the efficiency of nitrate reduction became limited at the high chloride concentrations of 106.5 and 213 mg/L as  $\text{Cl}^-$ . As has been described earlier, sodium ( $\text{Na}^+$ ) imposes only slightly inhibitive effect on nitrate reduction (Fig. 4.11); hence, it seems reasonable to infer that the  $\text{Cl}^-$  accelerates the corrosion of  $\text{Fe}^0$ , resulting in the promoting effect on nitrate removal. Choe et al. (2004) reported that chloride ion in solution induces pitting corrosion of the  $\text{Fe}^0$  surface, which could enhance surface reactivity or increase the reactive area of the  $\text{Fe}^0$  for  $\text{NO}_3^-$  reduction to occur.

To further clarify the effect of calcium alone on nitrate removal, experiments were designed by using the solution conditions described in the caption of Fig. 4.13. This figure indicates that under the same chloride content (106.5 mg/L) the profile of nitrate with higher calcium content, 60 mg/L (-○-) shows a higher nitrate than that of lower calcium content, 0 mg/L (-□-). In other words, calcium which is a divalent cation exhibits significant retarding effect on nitrate removal. On the other hand, if

looking into the two profiles with different chloride content in the absence of calcium, (-□-) and (-Δ-), it was found that the presence of chloride (106.5 mg/L) enhances the nitrate removal remarkably. It appears that cation like calcium suppresses  $\text{Fe}^{2+}$  dissolution from  $\text{Fe}^0$  surface, leading to inhibiting nitrate removal, whereas anion like chloride rapidly pulls Ferrous out of the  $\text{Fe}^0$  surface, resulting in more rapid reduction of nitrate, in addition to its pitting effect on the  $\text{Fe}^0$  surface.

As concluded from the above, calcium and chloride exhibit their effects on process performance in an opposite way. Knowing that calcium chloride dissociates into calcium and chloride easily in the solution, it was wondered that what will be the net effect on the process performance if calcium chloride of various concentrations is added into the solution, According to Fig. 4.14, the nitrate removals were almost the same under various calcium chloride concentrations as well as in the absence of other background species such as sodium chloride, sodium carbonate or humic acids. Based on such result, it might be well reasoned that competitive powers for both calcium and chloride ions are equivalent to each other only if their overall charge quantities are the same in the solution.

To further support such reasoning, experiments were designed and performed in the presence of sodium carbonate, which is anticipated the formation of calcium carbonate ( $\text{CaCO}_{3(s)}$ ) with its solubility product constant ( $K_{sp}$ ) of  $\text{CaCO}_3$  (aragonite) at  $25^\circ\text{C}$  is  $10^{-8.22}$  (Snoeyink and Jenkins, 1980). According to the experimental conditions described in Fig. 4.15, the initial molar concentrations of  $\text{Ca}^{2+}$  and  $\text{CO}_3^{2-}$  calculated from the lowest calcium chloride concentration (50 mg/L as  $\text{CaCO}_3$ ) and the constant sodium carbonate concentration (94 mg/L as  $\text{CaCO}_3$ ) were  $5 \times 10^{-4}$  and  $9.4 \times 10^{-4}$ , respectively. The product of initial calcium and carbonate concentrations is larger than their  $K_{sp}$ , indicating that the solution is supersaturated. Therefore, the overall charge quantity of chloride should be more than that of calcium due to the precipitation of some fraction of calcium ions in the form of  $\text{CaCO}_3$  during the initial period of higher pH values. On top of this, the release of hydroxide ions (Reaction (4.1)) may lead to locally high pH, and precipitation of calcium may occur on the  $\text{Fe}^0$  surface as well. Furthermore, it was reported that metal ions can form a complex with humic substances (Snoeyink and Jenkins, 1980). Both cases will lead to the decreasing of free calcium to chloride ratio as the calcium chloride increases from 50

to 300 mg/L as CaCO<sub>3</sub> in the solution. Consequently, as presented in Fig. 4.15, the higher the calcium chloride concentration, the higher nitrate removal, since charge quantity of chloride (promoting factor) outnumbers that of calcium ions (inhibiting factor). As reported by Westerhoff and James (2003), the formation of aragonite (CaCO<sub>3(s)</sub>) was observed on the surface of Fe<sup>0</sup>; this can lead to inactivation of Fe<sup>0</sup> particles. According to Phillips et al. (2000), the aragonite was formed *in situ* for a groundwater treatment by Fe<sup>0</sup> system with high calcium hardness groundwater. As a result, the water flow at the entrance of packed column will be restricted because cementation within the column decreased the permeability, ultimately requiring much higher influent flow.

#### **4.1.7 Iron precipitation by fluidized bed process**

##### *4.1.7.1 Effect of air flow rate*

According to Fe<sup>0</sup>/CO<sub>2</sub> process, a great amount of ferrous ion generated from zero-valent iron. The elimination of the ferrous iron is usually obtained by raising the water redox potential to oxidative range using oxygen gas in the air. To investigate the effect of air flow rate on the iron removal, the air flow rate were varied at 20, 100, 300 and 500 mL/min as shown in Fig. 4.16. pH of the solution was increased from 5.5 to around neutral (6.5 to 7.1) in all air flow rates as shown in Fig. 4.16(a). The changing pH increased very fast during the first 2 hr and then gradually increased after that. It was observed that the higher air flow rate was applied, the higher pH in the solution was found. The increasing pH is obviously due to the stripping of CO<sub>2</sub>, which was left over from previous carbonation process. Neutral pH was suitable for iron precipitation. The conversion of soluble ferrous ion to iron precipitate was shown in Fig. 4.16(b). It can be seen that ferrous concentration decreased rapidly with increasing air flow rate. The time for completely ferrous removal was found as 120, 90, 90 and 45 min at the air flow rates of 20, 100, 300 and 500 mL/min, respectively. Figure 4.16(c) showed that iron in the system rapidly decreased with increasing air flow rate in the first 1 hr and reaching a plateau afterward.

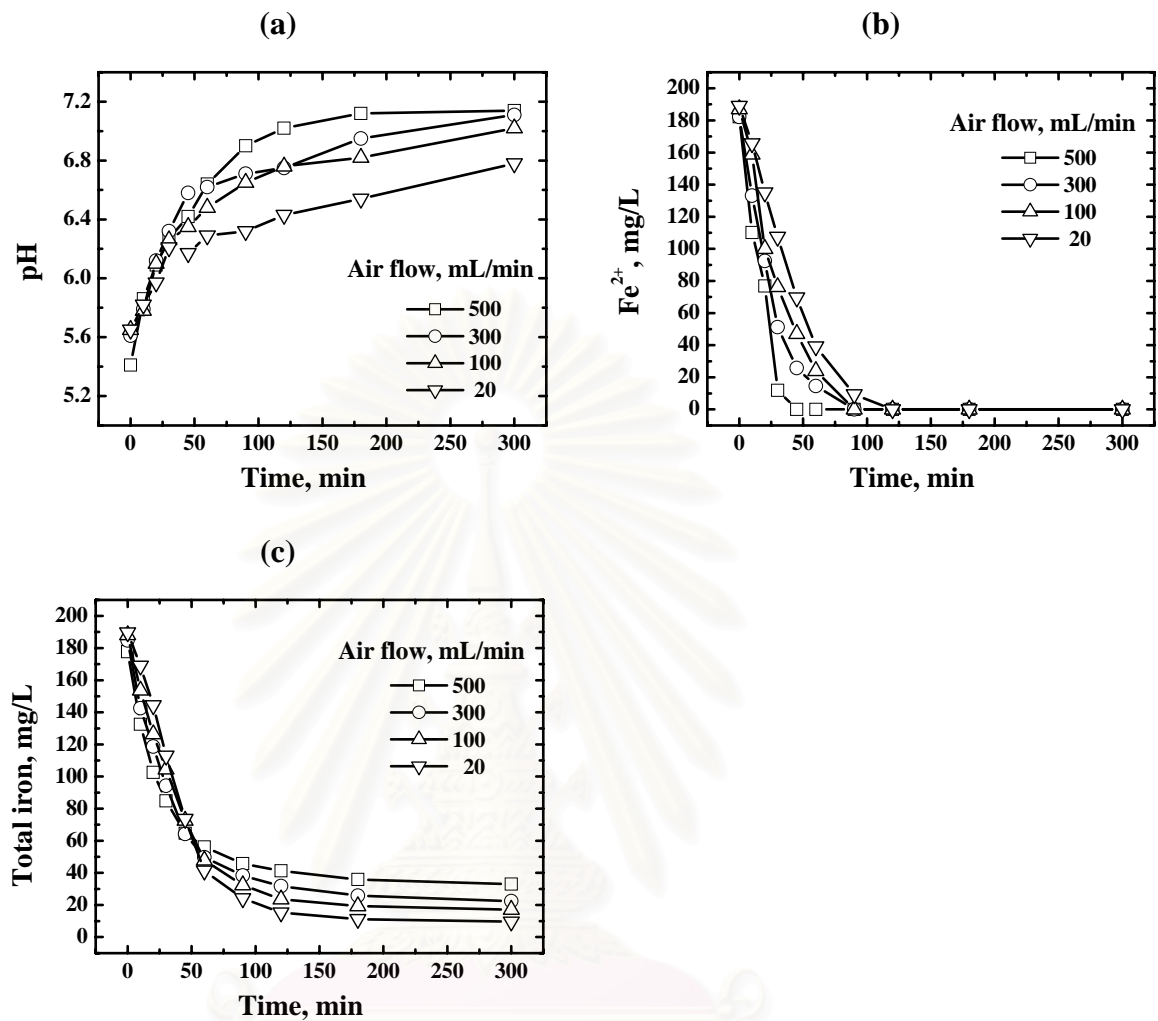


**Fig. 4.16 Effect of air flow rate on iron removal (a) pH, (b) Ferrous removal, (c) total iron removal.** The experiment was conducted by using various air flow rate from 20 to 500 mL/min with sand dosages at 400 g/L as well as bed expansion ratio of 0.5. The initial ferrous concentration was prepared from 2g Fe<sup>0</sup>/L.

The final residual iron at 5 hr was 9.6, 17.1, 22.3 and 33.0 mg/L for air flow rate of 20, 100, 300 and 500 mL/min, respectively. The iron removal efficiency at 5 hr was 95%, 88.2%, 90% and 81.4%, respectively. The lower ferrous removal at higher air flow rate related to the shear force between iron particle and sand surface. A large amount of air bubble generated from high air flow rate can impede the coating of iron onto sand due to abrasion at the surface of sand. Hence, the lower air flow rate for

ferrous removal in the fluidized sand bed reactor is preferred. Consequently, the air flow rate at 20 mL/min was selected as the optimal condition for operation.

#### *4.1.7.2 Effect of sand dosage*

Regarding the effect of sand dosage on the iron removal in fluidized bed process, Fig. 4.17(a) shows four different sand dosages of 200, 300, 400 and 500 g/L at the sand size of 0.42-0.59 mm. The initial iron concentration was 185 mg/L. It was found out that the iron removal was increased with the increasing sand dosage as expected. With the sand dosage of 200 g/L and 300 g/L, the iron removal was by 83% and 92% at 5 hr, respectively. As the sand dosage increased up to 400 and 500 g/L, the iron was removed by 94.97% and 95.25% at 5 hr. Hence, in view of benefit in ferrous removal, the optimum sand dosage of 400 g/L at sand size of 0.42-0.59 mm is recommended in the case of initial ferrous of 185 mg/L. Fig. 4.17(b) shows the iron precipitation with three different sand dosages of 200, 300, and 400 g/L at sand size of 0.096-0.21 mm. As for the ferrous removal, its removal appeared to be in proportion with the sand dosage. With the sand dosage of 200 g/L, the iron was removed by 82% in 5 hrs. As the sand dose increased to 300 and 400 g/L, the removal efficiency reached to 97% and 99%, respectively. This implies that 300 g/L of sand dosage is sufficiently enough to remove 185 mg/L of total iron from the solution. The effect of sand dosage on iron removal in fluidized bed process was considered to be due to the greater specific area for iron precipitation with the increasing of sand dosage. However, the applying sand dosage in excess amount was not necessary for increasing removal efficiency when precipitation between iron solid and sand become rate limited. Additionally, too much sand might increase the chance of collision among sands which remove the iron solid precipitated onto the surface of sand. Comparing the results of ferrous removal from different sand size, it demonstrates that the ferrous removal efficiency at sand size of 0.096-0.21 mm was greater than at sand size of 0.42-0.59 mm. This might be related to surface area of sand. The ferrous removal depends largely on the sand dosage or total surface area available to iron precipitation.

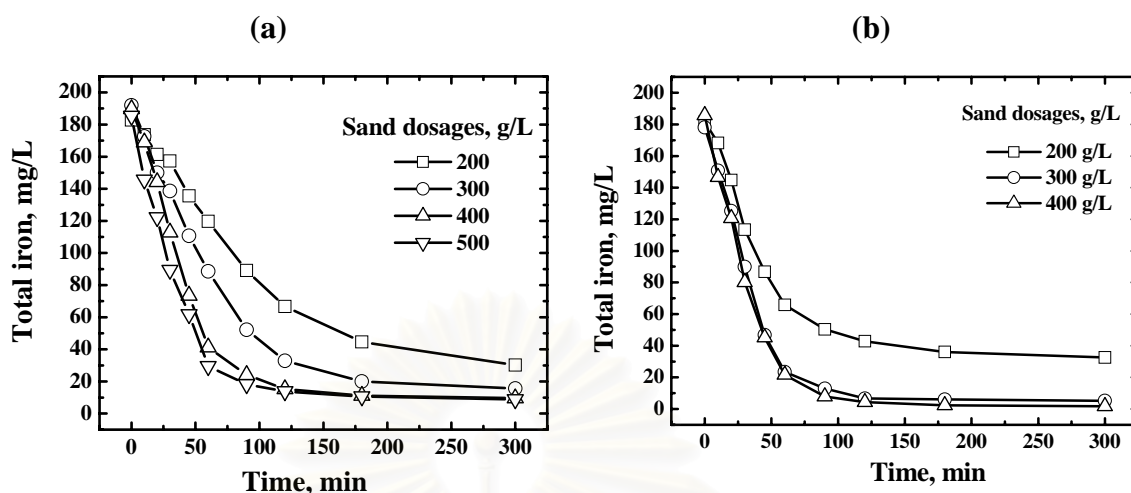


**Fig. 4.17 Effect of sand dosages on iron removal by fluidized bed process (a) 0.42-0.59 mm sand size, (b) 0.096-0.21 mm sand size.** The experiment was conducted by using various sand dosage from 200 to 500 g/L with air flow rate at 20 mL/min. The initial ferrous concentration was prepared from 2g  $\text{Fe}^0/\text{L}$ .

Generally, surface area of sand in small size is higher area than that in large size under the same weight. However, the application of small-size sand should be considered as well on its disadvantage of preparation. The small-size sand was not available in the environment therefore it has to be prepared by mechanical grinding and sieving which can increase the operating cost of this process. Therefore, the selection of sand size and sand dosage needed to be considered carefully prior to its application.

#### 4.1.7.3 Effect of initial iron concentration

To further understand the effect of initial iron concentration on the iron precipitation by fluidized bed process, the initial iron concentration was prepared at 121, 189, 275 and 350 mg/L from various  $\text{Fe}^0$  dosages as 1, 2, 4 and 6 g/L, respectively. The amount of sand dosage at sand size of 0.42-0.59 mm was 400 g/L with air flow rate at 20 mL/min. The bed expansion was controlled at 0.5. The effect of initial iron concentration was presented in Fig. 4.18. As seen in Fig. 4.18(a), the pH solution

increased to around neutral pH ( $6.5 \pm 0.5$ ) in all runs when air was introduced into the system. It can be seen in Fig. 4.18(b) that ferrous ion in different initial concentrations of 121, 189, 275 and 350 mg/L was completely removed at 90, 120, 120, and 180 min, respectively. According to iron removal in Fig. 4.18(c), iron was removed at 96% and 94% within 5 hr for the initial iron concentration of 121 mg/L and 189 mg/L. In contrast, the initial iron concentration of 275 mg/l and 350 mg/L was reduced to 49 mg/L (82% removal) and 130 mg/L (62% removal), respectively at 5 hr.

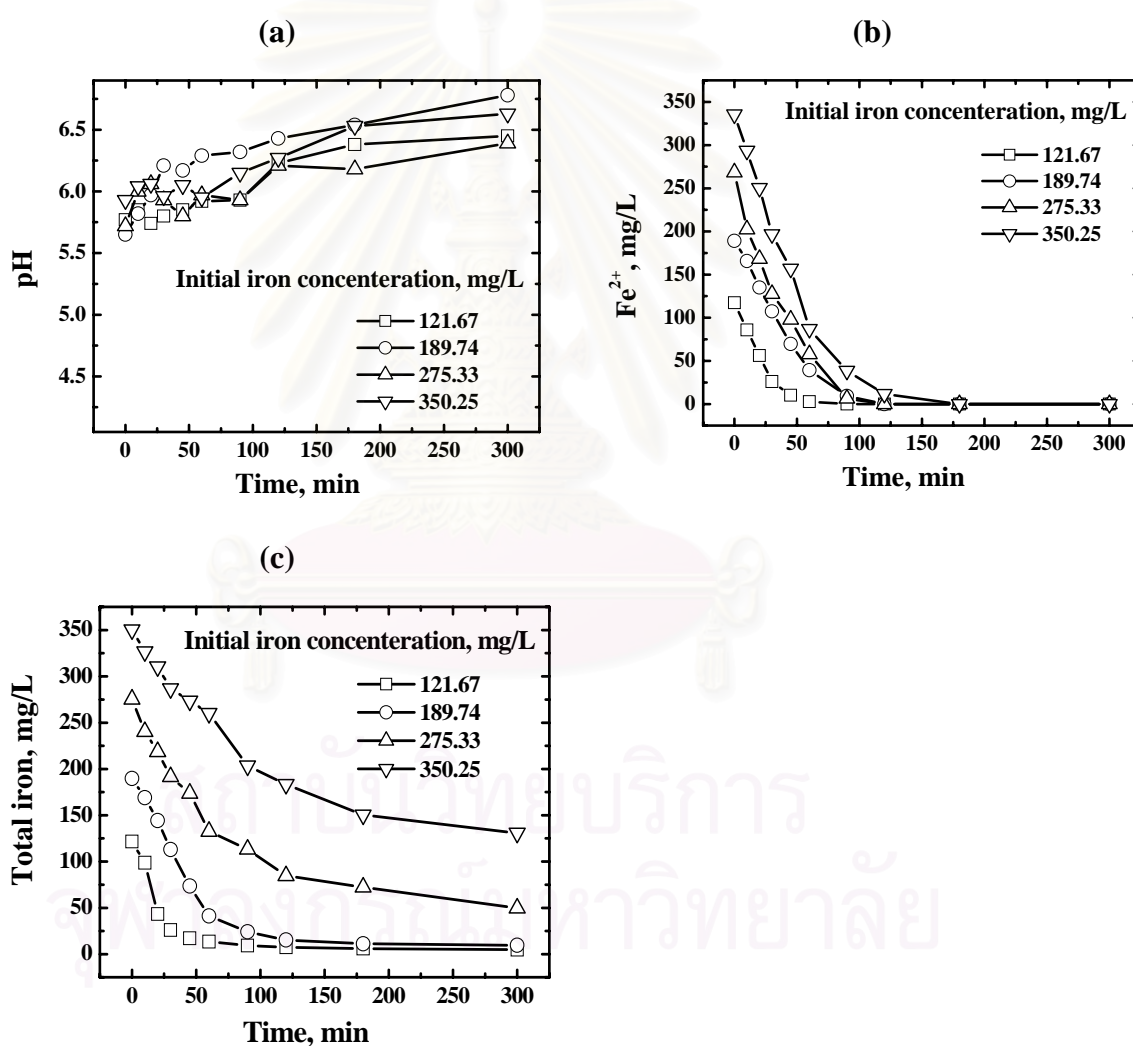


**Fig. 4.18 Effect of initial ferrous concentration on iron removal.** The experiment was conducted by using various sand dosages from 200 to 500 g/L with air flow rate at 20 mL/min. The initial ferrous concentration was prepared from 2 to 6 g  $Fe^0$ /L.



According to the mechanism of precipitation, the iron solid after converting by air will precipitation on sand surface in the favorable way. However, it is possible that some of iron solid form will combine together as discrete particle in the solution. These iron solids may not be easily to attach on the surface of sand. However, the iron residue at the initial iron concentration of 252 and 334 mg/L might be lower at the longer reaction time. Regarding on the apparent property of sand surface, the sand grain color changed from originally white-gray to light brown. The comparison of morphology between fresh and used sand was illustrated in Fig. 4.19. The surface of fresh sand was rough (Fig. 4.19(a)); however, it changed dramatically to become smooth after iron precipitation took place (Fig. 4.19(b)). Based on the spectrum of iron coated sand by SEM/EDS illustrated in Fig 4.20, only Si, Fe, and O signals can be observed in iron coated sand. In accordance with surface composition analysis by SEM-EDS presented in Table 4.4, weight percentage of iron on the sand surface was 1.9.

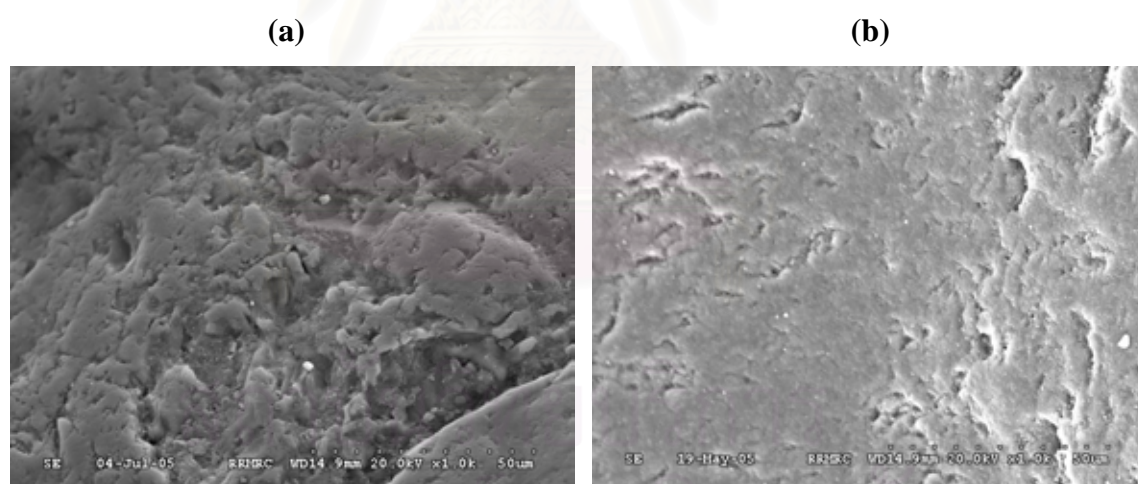


**Fig. 4.19** Morphology of iron pellets (a) fresh sand, and (b) iron coated sand. The material was investigated by SEM at 1.0 k.

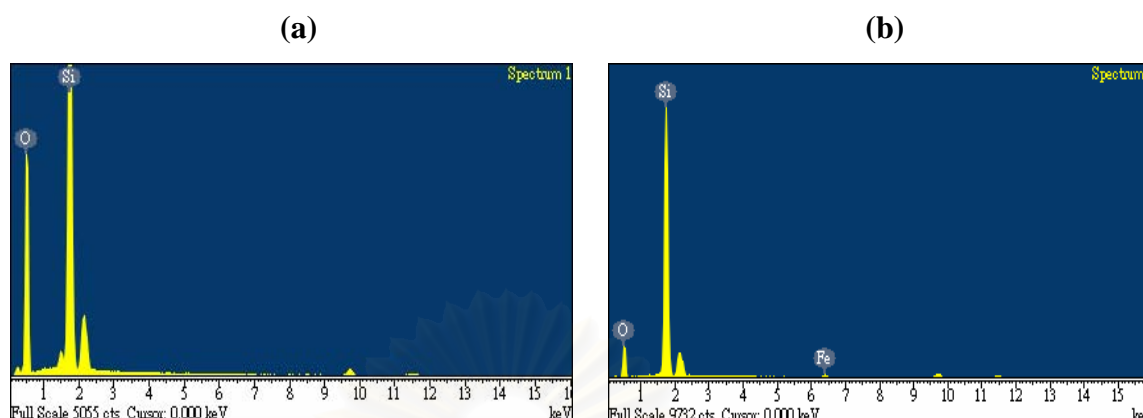


**Fig. 4.20** The distribution of fresh sand properties by SEM-EDS (a) fresh sand, and (b) iron coated sand.

**Table 4.4** Composition of iron coated sand by SEM-EDS.

Element	Fe	Si	O	Total
	% Weight	% Weight	% Weight	% Weight
Fresh sand	0	44.02	55.98	100
Iron coated sand	1.9	55.13	42.97	100

#### 4.1.8 Ammonia removal by air stripping process

##### 4.1.8.1 Effect of pH

As mentioned earlier, ammonium is the dominating end product in the nitrate reduction by  $\text{Fe}^0/\text{CO}_2$  process. Unfortunately, ammonium is an undesirable species. Therefore, a post treatment of separating ammonium from treated water is needed to assure a safe drinking water quality if the reduction process of  $\text{Fe}^0$  is employed for the treatment of nitrate-contaminated waters. According to Reaction (2.33), ammonium can be stripped out of aqueous phase under alkaline solution, especially at a pH level higher than 9.3. With this concept in mind, a follow-up experiment was designed and conducted to guarantee ammonium removal in solution. To investigate the effect of pH on the ammonia removal, the pH was varied at 10, 11, 12 and 13. Air flow rate

was set at 50 mL/min. The initial ammonium concentration was approximately 7.2 mg-N/L. As can be seen from Fig. 4.21 (a), the ammonia removal with pH at 10 and 11 was 97.2% and 98.6% at 4 hr, respectively.

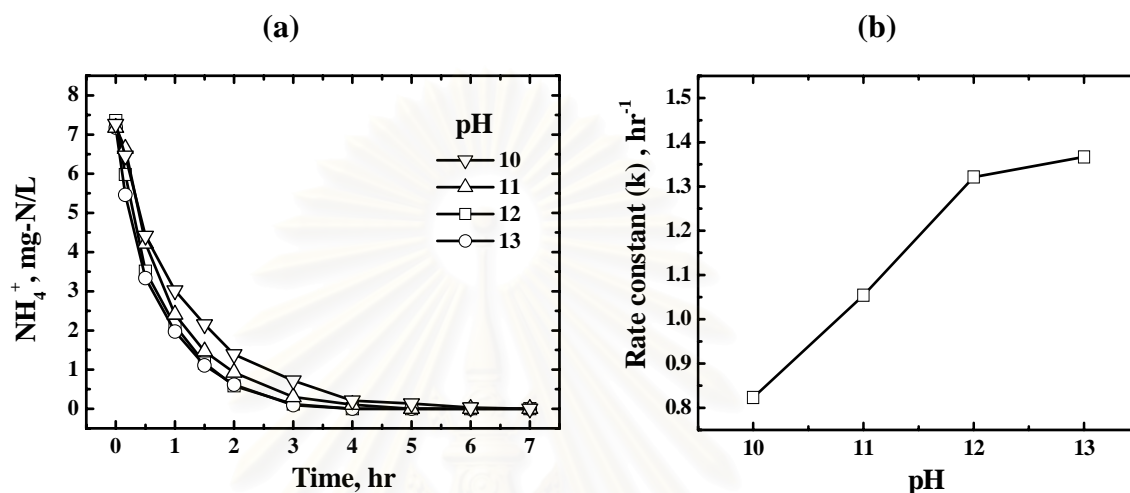


**Fig. 4.21 Effect of pH on ammonia removal by air stripping.** The experiment was conducted by using various controlled pH from 10 to 13 g/L with air flow rate at 50 mL/min. The initial ammonium concentration was 7.2 mg-N/L.

On the other hand, as pH was controlled at 12 and 13, the nitrate was completely removed at time of 4 hr in either case. In addition, the residual profiles of ammonium show no difference for pH controlled at 12 and 13, but the difference becomes quite significant as the pH was reduced from 12 to 11. For kinetic analysis, the ammonia stripping obeys a first-order kinetics. The result indicated that the initial pH greatly affected ammonia removal rates. The rate constant,  $k$ , of pH changed from  $0.82 \text{ hr}^{-1}$  at pH 10 to  $1.05$ ,  $1.32$ , and  $1.37 \text{ hr}^{-1}$  as pH increased to 11, 12, and 13, respectively (see Table A-24). The rate constant profile shows in Fig. 4.21(b) that rate constant linearly increases with increasing pH from 10 to 12. However, rate constant slightly increase from pH at 12 to 13. Hence, the optimum pH at 12 is recommended for ammonia stripping under the conditions of this study.

#### 4.1.8.2 Effect of air flow rate

Fig. 4.22 (a) presents the profile of ammonium removal by air stripping process with various air flow rates (10-50 L/min) and the pH was fixed at 12. The results showed that ammonium removal increased with increasing air flow rate.

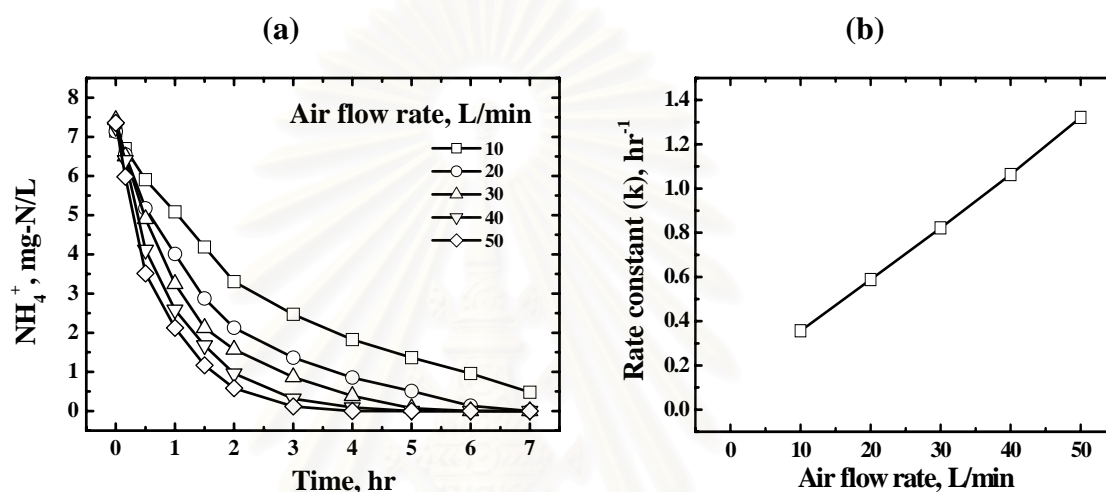


**Fig. 4.22 Effect of air flow rate on ammonia removal by air stripping.** The experiment was conducted by using various air flow rate from 15 to 50 L/min with controlled pH at 12. The initial ammonium concentration was 7.2 mg-N/L.

Ammonia removal efficiency with airflow rate of 10, 20, 30, 40 and 50 L/min were 74%, 88%, 94%, 98.8% and 100% at 4 hr, respectively. With the air flow rate at 50 L/min, the ammonium was completely removed at time of 4 hrs. Considering the kinetic analysis, the result shows in Fig. 4.22 (b) that rate constant increases proportionally with the increasing air flow rate, i.e., from  $0.36 \text{ hr}^{-1}$  to 0.59, 0.82, 1.06, and  $1.32 \text{ hr}^{-1}$  as the air flow rate increased from 10 L/min to 20, 30, 40 and, 50 L/min, respectively (see Table A-26). The increasing ammonia removal might be due to decreasing of film thickness between the interface of liquid and gas phase as a result from increasing air flow rate. In addition, the interfacial area between liquid and gas phases in which the mass transfer occurred also increased as the air flow rate increased.

#### 4.1.8.3 Effect of initial ammonia concentration

Fig. 4.23(a) presents the profile of ammonium removal by air stripping process under various initial ammonia concentrations at pH 12 and air flow rate at 50 mL/min.

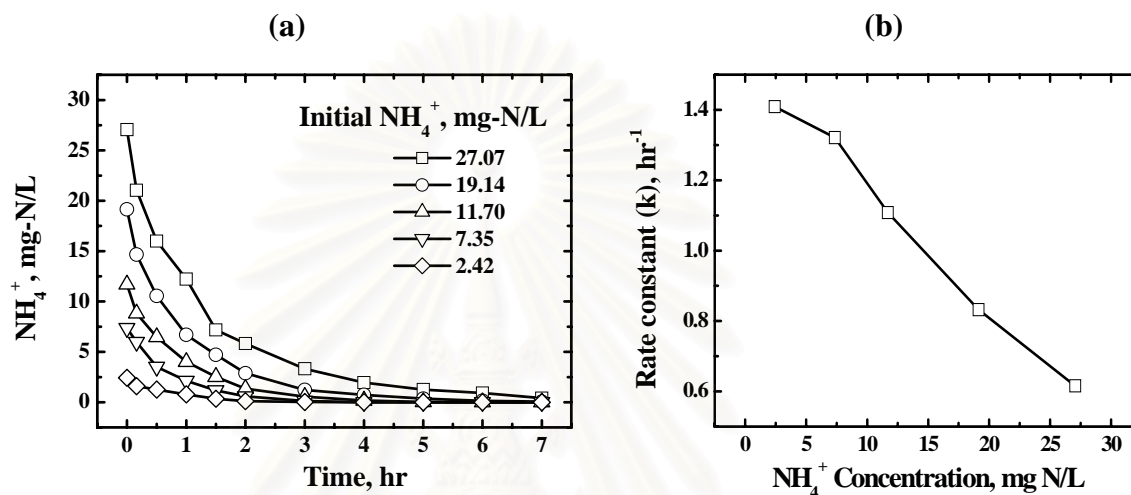


**Fig. 4.23 Effect of initial ammonium concentration on ammonia removal by air stripping.** The experiment was conducted by using various initial ammonium concentrations from 2.42 to 27.07 mg N/L with controlled pH at 12 as well as air flow rate at 50 L/min.

The result shows that initial ammonia concentration of 2.42, 7.35, 11.7 mg N/L was completely removed from the system at 4, 4, and 6 hr, respectively. On the other hand, at the initial ammonium concentrations of 19.7, and 27.07 mg N/L, some ammonia still remained at 7 hr, i.e., 0.059 and 0.418 mg N/L, respectively. Considering on kinetic analysis, the result indicates in Fig. 4.20(b) that rate constant decreases with the increasing ammonium concentration, i.e., decreased from  $1.4 \text{ hr}^{-1}$  to 1.32, 1.11, 0.83, and  $0.62 \text{ hr}^{-1}$  as the concentration of ammonium increased from 2.9 mg N/L to 8.3, 14.5, 23.2, and 20.03 mg N/L, respectively (see Table A-28). Therefore, it can be concluded that ammonia can be effectively removed to comply with the drinking water standard of 0.1 mg N/L by using air stripping. However, longer stripping period may be needed as the ammonia concentration increased.

## 4.2 Continuous mode study

### 4.2.1 Nitrate removal by Fe<sup>0</sup>/CO<sub>2</sub> process

#### 4.2.1.1 Effect of CO<sub>2</sub> flow rate

The removal of nitrate by Fe<sup>0</sup>/CO<sub>2</sub> was investigated at CO<sub>2</sub> flow rate from 100 to 800 mL/min, Fe<sup>0</sup> dosages of 40 g Fe<sup>0</sup>/L, and the initial nitrate concentration at 23 mg N/L. As can be seen in Fig. 4.24 (a), the pH profiles of CO<sub>2</sub> flow rate at 100, 200, 400 and 800 mL/min dropped rapidly from the neutral value to 5.21, 5.41, 5.53, and 5.76 respectively, within the first 10 min; however, it increased slightly to 5.92, 5.9, 5.87, and 5.76, respectively in the next 20 min, respectively. The decreasing profile of pH in the initial phase may be due to the dominating acidification reaction of CO<sub>2</sub> bubbling since zero-valent iron surface has not yet been activated. The reason for the pH rebounding is the consumption of hydrogen ions due to nitrate reduction as well as the generation of hydroxide ions due to reduction of oxygen and water molecule as mentioned earlier in the batch operation of NO<sub>3</sub><sup>-</sup>/Fe<sup>0</sup>/CO<sub>2</sub> process. The cause of gradually decreasing in pH after Fe<sup>0</sup> being activated was the loss of Fe<sup>0</sup> mass through its corrosion reaction in the system, leading to less consumption of H<sup>+</sup>. As presented in Fig. 4.24(b), the initial DO ranging from 7.0 to 7.5 mg/L dropped nearly to zero within the first 5 min regardless of Fe<sup>0</sup> dosages. Dissolved oxygen in the solution may be either stripped out of the system through CO<sub>2</sub> bubbling and/or reductively consumed by Fe<sup>0</sup>. As has been well understood, oxygen can act as a role of electron acceptor similar to the nitrate in the Fe<sup>0</sup> system. In regard to the ORP, Fig. 4.24(c) shows that the initial values of about 250±25 mV, indicating an oxidative environment, dropped considerably to -652, -680, -652, and -693 mV with the CO<sub>2</sub> flow rate of 100, 200, 400 and 800 mL/min, respectively, at time of 30 min. The ORP profiles of different CO<sub>2</sub> flow rate remained rather constant after 1 hr, which were -700, -712, -700, and -701 mV, respectively. Such negative ORP values indicate that the reducing environment has occurred in the Fe<sup>0</sup>/CO<sub>2</sub> system. However, the ORP value increased gradually as the reaction proceeded further.

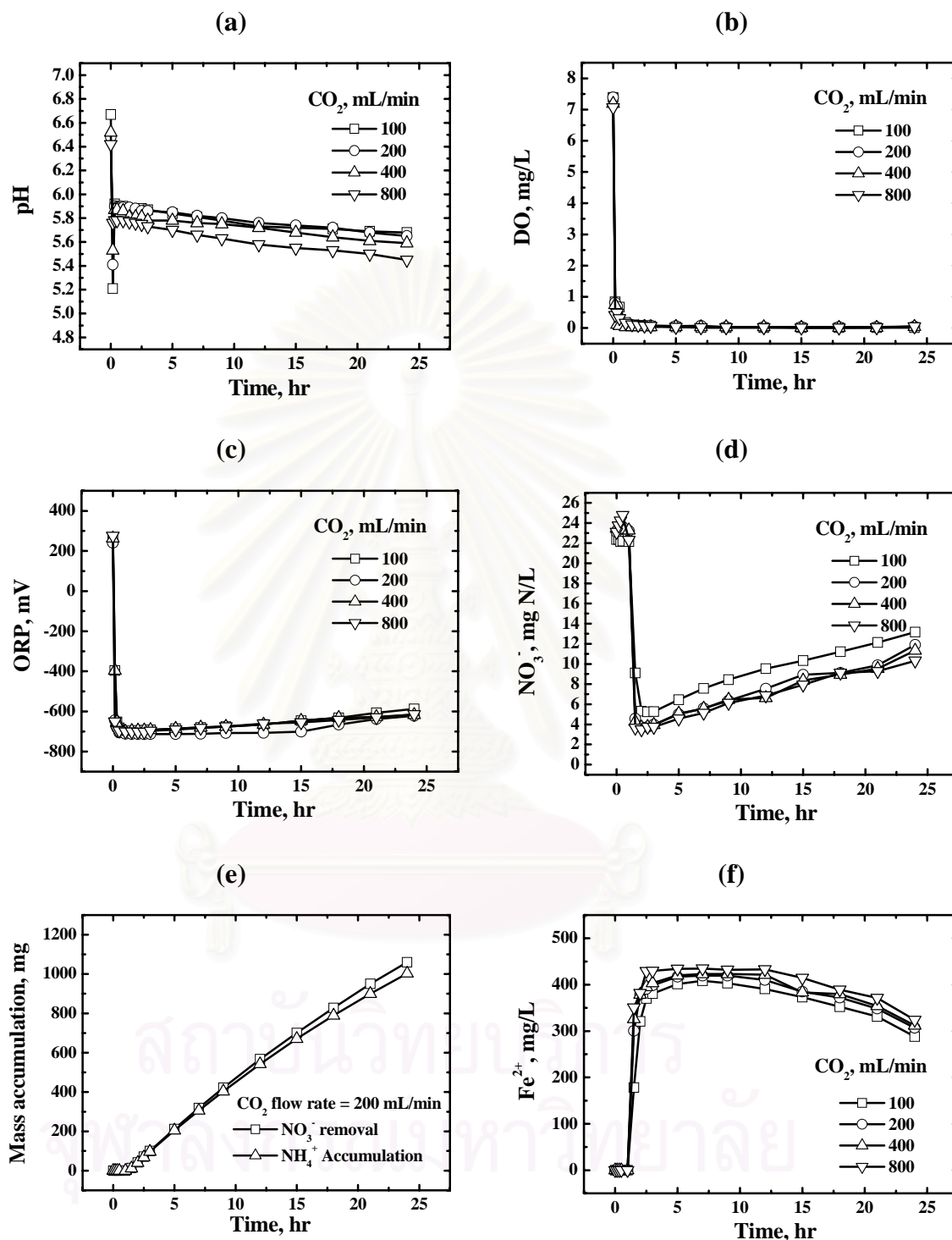


**Fig. 4.24** Effect of CO<sub>2</sub> bubbling rate on nitrate reduction (a) pH, (b) DO, (c) ORP, (d) nitrate residue, (e) mass balance at 200 mL/min of CO<sub>2</sub>, and (f) ferrous (Fe<sup>2+</sup>) accumulation. The initial NO<sub>3</sub><sup>-</sup> concentration was 23 mg-N/L. The experiment was conducted by using various CO<sub>2</sub> bubbling from 100 to 800 mL/min as well as Fe<sup>0</sup> dosages at 40 g. The feeding rate of NO<sub>3</sub><sup>-</sup> solution was 50 mL/min.

Theoretically, the more reductive environment created, the more rapid nitrate removal would occur. This is to say that ORP value can serve as an indicator for nitrate removal performance. In Fig. 4.24(d), it appears that nitrate concentration remained unchanged within the initial period of 1 hr. This may be due to the lapsed time for the treated nitrate solution transported from the first compartment, passing through the second compartment, to the effluent outlet. In addition, it also takes time to remove impurities from the  $\text{Fe}^0$  surface since it was used without any pretreatment. Following the lag phase, the nitrate residue dropped rapidly. The lowest residual  $\text{NO}_3^-$  concentration was observed at 2 hr. With the  $\text{CO}_2$  flow rate at 100 mL/min, the nitrate was removed by 76% at 2 hrs. As the  $\text{CO}_2$  flow rate increased up to 200, 400 and 800 mL/min, the nitrate was removed by 84%, 84%, and 84.8%, respectively, at 2 hrs. The nitrate removal efficiency shows no significant difference for  $\text{CO}_2$  bubbling rates from 200 to 800 mL/min. Therefore, it can be implied that the  $\text{CO}_2$  bubbling rate at 200 mL/min was the optimum one in the reaction system. Concerning the reaction by-product, nitrite ( $\text{NO}_2^-$ ) was not detected in the treated solution, whereas ammonium was the predominant nitrogen-containing species as shown in Fig. 4.24(e). The ammonium was produced rapidly when the nitrate reduction began, and its formation rate became reduced as the nitrate reduction rate was slowing down. The ammonium yield agrees very well with the nitrate disappearance on the basis of nitrogen mass balance between accumulated nitrate removal and ammonium formation, the difference of which was within  $\pm 5\%$ . In Fig. 4.24(f), the ferrous accumulation increased with increasing  $\text{CO}_2$  flow rate. It is interesting to point out that the initial lag phase for ferrous accumulation was observed for all  $\text{CO}_2$  flow rate. It might be due to the time required for ferrous ion to transfer from the first compartment, passing through the second compartment, to the effluent outlet. Moreover, the activation time of  $\text{Fe}^0$  surface is needed as well for removing impurities from the surface of  $\text{Fe}^0$ .

#### 4.2.1.2 Effect of $\text{Fe}^0$ dosages

To determine the optimal  $\text{Fe}^0$  dosage on nitrate reduction, 40, 60 and 80 g of  $\text{Fe}^0$  were used in the presence of  $\text{CO}_2$  bubbling at the flow rate of 200 mL/min and an initial nitrate concentration of 23 mg N/L.



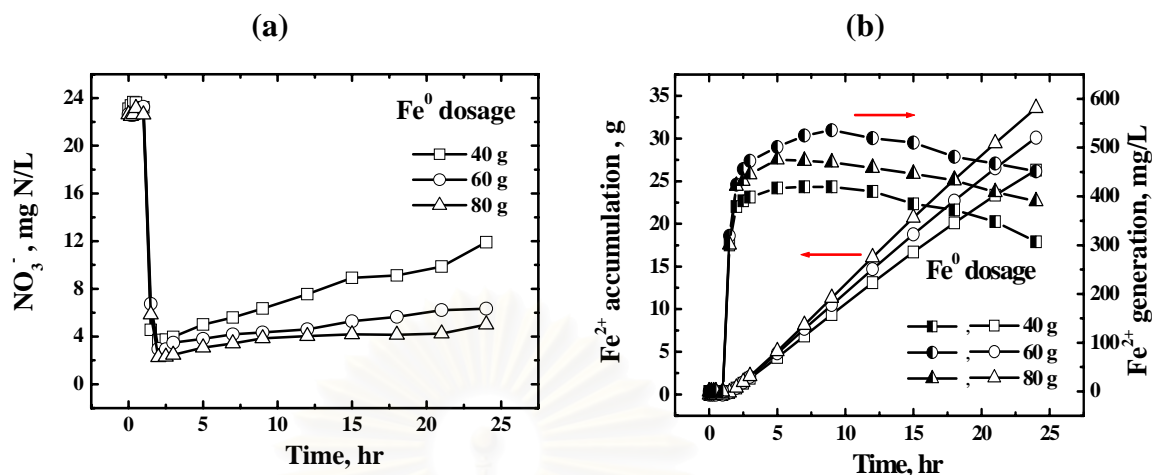


**Fig. 4.25 Effect of Fe<sup>0</sup> on nitrate reduction (a) nitrate reduction, and (b) ferrous accumulation.** The initial NO<sub>3</sub><sup>-</sup> concentration was 23 mg-N/L. The experiment was conducted by using various Fe<sup>0</sup> from 40 to 80 g as well as bubbling CO<sub>2</sub> at an inflow rate of 200 mL/min. The feeding rate of NO<sub>3</sub><sup>-</sup> solution was 50 mL/min.

In Fig. 4.25(a), it appears that nitrate concentration remained unchanged within the initial period of 1 hr. This may be due to the lapsed time for the treated nitrate solution transported from the first compartment, passing through the second compartment, to the effluent outlet. In addition, it also takes time to remove impurities from the Fe<sup>0</sup> surface since it was used without any pretreatment. Following the lag phase, the nitrate residue dropped rapidly. With the Fe<sup>0</sup> dosage of 40 g, the nitrate was removed by 83% at 2 hrs. As the initial Fe<sup>0</sup> increased up to 60 and 80 g, the nitrate was removed by 87% and 90%, respectively, at 2 hrs. Such a result implies that the higher the Fe<sup>0</sup> dosage, the lower the NO<sub>3</sub><sup>-</sup> residue in the reaction solution. With 40 g of Fe<sup>0</sup>, the nitrate concentration at 21 hrs was beyond the drinking water standard of 10 mg/L NO<sub>3</sub><sup>-</sup>-N. Therefore, the Fe<sup>0</sup> of 60 g was selected as the optimum dosage to remove 23 mg N/L of nitrate. In Fig. 4.25(b), the ferrous accumulation increased with increasing Fe<sup>0</sup> dosages. It is interesting to point out that the initial lag phase for ferrous accumulation was observed for all Fe<sup>0</sup> dosages. It might be due to the time required for ferrous ion to transfer from the first compartment, passing through the second compartment, to the effluent outlet. Moreover, the activation time

of  $\text{Fe}^0$  surface is needed as well for removing impurities from the surface of  $\text{Fe}^0$ . The ferrous accumulation rate in Fig. 4.25(b) appears to be in consistency with the rate of nitrate removal in Fig. 4.25(a). In other words, the nitrate removal is highly correlated with the ferrous concentration in the bulk solution. Therefore, monitoring of ferrous ion can provide a good prediction of the degree of nitrate being removed in the reaction system.

#### 4.2.1.3 Effect of $\text{NO}_3^-$ concentration

To investigate the effect of initial nitrate concentration on  $\text{Fe}^0/\text{CO}_2$  process, the initial nitrate concentration was varied from 6.6 to 46.2 mg N/L. The experiment was carried out with 60 g/L  $\text{Fe}^0$ , 200 mL/min  $\text{CO}_2$  inflow rates. Fig. 4.26(a) shows that the curves of all initial concentrations exist a lag phase over the initial period of 1 hr.

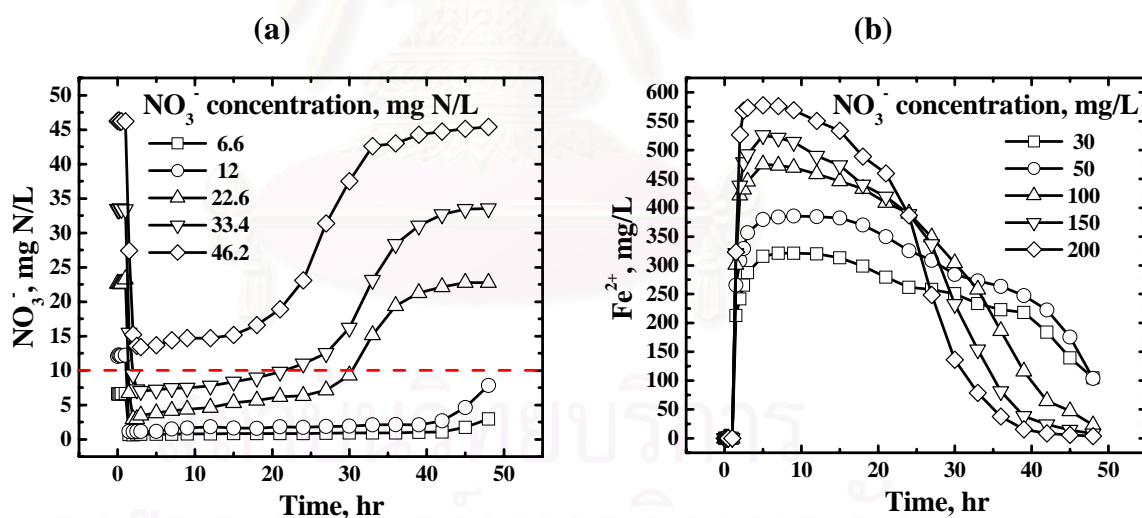


**Fig. 4.26** Effect of initial nitrate concentration on nitrate reduction. (a) nitrate reduction, and (b) ferrous accumulation. The initial  $\text{NO}_3^-$  concentration was various from 6.6 to 46.5 mg-N/L. The experiment was conducted by using 60 g of  $\text{Fe}^0$  as well as bubbling  $\text{CO}_2$  at an inflow rate of 200 mL/min. The feeding rate of  $\text{NO}_3^-$  solution was 50 mL/min.

The initial nitrate of 6.6, 12, 22.6, 33.4, and 46.2 mg N/L was reduced to 0.66 mg N/L (90% removed), 1.09 mg N/L (90% removed), 2.95 mg N/L (87% removed), 9.39 mg N/L (71% removed), and 13.57 mg N/L (70% removed), respectively, at 2 hr. It appears that the residual nitrate concentration increases with increasing initial nitrate concentration. Considering on  $\text{NO}_3^-$  standard, the  $\text{NO}_3^-$  concentration to be treated with 60 g/L of  $\text{Fe}^0$  can not be exceeded 33.4 mg N/L. From the profile of nitrate concentration at 46.2 mg N/L, the residual nitrate was beyond the standard. It might be due to the insufficient of  $\text{Fe}^0$  dosage or  $\text{CO}_2$  flow rate in the system. Therefore, the water contaminated with 46.2 mg N/L of nitrate should be treated with other conditions in order to meet the drinking water quality standard. The consumption of  $\text{Fe}^0$  increased with increasing initial nitrate concentration. It can be seen from ferrous formation as shown in Fig 4.26(b), ferrous formation increased with increasing initial nitrate concentration after lag phase. However, ferrous concentration at higher initial nitrate concentration will decrease rapidly earlier than that at lower initial concentration. From the nitrate removal profile, it shows that 60 g of  $\text{Fe}^0$  can be applied for treating 33.2 and 22.6 mg N/L of nitrate to below the standard for 21 hr and 30 hr, respectively. In addition, 60 g of  $\text{Fe}^0$  was enough to remove nitrate at 6.6 and 12 mg N/L for more than 48 hr.

#### *4.2.1.4 Effect of feeding solution rate*

In this part, the initial nitrate concentration,  $\text{Fe}^0$  dosage and  $\text{CO}_2$  bubbling rate were maintained constantly at 23 mg N/L, 60 g and 200 mL/min. The feeding rate of  $\text{NO}_3^-$  solution was various from 50 to 200 mL/min. The retention time at the feeding flow rate of 50, 100, and 200 mL/min was 4, 2, and 1 hr, respectively. Fig 4.27(a) shows that the lag phase was shorten as the feeding rate increased. The effluent nitrate was below the nitrate standard for all feeding rates. However, the residual nitrate was higher at higher feeding rate. It might be due to shorten reaction time for nitrate and  $\text{Fe}^0$ . In addition, the service time of  $\text{Fe}^0$  was decreased with increasing feeding solution rate.

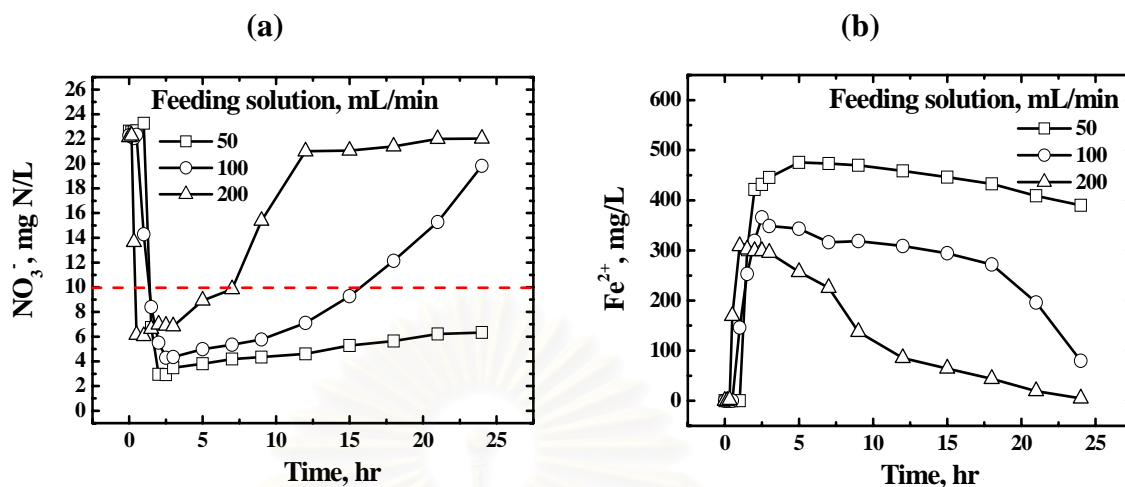


**Fig. 4.27 Effect of feeding solution rate on nitrate reduction (a) nitrate reduction, and (b) ferrous accumulation.** The initial  $\text{NO}_3^-$  concentration was 23 mg-N/L. The experiment was conducted by using 60 g of  $\text{Fe}^0$  as well as bubbling  $\text{CO}_2$  at an inflow rate of 200 mL/min. The feeding rate of  $\text{NO}_3^-$  solution was various from 50 to 200 mL/min.

60 g  $\text{Fe}^0$  can be applied for treating nitrate to below the standard value for 18 and 7 hr at 100 and 200 mL/min of feeding rate and more than 24 hr at 50 mL/min. As seen from ferrous formation after lag phase as shown in Fig 4.27(b), ferrous formation increased with increasing retention time. The increasing ferrous occurred from the longer reaction time of nitrate and  $\text{H}_2\text{O}$  reacted with  $\text{Fe}^0$ . However, ferrous concentration at higher liquid feeding rate will decrease rapidly than that at lower feeding rate. It might be due to the higher mass  $\text{Fe}^0$  consumption for  $\text{NO}_3^-$  removal occurred in higher liquid feeding rate.

#### 4.2.1.5 Effect of process operation

In the process operation, as shown in Fig. 4.28, the operating mode was divided into 2 steps, i.e., Step 1: the initial  $\text{Fe}^0$  of 60 g  $\text{Fe}^0$  was tested for 23 mg N/L of nitrate until its exhaustion without any supplement of  $\text{Fe}^0$  in order to determine an appropriate supplementing time; Step 2: the supplement of  $\text{Fe}^0$  was introduced into

the system when the effluent nitrate concentration was higher than 10 mg/L  $\text{NO}_3^-$ -N. This step was designed to control the effluent nitrate so that it can comply with the standard. The supplement of  $\text{Fe}^0$  was varied from 30 to 50 g to find the optimal  $\text{Fe}^0$  for continuous operation in continuous. In Step 1, pH dropped at the beginning and increased after 10 min. Then, it gradually decreased, similar to previous scenario. Moreover, it can be seen that pH significantly decreased after 33 hrs because of the decreasing  $\text{Fe}^0$  mass in the system. The  $\text{H}^+$  consumption for nitrate removal by  $\text{Fe}^0$ , as illustrated in Reaction 4.3, decreased as  $\text{Fe}^0$  mass in the system decreased; on the other hand, since the  $\text{CO}_2$  was continuously bubbled into the solution, the  $\text{H}^+$  began to build up in the system, resulting in the decrease of the pH. Not only can the pH indicate the reaction extent of the  $\text{Fe}^0$ , the DO, ORP and ferrous accumulation also relate to nitrate removal. As shown in Fig. 4.28(b), the increasing of DO value occurred when  $\text{Fe}^0$  in the system diminished. As mentioned earlier, the decreasing of DO in the solution was either stripped out of the system due to continuous  $\text{CO}_2$  purging or consumed reductively by  $\text{Fe}^0$  (see Reaction (4.2)). Therefore, the DO in the system raised up in the later time period as the  $\text{Fe}^0$  was used up completely. According to ORP profile in Fig. 4.28(c), it is shown that the ORP value changed from the negative to the positive, implying that the reductive environment was diminishing in the system. As seen from Fig. 4.28(d), the nitrate removal rate decreased as the reaction proceeded to a longer extend, particularly after 30 hr. This indicated that the residual mass of  $\text{Fe}^0$  was not sufficient for removing 23 mg N/L of nitrate at 50 mL/min of liquid feeding rate to the desired drinking water quality standard. In contrast, while nitrate removal decreased, the formations of ammonium and ferrous were decreasing as well, as illustrated in Figs. 4.28(e) and 4.28(f), respectively. At 48 hrs, the measured ferrous concentration was 22 mg/L, which accounts for the accumulated mass of 43 g, as compared to 60 g at the beginning stage. The unbalance of iron mass might be due to the formation of some iron complex species in the reactor and also the  $\text{Fe}^0$  residue in the recirculated pump. By visual observation, it can be seen that the color of solution changed from dark grey to light grey and to light yellow brown as the operation proceeded for 40 hrs. This depicts that the  $\text{Fe}^0$  in the reactor has been utilized completely in the reaction system.

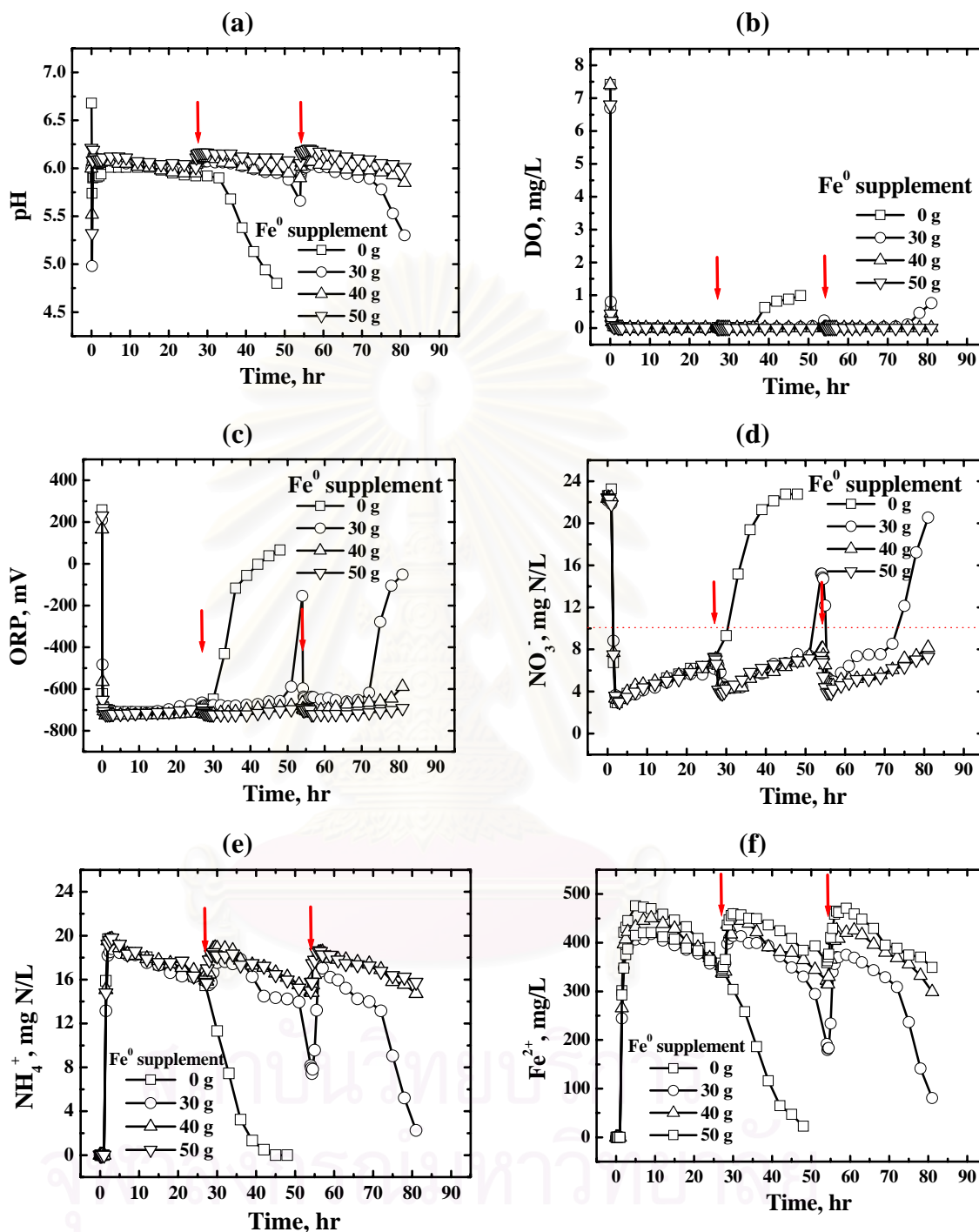


**Fig. 4.28** Effect of  $\text{Fe}^0$  supplement on nitrate reduction (a) pH, (b) DO, (c) ORP, (d) nitrate removal, (e) ammonium formation, (f) ferrous accumulation. The experiment was conducted under the conditions of  $\text{CO}_2$  bubbling rate of 200 mL/min and a recirculated flow of 90 L/min. The influent nitrate concentration was 23 mg N/L. The operating mode was divided into 2 steps. Step 1: the initial  $\text{Fe}^0$  of 60 g was tested until exhaustion, without any supplement of  $\text{Fe}^0$  (0 g  $\text{Fe}^0$  supplement). Step 2: The supplement of  $\text{Fe}^0$  such as 30, 40, and 50 g was introduced in the system at times of 27 hrs and 54 hrs, respectively.

Prior to the occurrence of breakthrough, the effluent solution was not colorless because  $\text{FeCO}_3$  (siderite) or  $\text{Fe}(\text{OH})_3$  (ferric hydroxide) can be also formed in the system. To ensure the compliance with effluent standard, it was found that extra  $\text{Fe}^0$  should have supplemented at every 27 hr rather than every 30 hr for safety factor consideration. In step 2, the supplement of fresh  $\text{Fe}^0$  such as 30, 40 and 50 g was decided at every 27 hr to control nitrate to less than 10 mg N/L. As seen in Fig. 4.28 (d), the supplement of  $\text{Fe}^0$  can assist to control the effluent nitrate not to be greater than 10 ppm-N when 40 and 50 g of  $\text{Fe}^0$  was added every 27 hr. The efficiency of nitrate removal increased after fresh of  $\text{Fe}^0$  supplement was introduced in the system. However, the supplement of  $\text{Fe}^0$  at 30 g could not assist to control nitrate to below the drinking water standard. It might be due to the mass of  $\text{Fe}^0$  in the system that was lower than during the first of 27 hr of operation. Regarding other indicators such as pH, DO, ORP as shown in Fig. 4.28 (a), (b) and (c), at the supplement of  $\text{Fe}^0$  40 g and 50 g  $\text{Fe}^0$ , a huge decreased in pH was not observed in the system. Moreover, DO in the system was very low at 0.02 mg/L. In addition, the ORP was in the range of -724 to -658 mV. In contrast, the indicator at the supplement of  $\text{Fe}^0$  at 30 g was shown that the profile was not steady in each parameter which is related to the nitrate removal result. Therefore, the supplement of  $\text{Fe}^0$  at 30 g was not suitable for controlling the system at every 27 hr. However, the optimal  $\text{Fe}^0$  supplement in the system should be considered for optimizing marginal benefit and controlling the concentration of ferrous ion as by product from  $\text{Fe}^0$ . As result, the effect of  $\text{Fe}^0$ , the higher  $\text{Fe}^0$  dosages, the higher ferrous concentration must occur in the system. Comparing the supplement of  $\text{Fe}^0$  at 40 g and 50 g, it can be said that the 40 g  $\text{Fe}^0$  of supplement can be the admirable  $\text{Fe}^0$  supplement for controlling nitrate removal efficiency and ferrous concentration formation.

#### **4.2.2 Ferrous removal by Iron precipitation process**

According to ferrous removal by iron precipitation, the experiments were conducted in a continuous process by varying sand dosages at the size of 0.42-0.59 mm from 10 to 20 kg with the air flow rate of 5 L/min and a bed expansion of 0.25 from original

level. The liquid feeding rate was 50 mL/min. In Fig. 4.29(a), pH of the system increased to around neutral (6.2 to 7.3). According pH from nitrate reduction process, pH was around 6.1. pH in this system can increase by using air for stripping  $\text{CO}_2$  from carbonation process. According to DO as shown in Fig. 4.29(b), DO in all experiments increased to around 6 to 10 mg/L. Regarding DO from nitrate reduction process, it was nearly zero. Oxygen from air flow could sufficiently oxidize ferrous ion to ferric ion and precipitate later. As seen in Fig. 4.29(c), the ORP value during 0 to 10 hr dropped to around -50 to 50 mV.

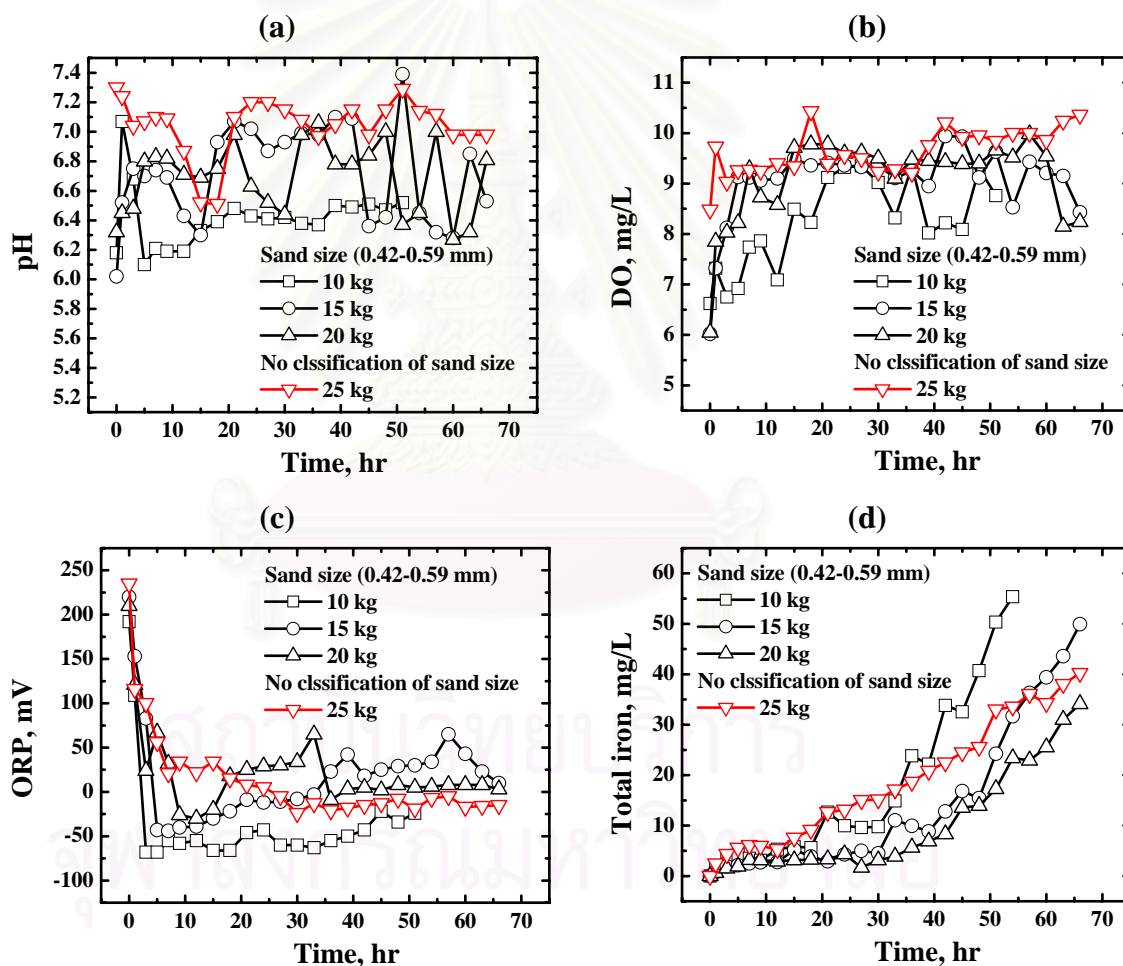


**Fig. 4.29 Effect of sand dosage on iron removal (a) pH, (b) DO, (c) ORP, and (d) total iron residue.** The experiment was conducted under the conditions of air flow rate of 5 L/min and a bed expansion of 0.25 from original level. The feeding rate of solution was 50 mL/min.



The decreased of ORP value in the beginning stage occur from ORP value in the solution of  $\text{Fe}^0/\text{CO}_2$  process around -720 mV combined with solution in the iron precipitation process which have initial value as around 180-230 mV. The iron removal for different sand dosage was shown in Fig. 4.29(d). Ferric ion was completely converted to iron solid form. In the first stage, total iron in the effluent increased slightly and remained steady for 15 hours; however, it increased rapidly afterward in the second stage. Residual iron for 10, 15, and 20 kg of sand within the first stage of 18, 30, and 36 hours, respectively, was not greater than 5 mg/L as compared to the feeding concentration of 320-450 mg/L. As the availability of sand surface for iron precipitation was limited in the second stage, more and more iron was leached out from the bed. It is necessary to mention that the effluent irons in all scenarios were still higher than the drinking water standard of 0.3 mg/L. This might be due to the shear force occurred on the sand surface as a result from fluidization flow rate. Bubble generated from air can impede the coating of iron onto sand due to abrasion at the surface of sand. Considering on the effect of sand size, it was found that size of 0.42-0.59 mm provided better iron removal than “no classification” size (commercial sand). Although their performances on iron removal were different, profiles of pH, DO, and ORP were quite similar regardless on sand size. Availability of sand surface is a very important factor affecting on the coating performance. For commercial sand, 66% of the sand has the size between 0.59-0.84 whereas 25% is between 0.42-0.59 as shown in Table 3.2. As we know, larger sand size has lower specific surface area than the smaller one. As a result, of the 25 kg of “no classification” sand, 16.5 kg has the diameter in between 0.59 and 0.84 mm whereas only 6.5 kg has the size between 0.42 and 0.59 mm. Therefore, it is not surprised that the iron removal efficiency of “no classification” sand was lower than those of 0.42-0.59 mm sand even it was supplied at a higher dosage. In conclusion, grain size for fluidized material is a very important issue that needed to be considered for system performance. Particularly those want to meet the drinking water standard. Air flow rate and bubble size which can impede the coating of iron onto sand surface are also other important factors that needed to be taken care as well. Future studies are required to investigate into more details regarding on this regard.

### 4.2.3 Ammonia removal by air stripping process

To investigate on the ammonia stripping efficiency, several experiments were conducted at pH 12 and air flow rates of 150 and 180 mL/min. Supernatant was re-neutralized by CO<sub>2</sub> at the flow rate of 400 mL/min. The initial NH<sub>4</sub><sup>+</sup> concentration was 23.9 mg N/L. The liquid feeding rate was 50 mL/min. In Fig 4.30(a), it was observed that pH was around neutral. Therefore, the bubbling of CO<sub>2</sub> at 400 mL/min was very efficient for controlling pH in neutral range. Ammonia removal was shown in Fig. 4.30(b). The results showed that the ammonia increased during initial stage of 7 hr. This may be due to the lapsed time for the treated ammonia solution to transport from the first tank of the cascade reactor, passing through the 6 tanks of cascade reactor, to the effluent outlet. The ammonia residual decreased with increasing air flow rate. The ammonia residual at air flow rate of 180 L/min and 150 mg N/L was approximately 2.3 and 3.6 mg N/L. The ammonia removal in each tank at 24 hr was shown in Fig. 4.30(c). The sample was collected at the effluent port of each tank. It was observed that ammonia concentration decreased with increasing the number of tank. Ammonia removal occurred significantly from the solution during high concentration as shown in tray NO.1 to 3. As the ammonia concentration decreased, the stripping rate decreased as well. Ammonia removal was slightly occurred in tray NO.6. It might be due to the pH in this tank which was controlled at neutral by CO<sub>2</sub> gas and was lower than the pK<sub>a</sub> of 9.3. Therefore, ammonia was hardly removed from the solution. Regarding drinking water standard, ammonia residual from preliminary test was beyond the standard. Therefore, an improvement of ammonia stripping system should be considered toward the air flow rate and stripping time. Increasing of air flow rate can increase the ammonia removal efficiency. However, the increasing of air flow rate might be related to the volume of the stripping tank. It can also reduce retention time for ammonia removal.

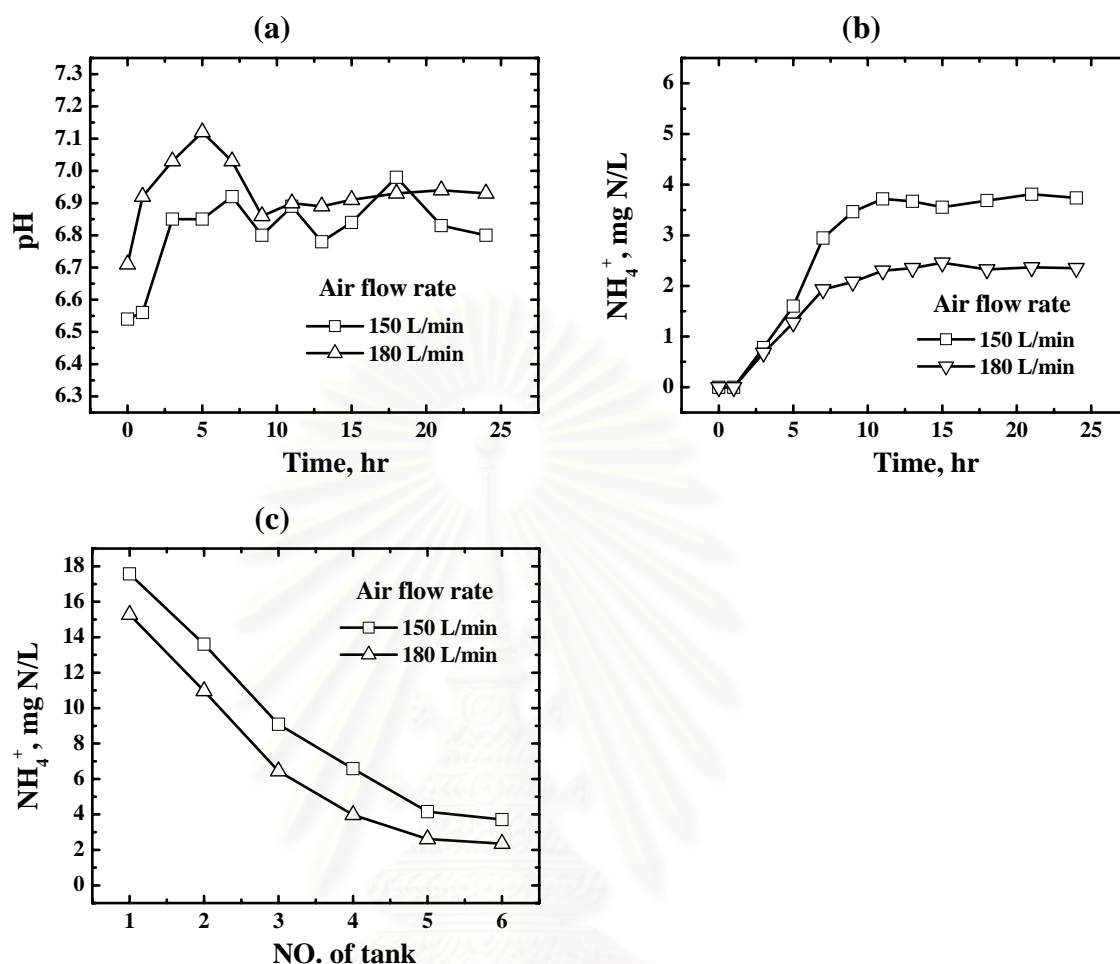


**Fig. 4.30 Effect of air flow rate on ammonia removal (a) pH, (b)  $\text{NH}_4^+$  removal, and (c)  $\text{NH}_4^+$  removal in each tray.** The experiment was conducted under the conditions of controlling pH at 12 and varying of air flow rate was 150 and 180 mL/min. Tray NO. 6 was used for adjusting pH to neutral by using  $\text{CO}_2$  flow rate at 400 mL/min. The initial  $\text{NH}_4^+$  concentration was 23.9 mg N/L. The feeding rate of solution was 50 mL/min.

### 4.3. Field Testing Study

#### 4.3.1 Nitrate reduction by $\text{Fe}^0/\text{CO}_2$ process

Nitrate removal between nitrate spiked in groundwater and RO water scenarios was compared. 40 g of  $\text{Fe}^0$  in the presence of  $\text{CO}_2$  bubbling with a constant flow rate of 200 mL/min and an initial nitrate concentration of 23 mg N/L was selected as the base conditions. The groundwater characteristic was shown in Table 3.3. According to pH in Fig. 4.31(a), pH profile of nitrate spiked RO water scenario

was observed to drop rapidly from the neutral value to 5.7 in 10 min; however that of nitrate spiked groundwater scenario dropped to around 5.9 at 10 min. The pH of profile in groundwater was slightly higher than that of profile in RO water. It might be from alkalinity from water quality. Then, pH profile of RO water and groundwater increased to 6 after 20 min and 6.2 after 1 hr, respectively. This was indicated activation of zero-valent iron surface for the groundwater test was taken time longer than that for RO water test. It might be effect of water characteristic such as dissolve organic carbon that might inhibit the surface of  $\text{Fe}^0$ . During the operation, pH profile gradually decreased and significantly dropped as shown at 27 hr for RO water test and at 30 hr for groundwater test. The different time of significantly decreasing pH for two tests was related to the remaining mass of  $\text{Fe}^0$  dosage in the system. The loss of  $\text{Fe}^0$  mass through its corrosion reaction in the system can lead to less consumption of  $\text{H}^+$ , therefore, decreasing of pH significantly can obviously occurred in the solution. As presented in Fig. 4.31(b), the DO of profile dropped nearly zero within 5 min. However, DO increased when the system was operated at longer time. It was due to the decreasing of  $\text{Fe}^0$  mass in the system. Therefore, oxygen consumed by  $\text{Fe}^0$  was lower. In regard to ORP (Fig. 4.31(c)), the ORP value in the both systems decreased significantly from positive to negative value. It can be pointed out that the reducing environment occurred in the system. However, the ORP profile of RO water significantly increased at 36 hr sooner than that of groundwater which began after 39 hr. In Fig. 4.31(d), it appears that nitrate of nitrated spiked in RO water scenario remained unchanged within the initial period of 1 hr. This may be due to the lag time for the treated nitrate solution to transport from the first compartment, passed through the second compartment, to the effluent outlet. In addition, it also takes time to remove impurities from the  $\text{Fe}^0$  surface since it was used without any pretreatment. In contrast, nitrate of nitrated spiked in groundwater remained unchanged within the first 1.5 hr. Therefore, it showed that water characteristic of groundwater might affect the  $\text{Fe}^0$  surface. It has to take longer time to activated  $\text{Fe}^0$  surface. Following the lag phase, the nitrate dropped rapidly. The comparison nitrate removal profile between RO water test and groundwater test showed that the residual nitrate in RO water test was better than that in groundwater test.

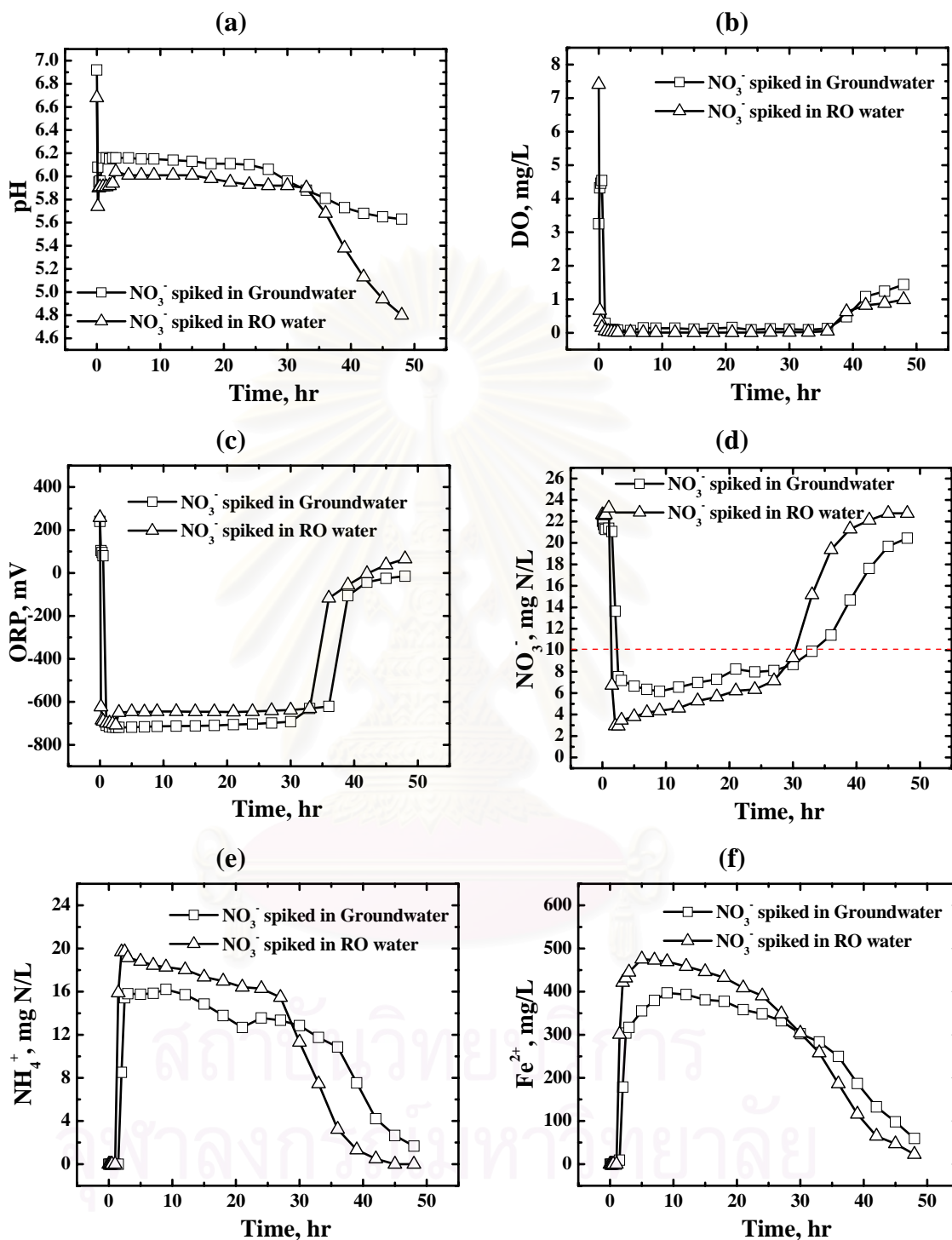


**Fig. 4.31 Comparison system performance between  $\text{NO}_3^-$  spiked groundwater and  $\text{NO}_3^-$  spiked RO water (a) pH, (b) DO, (c) ORP, (d)  $\text{NO}_3^-$  removal, (e)  $\text{NH}_4^+$  formation, and (f)  $\text{Fe}^{2+}$  formation.** The experiment was conducted under the conditions of  $\text{CO}_2$  bubbling rate of 200 mL/min and a recirculated flow of 90 L/min. The influent nitrate concentration was 23 mg N/L. the initial  $\text{Fe}^0$  of 60 g was tested.

It might be due to the inhibiting effect of the water chemistry of groundwater to nitrate removal such as dissolved organic carbon and  $\text{Ca}^{2+}$ . However, nitrate removal in groundwater test can occur more than 70%. It might be promoted by chloride that was found very high in the groundwater. Nevertheless, nitrate removal in groundwater was greater than that in RO water test of nitrate spiked in RO water after 30 hr. It was related to the remaining of  $\text{Fe}^0$  mass in the system. The higher consumption of  $\text{Fe}^0$  with greater nitrate removal for RO water test was occurred comparing with groundwater test. Therefore, the utilization of  $\text{Fe}^0$  mass for nitrate reduction was not enough when the diminishing of  $\text{Fe}^0$  was happened in long time operation. Concerning the by-product of reaction, ammonium was produced rapidly when the nitrate reduction began as shown in Fig. 4.31(e). The ammonium formation rate became decreasing when the nitrate reduction rate slowed down. Ferrous formation occurred when the nitrate reduction began. It is interesting to point out that the initial lag phase for ferrous accumulation was observed for both tests. It might be due to the time required for ferrous ion to transfer from the first compartment, passing through the second compartment, to the effluent outlet. Moreover, the activation time of  $\text{Fe}^0$  surface is needed as well for removing impurities from the surface of  $\text{Fe}^0$ . As seen in Fig. 4.31(f), the ferrous formation in the test of nitrate spiked in RO water scenario was higher than that in the groundwater scenario from lag phase to 30 hr. However, ferrous formation in the nitrate spiked in groundwater scenario was higher than that RO water after 30 hr. It was due to the remaining of  $\text{Fe}^0$  mass in the system related to corrosion of  $\text{Fe}^0$  process as mentioned above in nitrate removal section. To ensure the compliance with effluent standard, it was found that extra  $\text{Fe}^0$  should have been supplemented at every 27 hr rather than every 30 hr for safety factor consideration.

To investigate process operation, the supplement of 40 g of fresh  $\text{Fe}^0$  was decided at every 27 hr to control nitrate to be less than 10 mg N/L. As seen in Fig. 4.31(d), the supplement of  $\text{Fe}^0$  can assist to control nitrate removal effectively. The efficiency of nitrate removal can increased after fresh  $\text{Fe}^0$  was introduced in the system. Regarding on indicator other such as pH, DO, ORP in Fig. 4.32(a), (b) and (c), with the supplement of 40 g  $\text{Fe}^0$ , pH did not decrease significantly. Moreover, DO in the system was stable around 0.02 mg/L. In addition, the ORP was steady approximately -700 mV. As a result, it can be said that the supplement of 40 g  $\text{Fe}^0$  can

be the admirable  $\text{Fe}^0$  supplement for controlling nitrate removal efficiency to achieve drinking water standard. However, the optimal  $\text{Fe}^0$  supplement in the system should be considered for optimizing marginal benefit and controlling the concentration of ferrous ion as by product from  $\text{Fe}^0$ . Therefore the optimal  $\text{Fe}^0$  supplement for groundwater needs to be studied further.

### 4.3.2 Ferrous removal by iron precipitation process

The effectiveness of ferrous removal by iron precipitation was tested in groundwater and RO water. In Fig. 4.33(a), pH of groundwater was found to be higher than that of RO when air flow rate at 5 L/min was introduced into the system. However, it can be seen that pH of the solution was around neutral pH, i.e., 7.6 for ground water and 6.8 for RO water. DO of groundwater test and RO water test increased to around 11 and 10 mg/L, respectively, as shown in Fig. 4.33(b). Since the DO in the solution after nitrate reduction was nearly zero; therefore, it can be said that oxygen from air flow was sufficient for oxidizing ferrous ion to ferric ion which, it will precipitate later. As seen in Fig. 4.33(c), the ORP value of groundwater test decreased from 212 mV to  $-30 \pm 20$  mV from 149 mV to  $-50 \pm 20$  mV for RO water experiment. According to iron removal as shown in Fig. 4.33(d), iron residual profile of groundwater test was higher than that of RO water test. Even though, the iron concentration from  $\text{Fe}^0/\text{CO}_2$  process in groundwater test was higher than that in RO test as around 450 mg/L and 380 mg/L, respectively. The primary reason for low iron removal in groundwater test might be due to the competition between iron and calcium precipitated on sand surface.  $\text{CaCO}_{3(s)}$  and  $\text{Ca}(\text{HCO}_3)_{2(s)}$  can form in the system with the high calcium-hardness groundwater (Chen et al, 2000). Therefore, not only iron hydroxide was mainly found on the sand surface, but also  $\text{CaCO}_{3(s)}$  and  $\text{Ca}(\text{HCO}_3)_{2(s)}$  might begin to dominate on porosity of sand. Therefore, the application of iron precipitation in sand fluidization for groundwater should consider the level of calcium because calcium might impede iron precipitation on the sand. Regarding on nitrate as shown in Fig. 4.33(e), it was shown that nitrate profile increased rapidly in the beginning stage.

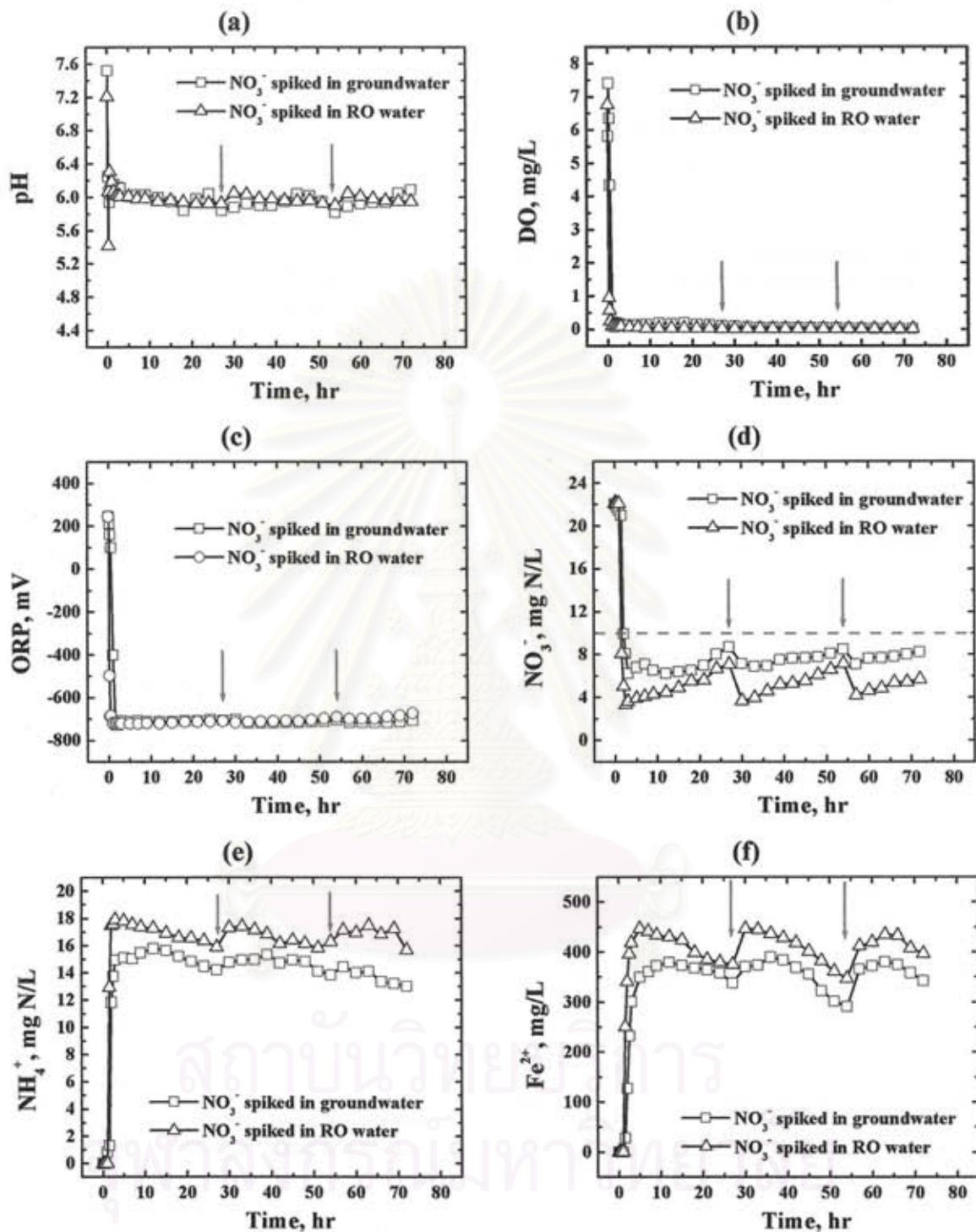


**Fig. 4.32** Performance comparison of nitrate reduction by  $\text{Fe}^0/\text{CO}_2$  in integrated system between  $\text{NO}_3^-$  spiked groundwater and  $\text{NO}_3^-$  spiked RO water (a) pH, (b) DO, (c) ORP, (d)  $\text{NO}_3^-$  removal, (e)  $\text{NH}_4^+$  formation, and (f)  $\text{Fe}^{2+}$  formation. The experiment was conducted under the conditions of  $\text{CO}_2$  bubbling rate of 200 mL/min and a recirculated flow of 90 L/min. The influent nitrate concentration was 23 mg N/L. the initial  $\text{Fe}^0$  of 60 g was tested. The 40g of  $\text{Fe}^0$  supplement was introduced in the system at times of 27 hrs and 54 hrs, respectively.



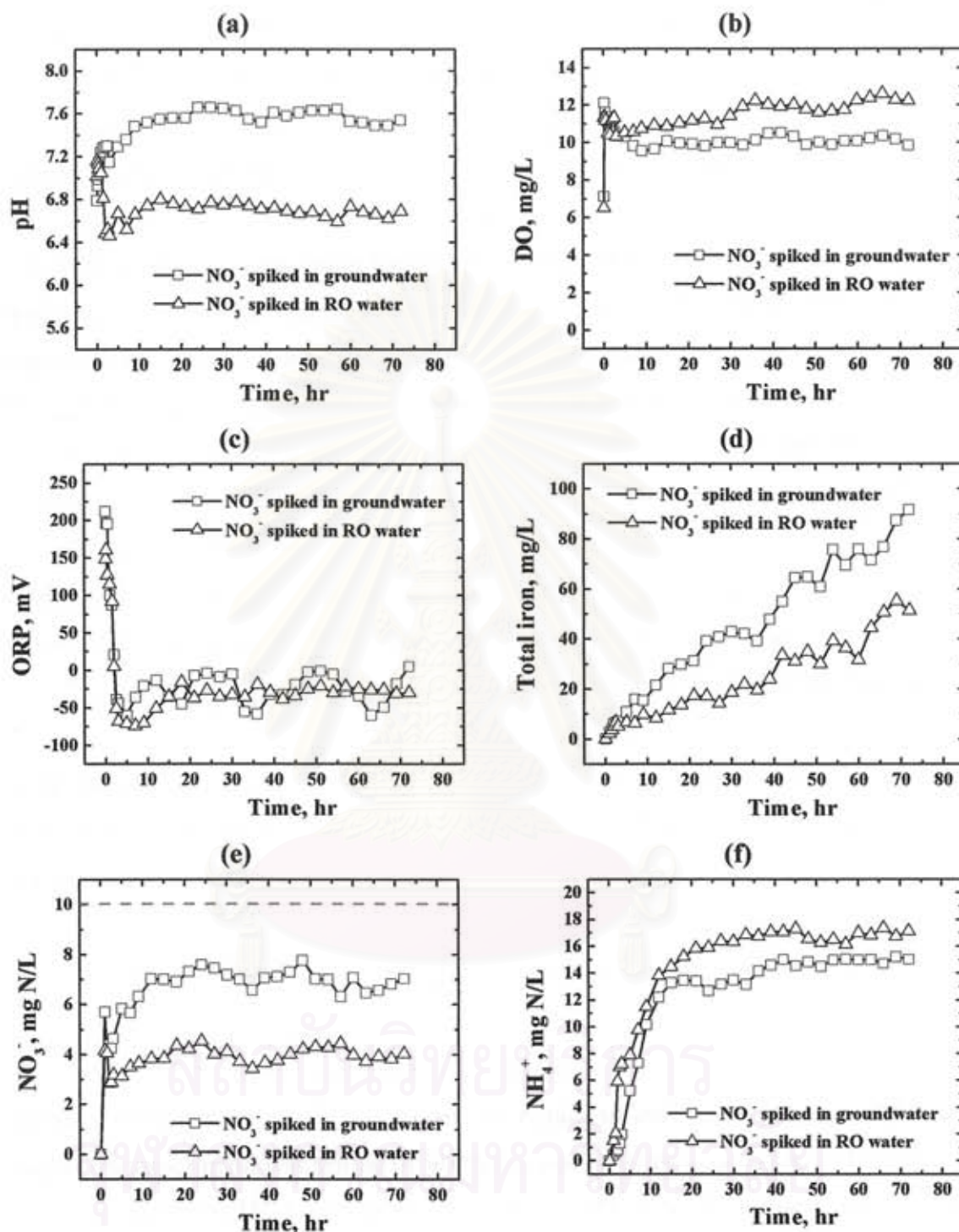


**Fig. 4.33** Performance comparison of iron precipitation in integrated system between  $\text{NO}_3^-$  spiked groundwater and  $\text{NO}_3^-$ -spiked RO water (a) pH, (b) DO, (c) ORP, (d)  $\text{NO}_3^-$  residue, (e)  $\text{NH}_4^+$  residue, and (f)  $\text{Fe}^{2+}$  residue. The experiment was conducted under the conditions of air flow rate of 5 L/min and a bed expansion of 0.25 from original level. The feeding rate of solution was 50 mL/min.

The rapid increase of nitrate and ammonium value in the beginning stage was due to the high nitrate solution from  $\text{Fe}^0/\text{CO}_2$  process mixing with RO water in the iron precipitation process during the first hour leading, to the dilution of nitration concentration in the initial stage. However, nitrate remained between 6 and 8 mg N/L in groundwater test and between 3 and 5 mg N/L in RO water test after system was steady. According to ammonium formation as shown in Fig. 4.33(f), it was observed that ammonium profile gradually increased in the beginning stage of 10 hr and remained quite steady between 6 to 8 mg N/L in groundwater test and between 15 and 17 mg N/L, respectively. Westerhoff et al. (2003) mentioned about the possibility of ammonium and nitrate sorption onto precipitated metal oxides. They found that iron oxides had point of zero charge between 5 and 8.5 whereas the pH observed in the groundwater and RO water were approximately 6.8 and 7.6, respectively. Hence, certain surface of the oxides would have net negative charges and allowed ammonium ion adsorption to occur. However, nitrate sorption could occur via sorption onto some specific positively charged surfaces through electrostatic attraction or ligand exchange (i.e., surface hydroxide; green rust). The results from this study; nevertheless, indicated the difference in input and output concentration of  $\text{NO}_3^-$  and  $\text{NH}_4^+$ , if any, were small. It implied that the sorption of  $\text{NO}_3^-$  and  $\text{NH}_4^+$  onto metal oxide surface was not insignificant.

### 4.3.3 Ammonia removal by air stripping process

The comparison of ammonia removal by air stripping was tested between the ferrous solution produced from  $\text{Fe}^0/\text{CO}_2$  process of nitrate spiked in groundwater and RO water. The experiment was started by using RO water. pH was controlled at 12 and air flow rate was set at 180 L/min from tray NO. 1 to NO. 5. Solution pH for tray NO.6 was controlled at neutral by recarbonation with 400 mL/min of  $\text{CO}_2$  gas as shown in Fig. 4.34(a). Regarding on DO in Fig. 4.34(c), DO dropped from the initial value of 8.5 and 6.5 to around 4 mg/L for RO water test and 2 mg/L for groundwater, respectively. This might be due to oxygen stripping by  $\text{CO}_2$ . According to ORP value in Fig. 4.34(c), it showed that ORP was positive in both of tests. Ammonia removal profile was shown in Fig. 4.34(d).

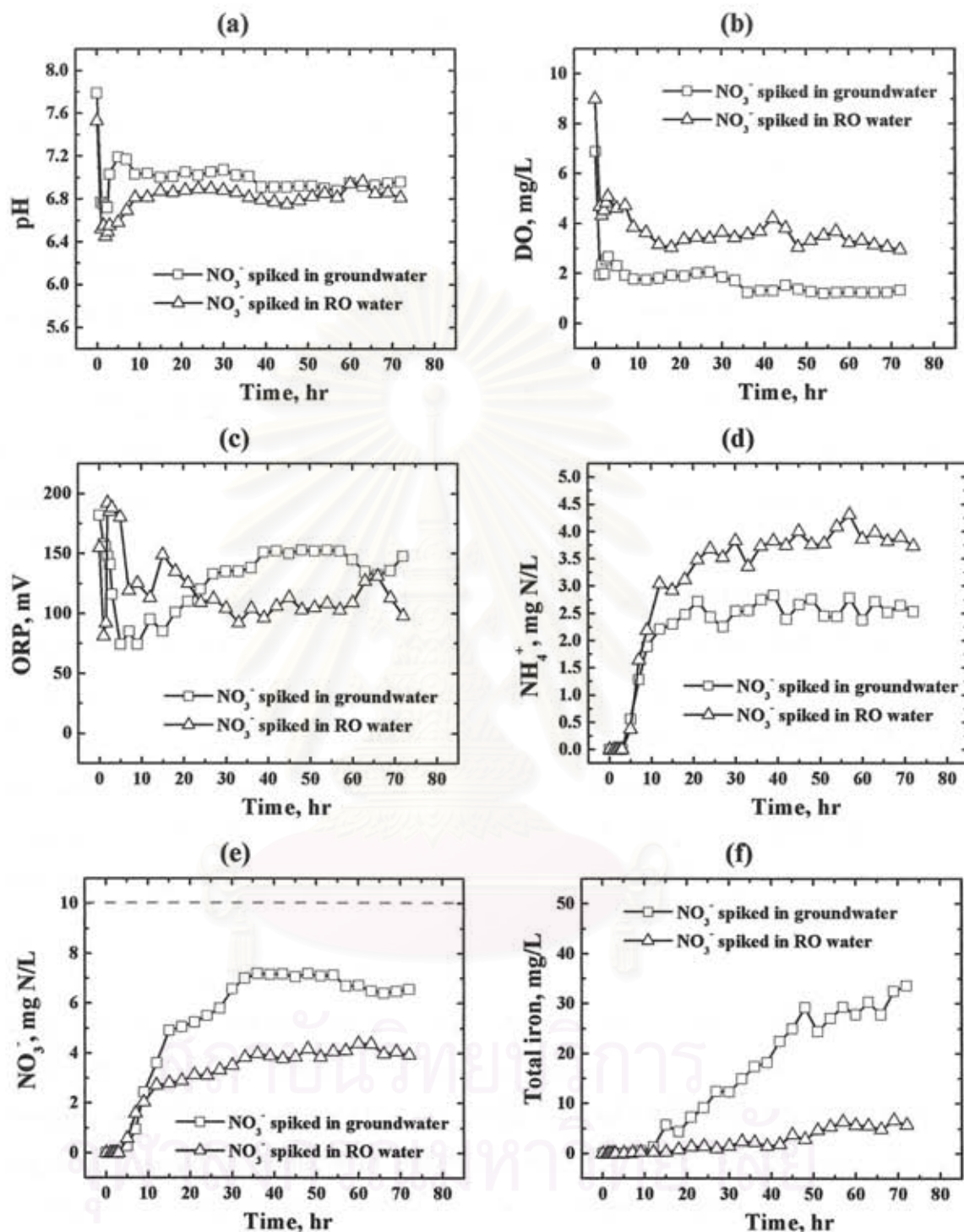


**Fig. 4.34 Performance comparison of ammonia stripping in integrated system between  $\text{NO}_3^-$  spiked groundwater and  $\text{NO}_3^-$ -spiked RO water (a) pH, (b) DO, (c) ORP, (d)  $\text{NO}_3^-$  residue, (e)  $\text{NH}_4^+$  residue, and (f)  $\text{Fe}^{2+}$  residue. The experiment was conducted under the conditions of controlling pH at 12 and air flow rate 180 L/min. Tray NO. 6 was used for adjusting pH to neutral by using  $\text{CO}_2$  flow rate at 400 mL/min. The feeding rate of solution was 50 mL/min.**

The gradually increasing of ammonium profile from 0 to 10 hr was due to time spent for solution to flow from tray NO. 1 to tray NO. 6. Ammonium concentration from the iron precipitation unit for groundwater test and RO water test was 14 and 17 mg N/L, respectively. It decreased to around 2.5 mg N/L for groundwater test and 3.5 mg N/L for RO test after the system was steady. High ammonium concentration beyond the drinking standard might be due to insufficient of the air flow rate for stripping of ammonia from the system as well as the stripping time. It should be studied further to search for the more effective setup for this process to achieve the drinking water standard. Regarding nitrate residual in Fig. 4.34(e), nitrate was less than 10 mg N/L in both tests. Nitrate after 10 hr remained between 6 and 8 mg N/L in groundwater test and between 3 and 5 mg N/L. Therefore, nitrate concentration can meet the standard of the drinking water. Surprisingly, the precipitation of iron in the ammonia stripping tank was also found in both of tests. Therefore, iron residual from the effluents in both tests were lower than inlet iron concentration derived from precipitation process as shown in Fig. 4.34(f). However, iron precipitation was obviously seen in the RO water test more than in groundwater. Iron precipitation can be observed from the bottom of ammonia stripping tank and the solution became clearer than in the iron precipitation tank. The iron residual profile of groundwater test gradually increased with time. It can be seen that the color of solution was still yellow brown in ammonia stripping tank. In addition, some white solids were observed in the groundwater test and expected to be calcium carbonate and/or magnesium hydroxide. Calcium and magnesium in groundwater were 42.8 mg/L and 26.7 mg/L, respectively as shown in Table 3.3. At pH 12, all carbonate species would be in the form of  $\text{CO}_3^{2-}$  which could combine with  $\text{Ca}^{2+}$  and precipitated out in the form of  $\text{CaCO}_3$ . By the same focus, magnesium could combine with hydroxide and precipitate out. However, these divalent cations did not exist in RO water; as result, no precipitate occurred in the reactor of ammonia stripping.

## CHAPTER V

### CONCLUSIONS AND SUGGESTIONS FOR FUTURE WORKS

#### 5.1 Conclusions

##### 5.1.1 Batch mode study

The  $\text{Fe}^0/\text{CO}_2$  process was investigated for removing nitrate from aqueous solution under various operating conditions. As a result, the bubbling of  $\text{CO}_2$  flow rate at 200 mL/min was sufficient for supplying  $\text{H}^+$  to create a favorable acidic environment for the nitrate reduction. The nitrate removal behavior can be described by an S-curve equation successfully, the  $t_{1/2}$  in which depends on the  $\text{Fe}^0$  dosages of relatively small values under various initial nitrate concentrations. In other words, the higher the  $\text{Fe}^0$  dosage, the lower the  $\text{NO}_3^-$  residue in the reaction solution, however, the marginal benefit is decreasing as the  $\text{Fe}^0$  is applied in excess. With various operating modes, the removal efficiency of  $\text{NO}_3^-$  by  $\text{Fe}^0$  decreases with increasing number of batch treatment. In addition, the batch mode with treated solution emptied and freshly refilled (Mode 2) outperforms the one (Mode 1), which was operated by retaining the treated solution and spiking concentrated nitrate into it for the next batch treatment. One key reason behind such phenomenon exists in the difference of pH variation. In Mode 1, the pH was seen to increase gradually along the reaction time within each batch treatment, leading to the deterioration of nitrate removal performance. Another reason is due to the concentration gradient of  $\text{Fe}^{2+}$  between bulk solution and  $\text{Fe}^0$  surface becoming smaller and smaller in Mode 1, and ultimately this result in stronger suppression of  $\text{Fe}^{2+}$  dissolution from the  $\text{Fe}^0$  surface. In addition, measure of the optimum  $\text{Fe}^0$  supplement needs to be taken to guarantee satisfactory nitrate removal in batch operation using the  $\text{Fe}^0/\text{CO}_2$  process.

With various water characteristics, it is concluded that nitrate removal decreased remarkably with increasing humic acid concentration. The blockage of reactive sites may occur from adsorption of humic acid onto the surface of  $\text{Fe}^0$ . In

addition, calcium ions inhibit the removal of nitrate significantly due to its suppression of  $\text{Fe}^{2+}$  dissolution from  $\text{Fe}^0$  surface as well as calcium carbonate coating onto  $\text{Fe}^0$  surface if there's the presence of  $\text{CO}_3^{2-}$  in solution under alkaline condition. On the contrary, increasing chloride concentration leads to the increase of nitrate reduction efficiency. Chloride ions in solution inducing pitting corrosion of the  $\text{Fe}^0$  surface could enhance surface reactivity or increase reactive surface area of the  $\text{Fe}^0$  for  $\text{NO}_3^-$  reduction to occur. In addition, chloride ions may also pull  $\text{Fe}^{2+}$  out of the  $\text{Fe}^0$  surface, leading to a higher reduction rate of nitrate. Other background species such as sodium ions imposes only slight inhibition on nitrate reduction. Under the studied condition, water molecule was found to play an important role of consuming electrons in a significant way.

The ferrous removal from the  $\text{Fe}^0/\text{CO}_2$  process was investigated by using the fluidized sand bed reactor. Air was selected for converting ferrous ion to iron solid form. The results show that the lower air flow rate for ferrous removal in the fluidized sand bed reactor is preferred. Consequently, the air flow rate at 20 ml/min was selected as the optimal air flow rate for operation. Regarding sand dosage, the optimum sand dosage of 400 g/L at sand size of 0.42-0.59 mm is recommended in the case of initial ferrous of 185 mg/L. 300 g/L of sand dosage at sand size of 0.096-0.21 mm is sufficiently enough to remove 185 mg/L of total iron from the solution. The effect of sand dosage on iron removal in fluidized bed process was considered to be due to the greater specific area for iron precipitation with the increasing of sand dosage. Percent iron removal decrease with increasing iron concentration. Under the studied condition, air flow rate and surface area of sand was found to play an important role for iron precipitation process.

Ammonium is the dominating end product in the nitrate reduction by  $\text{Fe}^0/\text{CO}_2$  process. The optimum pH at 12 is recommended for operated pH. The result showed that ammonium removal increased with increasing air flow rate. Considering on kinetic analysis, rate constant decreases with the increasing ammonium concentration.

### 5.1.2 Continuous mode study

Innovative reactor was designed and investigated for removing nitrate from aqueous solution. The 23.5 mg-N/L of nitrate can be reduced to 2.93 mg-N/L within 2.5 hrs by using the condition as follows: 3 L/hr of the influent feeding rate, 60 g of Fe<sup>0</sup> dosage, and 200 mL/min of CO<sub>2</sub> gas inflow rate. The higher mass Fe<sup>0</sup> consumption for NO<sub>3</sub><sup>-</sup> removal occurred in higher nitrate concentration and feeding solution. The measure of the optimum Fe<sup>0</sup> supplement needs to be taken to guarantee satisfactory nitrate removal in batch operation using the Fe<sup>0</sup>/CO<sub>2</sub> process. In this study, the supplement of 40 g of Fe<sup>0</sup> at every 27 hrs was found to be sufficient to consistently maintain the residual nitrate at a level that complies with the drinking water quality standard and ferrous concentration formation in the system.

According to ferrous removal by iron precipitation, time of utilizing sand for iron removal increases with increasing sand dosage. The greater specific area of sand in smaller size can increase the iron removal efficiency. However, air bubble can impede the coating of iron onto sand due to abrasion at the surface of sand.

Regarding on ammonia removal by air stripping, the increasing of air flow rate can increase the ammonia removal efficiency. In addition, the increasing retention time can increase ammonia removal efficiency also.

### 5.1.3 Field testing study

Fe<sup>0</sup>/CO<sub>2</sub> process was selected as an innovative purification technology for treating nitrate-contaminated groundwater of Chia Nan University of Pharmacy and Science. The comparison nitrate removal profile between RO water test and groundwater test showed that the residual nitrate in RO water test was better than that in groundwater test. It might be due to the inhibiting effect of the water chemistry of groundwater to nitrate removal such as dissolved organic carbon and Ca<sup>2+</sup>. However, nitrate removal in groundwater test can occur more than 70%. It might be promoted by chloride that was found very high in the groundwater. Regarding process operation, the 40 g Fe<sup>0</sup> of supplement can be the admirable Fe<sup>0</sup> supplement for controlling nitrate removal efficiency to achieve drinking water standard at every 27

hr.

According to iron removal, iron residual of groundwater test was higher than that of RO water test. The competition between iron and calcium which precipitated on sand surface might be the reason.  $\text{CaCO}_3$  (s) and  $\text{Ca}(\text{HCO}_3)_2$  can form in the system with the high calcium hardness in groundwater. Therefore, not only iron hydroxide was mainly found on the sand surface, but also  $\text{CaCO}_3$  (s) and  $\text{Ca}(\text{HCO}_3)_2$  (s) might begin to dominate on porosity of sand. Therefore, the application of iron precipitation in sand fluidization for groundwater should consider the level of calcium in the process because calcium might impede iron precipitation on the sand.

Regarding on ammonia stripping, ammonium residual of RO water test was higher than that of groundwater test. It might be the reason of ammonium concentration from the iron precipitation process at groundwater test higher than RO water test as 17 mg N/L and 14 mg N/L, respectively. The precipitation of iron solid occurred in the ammonia stripping tank. iron precipitation was obviously seen in the RO water test more than in groundwater. At pH 12, all carbonate species would be in the form of  $\text{CO}_3^{2-}$  which could combine with  $\text{Ca}^{2+}$  and precipitated out in the form of  $\text{CaCO}_3$ . By the same focus, magnesium could combine with hydroxide and precipitate out. However, these divalent cations did not exist in RO water; as result, no precipitate occurred in the reactor of ammonia stripping.

## 5.2 Suggestions for future work

Dissolved organic carbon and hardness which have negative effect on the system performance were found in a significant amount in the groundwater at Chia Nan University of Pharmacy and Science. Therefore, removal of these constituents either by precipitation or adsorption maybe necessary in order to improve this integrated system. Moreover, the effect of  $\text{Mg}^{2+}$  on the nitrate removal by  $\text{Fe}^0/\text{CO}_2$  was recommended to study further.

Air bubble can impede the coating of iron onto sand due to abrasion at the sand surface. The decreasing of air flow rate can lower the shear force between sand surface and iron solid. However, the converting ferrous to ferric and sequentially to iron hydroxide should be considered. Feeding  $\text{H}_2\text{O}_2$  in the system can be an efficient



alternative for converting  $\text{Fe}^{2+}$  to  $\text{Fe}^{3+}$ . Nonetheless, the optimal ratio of  $\text{H}_2\text{O}_2$  and air flow rate needs to be investigated further.

Air bubble size is also an important factor for ammonia stripping. With finer bubble size, stripping time as well as air flow rate may be reduced while maintaining similar effectiveness. Further study on the effect of bubble size is required.

In view of application, iron coated sand possesses an advantage for degradation of organic contaminants simultaneously present in the treated water stream via Fenton-like oxidation with an addition of  $\text{H}_2\text{O}_2$ . It would be very interesting to study on the use of iron coated sand as a  $\text{Fe}^{3+}$  source for Fenton-like reaction. In addition, it is also worthwhile to study on its adsorption capacity for heavy metals.

The complete system of nitrate reduction, ferrous precipitation and ammonia stripping needs to be compared with other relevant methods such as ion exchange, denitrification by biological process on the basis of system performance and cost-effectiveness.

## REFERENCES

- Agrawal, A. and Tratnyek, P.G. (1996). Reduction of nitro aromatic compounds by zero-valent iron metal. Environmental Science and Technology 36, 299-306.
- Alowitz, M.J. and Scherer, M.M. (2002). Kinetics of nitrate, nitrite, and Cr(VI) reduction by iron metal. Environmental Science and Technology 36: 299-306.
- Banens, R.J. and Devis, J.R. (1998). Comprehensive approaches to eutrophication management: the Australian example. Water Science and Technology 37: 217-225.
- Benjamin M.M. (2002). Water chemistry (1<sup>st</sup> ed.). New York: McGraw-Hill.
- Bigg, T. and Judd, S.J. (2000) Zero-valent iron for water treatment. Environmental Technology 21: 661-670.
- Bonmati, A. and Flotats, X. (2003). Air stripping of ammonia from pig slurry: characterization and feasibility as a pre- or post-treatment to mesophilic anaerobic digestion. Waste Management 23: 261-272.
- Cao, J., Wei, L., Huang, Q., Wang, L. and Han, S. (1999). Reducing degradation of azo dye by zero-valent iron in aqueous solution. Chemosphere 38(3): 565-571.
- Chang, H.L., Hwang, R.J., Gung, H.B., Horng, S.J. and Su, J.L. (2002). Heterotrophic-denitrification pilot study in Hsin-Chia Water Treatment Plant on Nan-Tou operation station. Proceedings, The 8<sup>th</sup> International Conference on Drinking Water Management and Treatment Technologies, May 27-29, Chung Shan University, Kaohsiung, Taiwan: 3-14 – 3-30.
- Chen, H.Y., Yeh, H.H., Tsai, M.C. and Lai, W.L. (2000). The application of fluidized bed crystallization in drinking water softening. Journal of the Chinese Institute of Environmental Engineering 10: 177-184.
- Chen, Y.M., Li, C.W. and Chen, S.S. (2005). Fluidized zero valent iron bed reactor for nitrate removal. Chemosphere 59: 753-759.
- Cheng, I.F., Muftikian, R., Fernando, Q. and Korte, N. (1997). Reduction of nitrate to ammonia by zero-valent iron. Chemosphere 35: 2689-2695.
- Cheng, S.F. and Wu, S.C. (2000). The enhancement methods for the degradation of TCE by zero-valent metals. Chemosphere 41:1263-1270.

- Coehn, M. (1979). Dissolution of iron. In Corrosion Chemistry, ed. Brubaker, G.R., Beverly, P. and Phipps, P. Washington, D.C.: American Chemical Society.
- Chew, C.F. and Zhang, T.C. (1998). In situ remediation of nitrate contaminated groundwater by electrokinetics/iron wall processes. Water Science and Technology 36: 135-142.
- Choe, S., Chang, Y.Y., Hwang, K.Y. and Khim, J. (2000). Kinetics of reductive denitrification by nanoscale zero-valent iron. Chemosphere 41: 1307-1311.
- Choe, S., Liljestrand, H.M. and Khim, J. (2004). Nitrate reduction by zero-valent iron under different pH regimes. Applied Geochemistry 19: 335-342.
- Chuang, F.W., Larson, R.A., Wessman, M.S. (1995). Zero-valent iron promoted dechlorination of polychlorinated biphenyls. Environmental Science and Technology 29: 2460-2463.
- Cheung, K.C., Chu, L.M. and Wong, M.H. (1997). Ammonia stripping as a pretreatment for landfill leachate. Water, Air, and Soil Pollution 94, 209-221.
- Fan L.H. (1989). Gas-Liquid-Solid Fluidization Engineering. Butterworths Publishers, Miami, MA.
- Flis, J. (1991). Stress corrosion cracking of structural steels in nitrate solutions. In: Flis, J. (Ed.), Corrosion of Metals and Hydrogen-Related Phenomena. Materials Science Monograph, Vol. 59. Elsevier, Amsterdam, NL, pp. 57-94.
- Furukawa, Y., Kim, J.W., Watkins, J. and Wilkin, R.T. (2002). Formation of ferrihydrite and associated iron corrosion products in permeable reactive barriers of zero-valent iron. Environmental Science and Technology 36: 5469-5475.
- Gillham, R.W. and O'Hammesin, S.F. (1994). Enhanced degradation of halogenated aliphatics by zero-valent iron. Ground Water 32(6): 958-967.
- Gonzalez Benito, G. and Garcia Cubero, M.T. (1996). Ammonia elimination from beet sugar factory condensate streams by a stripping absorption system. Zuckerindustrie 121: 721-726.
- Gotpagar, J., Grulke, E., Tsang, T. and Bhattacharyya, D. (1997). Reductive dehalogenation of trichloroethylene using zero-valent iron. Environmental Progress 16(2): 137-142.

- Hsu, C.Y., Liao, C.H. and Lu, M.C. (2004). Treatment of aqueous nitrate by zero valent iron powder in the presence of CO<sub>2</sub> bubbling. Groundwater Monitoring and Remediation 24(4): 82-87.
- Hu, H.Y., Goto, N., Fujie, K., Kasakusa, T. and Tsubone, T. (2001). Reductive treatment characteristics of nitrate by metallic iron in aquatic solution. Journal of Chemical Engineering of Japan 34: 1097-1102.
- Huang, C.P., Wang, H.W. and Chiu, P.C. (1998) Nitrate reduction by metallic iron. Water Research 32: 2257-2264.
- Huang, Y.H. and Zheng, T.C. (2002). Kinetics of nitrate reduction by iron at near neutral pH. Journal of Environmental Engineering 128: 604-611.
- Huang, Y.H. and Zheng, T.C. (2004). Effects of low pH on nitrate reduction by iron powder. Water Research 38: 2631-2642.
- Kelly, E.J. (1965). The active iron electrode: iron dissolution and hydrogen evolution reactions in acidic sulfate solutions. Journal of Electrochemistry Society 112(2): 679-687.
- Janus, H.M. and Van Der Roest, H.F. (1997). Don't reject the idea of treating reject water. Water Science and Technology 35(10):27-34.
- Kabdasli, I., Tunay, O., Ozturk, I., Yilmaz, S. and Arikan, O. (2000). Ammonia removal from young landfill leachate by magnesium ammonium phosphate precipitation and air stripping. Water Science and Technology 41(1), 237-240.
- Karen M.M. (1987). Nitrate in drinking water. Available online at [[http://ohioline.osu.edu/b744/b744\\_5.html](http://ohioline.osu.edu/b744/b744_5.html)].
- Kielemoes, J., De Boever, P. and Verstraete, W. (2000). Influence of denitrification on the corrosion of iron and stainless steel powder. Environmental Science and Technology 34: 663-671.
- Kim, Y.H. and Carraway, E.R. (2000). Dechlorination of pentachlorophenol by zero valent iron and modified zero valent iron. Environmental Science and Technology 34: 2014-2017.
- Liao, P.H., Chen, A. and Lo, K.V. (1995). Removal of nitrogen from swine manure wastewaters by ammonia stripping. Bioresource Technology 54: 17-20.
- Liao, C.H., Kang, S.F. and Hsu, Y.W. (2003). Characteristics of reductive removal of nitrate by suspended zero-valent iron powder. Journal of the Chinese Institute of Environmental Engineering 13(4): 251-261.

- Liao, C.H., Kang, S.F. and Hsu, Y.W. (2003). Zero-valent iron reduction of nitrate in the presence of ultraviolet light, organic matter and hydrogen peroxide. Water Research 37: 4109-4118.
- Lide, D. (1993). Handbook of Chemistry and Physics. A Ready-reference Book of Chemical and Physical Data. CRC Press, Boca Raton.
- Matheson, L.J. and Tratnyek, P.G. (1994). Reductive dehalogenation of chlorinated methanes by iron metal. Environmental Science and Technology 28: 2045-2053.
- Menzer, R.E. (1991). Water and soil pollutants. In: AMDUR, M.O.; DOULL, J.; KLAASEN, C.D. Toxicology: the basic science of poisons. New York: Casarett & Doull's: pp. 872-902.
- Monicha, V.K. and Prabhakar, A.V.S. (1988). Ammonia removal and recovery from urea fertilizer plant waste. Environmental Technology Letters 9: 655-664.
- Nam, S. and Tratnyek, P.G. (2000). Reduction of azo dyes with zero-valent iron. Water Research 34(6): 1837-1845.
- Orth, W.S. and Grillham, R.W. (1996). Dechlorination of trichloroethene in aqueous solution using  $\text{Fe}^0$ . Environmental Science and Technology 30: 66-71.
- Phillip D.H., Gu B., Watson D.B., Roh Y., Liang L. and Lee S. Y. (2000). Performance Evaluation of a Zerovalent Iron Reactive Barrier: Mineralogical Characteristics. Environmental Science and Technology 34: 4169-4176.
- Piromlert, S. (1995). Nitrate affected groundwater in northeast Thailand. Proceedings, International Conference on Geology and Mineral Resources of Indochina (Geo-Indo'95): 513-520.
- Piron, D.L. (1991). Prediction of corrosion tendencies. In The Electrochemistry of Corrosion. Houston, Texas: NACE International-The Corrosion Society: pp. 37-61.
- Ponder, S.M., Darab, J.G. and Mallouk, T.E. (2000). Remediation of Cr(IV) and Pb(II) Aqueous solutions using Supported nanoscale zero-valent iron. Environmental Science and Technology 34: 2564-2569.
- Sayles, G.D., You, G., Wang, M. and Kupferle, M. (1997). DDT, DDD, and DDE dechlorination by zero-valent iron. Environmental Science and Technology 31: 3448-3454.

- Seller, R.M. (1980). Spectrophotometric Determination of Hydrogen Peroxide Using Potassium (IV) Oxalate. Analyst 105 (10): 950-954.
- Siantar, D.P., Schreier, C.G., Chou, C.S. and Reinhard, M. (1996). Treatment of 1,2-dibromo-3-chloropropane and nitrate contaminated water with zero-valent iron or hydrogen/palladium catalysts. Water Research 30: 2315–2322
- Singh, J., Comfort, D.D. and Shea, P.J. (1998). Remediating RDX-contaminated water and soil using zero-valent iron. Journal of Environmental Quality 27: 1240-1245.
- Snoeyink, V. and Jenkins, D. (1980). Water Chemistry, John Wiley & Sons, Inc.
- Standard Methods for the Examination of Water and Wastewater, 19th ed. (1995) American Public Health Association/American Water Works Association/Water Environment Federation, Washington DC.
- Su, C. and Puls, R.W. (2004). Nitrate reduction by zero valent iron: effects of formate, oxalate, citrate, chloride, sulfate, borate, and phosphate. Environmental Science and Technology 38(9): 2715-2720.
- Schiweck, H. and Nahle, C. (1990). Removal of ammonia from condensates and surplus condenser water by stripping with air. Zuckerindustrie 115: 639-647.
- Thorndahl, U. (1992). Nitrogen removal by treatment of reject water. In: Proceeding of European Conference on Nutrient Removal from Wastewater, Leeds: pp. 1-15.
- Till, B.A., Weathers, L.J. and Alvarez, P.J.J. (1998). Fe<sup>0</sup> supported autotrophic denitrification. Environmental Science and Technology 32: 634-639.
- Tratnyek, P.G., Scherer, M.M., Deng, B. and Hu, S. (2001). Effect of natural organic matter, anthropogenic surfactants, and model quinines on the reduction of contaminants by zero-valent iron. Water Research 35 (18): 4435-4443.
- U.S. EPA. (2000). Wastewater Technology Fact Sheet Ammonia stripping EPA 832-F-00-019, Washington D.C.
- Van Der Veen, C. and Graveland, A. (1988). Central softening by crystallization in a fluidized-bed process. Journal AWWA: 51-56.
- Watergroup (1990). Purification reject water from sewage treatment plants. Results of test run with pilot plant at the Saltebakkens Sewage Treatment Plant, Frederikshavn, Denmark. Watergroup Technical Letter: pp. 1-9.

- Walton, G. (1951). Survey of literature relating to infant methemoglobinemia due to nitrate-contaminated water. American Journal of Public Health 41: 986-995.
- Westerhoff, P. (2003). Reduction of nitrate, bromate, and chlorate by zero valent iron ( $\text{Fe}^0$ ). Journal of Environmental Engineering 129: 10-16.
- Westerhoff, P. and James, J. (2003). Nitrate removal in zero-valent iron packed columns. Water Research 37: 1818-1830.
- Wilkin, R.T., Puls, R.W. and Sewell, G.W. (2003). Long-term performance of permeable reactive barriers using zero-valent iron: geochemical and microbiological effects. Ground Water 41: 493-503.
- Whitman, G. W., Russell, R. P. and Altieri, V. J. (1924). Effect of hydrogen-ion concentration on the submerged corrosion of steel. Industrial & Engineering Chemistry Research 16: 665-670.
- Yang, G.C.C. and Lee, H.L. (2005). Chemical reduction of nitrate by nanosized iron: kinetics and pathways. Water Research 39: 884-894.
- Young, G.K., Bungay, H.R., Brown, L.M. and Parsons, W.A. (1964). Chemical reduction of nitrate in water. Journal of Water Pollution Control Federation 36: 395-398.
- Zawaideh, L.L. and Zhang, T.C. (1998). The effect of pH and addition of an organic buffer (HEPES) on nitrate transformation in  $\text{Fe}^0$ -water system. Water Science and Technology 38: 107-115.
- Zhou, P., Huang, J.C., Li, A.W.F. and Wei, S. (1999). Heavy metal removal from wastewater in fluidized bed reactor. Water Research 33: 1918-1924.



## APPENDICES

สถาบันวิทยบริการ  
จุฬาลงกรณ์มหาวิทยาลัย



## APPENDIX A

### Batch mode study of nitrate reduction by Fe<sup>0</sup>/CO<sub>2</sub> process

Table A-1 Effect of CO<sub>2</sub> inflow rates on aqueous solution

(a) CO<sub>2</sub> = 100 mL/min

Time (min)	pH	DO (mg/L)	ORP (mV)
0	6.76	6.68	274
10	3.76	2.22	300
20	3.72	0.42	329
30	3.69	0.32	340
40	3.73	0.21	345

(b) CO<sub>2</sub> = 200 mL/min

Time (min)	pH	DO (mg/L)	ORP (mV)
0	6.81	7.1	254
10	3.49	0.16	288
20	3.51	0.12	292
30	3.51	0.11	299
40	3.52	0.1	303

**Table A-1 Effect of CO<sub>2</sub> inflow rates on aqueous solution (Continue)****(c) CO<sub>2</sub> = 400 mL/min**

<b>Time (min)</b>	<b>pH</b>	<b>DO (mg/L)</b>	<b>ORP (mV)</b>
0	7.51	7.51	187
10	3.29	0.28	232
20	3.32	0.2	247
30	3.31	0.16	258
40	3.26	0.14	268

**Table A-2 Effect of Fe<sup>0</sup> dosages on aqueous solution****(a) Fe<sup>0</sup> = 0 g/L**

<b>Time (min)</b>	<b>pH</b>	<b>DO (mg/L)</b>	<b>ORP (mV)</b>	<b>Fe<sup>2+</sup> (mg/L)</b>
0	6.81	7.1	254	0
10	3.49	0.16	288	0
20	3.51	0.12	292	0
30	3.51	0.11	299	0
40	3.52	0.1	303	0

**(b) Fe<sup>0</sup> = 1 g/L**

<b>Time (min)</b>	<b>pH</b>	<b>DO (mg/L)</b>	<b>ORP (mV)</b>	<b>Fe<sup>2+</sup> (mg/L)</b>
0	6.99	6.44	224	0
10	4.37	0.24	-670	30.0
20	4.75	0.11	-699	54.4
30	5	0.16	-705	78.5
40	5.07	0.11	-715	93.3

**Table A-2 Effect of Fe<sup>0</sup> dosages on aqueous solution (Continue)****(c) Fe<sup>0</sup> = 2 g/L**

Time (min)	pH	DO (mg/L)	ORP (mV)	Fe <sup>2+</sup> (mg/L)
0	7.21	6.2	183	0
10	4.73	0.09	-664	65.37
20	5.02	0.07	-682	109.54
30	5.17	0.06	-684	152.79
40	5.26	0.06	-689	179.29

**(d) Fe<sup>0</sup> = 4 g/L**

Time (min)	pH	DO (mg/L)	ORP (mV)	Fe <sup>2+</sup> (mg/L)
0	6.05	7.4	216	0.00
10	4.73	0.14	-703	92.24
20	5.01	0.09	-710	147.76
30	5.16	0.08	-714	180.69
40	5.24	0.07	-716	224.21

**Table A-3 Effect of CO<sub>2</sub> bubbling rate on nitrate reduction****(a). CO<sub>2</sub> = 0 mL/min**

Time (min)	pH	DO (mg/L)	ORP (mV)	Fe <sup>2+</sup> (mg/L)	NO <sub>3</sub> <sup>-</sup> (mg/L)	NO <sub>3</sub> <sup>-</sup> (mgN/L)	NH <sub>4</sub> <sup>+</sup> (mg/L)	NH <sub>4</sub> <sup>+</sup> (mgN/L)	Total N (mgN/L)
0	7.13	5.44	181	0	28.91	6.528	0.00	0.00	6.52
5	7.51	6.06	353	0	29.45	6.65	0.00	0.00	6.65
10	7.26	5.99	356	0	30.83	6.96	0.00	0.00	6.96
20	6.85	5.91	362	0.27	29.37	6.63	0.00	0.00	6.63
30	6.64	6.38	372	0.54	29.98	6.77	0.00	0.00	6.77
40	6.63	6.62	370	0.67	29.60	6.68	0.00	0.00	6.68
60	6.63	6.75	368	1.1	29.52	6.66	0.00	0.00	6.66

**Table A-3 Effect of CO<sub>2</sub> bubbling rate on nitrate reduction (Continue)****(b). CO<sub>2</sub> = 100 mL/min**

<b>Time (min)</b>	<b>pH</b>	<b>DO (mg/L)</b>	<b>ORP (mV)</b>	<b>Fe<sup>2+</sup> (mg/L)</b>	<b>NO<sub>3</sub><sup>-</sup> (mg/L)</b>	<b>NO<sub>3</sub><sup>-</sup> (mgN/L)</b>	<b>NH<sub>4</sub><sup>+</sup> (mg/L)</b>	<b>NH<sub>4</sub><sup>+</sup> (mgN/L)</b>	<b>Total N (mgN/L)</b>
0	8.21	5.33	158	0.00	29.42	6.64	0.00	0.00	6.64
5	3.56	0.85	13	0.00	29.31	6.62	0.00	0.00	6.62
10	3.59	0.22	-160	13.39	25.73	5.81	0.80	0.62	6.43
20	5.11	0.19	-501	116.34	5.11	1.15	6.90	5.37	6.52
30	5.25	0.17	-521	154.84	1.78	0.40	7.49	5.83	6.23
40	5.37	0.16	-503	173.25	0.00	0.00	8.10	6.30	6.30
60	5.38	0.15	-501	196.41	0.00	0.00	8.36	6.50	6.50

**(c). CO<sub>2</sub> = 200 mL/min**

<b>Time (min)</b>	<b>pH</b>	<b>DO (mg/L)</b>	<b>ORP (mV)</b>	<b>Fe<sup>2+</sup> (mg/L)</b>	<b>NO<sub>3</sub><sup>-</sup> (mg/L)</b>	<b>NO<sub>3</sub><sup>-</sup> (mgN/L)</b>	<b>NH<sub>4</sub><sup>+</sup> (mg/L)</b>	<b>NH<sub>4</sub><sup>+</sup> (mgN/L)</b>	<b>Total N (mgN/L)</b>
0	6.58	7.08	179	0.00	29.51	6.66	0.00	0.00	6.66
5	3.7	0.65	105	9.34	28.13	6.35	0.42	0.32	6.68
10	4.87	0.39	-567	72.67	14.96	3.38	4.19	3.26	6.64
20	5.38	0.19	-674	125.82	2.72	0.61	7.54	5.86	6.48
30	5.45	0.13	-688	166.28	0.00	0.00	8.25	6.42	6.42
40	5.5	0.09	-690	189.44	0.00	0.00	8.45	6.57	6.57
60	5.57	0.06	-651	225.43	0.00	0.00	8.47	6.59	6.59

**Table A-3 Effect of CO<sub>2</sub> bubbling rate on nitrate reduction (Continue)****(d). CO<sub>2</sub> = 400 mL/min**

<b>Time (min)</b>	<b>pH</b>	<b>DO (mg/L)</b>	<b>ORP (mV)</b>	<b>Fe<sup>2+</sup> (mg/L)</b>	<b>NO<sub>3</sub><sup>-</sup> (mg/L)</b>	<b>NO<sub>3</sub><sup>-</sup> (mgN/L)</b>	<b>NH<sub>4</sub><sup>+</sup> (mg/L)</b>	<b>NH<sub>4</sub><sup>+</sup> (mgN/L)</b>	<b>Total N (mgN/L)</b>
0	7.31	5.19	158	0.00	29.35	6.63	0.00	0.00	6.63
5	3.85	0.77	62	41.29	26.34	5.95	0.60	0.47	6.41
10	4.93	0.33	-637	106.29	12.66	2.86	4.50	3.50	6.36
20	5.31	0.11	-732	172.69	2.06	0.47	7.80	6.07	6.53
30	5.36	0.09	-722	187.20	0.00	0.00	8.35	6.49	6.49
40	5.39	0.08	-716	207.60	0.00	0.00	8.42	6.55	6.55
60	5.5	0.06	-702	243.28	0.00	0.00	8.46	6.58	6.58

**Table A-4 Effect of Fe<sup>0</sup> dosages on the initial nitrate of 30 mg/L****(a). Fe<sup>0</sup> = 1 g/L**

<b>Time (min)</b>	<b>pH</b>	<b>DO (mg/L)</b>	<b>ORP (mV)</b>	<b>Fe<sup>2+</sup> (mg/L)</b>	<b>NO<sub>3</sub><sup>-</sup> (mg/L)</b>	<b>NO<sub>3</sub><sup>-</sup> (mgN/L)</b>	<b>NH<sub>4</sub><sup>+</sup> (mg/L)</b>	<b>NH<sub>4</sub><sup>+</sup> (mgN/L)</b>	<b>Total N (mgN/L)</b>
0	6.43	7.33	135	0.00	30.79	6.95	0.00	0.00	6.95
5	3.51	1.16	157	2.09	29.73	6.71	0.00	0.00	6.71
10	4.5	0.79	-111	50.22	21.59	4.87	2.3	1.79	6.66
20	5.2	0.57	-644	131.13	7.66	1.73	6.25	4.86	6.59
30	5.33	0.51	-643	143.96	2.64	0.6	7.94	6.18	6.77
40	5.37	0.47	-662	162.09	1.49	0.34	8.35	6.49	6.83
60	5.42	0.43	-683	170.74	1.19	0.27	8.40	6.53	6.80

**Table A-4 Effect of Fe<sup>0</sup> dosages on the initial nitrate of 30 mg/L (Continue)****(b). Fe<sup>0</sup> = 2 g/L**

<b>Time (min)</b>	<b>pH</b>	<b>DO (mg/L)</b>	<b>ORP (mV)</b>	<b>Fe<sup>2+</sup> (mg/L)</b>	<b>NO<sub>3</sub><sup>-</sup> (mg/L)</b>	<b>NO<sub>3</sub><sup>-</sup> (mgN/L)</b>	<b>NH<sub>4</sub><sup>+</sup> (mg/L)</b>	<b>NH<sub>4</sub><sup>+</sup> (mgN/L)</b>	<b>Total N (mgN/L)</b>
0	6.58	7.08	179	0	29.51	6.66	0.00	0.00	6.66
5	3.7	0.65	105	9.34	28.13	6.35	0.42	0.32	6.68
10	4.87	0.39	-567	72.67	14.96	3.38	4.19	3.26	6.64
20	5.38	0.19	-674	125.82	2.72	0.61	7.54	5.86	6.48
30	5.45	0.13	-688	166.28	0.00	0.00	8.25	6.42	6.42
40	5.5	0.09	-690	189.44	0.00	0.00	8.45	6.57	6.57
60	5.57	0.06	-651	225.43	0.00	0.00	8.47	6.59	6.59

**(c). Fe<sup>0</sup> = 4 g/L**

<b>Time (min)</b>	<b>pH</b>	<b>DO (mg/L)</b>	<b>ORP (mV)</b>	<b>Fe<sup>2+</sup> (mg/L)</b>	<b>NO<sub>3</sub><sup>-</sup> (mg/L)</b>	<b>NO<sub>3</sub><sup>-</sup> (mgN/L)</b>	<b>NH<sub>4</sub><sup>+</sup> (mg/L)</b>	<b>NH<sub>4</sub><sup>+</sup> (mgN/L)</b>	<b>Total N (mgN/L)</b>
0	6.99	7.57	179	0.00	32.16	7.26	0.00	0.00	7.26
5	4.39	2.26	93	2.65	31.17	7.04	0.35	0.27	7.31
10	5.15	0.72	-551	80.49	18.01	4.07	3.9	3.03	7.10
20	5.55	0.40	-805	170.46	3.17	0.72	8.05	6.26	6.98
30	5.61	0.29	-841	211.20	0.00	0.00	8.95	6.96	6.96
40	5.66	0.23	-844	241.05	0.00	0.00	9.05	7.04	7.04
60	5.72	0.16	-913	285.69	0.00	0.00	9.08	7.06	7.06

**Table A-5 Effect of Fe<sup>0</sup> dosages on the initial nitrate of 50 mg/L****(a) Fe<sup>0</sup> = 2 g/L**

<b>Time (min)</b>	<b>pH</b>	<b>DO (mg/L)</b>	<b>ORP (mV)</b>	<b>Fe<sup>2+</sup> (mg/L)</b>	<b>NO<sub>3</sub><sup>-</sup> (mg/L)</b>	<b>NO<sub>3</sub><sup>-</sup> (mgN/L)</b>	<b>NH<sub>4</sub><sup>+</sup> (mg/L)</b>	<b>NH<sub>4</sub><sup>+</sup> (mgN/L)</b>	<b>Total N (mgN/L)</b>
0	6.62	6.15	204	0.00	45.95	10.38	0.00	0.00	10.38
5	3.51	2.81	-459	6.98	43.78	9.89	0.51	0.65	10.39
10	4.22	0.71	-518	12.97	37.92	8.56	1.71	2.20	10.27
20	5.29	0.69	-692	121.64	17.72	4.00	6.12	7.87	10.12
30	5.50	0.27	-682	189.44	7.51	1.70	8.52	10.96	10.22
40	5.53	0.19	-700	215.39	4.75	1.07	9.18	11.80	10.25
60	5.58	0.1	-676	244.68	3.37	0.76	9.52	12.24	10.28

**(b) Fe<sup>0</sup> = 3 g/L**

<b>Time (min)</b>	<b>pH</b>	<b>DO (mg/L)</b>	<b>ORP (mV)</b>	<b>Fe<sup>2+</sup> (mg/L)</b>	<b>NO<sub>3</sub><sup>-</sup> (mg/L)</b>	<b>NO<sub>3</sub><sup>-</sup> (mgN/L)</b>	<b>NH<sub>4</sub><sup>+</sup> (mg/L)</b>	<b>NH<sub>4</sub><sup>+</sup> (mgN/L)</b>	<b>Total N (mgN/L)</b>
0	6.75	6.82	448	0.00	45.53	10.28	0.00	0.00	10.28
5	4.76	0.22	-195	26.94	42.18	9.52	1.45	1.12	10.65
10	5.59	0.16	-544	122.92	21.48	4.85	8.13	6.32	11.17
20	5.82	0.14	-569	204.66	6.55	1.48	12.68	9.86	11.34
30	5.90	0.09	-625	240.93	2.61	0.59	13.76	10.70	11.29
40	5.94	0.06	-638	256.00	1.20	0.27	14.18	11.03	11.30
60	5.98	0.03	-654	303.60	0.00	0.00	14.40	11.20	11.20

**Table A-5 Effect of Fe<sup>0</sup> dosages on the initial nitrate of 50 mg/L (Continue)**

**(c) Fe<sup>0</sup> = 4 g/L**

<b>Time (min)</b>	<b>pH</b>	<b>DO (mg/L)</b>	<b>ORP (mV)</b>	<b>Fe<sup>2+</sup> (mg/L)</b>	<b>NO<sub>3</sub><sup>-</sup> (mg/L)</b>	<b>NO<sub>3</sub><sup>-</sup> (mgN/L)</b>	<b>NH<sub>4</sub><sup>+</sup> (mg/L)</b>	<b>NH<sub>4</sub><sup>+</sup> (mgN/L)</b>	<b>Total N (mgN/L)</b>
0	7.10	5.79	454	0.00	44.65	10.08	0.00	0.00	10.08
5	4.69	0.19	-501	41.73	40.50	9.14	2.34	1.82	10.97
10	5.48	0.16	-653	149.42	18.13	4.09	9.89	7.69	11.79
20	5.69	0.11	-672	233.12	3.90	0.88	14.07	10.94	11.82
30	5.74	0.09	-681	251.26	1.49	0.34	14.65	11.40	11.73
40	5.76	0.04	-697	278.60	0.00	0.00	14.72	11.45	11.45
60	5.80	0.03	-698	309.01	0.00	0.00	14.91	11.59	11.59



**Table A-6 Effect of Fe<sup>0</sup> dosages on the initial nitrate of 100 mg/L****(a) Fe<sup>0</sup> = 2 g/L**

<b>Time (min)</b>	<b>pH</b>	<b>DO (mg/L)</b>	<b>ORP (mV)</b>	<b>Fe<sup>2+</sup> (mg/L)</b>	<b>NO<sub>3</sub><sup>-</sup> (mg/L)</b>	<b>NO<sub>3</sub><sup>-</sup> (mgN/L)</b>	<b>NH<sub>4</sub><sup>+</sup> (mg/L)</b>	<b>NH<sub>4</sub><sup>+</sup> (mgN/L)</b>	<b>Total N (mgN/L)</b>
0	6.88	7.06	465	0.00	107.16	24.20	0.00	0.00	24.20
5	4.32	0.49	163	12.16	105.19	23.75	1.09	0.84	24.60
10	5.27	0.39	-539	102.55	83.60	18.88	8.47	6.59	25.46
20	5.59	0.5	-600	203.83	54.30	12.26	16.44	12.79	25.05
30	5.71	0.45	-621	268.28	38.40	8.67	19.80	15.40	24.07
40	5.78	0.4	-632	311.24	28.27	6.38	22.56	17.55	23.93
60	5.83	0.35	-638	359.51	17.73	4.00	24.94	19.40	23.40

**(b) Fe<sup>0</sup> = 4 g/L**

<b>Time (min)</b>	<b>pH</b>	<b>DO (mg/L)</b>	<b>ORP (mV)</b>	<b>Fe<sup>2+</sup> (mg/L)</b>	<b>NO<sub>3</sub><sup>-</sup> (mg/L)</b>	<b>NO<sub>3</sub><sup>-</sup> (mgN/L)</b>	<b>NH<sub>4</sub><sup>+</sup> (mg/L)</b>	<b>NH<sub>4</sub><sup>+</sup> (mgN/L)</b>	<b>Total N (mgN/L)</b>
0	6.75	6.20	462	0.00	105.79	23.89	0.00	0.00	23.89
5	4.65	0.22	-84	36.43	94.90	21.43	1.54	1.20	22.63
10	5.46	0.16	-620	156.68	63.57	14.35	10.95	8.52	22.87
20	5.78	0.11	-668	287.80	35.01	7.90	20.99	16.33	24.23
30	5.89	0.06	-673	351.42	21.61	4.88	24.61	19.14	24.02
40	5.92	0.03	-675	388.80	14.63	3.30	26.49	20.60	23.91
60	5.95	0.03	-680	436.23	8.06	1.82	27.57	21.44	23.26

**Table A-6 Effect of Fe<sup>0</sup> dosages on the initial nitrate of 100 mg/L (Continue)****(c) Fe<sup>0</sup> = 5 g/L**

<b>Time (min)</b>	<b>pH</b>	<b>DO (mg/L)</b>	<b>ORP (mV)</b>	<b>Fe<sup>2+</sup> (mg/L)</b>	<b>NO<sub>3</sub><sup>-</sup> (mg/L)</b>	<b>NO<sub>3</sub><sup>-</sup> (mgN/L)</b>	<b>NH<sub>4</sub><sup>+</sup> (mg/L)</b>	<b>NH<sub>4</sub><sup>+</sup> (mgN/L)</b>	<b>Total N (mgN/L)</b>
0	6.75	6.82	483	0.00	98.41	22.22	0.00	0.00	22.22
5	4.76	0.18	-65	45.52	90.11	20.35	3.16	2.46	22.81
10	5.59	0.15	-636	171.06	56.36	12.73	14.28	11.11	23.83
20	5.82	0.16	-665	312.89	27.71	6.26	22.81	17.74	24.00
30	5.9	0.08	-679	382.63	15.54	3.51	25.76	20.04	23.55
40	5.94	0.05	-683	417.51	10.57	2.39	27.06	21.05	23.44
60	5.98	0.03	-692	457.03	5.62	1.27	28.32	22.02	23.29

**(d) Fe<sup>0</sup> = 6 g/L**

<b>Time (min)</b>	<b>pH</b>	<b>DO (mg/L)</b>	<b>ORP (mV)</b>	<b>Fe<sup>2+</sup> (mg/L)</b>	<b>NO<sub>3</sub><sup>-</sup> (mg/L)</b>	<b>NO<sub>3</sub><sup>-</sup> (mgN/L)</b>	<b>NH<sub>4</sub><sup>+</sup> (mg/L)</b>	<b>NH<sub>4</sub><sup>+</sup> (mgN/L)</b>	<b>Total N (mgN/L)</b>
0	6.52	5.71	453	0.00	98.41	22.22	0.00	0.00	22.22
5	4.29	0.41	-254	56.24	90.63	20.47	3.04	2.36	22.83
10	5.43	0.32	-632	196.02	57.63	13.01	13.25	10.31	23.32
20	5.77	0.3	-692	334.40	25.13	5.67	20.70	16.10	21.77
30	5.89	0.29	-698	401.63	14.14	3.19	23.15	18.01	21.20
40	5.96	0.28	-705	430.65	8.97	2.02	25.09	19.52	21.54
60	6.04	0.21	-717	469.43	4.54	1.03	26.33	20.48	21.50

**Table A-7 Values of constants in the proposed sigmoidal model equation for nitrate reduction (Y).**

<b>Initial NO<sub>3</sub><sup>-</sup> (mg N/L)</b>	<b>Fe<sup>0</sup> (g/L)</b>	<b>A<sub>1</sub> (mg N/L)</b>	<b>A<sub>2</sub> (mg N/L)</b>	<b>t<sub>1/2</sub> (min)</b>	<b>W (min)</b>	<b>R<sup>2</sup></b>
<b>6.95</b>	1	7.549	0.333	13.002	4.765	0.997
	2	6.778	0.137	9.950	2.011	0.995
	4	7.590	0.110	10.518	2.664	0.994
<b>10.25</b>	2	10.880	0.912	16.069	5.182	0.999
	3	10.551	0.550	9.461	2.247	0.990
	4	10.221	0.289	9.079	1.986	0.996
<b>23.14</b>	2	30.861	4.204	12.691	10.124	0.991
	4	34.736	2.304	6.617	8.680	0.991
	5	28.238	1.953	8.845	6.562	0.989
	6	26.692	1.767	9.821	5.822	0.991

สถาบันวิทยบริการ  
จุฬาลงกรณ์มหาวิทยาลัย

**Table A-8 Values of constants in the proposed sigmoidal model equation for ferrous accumulation (Y).**

<b>Initial NO<sub>3</sub><sup>-</sup> (mg N/L)</b>	<b>Fe<sup>0</sup> (g/L)</b>	<b>A<sub>1</sub> (mg/L)</b>	<b>A<sub>2</sub> (mg/L)</b>	<b>t<sub>1/2</sub> (min)</b>	<b>W (min)</b>	<b>R<sup>2</sup></b>
<b>6.95</b>	1	0	159.695	13.893	3.834	0.984
	2	0	211.394	18.178	7.322	0.965
	4	0	261.138	17.266	6.138	0.965
<b>10.25</b>	2	0	229.545	20.385	4.993	0.989
	3	0	271.367	13.699	5.329	0.960
	4	0	273.390	10.073	3.467	0.966
<b>23.14</b>	2	0	338.713	18.265	6.840	0.974
	4	0	405.016	14.808	5.781	0.975
	5	0	428.825	14.163	5.516	0.980
	6	0	438.790	12.958	5.190	0.978

สถาบันวิทยบริการ  
จุฬาลงกรณ์มหาวิทยาลัย

**Table A-9 Values of constants in the proposed sigmoidal model equation for ammonium formation (Y).**

Initial NO <sub>3</sub> <sup>-</sup> (mg N/L)	Fe <sup>0</sup> (g/L)	A <sub>1</sub> (mg N/L)	A <sub>2</sub> (mg N/L)	t <sub>1/2</sub> (min)	W (min)	R <sup>2</sup>
<b>6.95</b>	1	0	6.446	15.079	4.091	0.992
	2	0	6.368	9.937	1.788	0.994
	4	0	6.854	10.566	2.081	0.993
<b>10.25</b>	2	0	9.298	17.127	4.640	0.998
	3	0	10.718	9.291	2.060	0.992
	4	0	11.357	8.468	2.074	0.998
<b>23.14</b>	2	0	18.025	15.253	5.544	0.973
	4	0	20.400	12.871	4.292	0.983
	5	0	20.400	9.812	2.757	0.983
	6	0	18.729	9.809	2.878	0.977

สถาบันวิทยบริการ  
จุฬาลงกรณ์มหาวิทยาลัย

**Table A-10 Effect of operation mode on nitrate reduction****(a) Mode 1**

<b>Time (min)</b>	<b>pH</b>	<b>DO (mg/L)</b>	<b>ORP (mV)</b>	<b>Fe<sup>2+</sup> (mg/L)</b>	<b>NO<sub>3</sub><sup>-</sup> (mg/L)</b>	<b>NO<sub>3</sub> (mgN/L)</b>	<b>NH<sub>4</sub><sup>+</sup> (mg/L)</b>	<b>NH<sub>4</sub><sup>+</sup> (mgN/L)</b>	<b>Total N (mgN/L)</b>
0	7.33	5.91	196	0	27.33	6.17	0.00	0.00	6.17
5	3.95	0.66	-167	5	25.69	5.80	0.30	0.23	6.03
10	5.05	0.21	-472	66	14.33	3.24	3.50	2.72	5.96
20	5.5	0.15	-571	139	3.17	0.72	5.65	4.40	5.11
30	5.55	0.11	-580	166	0.00	0.00	6.57	5.11	5.11
40	5.57	0.07	-581	174	0.00	0.00	7.45	5.79	5.79
60	5.62	0.06	-588	200	0.00	0.00	7.74	6.02	6.02
61	5.63	0.06	-586	194	24.46	5.52	7.74	6.02	5.52
65	5.63	0.06	-600	215	19.25	4.35	7.00	5.44	9.79
70	5.73	0.06	-603	239	14.81	3.34	8.30	6.46	9.80
80	5.79	0.05	-603	277	9.25	2.09	9.50	7.39	9.48
90	5.82	0.05	-599	299	6.30	1.42	10.42	8.10	9.53
100	5.88	0.04	-597	311	4.65	1.05	10.60	8.24	9.29
120	5.86	0.03	-541	332	3.33	0.75	11.20	8.71	9.46
121	5.85	0.05	-537	312	27.58	6.23	11.20	8.71	6.23
125	5.87	0.04	-537	326	25.10	5.67	12.23	9.51	15.18
130	5.88	0.04	-544	337	22.54	5.09	12.44	9.68	14.77
140	5.91	0.04	-552	360	18.19	4.11	13.40	10.42	14.53
150	5.94	0.04	-555	376	14.72	3.32	14.29	11.12	14.44
160	5.96	0.02	-559	399	12.57	2.84	14.36	11.17	14.01
180	5.98	0.02	-571	422	9.62	2.17	15.75	12.25	14.42

**Table A-10 Effect of operation mode on nitrate reduction (Continue)****(b) Mode 2**

Time (min)	pH	DO (mg/L)	ORP (mV)	Fe <sup>2+</sup> (mg/L)	NO <sub>3</sub> (mg/L)	NO <sub>3</sub> <sup>-</sup> (mgN/L)	NH <sub>4</sub> <sup>+</sup> (mg/L)	NH <sub>4</sub> <sup>+</sup> (mgN/L)	Total N (mgN/L)
0	5.66	5.66	230	0	29.65	6.69	0.00	0.00	6.69
5	0.31	0.31	-42	7	26.83	6.06	0.45	0.35	6.41
10	0.36	0.36	-56	54	14.82	3.35	3.60	2.80	6.15
20	0.14	0.14	-512	134	2.30	0.52	7.20	5.60	6.12
30	0.1	0.1	-524	167	0.00	0.00	8.10	6.30	6.30
40	0.08	0.08	-535	181	0.00	0.00	8.33	6.48	6.48
60	0.06	0.06	-555	222	0.00	0.00	8.50	6.61	6.61
61	0.44	0.44	380	0	30.13	6.80	0.00	0.00	6.80
65	0.08	0.08	32	64	19.37	4.37	2.60	2.02	6.40
70	0.06	0.06	-461	107	10.02	2.26	5.20	4.04	6.31
80	0.05	0.05	-480	147	2.46	0.55	7.50	5.83	6.39
90	0.04	0.04	-491	167	0.00	0.00	8.50	6.61	6.61
100	0.04	0.04	-494	177	0.00	0.00	8.56	6.66	6.66
120	0.03	0.03	-549	183	0.00	0.00	8.66	6.74	6.74
121	6.3	6.3	303	0	30.65	6.92	0.00	0.00	6.92
125	0.07	0.07	32	38	21.53	4.86	2.50	1.94	6.81
130	0.04	0.04	-466	87	12.81	2.89	4.90	3.81	6.70
140	0.04	0.04	-485	127	3.76	0.85	7.40	5.76	6.60
150	0.03	0.03	-492	150	1.68	0.38	7.90	6.14	6.52
160	0.02	0.02	-495	153	2.31	0.52	8.34	6.49	7.01
180	0.03	0.03	-501	159	0.00	0.00	9.20	7.16	7.16

**Table A-11 Effect of supplement of Fe<sup>0</sup> on operation mode 2****(a) Fe<sup>0</sup> = 0 g**

<b>Time (min)</b>	<b>pH</b>	<b>DO (mg/L)</b>	<b>ORP (mV)</b>	<b>Fe<sup>2+</sup> (mg/L)</b>	<b>NO<sub>3</sub> (mg/L)</b>	<b>NO<sub>3</sub><sup>-</sup> (mgN/L)</b>	<b>NH<sub>4</sub><sup>+</sup> (mg/L)</b>	<b>NH<sub>4</sub><sup>+</sup> (mgN/L)</b>	<b>Total N (mgN/L)</b>
0	5.66	5.66	230	0	29.65	6.69	0.00	0.00	6.69
5	0.31	0.31	-42	7	26.83	6.06	0.45	0.35	6.41
10	0.36	0.36	-56	54	14.82	3.35	3.60	2.80	6.15
20	0.14	0.14	-512	134	2.30	0.52	7.20	5.60	6.12
30	0.1	0.1	-524	167	0.00	0.00	8.10	6.30	6.30
40	0.08	0.08	-535	181	0.00	0.00	8.33	6.48	6.48
60	0.06	0.06	-555	222	0.00	0.00	8.50	6.61	6.61
61	0.44	0.44	380	0	30.13	6.80	0.00	0.00	6.80
65	0.08	0.08	32	64	19.37	4.37	2.60	2.02	6.40
70	0.06	0.06	-461	107	10.02	2.26	5.20	4.04	6.31
80	0.05	0.05	-480	147	2.46	0.55	7.50	5.83	6.39
90	0.04	0.04	-491	167	0.00	0.00	8.50	6.61	6.61
100	0.04	0.04	-494	177	0.00	0.00	8.56	6.66	6.66
120	0.03	0.03	-549	183	0.00	0.00	8.66	6.74	6.74
121	6.3	6.3	303	0	30.65	6.92	0.00	0.00	6.92
125	0.07	0.07	32	38	21.53	4.86	2.50	1.94	6.81
130	0.04	0.04	-466	87	12.81	2.89	4.90	3.81	6.70
140	0.04	0.04	-485	127	3.76	0.85	7.40	5.76	6.60
150	0.03	0.03	-492	150	1.68	0.38	7.90	6.14	6.52
160	0.02	0.02	-495	153	2.31	0.52	8.34	6.49	7.01
180	0.03	0.03	-501	159	0.00	0.00	9.20	7.16	7.16



**Table A-11 Effect of supplement of Fe<sup>0</sup> on operation mode 2 (Continue)****(b) Fe<sup>0</sup> = 0.25 g**

<b>Time (min)</b>	<b>pH</b>	<b>DO (mg/L)</b>	<b>ORP (mV)</b>	<b>Fe<sup>2+</sup> (mg/L)</b>	<b>NO<sub>3</sub> (mg/L)</b>	<b>NO<sub>3</sub><sup>-</sup> (mgN/L)</b>	<b>NH<sub>4</sub><sup>+</sup> (mg/L)</b>	<b>NH<sub>4</sub><sup>+</sup> (mgN/L)</b>	<b>Total N (mgN/L)</b>
0	7.21	5.69	354	0	29.87	6.74	0.00	0.00	6.74
5	4.05	0.79	201	7	28.11	6.35	0.30	0.23	6.58
10	5.13	0.21	-70	88	12.73	2.87	4.85	3.77	6.65
20	5.44	0.1	-612	148	2.01	0.45	7.81	6.07	6.53
30	5.48	0.07	-618	167	0.00	0.00	8.39	6.53	6.53
40	5.51	0.05	-621	185	0.00	0.00	8.25	6.42	6.42
60	5.58	0.04	-634	214	0.00	0.00	8.55	6.65	6.65
61	6.41	5.19	282	0	28.66	6.47	0.00	0.00	6.47
65	5.13	0.06	-498	77	17.29	3.90	2.89	2.25	6.15
70	5.33	0.04	-506	126	7.60	1.72	6.28	4.89	6.60
80	5.47	0.03	-518	164	1.73	0.39	8.49	6.60	6.99
90	5.5	0.03	-520	188	0.00	0.00	8.52	6.63	6.63
100	5.53	0.03	-522	194	0.00	0.00	8.30	6.45	6.45
120	5.57	0.03	-532	207	0.00	0.00	8.16	6.34	6.34
121	6.23	4.84	361	0	28.97	6.54	0.00	0.00	6.54
125	5.05	0.06	-268	68	19.27	4.35	2.50	1.94	6.29
130	5.39	0.04	-474	117	8.62	1.95	5.77	4.49	6.43
140	5.46	0.04	-488	157	2.02	0.46	7.50	5.83	6.29
150	5.49	0.03	-492	172	0.00	0.00	8.05	6.26	6.26
160	5.52	0.03	-494	173	0.00	0.00	8.22	6.39	6.39
180	5.56	0.03	-497	198	0.00	0.00	8.36	6.50	6.50

**Table A-11 Effect of supplement of Fe<sup>0</sup> on operation mode 2 (Continue)****(c) Fe<sup>0</sup> = 1 g**

<b>Time (min)</b>	<b>pH</b>	<b>DO (mg/L)</b>	<b>ORP (mV)</b>	<b>Fe<sup>2+</sup> (mg/L)</b>	<b>NO<sub>3</sub> (mg/L)</b>	<b>NO<sub>3</sub><sup>-</sup> (mgN/L)</b>	<b>NH<sub>4</sub><sup>+</sup> (mg/L)</b>	<b>NH<sub>4</sub><sup>+</sup> (mgN/L)</b>	<b>Total N (mgN/L)</b>
0	6.99	5.93	214	0	29.48	6.66	0.00	0.00	6.66
5	4.42	0.83	153	66	21.95	4.96	2.00	1.56	6.51
10	5.26	0.2	-501	100	10.04	2.27	5.70	4.43	6.70
20	5.49	0.07	-541	153	1.54	0.35	7.95	6.18	6.53
30	5.51	0.05	-550	166	0.00	0.00	8.31	6.46	6.46
40	5.51	0.04	-555	182	0.00	0.00	8.43	6.56	6.56
60	5.54	0.04	-563	212	0.00	0.00	8.91	6.93	6.93
61	7.1	5.38	188	0	30.05	6.79	0.00	0.00	6.79
65	5.06	0.09	-495	81	17.19	3.88	3.50	2.72	6.60
70	5.32	0.05	-529	134	5.95	1.34	6.59	5.13	6.47
80	5.44	0.03	-535	181	0.00	0.00	8.07	6.27	6.27
90	5.48	0.03	-540	195	0.00	0.00	8.29	6.44	6.44
100	5.51	0.03	-543	209	0.00	0.00	8.45	6.57	6.57
120	5.56	0.03	-557	232	0.00	0.00	8.55	6.65	6.65
121	6.71	5.38	169	0	29.89	6.75	0.00	0.00	6.75
125	5.33	0.12	-272	95	14.06	3.18	4.00	3.11	6.29
130	5.37	0.07	-505	153	3.70	0.83	7.40	5.76	6.59
140	5.47	0.04	-531	186	0.00	0.00	8.51	6.62	6.62
150	5.5	0.03	-540	205	0.00	0.00	8.46	6.58	6.58
160	5.55	0.03	-543	214	0.00	0.00	8.32	6.47	6.47
180	5.63	0.03	-551	249	0.00	0.00	8.53	6.63	6.63

**Table A-12 Effect of humic acid concentrations without other background species****(a) TOC = 0.6 mg/L**

<b>Time (min)</b>	<b>pH</b>	<b>DO (mg/L)</b>	<b>ORP (mV)</b>	<b>Fe<sup>2+</sup> (mg/L)</b>	<b>NO<sub>3</sub><sup>-</sup> (mg/L)</b>	<b>NO<sub>3</sub><sup>-</sup> (mgN/L)</b>	<b>NH<sub>4</sub><sup>+</sup> (mg/L)</b>	<b>NH<sub>4</sub><sup>+</sup> (mgN/L)</b>	<b>Total N (mgN/L)</b>
0	6.84	6.41	275	0.00	30.02	6.78	0.00	0.00	6.78
5	4.04	1.09	375	0.56	29.16	6.58	0.00	0.00	6.58
10	4.04	0.47	314	1.81	29.59	6.68	0.00	0.00	6.68
20	4.28	0.39	227	5.30	29.33	6.62	0.00	0.00	6.62
30	4.65	0.36	100	15.48	28.22	6.37	0.40	0.31	6.68
40	5.02	0.3	-46	31.53	24.54	5.54	1.50	1.17	6.71
60	5.33	0.23	-462	73.65	17.69	3.99	3.50	2.72	6.72
90	5.56	0.19	-458	128.90	8.53	1.93	6.50	5.06	6.98

**(b) TOC = 1 mg/L**

<b>Time (min)</b>	<b>pH</b>	<b>DO (mg/L)</b>	<b>ORP (mV)</b>	<b>Fe<sup>2+</sup> (mg/L)</b>	<b>NO<sub>3</sub><sup>-</sup> (mg/L)</b>	<b>NO<sub>3</sub><sup>-</sup> (mgN/L)</b>	<b>NH<sub>4</sub><sup>+</sup> (mg/L)</b>	<b>NH<sub>4</sub><sup>+</sup> (mgN/L)</b>	<b>Total N (mgN/L)</b>
0	6.82	6.95	210	0.00	31.98	7.22	0.00	0.00	7.22
5	3.94	0.89	373	0.56	30.96	6.99	0.00	0.00	6.99
10	3.97	0.12	343	0.70	30.87	6.97	0.00	0.00	6.97
20	4	0.11	303	1.39	30.25	6.83	0.00	0.00	6.83
30	4.09	0.14	260	3.21	30.19	6.82	0.00	0.00	6.82
40	4.41	0.08	196	8.23	28.90	6.53	0.00	0.00	6.53
60	4.94	0.05	-166	42.97	27.10	6.12	1.45	1.13	7.25
90	5.34	0.06	-440	108.81	19.14	4.32	3.80	2.96	7.28

**Table A-12 Effect of humic acid concentrations without other background species****(Continue)****(c) TOC = 1.9 mg/L**

<b>Time (min)</b>	<b>pH</b>	<b>DO (mg/L)</b>	<b>ORP (mV)</b>	<b>Fe<sup>2+</sup> (mg/L)</b>	<b>NO<sub>3</sub><sup>-</sup> (mg/L)</b>	<b>NO<sub>3</sub><sup>-</sup> (mgN/L)</b>	<b>NH<sub>4</sub><sup>+</sup> (mg/L)</b>	<b>NH<sub>4</sub><sup>+</sup> (mgN/L)</b>	<b>Total N (mgN/L)</b>
0	7.11	6.72	172	0.00	30.88	6.97	0.00	0.00	6.97
5	4.1	0.92	361	0.98	30.96	6.99	0.00	0.00	6.99
10	4.09	0.81	338	0.00	30.53	6.89	0.00	0.00	6.89
20	4.04	0.78	305	0.28	30.36	6.85	0.00	0.00	6.85
30	4.09	0.21	207	1.26	28.47	6.43	0.00	0.00	6.43
40	4.14	0.11	235	1.81	29.93	6.76	0.00	0.00	6.76
60	4.32	0.08	125	7.95	29.93	6.76	0.50	0.39	7.15
90	4.86	0.06	-289	38.78	28.90	6.53	0.70	0.54	7.07

**(d) TOC = 4.2 mg/L**

<b>Time (min)</b>	<b>pH</b>	<b>DO (mg/L)</b>	<b>ORP (mV)</b>	<b>Fe<sup>2+</sup> (mg/L)</b>	<b>NO<sub>3</sub><sup>-</sup> (mg/L)</b>	<b>NO<sub>3</sub><sup>-</sup> (mgN/L)</b>	<b>NH<sub>4</sub><sup>+</sup> (mg/L)</b>	<b>NH<sub>4</sub><sup>+</sup> (mgN/L)</b>	<b>Total N (mgN/L)</b>
0	7.1	4.76	159	0.00	30.44	6.87	0.00	0.00	6.87
5	3.61	2.12	418	0.00	30.22	6.82	0.00	0.00	6.82
10	3.63	0.71	347	1.95	30.53	6.89	0.00	0.00	6.89
20	3.65	0.23	294	2.09	30.22	6.82	0.00	0.00	6.82
30	3.71	0.16	243	2.37	30.29	6.84	0.00	0.00	6.84
40	3.73	0.07	168	2.65	30.06	6.79	0.00	0.00	6.79
60	3.84	0.06	-312	3.77	30.06	6.79	0.00	0.00	6.79
90	4.4	0.03	-397	20.09	28.30	6.39	0.72	0.56	6.95

**Table A-13 Effect of humic acid concentrations with other background species****(a) TOC = 0.36 mg/L**

<b>Time (min)</b>	<b>pH</b>	<b>DO (mg/L)</b>	<b>ORP (mV)</b>	<b>Fe<sup>2+</sup> (mg/L)</b>	<b>NO<sub>3</sub><sup>-</sup> (mg/L)</b>	<b>NO<sub>3</sub><sup>-</sup> (mgN/L)</b>	<b>NH<sub>4</sub><sup>+</sup> (mg/L)</b>	<b>NH<sub>4</sub><sup>+</sup> (mgN/L)</b>	<b>Total N (mgN/L)</b>
0	7.04	5.61	180	0.00	30.31	6.84	0.00	0.00	6.84
5	4.4	1.86	298	0.14	30.15	6.81	0.00	0.00	6.81
10	4.38	0.72	285	0.56	30.47	6.88	0.00	0.00	6.88
20	4.41	0.68	235	2.23	29.67	6.70	0.00	0.00	6.70
30	4.57	0.43	172	9.90	28.08	6.34	0.50	0.39	6.73
40	4.81	0.21	103	24.83	24.43	5.52	1.50	1.17	6.68
60	5.19	0.11	-43	75.89	14.43	3.26	4.50	3.50	6.76
90	5.47	0.08	-436	141.17	4.66	1.05	7.48	5.82	6.87

**(b) TOC = 0.55 mg/L**

<b>Time (min)</b>	<b>pH</b>	<b>DO (mg/L)</b>	<b>ORP (mV)</b>	<b>Fe<sup>2+</sup> (mg/L)</b>	<b>NO<sub>3</sub><sup>-</sup> (mg/L)</b>	<b>NO<sub>3</sub><sup>-</sup> (mgN/L)</b>	<b>NH<sub>4</sub><sup>+</sup> (mg/L)</b>	<b>NH<sub>4</sub><sup>+</sup> (mgN/L)</b>	<b>Total N (mgN/L)</b>
0	7.04	6.02	185	0.00	30.62	6.92	0.00	0.00	6.92
5	4.47	0.99	281	0.98	29.59	6.68	0.00	0.00	6.68
10	4.44	0.35	269	0.28	30.23	6.83	0.00	0.00	6.83
20	4.47	0.24	231	1.26	29.51	6.66	0.00	0.00	6.66
30	4.53	0.18	195	3.77	28.48	6.43	0.35	0.27	6.70
40	4.63	0.18	158	9.21	27.85	6.29	0.70	0.54	6.83
60	4.93	0.12	63	33.48	23.00	5.19	2.00	1.90	7.09
90	5.29	0.06	-256	87.05	12.28	2.77	5.20	4.04	6.82

**Table A-13 Effect of humic acid concentrations with other background species  
(Continue)**

**(c) TOC = 0.93 mg/L**

<b>Time (min)</b>	<b>pH</b>	<b>DO (mg/L)</b>	<b>ORP (mV)</b>	<b>Fe<sup>2+</sup> (mg/L)</b>	<b>NO<sub>3</sub><sup>-</sup> (mg/L)</b>	<b>NO<sub>3</sub><sup>-</sup> (mgN/L)</b>	<b>NH<sub>4</sub><sup>+</sup> (mg/L)</b>	<b>NH<sub>4</sub><sup>+</sup> (mgN/L)</b>	<b>Total N (mgN/L)</b>
0	7.05	5.51	212	0.00	30.37	6.86	0.00	0.00	6.86
5	4.34	1.16	255	0.84	29.02	6.55	0.00	0.00	6.55
10	4.35	0.16	229	1.67	28.47	6.43	0.00	0.00	6.43
20	4.4	0.07	196	2.51	28.78	6.50	0.00	0.00	6.50
30	4.44	0.05	169	5.30	27.91	6.30	0.40	0.31	6.61
40	4.5	0.04	147	6.00	27.99	6.32	0.55	0.43	6.75
60	4.65	0.02	92	12.83	25.93	5.85	1.25	0.97	6.83
90	4.95	0.02	-17	37.67	21.73	4.91	2.70	2.10	7.01

**(d) TOC = 1.34 mg/L**

<b>Time (min)</b>	<b>pH</b>	<b>DO (mg/L)</b>	<b>ORP (mV)</b>	<b>Fe<sup>2+</sup> (mg/L)</b>	<b>NO<sub>3</sub><sup>-</sup> (mg/L)</b>	<b>NO<sub>3</sub><sup>-</sup> (mgN/L)</b>	<b>NH<sub>4</sub><sup>+</sup> (mg/L)</b>	<b>NH<sub>4</sub><sup>+</sup> (mgN/L)</b>	<b>Total N (mgN/L)</b>
0	7.03	5.4	208	0.00	30.61	6.91	0.00	0.00	6.91
5	4.48	1.21	270	0.00	30.29	6.84	0.00	0.00	6.84
10	4.46	0.46	254	0.00	30.61	6.91	0.00	0.00	6.91
20	4.47	0.18	224	0.84	30.69	6.93	0.00	0.00	6.93
30	4.48	0.11	200	1.12	30.45	6.88	0.00	0.00	6.88
40	4.5	0.08	182	1.67	30.29	6.84	0.00	0.00	6.84
60	4.57	0.05	134	4.88	29.66	6.70	0.19	0.25	6.89
90	4.84	0.04	19	24.27	26.17	5.91	0.70	0.90	6.61

**Table A-13 Effect of humic acid concentrations with other background species  
(Continue)**

**(e) TOC = 2.29 mg/L**

<b>Time (min)</b>	<b>pH</b>	<b>DO (mg/L)</b>	<b>ORP (mV)</b>	<b>Fe<sup>2+</sup> (mg/L)</b>	<b>NO<sub>3</sub><sup>-</sup> (mg/L)</b>	<b>NO<sub>3</sub><sup>-</sup> (mgN/L)</b>	<b>NH<sub>4</sub><sup>+</sup> (mg/L)</b>	<b>NH<sub>4</sub><sup>+</sup> (mgN/L)</b>	<b>Total N (mgN/L)</b>
0	7.03	5.72	196	0.00	30.84	6.96	0.00	0.00	6.96
5	4.55	0.93	260	0.14	30.77	6.95	0.00	0.00	6.95
10	4.55	0.32	245	0.28	30.77	6.95	0.00	0.00	6.95
20	4.55	0.15	218	0.00	30.77	6.95	0.00	0.00	6.95
30	4.54	0.1	188	3.07	30.69	6.93	0.00	0.00	6.93
40	4.57	0.07	162	1.53	30.53	6.89	0.00	0.00	6.89
60	4.61	0.06	91	4.60	29.97	6.77	0.20	0.16	6.92
90	4.88	0.03	-50	22.88	27.04	6.11	0.80	0.62	6.73

สถาบันวิทยบริการ  
จุฬาลงกรณ์มหาวิทยาลัย

**Table A-14 Effect of sodium carbonate without other background species****(a) Na<sub>2</sub>CO<sub>3</sub> = 47 mg/L as CaCO<sub>3</sub>**

<b>Time (min)</b>	<b>pH</b>	<b>DO (mg/L)</b>	<b>ORP (mV)</b>	<b>Fe<sup>2+</sup> (mg/L)</b>	<b>NO<sub>3</sub><sup>-</sup> (mg/L)</b>	<b>NO<sub>3</sub><sup>-</sup> (mgN/L)</b>	<b>NH<sub>4</sub><sup>+</sup> (mg/L)</b>	<b>NH<sub>4</sub><sup>+</sup> (mgN/L)</b>	<b>Total N (mgN/L)</b>
0	6.74	5.8	293	0.00	29.98	6.77	0.00	0.00	6.77
5	3.98	0.64	342	0.00	29.00	6.55	0.00	0.00	6.55
10	4.59	0.36	-466	35.99	20.63	4.66	3.00	2.33	6.99
20	5.37	0.06	-564	140.34	4.36	0.98	7.50	5.83	6.82
30	5.48	0.04	-579	181.91	0.00	0.00	8.70	6.77	6.77
40	5.52	0.04	-578	197.25	0.00	0.00	8.50	6.61	6.61
60	5.59	0.03	-589	221.25	0.00	0.00	8.60	6.69	6.69
90	5.66	0.02	-597	249.15	0.00	0.00	8.90	6.92	6.92

**(b) Na<sub>2</sub>CO<sub>3</sub> = 94 mg/L as CaCO<sub>3</sub>**

<b>Time (min)</b>	<b>pH</b>	<b>DO (mg/L)</b>	<b>ORP (mV)</b>	<b>Fe<sup>2+</sup> (mg/L)</b>	<b>NO<sub>3</sub><sup>-</sup> (mg/L)</b>	<b>NO<sub>3</sub><sup>-</sup> (mgN/L)</b>	<b>NH<sub>4</sub><sup>+</sup> (mg/L)</b>	<b>NH<sub>4</sub><sup>+</sup> (mgN/L)</b>	<b>Total N (mgN/L)</b>
0	6.78	7.01	209	0.00	27.73	6.26	0.00	0.00	6.38
5	4.52	0.5	186	3.63	26.64	6.01	0.39	0.50	6.16
10	5.06	0.06	-76	62.22	15.69	3.45	3.58	4.60	6.43
20	5.44	0.03	-507	145.92	2.57	0.58	5.60	7.20	6.09
30	5.49	0.02	-514	171.59	0.00	0.00	6.11	7.85	6.11
40	5.52	0.02	-514	183.02	0.00	0.00	6.14	7.90	6.14
60	5.58	0.02	-536	214.27	0.00	0.00	6.46	8.30	6.46
90	5.65	0.02	-539	246.08	0.00	0.00	6.42	8.25	6.42



**Table A-14 Effect of sodium carbonate without other background species  
(Continue)**

**(c)  $\text{Na}_2\text{CO}_3 = 141 \text{ mg/L as CaCO}_3$**

Time (min)	pH	DO (mg/L)	ORP (mV)	$\text{Fe}^{2+}$ (mg/L)	$\text{NO}_3^-$ (mg/L)	$\text{NO}_3^-$ (mgN/L)	$\text{NH}_4^+$ (mg/L)	$\text{NH}_4^+$ (mgN/L)	Total N (mgN/L)
0	6.9	6.22	0.00	0.00	29.52	6.67	0.00	0.00	6.67
5	4.51	0.47	6.42	6.42	28.20	6.37	0.00	0.00	6.37
10	5.17	0.05	79.24	79.24	15.00	3.39	3.34	4.30	6.73
20	5.46	0.03	150.38	150.38	2.63	0.59	5.91	7.60	6.50
30	5.52	0.03	172.42	172.42	0.00	0.00	6.53	8.40	6.53
40	5.56	0.03	187.77	187.77	0.00	0.00	6.46	8.30	6.46
60	5.61	0.02	219.85	219.85	0.00	0.00	6.84	8.80	6.84
90	5.68	0.02	270.35	270.35	0.00	0.00	6.38	8.20	6.38

สถาบันวิทยบริการ  
จุฬาลงกรณ์มหาวิทยาลัย

**Table A-15 Effect of sodium carbonate with other background species****(a) Na<sub>2</sub>CO<sub>3</sub> = 47 mg/L as CaCO<sub>3</sub>**

<b>Time (min)</b>	<b>pH</b>	<b>DO (mg/L)</b>	<b>ORP (mV)</b>	<b>Fe<sup>2+</sup> (mg/L)</b>	<b>NO<sub>3</sub><sup>-</sup> (mg/L)</b>	<b>NO<sub>3</sub><sup>-</sup> (mgN/L)</b>	<b>NH<sub>4</sub><sup>+</sup> (mg/L)</b>	<b>NH<sub>4</sub><sup>+</sup> (mgN/L)</b>	<b>Total N (mgN/L)</b>
0	7.03	6.22	185	0.00	30.62	6.92	0.00	0.00	6.92
5	4.2	1.35	283	0.14	30.47	6.88	0.00	0.00	6.88
10	4.19	0.94	265	0.14	30.39	6.86	0.00	0.00	6.86
20	4.22	0.35	239	0.98	30.23	6.83	0.00	0.00	6.83
30	4.27	0.26	210	2.93	29.77	6.72	0.00	0.00	6.72
40	4.39	0.07	170	7.25	28.99	6.55	0.23	0.30	6.78
60	4.72	0.04	100	23.44	25.16	5.68	1.40	1.80	7.08
90	5.11	0.02	-91	64.73	15.96	3.60	3.41	4.38	7.01

**(b) Na<sub>2</sub>CO<sub>3</sub> = 94 mg/L as CaCO<sub>3</sub>**

<b>Time (min)</b>	<b>pH</b>	<b>DO (mg/L)</b>	<b>ORP (mV)</b>	<b>Fe<sup>2+</sup> (mg/L)</b>	<b>NO<sub>3</sub><sup>-</sup> (mg/L)</b>	<b>NO<sub>3</sub><sup>-</sup> (mgN/L)</b>	<b>NH<sub>4</sub><sup>+</sup> (mg/L)</b>	<b>NH<sub>4</sub><sup>+</sup> (mgN/L)</b>	<b>Total N (mgN/L)</b>
0	7.04	6.02	185	0.00	30.62	6.92	0.00	0.00	6.92
5	4.47	0.99	281	0.98	29.59	6.68	0.00	0.00	6.68
10	4.44	0.35	269	0.28	30.23	6.83	0.00	0.00	6.83
20	4.47	0.24	231	1.26	29.51	6.66	0.00	0.00	6.66
30	4.53	0.18	195	3.77	28.48	6.43	0.00	0.00	6.43
40	4.63	0.18	158	9.21	27.85	6.29	0.00	0.00	6.29
60	4.93	0.12	63	33.48	23.00	5.19	1.95	1.52	6.71
90	5.29	0.06	-256	87.05	12.28	2.77	5.50	4.28	7.05

**Table A-15 Effect of sodium carbonate with other background species (Continue)****(c) Na<sub>2</sub>CO<sub>3</sub> = 141 mg/L as CaCO<sub>3</sub>**

<b>Time (min)</b>	<b>pH</b>	<b>DO (mg/L)</b>	<b>ORP (mV)</b>	<b>Fe<sup>2+</sup> (mg/L)</b>	<b>NO<sub>3</sub><sup>-</sup> (mg/L)</b>	<b>NO<sub>3</sub><sup>-</sup> (mgN/L)</b>	<b>NH<sub>4</sub><sup>+</sup> (mg/L)</b>	<b>NH<sub>4</sub><sup>+</sup> (mgN/L)</b>	<b>Total N (mgN/L)</b>
0	7.19	5.56	219	0.00	29.69	6.70	0.00	0.00	6.70
5	4.72	1.21	226	0.84	30.16	6.81	0.00	0.00	6.81
10	4.71	0.14	192	1.40	29.61	6.69	0.00	0.00	6.69
20	4.74	0.05	174	2.93	29.45	6.65	0.00	0.00	6.65
30	4.76	0.04	153	5.02	28.67	6.47	0.00	0.00	6.47
40	4.81	0.03	128	8.79	27.82	6.28	0.00	0.00	6.28
60	4.94	0.02	66	24.97	23.76	5.37	1.55	1.21	6.57
90	5.27	0.03	-78	71.70	13.31	3.01	4.50	3.50	6.51

  
 สถาบันวิทยบริการ  
 จุฬาลงกรณ์มหาวิทยาลัย

**Table A-16 Effect of sodium chloride****(a) NaCl = 35.5 mg/L as Cl<sup>-</sup>**

<b>Time (min)</b>	<b>pH</b>	<b>DO (mg/L)</b>	<b>ORP (mV)</b>	<b>Fe<sup>2+</sup> (mg/L)</b>	<b>NO<sub>3</sub><sup>-</sup> (mg/L)</b>	<b>NO<sub>3</sub><sup>-</sup> (mgN/L)</b>	<b>NH<sub>4</sub><sup>+</sup> (mg/L)</b>	<b>NH<sub>4</sub><sup>+</sup> (mgN/L)</b>	<b>Total N (mgN/L)</b>
0	7.14	5.63	207	0.00	29.56	6.67	0.00	0.00	6.67
5	4.49	1.56	226	0.98	29.17	6.59	0.00	0.00	6.59
10	4.51	0.45	193	3.07	29.09	6.57	0.00	0.00	6.57
20	4.72	0.28	103	15.07	28.00	6.32	0.00	0.00	6.32
30	4.95	0.18	-6	33.48	21.53	4.86	2.60	2.02	6.88
40	5.17	0.11	-241	64.73	13.57	3.06	4.60	3.58	6.64
60	5.42	0.09	-431	118.85	5.93	1.34	6.80	5.29	6.63
90	5.56	0.06	-460	175.21	3.35	0.76	7.40	5.76	6.51

**(b) NaCl = 106.5 mg/L as Cl<sup>-</sup>**

<b>Time (min)</b>	<b>pH</b>	<b>DO (mg/L)</b>	<b>ORP (mV)</b>	<b>Fe<sup>2+</sup> (mg/L)</b>	<b>NO<sub>3</sub><sup>-</sup> (mg/L)</b>	<b>NO<sub>3</sub><sup>-</sup> (mgN/L)</b>	<b>NH<sub>4</sub><sup>+</sup> (mg/L)</b>	<b>NH<sub>4</sub><sup>+</sup> (mgN/L)</b>	<b>Total N (mgN/L)</b>
0	6.98	5.8	216	0.00	6.66	29.48	0.00	0.00	6.66
5	4.6	1.88	253	1.40	6.71	29.72	0.00	0.00	6.71
10	4.61	0.46	201	3.63	6.62	29.33	0.00	0.00	6.62
20	4.8	0.17	11	22.60	5.71	25.27	1.20	0.93	6.64
30	5.22	0.08	-318	68.91	3.66	16.22	3.50	2.72	6.39
40	5.41	0.06	-414	110.48	1.92	8.50	5.80	4.51	6.43
60	5.54	0.03	-437	154.29	0.93	4.13	7.40	5.76	6.69
90	5.62	0.02	-448	189.44	0.62	2.73	7.85	6.11	6.72

**Table A-16 Effect of sodium chloride (Continue)****(c) NaCl = 213 mg/L as Cl<sup>-</sup>**

<b>Time (min)</b>	<b>pH</b>	<b>DO (mg/L)</b>	<b>ORP (mV)</b>	<b>Fe<sup>2+</sup> (mg/L)</b>	<b>NO<sub>3</sub><sup>-</sup> (mg/L)</b>	<b>NO<sub>3</sub><sup>-</sup> (mgN/L)</b>	<b>NH<sub>4</sub><sup>+</sup> (mg/L)</b>	<b>NH<sub>4</sub><sup>+</sup> (mgN/L)</b>	<b>Total N (mgN/L)</b>
0	6.86	6.01	196	0.00	30.50	6.89	0.00	0.00	6.89
5	4.56	1.21	230	2.23	30.03	6.78	0.00	0.00	6.78
10	4.59	0.41	191	5.02	29.64	6.69	0.00	0.00	6.69
20	4.91	0.19	33	27.90	24.65	5.57	1.50	1.17	6.73
30	5.25	0.11	-286	73.10	15.68	3.54	3.90	3.03	6.57
40	5.43	0.1	-380	114.67	8.73	1.97	6.20	4.82	6.79
60	5.56	0.08	-422	159.03	3.90	0.88	7.65	5.95	6.83
90	5.64	0.06	-501	196.14	2.73	0.62	7.85	6.11	6.72

สถาบันวิทยบริการ  
จุฬาลงกรณ์มหาวิทยาลัย

**Table A-17 Effect of calcium chloride without other background species****(a) CaCl<sub>2</sub>·2H<sub>2</sub>O = 50 mg/L as Cl<sup>-</sup>**

<b>Time (min)</b>	<b>pH</b>	<b>DO (mg/L)</b>	<b>ORP (mV)</b>	<b>Fe<sup>2+</sup> (mg/L)</b>	<b>NO<sub>3</sub><sup>-</sup> (mg/L)</b>	<b>NO<sub>3</sub><sup>-</sup> (mgN/L)</b>	<b>NH<sub>4</sub><sup>+</sup> (mg/L)</b>	<b>NH<sub>4</sub><sup>+</sup> (mgN/L)</b>	<b>Total N (mgN/L)</b>
0	6.87	6.74	163	0.00	6.94	30.75	0.00	0.00	6.94
5	3.84	0.72	319	11.72	6.16	27.28	0.39	0.50	6.55
10	4.74	0.09	-483	49.38	4.02	17.82	2.64	3.40	6.67
20	5.36	0.05	-565	141.45	0.67	2.96	5.68	7.30	6.35
30	5.42	0.05	-564	159.59	0.00	0.00	6.30	8.10	6.30
40	5.46	0.04	-561	186.09	0.00	0.00	6.65	8.55	6.65
60	5.52	0.03	-572	204.23	0.00	0.00	6.73	8.65	6.73
90	5.61	0.03	-587	241.34	0.00	0.00	6.78	8.72	6.78

**(b) CaCl<sub>2</sub>·2H<sub>2</sub>O = 150 mg/L as Cl<sup>-</sup>**

<b>Time (min)</b>	<b>pH</b>	<b>DO (mg/L)</b>	<b>ORP (mV)</b>	<b>Fe<sup>2+</sup> (mg/L)</b>	<b>NO<sub>3</sub><sup>-</sup> (mg/L)</b>	<b>NO<sub>3</sub><sup>-</sup> (mgN/L)</b>	<b>NH<sub>4</sub><sup>+</sup> (mg/L)</b>	<b>NH<sub>4</sub><sup>+</sup> (mgN/L)</b>	<b>Total N (mgN/L)</b>
0	6.75	6.94	293	0.00	28.27	6.38	0.00	0.00	6.38
5	4.18	0.34	195	12.28	25.55	5.77	0.55	0.43	6.20
10	5.13	0.07	-476	84.82	12.63	2.85	4.25	3.31	6.16
20	5.42	0.04	-495	157.64	2.16	0.49	7.55	5.87	6.36
30	5.46	0.03	-502	172.14	0.00	0.00	7.85	6.11	6.11
40	5.5	0.03	-501	187.77	0.00	0.00	7.90	6.14	6.14
60	5.56	0.02	-509	211.20	0.00	0.00	7.93	6.17	6.17
90	5.63	0.02	-514	279.28	0.00	0.00	7.90	6.14	6.14

**Table A-17 Effect of calcium chloride without other background species (Continue)****(c)  $\text{CaCl}_2 \cdot 2\text{H}_2\text{O} = 300 \text{ mg/L as Cl}^-$** 

<b>Time (min)</b>	<b>pH</b>	<b>DO (mg/L)</b>	<b>ORP (mV)</b>	<b><math>\text{Fe}^{2+}</math> (mg/L)</b>	<b><math>\text{NO}_3^-</math> (mg/L)</b>	<b><math>\text{NO}_3^-</math> (mgN/L)</b>	<b><math>\text{NH}_4^+</math> (mg/L)</b>	<b><math>\text{NH}_4^+</math> (mgN/L)</b>	<b>Total N (mgN/L)</b>
0	6.87	6.52	274	0.00	6.94	30.75	0.00	0.00	6.94
5	4.26	0.75	166	1.67	6.16	27.28	0.50	0.39	6.55
10	4.98	0.21	-446	64.45	4.02	17.82	3.40	2.64	6.67
20	5.32	0.05	-481	116.62	0.67	2.96	7.30	5.68	6.35
30	5.4	0.05	-486	139.78	0.00	0.00	8.10	6.30	6.30
40	5.44	0.03	-493	151.22	0.00	0.00	8.42	6.55	6.55
60	5.49	0.03	-508	167.40	0.00	0.00	8.55	6.65	6.65
90	5.56	0.02	-536	200.32	0.00	0.00	8.88	6.91	6.91

  
 สถาบันวิทยบริการ  
 จุฬาลงกรณ์มหาวิทยาลัย

**Table A-18 Effect of calcium chloride with other background species****(a) CaCl<sub>2</sub>·2H<sub>2</sub>O = 50 mg/L as Cl<sup>-</sup>**

<b>Time (min)</b>	<b>pH</b>	<b>DO (mg/L)</b>	<b>ORP (mV)</b>	<b>Fe<sup>2+</sup> (mg/L)</b>	<b>NO<sub>3</sub><sup>-</sup> (mg/L)</b>	<b>NO<sub>3</sub><sup>-</sup> (mgN/L)</b>	<b>NH<sub>4</sub><sup>+</sup> (mg/L)</b>	<b>NH<sub>4</sub><sup>+</sup> (mgN/L)</b>	<b>Total N (mgN/L)</b>
0	7.07	5.81	204	0.00	30.08	6.79	0.00	0.00	0.00
5	4.36	1.21	325	0.14	29.84	6.74	0.00	0.00	0.00
10	4.32	0.29	295	0.14	29.53	6.67	0.00	0.00	0.00
20	4.33	0.17	225	0.00	29.61	6.69	0.00	0.00	0.00
30	4.38	0.12	220	0.84	29.22	6.60	0.00	0.00	0.00
40	4.45	0.09	187	3.49	28.91	6.53	0.00	0.00	0.00
60	4.71	0.07	108	13.39	26.33	5.95	0.00	0.95	0.74
90	5.1	0.05	-54	48.83	19.16	4.33	0.00	3.30	2.57

**(b) CaCl<sub>2</sub>·2H<sub>2</sub>O = 150 mg/L as Cl<sup>-</sup>**

<b>Time (min)</b>	<b>pH</b>	<b>DO (mg/L)</b>	<b>ORP (mV)</b>	<b>Fe<sup>2+</sup> (mg/L)</b>	<b>NO<sub>3</sub><sup>-</sup> (mg/L)</b>	<b>NO<sub>3</sub><sup>-</sup> (mgN/L)</b>	<b>NH<sub>4</sub><sup>+</sup> (mg/L)</b>	<b>NH<sub>4</sub><sup>+</sup> (mgN/L)</b>	<b>Total N (mgN/L)</b>
0	7.04	6.02	185	0.00	30.62	6.92	0.00	0.00	6.92
5	4.47	0.99	281	0.98	30.59	6.91	0.00	0.00	6.91
10	4.44	0.35	269	0.28	30.23	6.83	0.00	0.00	6.83
20	4.47	0.24	231	1.26	29.51	6.66	0.00	0.00	6.66
30	4.53	0.18	195	3.77	28.48	6.43	0.00	0.00	6.43
40	4.63	0.18	158	9.21	27.85	6.29	0.00	0.00	6.29
60	4.93	0.12	63	33.48	23.00	5.19	1.85	1.44	6.63
90	5.29	0.06	-256	87.05	12.28	2.77	5.25	4.08	6.86



**Table A-18 Effect of calcium chloride with other background species (Continue)****(c)  $\text{CaCl}_2 \cdot 2\text{H}_2\text{O} = 300 \text{ mg/L as Cl}^-$** 

<b>Time (min)</b>	<b>pH</b>	<b>DO (mg/L)</b>	<b>ORP (mV)</b>	<b><math>\text{Fe}^{2+}</math> (mg/L)</b>	<b><math>\text{NO}_3^-</math> (mg/L)</b>	<b><math>\text{NO}_3^-</math> (mgN/L)</b>	<b><math>\text{NH}_4^+</math> (mg/L)</b>	<b><math>\text{NH}_4^+</math> (mgN/L)</b>	<b>Total N (mgN/L)</b>
0	7.13	6.18	180	0.00	31.56	7.13	0.00	0.00	7.13
5	4.47	0.69	260	0.42	31.48	7.11	0.00	0.00	7.11
10	4.47	0.17	247	0.42	31.35	7.08	0.00	0.00	7.08
20	4.5	0.07	187	1.67	31.25	7.06	0.00	0.00	7.06
30	4.58	0.06	90	5.44	30.47	6.88	0.00	0.00	6.88
40	4.75	0.04	-16	15.07	27.97	6.32	0.90	0.70	7.02
60	5.2	0.03	-306	66.96	17.05	3.85	4.10	3.19	7.04
90	5.53	0.03	-513	153.17	5.12	1.16	7.60	5.91	7.07

  
 สถาบันวิทยบริการ  
 จุฬาลงกรณ์มหาวิทยาลัย

### Batch mode study of ferrous removal by iron precipitation process

**Table A-19 Effect of air flow rate on ferrous removal.**

**(a) Air flow rate = 20 mL/min**

<b>Time (min)</b>	<b>pH</b>	<b>DO (mg/L)</b>	<b>ORP (mV)</b>	<b>Fe<sup>2+</sup> (mg/l)</b>	<b>Total iron (mg/L)</b>
0	5.65	0.78	-204	189.04	189.74
10	5.82	1.66	-107	165.64	168.95
20	5.97	2.17	-111	135.03	144.29
30	6.21	3.73	-112	107.38	112.89
45	6.17	4.85	-78	69.63	73.54
60	6.29	4.87	-40	39.22	41.27
90	6.32	5.19	-12	9.36	24.10
120	6.43	5.82	58	0.00	15.29
180	6.54	7.26	164	0.00	11.21
300	6.78	7.38	250	0.00	9.57

**Table A-19 Effect of air flow rate on ferrous removal (Continue)****(b) Air flow rate = 100 mL/min**

<b>Time (min)</b>	<b>pH</b>	<b>DO (mg/L)</b>	<b>ORP (mV)</b>	<b>Fe<sup>2+</sup> (mg/l)</b>	<b>Total iron (mg/L)</b>
0	5.65	0.86	-191	187.09	188.14
10	5.78	0.28	-167	158.80	153.63
20	6.10	4.51	-91	100.04	126.40
30	6.26	4.68	-63	76.29	104.52
45	6.35	5.45	-48	47.12	72.56
60	6.48	7.09	2	23.98	47.77
90	6.65	6.67	57	0.00	32.35
120	6.76	7.32	86	0.00	23.58
180	6.82	7.80	112	0.00	19.28
300	7.02	7.86	152	0.00	17.10

**(c) Air flow rate = 300 mL/min**

<b>Time (min)</b>	<b>pH</b>	<b>DO (mg/L)</b>	<b>ORP (mV)</b>	<b>Fe<sup>2+</sup> (mg/l)</b>	<b>Total iron (mg/L)</b>
0	5.61	0.88	-120	182.15	184.82
10	5.79	2.20	-106	133.14	142.54
20	6.12	3.05	-93	92.50	118.72
30	6.32	4.81	-72	51.23	94.28
45	6.58	6.89	-55	25.82	64.21
60	6.62	7.02	-27	14.56	49.79
90	6.71	7.80	-4	0.00	38.32
120	6.75	7.75	54	0.00	31.69
180	6.95	7.58	102	0.00	25.78
300	7.11	7.42	134	0.00	22.33

**Table A-19 Effect of air flow rate on ferrous removal (Continue)****(d) Air flow rate = 500 mL/min**

<b>Time (min)</b>	<b>pH</b>	<b>DO (mg/L)</b>	<b>ORP (mV)</b>	<b>Fe<sup>2+</sup> (mg/l)</b>	<b>Total iron (mg/L)</b>
0	5.41	0.61	-133	182.15	177.74
10	5.86	4.82	-63	110.15	132.54
20	6.09	6.73	-19	76.88	102.56
30	6.27	7.58	2	11.88	84.82
45	6.42	7.64	100	0.00	64.66
60	6.64	7.62	203	0.00	56.12
90	6.90	7.95	218	0.00	45.74
120	7.02	7.82	230	0.00	41.26
180	7.12	8.02	246	0.00	35.92
300	7.14	7.81	258	0.00	33.02

**Table A-20 Effect of sand dosages at 0.42-0.59 mm sand size on iron removal by fluidized bed process**

**(a) Sand dosages = 200 g/L**

<b>Time (min)</b>	<b>pH</b>	<b>DO (mg/L)</b>	<b>ORP (mV)</b>	<b>Fe<sup>2+</sup> (mg/l)</b>	<b>Total iron (mg/L)</b>
0	5.84	0.91	-156	185.62	182.80
10	5.62	1.59	-134	155.14	173.60
20	5.87	3.57	-113	132.75	161.40
30	5.99	3.92	-84	113.67	157.30
45	6.22	5.69	-66	86.24	135.60
60	6.14	6.35	-18	53.04	119.70
90	6.39	6.75	28	23.18	89.10
120	6.33	6.88	76	4.22	66.70
180	6.55	7.18	134	0.00	44.60
300	6.81	7.01	186	0.00	30.20

**Table A-20 Effect of sand dosages at 0.42-0.59 mm sand size on iron removal by fluidized bed process (Continue)**

**(b) Sand dosages = 300 g/L**

<b>Time (min)</b>	<b>pH</b>	<b>DO (mg/L)</b>	<b>ORP (mV)</b>	<b>Fe<sup>2+</sup> (mg/l)</b>	<b>Total iron (mg/L)</b>
0	5.65	0.94	-121	179.55	192.00
10	5.78	1.39	-112	157.51	172.60
20	5.90	3.13	-101	124.59	150.00
30	5.83	4.57	-96	98.49	138.60
45	6.12	5.43	-83	67.23	110.70
60	6.25	5.64	-53	40.21	88.60
90	6.30	6.48	20	12.78	52.20
120	6.32	6.96	58	0.00	32.80
180	6.48	6.18	104	0.00	20.00
300	6.67	6.98	200	0.00	15.60

**(c) Sand dosages = 400 g/L**

<b>Time (min)</b>	<b>pH</b>	<b>DO (mg/L)</b>	<b>ORP (mV)</b>	<b>Fe<sup>2+</sup> (mg/l)</b>	<b>Total iron (mg/L)</b>
0	5.65	0.78	-204	189.04	189.74
10	5.82	1.66	-107	165.64	168.95
20	5.97	2.17	-111	135.03	144.29
30	6.21	3.73	-112	107.38	112.89
45	6.17	4.85	-78	69.63	73.54
60	6.29	4.87	-40	39.22	41.27
90	6.32	5.19	-12	9.36	24.10
120	6.43	5.82	58	0.00	15.29
180	6.54	7.26	164	0.00	11.21
300	6.78	7.38	250	0.00	9.57

**Table A-20 Effect of sand dosages at 0.42-0.59 mm sand size on iron removal by fluidized bed process (Continue)**

**(d) Sand dosages = 500 g/L**

<b>Time (min)</b>	<b>pH</b>	<b>DO (mg/L)</b>	<b>ORP (mV)</b>	<b>Fe<sup>2+</sup> (mg/l)</b>	<b>Total iron (mg/L)</b>
0	5.72	1.02	-126	176.50	185.40
10	5.93	1.98	-91	150.17	145.60
20	5.81	2.36	-95	123.98	122.20
30	6.11	4.12	-102	96.83	89.40
45	6.09	5.67	-89	72.56	61.80
60	6.35	5.24	-78	33.62	29.40
90	6.44	6.35	-5	6.36	18.20
120	6.50	6.80	54	1.20	13.80
180	6.55	7.13	102	0.00	10.60
300	6.58	7.68	196	0.00	8.80

**Table A-21 Effect of sand dosages at 0.096-0.21 mm sand size on iron removal by fluidized bed process.**

**(a) Sand dosages = 200 g/L**

<b>Time (min)</b>	<b>pH</b>	<b>DO (mg/L)</b>	<b>ORP (mV)</b>	<b>Fe<sup>2+</sup> (mg/l)</b>	<b>Total iron (mg/L)</b>
0	5.56	0.75	-120	177.00	181.60
10	5.75	1.39	-103	165.13	168.20
20	5.86	3.58	-106	142.51	144.80
30	6.01	3.68	-103	110.73	113.40
45	6.11	3.76	-55	80.27	86.80
60	6.16	5.58	33	30.88	65.80
90	6.14	7.89	138	4.06	50.40
120	6.36	7.84	174	0.00	42.90
180	6.42	7.94	263	0.00	36.12
300	6.54	7.59	274	0.00	32.60



**Table A-21 Effect of sand dosages at 0.096-0.21 mm sand size on iron removal by fluidized bed process (Continue)**

**(b) Sand dosages = 300 g/L**

<b>Time (min)</b>	<b>pH</b>	<b>DO (mg/L)</b>	<b>ORP (mV)</b>	<b>Fe<sup>2+</sup> (mg/l)</b>	<b>Total iron (mg/L)</b>
0	5.75	0.76	-158	176.00	178.1
10	6.13	1.04	-108	148.63	150.8
20	6.20	1.39	-113	126.77	125.2
30	6.15	1.65	-110	85.47	89.89
45	6.02	1.98	-87	40.27	46.8
60	6.21	3.79	-22	20.89	23.52
90	6.22	6.32	86	2.29	12.99
120	6.32	7.41	159	0.00	6.68
180	6.44	7.60	240	0.00	6.12
300	6.54	7.74	270	0.00	5.21

**(c) Sand dosages = 400 g/L**

<b>Time (min)</b>	<b>pH</b>	<b>DO (mg/L)</b>	<b>ORP (mV)</b>	<b>Fe<sup>2+</sup> (mg/l)</b>	<b>Total iron (mg/L)</b>
0	5.79	0.89	-119	181.00	185.80
10	5.94	1.02	-106	142.27	146.60
20	6.01	1.12	-116	118.53	120.70
30	6.04	1.44	-101	78.61	80.20
45	5.96	2.08	-70	42.81	45.20
60	6.08	2.90	-1	20.51	21.60
90	6.13	5.87	126	1.51	7.90
120	6.32	7.31	181	0.00	4.33
180	6.39	7.78	252	0.00	2.34
300	6.49	8.24	286	0.00	1.72

**Table A-22 Effect of initial ferrous concentration on iron removal by fluidized bed process.**

**(a) Ferrous ion generated from Fe<sup>0</sup> at 1 g/L**

<b>Time (min)</b>	<b>pH</b>	<b>DO (mg/L)</b>	<b>ORP (mV)</b>	<b>Fe<sup>2+</sup> (mg/l)</b>	<b>Total iron (mg/L)</b>
0	5.77	1.64	-114	117.33	121.67
10	5.85	7.21	-108	85.81	98.67
20	5.74	6.89	-73	56.10	43.33
30	5.80	7.66	-27	26.10	26.08
45	5.85	8.20	48	10.25	17.13
60	5.92	7.30	126	2.68	13.53
90	5.93	7.22	170	0.00	9.17
120	6.23	8.54	187	0.00	7.33
180	6.38	8.39	269	0.00	6.02
300	6.45	8.56	266	0.00	4.82

**Table A-22 Effect of initial ferrous concentration on iron removal by fluidized bed process (Continue)**

**(b) Ferrous ion generated from Fe<sup>0</sup> at 2 g/L**

<b>Time (min)</b>	<b>pH</b>	<b>DO (mg/L)</b>	<b>ORP (mV)</b>	<b>Fe<sup>2+</sup> (mg/l)</b>	<b>Total iron (mg/L)</b>
0	5.65	0.78	-204	189.04	189.74
10	5.82	1.66	-107	165.64	168.95
20	5.97	2.17	-111	135.03	144.29
30	6.21	3.73	-112	107.38	112.89
45	6.17	4.85	-78	69.63	73.54
60	6.29	4.87	-40	39.22	41.27
90	6.32	5.19	-12	9.36	24.10
120	6.43	5.82	58	0.00	15.30
180	6.54	7.26	164	0.00	11.21
300	6.78	7.38	250	0.00	9.57

**(c) Ferrous ion generated from Fe<sup>0</sup> at 4 g/L**

<b>Time (min)</b>	<b>pH</b>	<b>DO (mg/L)</b>	<b>ORP (mV)</b>	<b>Fe<sup>2+</sup> (mg/l)</b>	<b>Total iron (mg/L)</b>
0	5.72	1.31	-254	268.45	275.33
10	6.00	3.43	-180	202.52	240.33
20	6.06	5.03	-140	168.26	218.67
30	5.93	6.17	-120	127.72	191.57
45	5.80	6.63	-46	97.80	173.67
60	5.97	7.12	17	57.80	132.59
90	5.93	7.53	70	6.36	113.30
120	6.21	7.23	123	0.00	84.67
180	6.18	7.36	204	0.00	72.33
300	6.39	7.40	220	0.00	49.67

**Table A-22 Effect of initial ferrous concentration on iron removal by fluidized bed process (Continue)**

**(d) Ferrous ion generated from Fe<sup>0</sup> at 6 g/L**

<b>Time (min)</b>	<b>pH</b>	<b>DO (mg/L)</b>	<b>ORP (mV)</b>	<b>Fe<sup>2+</sup> (mg/l)</b>	<b>Total iron (mg/L)</b>
0	5.93	0.78	-176	335.45	350.25
10	6.04	4.53	-137	293.40	326.67
20	6.06	4.00	-121	250.27	310.33
30	5.96	3.04	-66	196.72	286.67
45	6.05	5.35	114	156.81	273.33
60	5.95	7.97	185	86.81	260.00
90	6.15	8.99	233	38.50	203.33
120	6.27	9.21	263	11.50	183.33
180	6.53	9.85	304	0.00	150.25
300	6.63	9.61	283	0.00	130.67

สถาบันวิทยบริการ  
จุฬาลงกรณ์มหาวิทยาลัย

### Batch mode study of ammonia removal by air stripping process

**Table A-23 Effect of pH on ammonia removal by air stripping.**

Time (hr)	NH <sub>4</sub> <sup>+</sup> (mg-N/L)			
	pH 10	pH 11	pH 12	pH 13
0	7.27	7.18	7.36	7.18
0.16	6.46	6.64	5.98	5.46
0.5	4.41	4.22	3.51	3.33
1	3.02	2.41	2.12	1.97
1.5	2.15	1.47	1.17	1.11
2	1.39	0.93	0.58	0.61
3	0.72	0.30	0.12	0.09
4	0.21	0.10	0.00	0.00
5	0.13	0.00	0.00	0.00
6	0.03	0.00	0.00	0.00
7	0.00	0.00	0.00	0.00

**Table A-24 pseudo-first order rate constant at different pH operation**

pH	Rate constant (k), hr <sup>-1</sup>
10	0.82
11	1.05
12	1.32
13	1.37

**Table A-25 Effect of air flow rate on ammonia removal by air stripping.**

Time (hr)	NH <sub>4</sub> <sup>+</sup> (mg-N/L)				
	10 L/min	20 L/min	30 L/min	40 L/min	50 L/min
0	7.15	7.13	7.43	7.25	7.36
0.16	6.70	6.55	6.51	6.40	5.98
0.5	5.91	5.17	4.91	4.11	3.51
1	5.08	4.01	3.25	2.59	2.12
1.5	4.19	2.87	2.12	1.67	1.17
2	3.30	2.12	1.57	0.96	0.58
3	2.47	1.36	0.87	0.31	0.12
4	1.82	0.85	0.39	0.09	0.00
5	1.36	0.51	0.07	0.00	0.00
6	0.96	0.13	0.00	0.00	0.00
7	0.48	0.00	0.00	0.00	0.00

**Table A-26 pseudo-first order rate constant at different air flow rate**

pH	Rate constant, hr <sup>-1</sup>
10	0.36
20	0.59
30	0.82
40	1.06
50	1.32

**Table A-27 Effect of initial ammonium concentration on ammonia removal by air stripping.**

Time (hr)	NH <sub>4</sub> <sup>+</sup> (mg-N/L)				
	27.07 mg N/L	19.07 mg N/L	11.70 mg N/L	7.36 mg N/L	2.42 mg N/L
0	27.07	19.14	11.70	7.36	2.42
0.16	21.05	14.66	8.82	5.98	1.60
0.5	16.00	10.54	6.47	3.51	1.26
1	12.23	6.69	4.02	2.12	0.78
1.5	7.18	4.71	2.53	1.17	0.34
2	5.83	2.88	1.35	0.58	0.11
3	3.33	1.22	0.55	0.12	0.02
4	1.94	0.73	0.18	0.00	0.00
5	1.26	0.36	0.03	0.00	0.00
6	0.93	0.13	0.00	0.00	0.00
7	0.42	0.06	0.00	0.00	0.00

**Table A-28 pseudo-first order rate constant at different initial ammonium concentration**

Initial NH <sub>4</sub> <sup>+</sup> , mg N/L	Rate constant, hr <sup>-1</sup>
2.42	1.40
7.35	1.32
11.7	1.11
19.14	0.83
27.06	0.62

### Continuous mode study of nitrate reduction by Fe<sup>0</sup>/CO<sub>2</sub> process

**Table A-29 Effect of CO<sub>2</sub> bubbling rate on nitrate reduction**

**(a). CO<sub>2</sub> = 100 mL/min**

Time (hr)	pH	DO (mg/L)	ORP (mV)	Fe <sup>2+</sup> (mg/L)	NO <sub>3</sub> <sup>-</sup> (mg/L)	NO <sub>3</sub> <sup>-</sup> (mgN/L)	NH <sub>4</sub> <sup>+</sup> (mg/L)	NH <sub>4</sub> <sup>+</sup> (mgN/L)
0	6.67	7.39	255	0.00	98.99	22.35	0.00	0.00
0.16	5.21	0.84	-396	0.00	99.07	22.37	0.00	0.00
0.33	5.92	0.64	-652	0.00	98.08	22.14	0.00	0.00
0.5	5.9	0.67	-682	0.00	98.29	22.19	0.00	0.00
1	5.9	0.18	-700	0.00	98.08	22.14	0.00	0.00
1.5	5.87	0.1	-697	178.07	40.28	9.09	17.04	13.25
2	5.87	0.08	-695	320.89	23.49	5.30	21.92	17.04
2.5	5.88	0.07	-694	370.02	23.23	5.24	21.99	17.10
3	5.87	0.06	-692	380.46	23.32	5.26	21.96	17.08
5	5.84	0.03	-686	401.53	28.55	6.44	20.45	15.90
7	5.81	0.01	-680	408.29	33.54	7.57	19.00	14.77
9	5.78	0.01	-676	403.21	37.36	8.43	17.89	13.91
12	5.73	0.01	-665	390.85	42.21	9.53	16.48	12.82
15	5.72	0.01	-646	373.02	45.74	10.33	15.45	12.02
18	5.71	0.01	-632	352.55	49.66	11.21	14.32	11.13
21	5.69	0.01	-607	331.11	53.71	12.12	13.14	10.22
24	5.68	0.01	-587	288.03	58.31	13.16	11.81	9.185

สถาบันวิทยบริการ  
จุฬาลงกรณ์มหาวิทยาลัย



**Table A-29 Effect of CO<sub>2</sub> bubbling rate on nitrate reduction (Continue)****(b). CO<sub>2</sub> = 200 mL/min**

<b>Time (hr)</b>	<b>pH</b>	<b>DO (mg/L)</b>	<b>ORP (mV)</b>	<b>Fe<sup>2+</sup> (mg/L)</b>	<b>NO<sub>3</sub><sup>-</sup> (mg/L)</b>	<b>NO<sub>3</sub><sup>-</sup> (mgN/L)</b>	<b>NH<sub>4</sub><sup>+</sup> (mg/L)</b>	<b>NH<sub>4</sub><sup>+</sup> (mgN/L)</b>
0	6.48	7.39	248	0.00	102.30	23.10	0.00	0.00
0.16	5.41	0.81	-644	0.00	103.54	23.38	0.00	0.00
0.33	5.90	0.69	-670	0.00	104.80	23.66	0.00	0.00
0.5	5.89	0.26	-689	0.00	104.61	23.62	0.00	0.00
1	5.89	0.10	-702	0.00	102.82	23.22	0.00	0.00
1.5	5.89	0.09	-699	300.62	20.22	4.57	23.83	18.53
2	5.88	0.08	-695	378.99	16.45	3.71	24.92	19.39
2.5	5.86	0.08	-696	390.78	16.56	3.74	24.89	19.36
3	5.86	0.08	-700	398.58	17.58	3.97	24.60	19.13
5	5.85	0.06	-690	417.12	22.20	5.01	23.25	18.09
7	5.82	0.07	-686	419.56	24.75	5.59	22.51	17.51
9	5.80	0.03	-687	419.56	28.10	6.35	21.54	16.75
12	5.76	0.03	-685	410.02	33.42	7.55	20.00	15.55
15	5.74	0.03	-683	384.92	39.51	8.92	18.23	14.18
18	5.72	0.03	-666	372.24	40.38	9.12	17.98	13.98
21	5.68	0.03	-638	348.33	43.71	9.87	17.01	13.23
24	5.65	0.05	-548	306.86	52.72	11.91	14.39	11.20

สถาบันวิทยบริการ  
จุฬาลงกรณ์มหาวิทยาลัย

Table A-29 Effect of CO<sub>2</sub> bubbling rate on nitrate reduction (Continue)(c). CO<sub>2</sub> = 400 mL/min

Time (hr)	pH	DO (mg/L)	ORP (mV)	Fe <sup>2+</sup> (mg/L)	NO <sub>3</sub> <sup>-</sup> (mg/L)	NO <sub>3</sub> <sup>-</sup> (mgN/L)	NH <sub>4</sub> <sup>+</sup> (mg/L)	NH <sub>4</sub> <sup>+</sup> (mgN/L)
0	6.52	7.19	263	0.00	103.92	23.47	0.00	0.00
0.16	5.53	0.74	-396	0.00	103.71	23.42	0.00	0.00
0.33	5.87	0.11	-652	0.00	103.96	23.47	0.00	0.00
0.5	5.87	0.07	-682	0.00	103.42	23.35	0.00	0.00
1	5.86	0.03	-700	0.00	103.12	23.28	0.00	0.00
1.5	5.81	0.03	-697	325.89	18.90	4.27	24.68	19.19
2	5.81	0.03	-695	378.57	16.40	3.70	25.41	19.76
2.5	5.81	0.04	-694	395.16	16.60	3.75	25.35	19.71
3	5.78	0.03	-692	403.46	17.49	3.95	25.09	19.51
5	5.78	0.04	-686	420.04	22.48	5.08	23.64	18.39
7	5.76	0.03	-680	422.97	24.61	5.56	23.02	17.90
9	5.75	0.03	-676	422.97	28.60	6.46	21.86	17.00
12	5.72	0.03	-665	421.33	29.34	6.62	20.49	15.93
15	5.68	0.01	-646	383.45	37.02	8.36	18.84	14.65
18	5.64	0.01	-632	379.55	39.58	8.94	18.68	14.52
21	5.61	0.01	-627	354.18	42.21	9.53	17.62	13.70
24	5.59	0.04	-617	312.23	50.20	11.34	15.59	12.13

**Table A-29 Effect of CO<sub>2</sub> bubbling rate on nitrate reduction (Continue)****(d). CO<sub>2</sub> = 800 mL/min**

<b>Time (hr)</b>	<b>pH</b>	<b>DO (mg/L)</b>	<b>ORP (mV)</b>	<b>Fe<sup>2+</sup> (mg/L)</b>	<b>NO<sub>3</sub><sup>-</sup> (mg/L)</b>	<b>NO<sub>3</sub><sup>-</sup> (mgN/L)</b>	<b>NH<sub>4</sub><sup>+</sup> (mg/L)</b>	<b>NH<sub>4</sub><sup>+</sup> (mgN/L)</b>
0	6.42	7.07	275	0.00	102.30	23.10	0.00	0.00
0.16	5.76	0.41	-651	0.00	105.13	23.74	0.00	0.00
0.33	5.78	0.49	-693	0.00	107.30	24.23	0.00	0.00
0.5	5.78	0.31	-696	0.00	109.72	24.78	0.00	0.00
1	5.78	0.16	-701	0.00	98.82	22.31	0.00	0.00
1.5	5.77	0.11	-701	350.77	16.22	3.66	24.70	19.21
2	5.76	0.09	-702	381.99	15.45	3.49	24.92	19.38
2.5	5.75	0.07	-702	429.31	16.56	3.74	24.89	19.36
3	5.73	0.06	-697	429.80	16.58	3.74	24.59	19.13
5	5.7	0.03	-691	434.31	20.20	4.56	23.25	18.08
7	5.66	0.02	-683	434.68	22.75	5.14	22.51	17.51
9	5.63	0.02	-675	432.24	27.10	6.12	21.54	16.75
12	5.58	0.02	-661	433.21	30.42	6.87	19.99	15.55
15	5.55	0.01	-655	414.43	35.11	7.93	18.63	14.49
18	5.53	0.01	-643	389.23	40.38	9.12	17.97	13.98
21	5.5	0.02	-630	371.26	41.11	9.28	17.18	13.36
24	5.45	0.05	-614	323.93	45.72	10.32	14.97	11.64

สถาบันวิทยบริการ  
จุฬาลงกรณ์มหาวิทยาลัย

**Table A-30 Effect of Fe<sup>0</sup> dosages on nitrate reduction****(a). Fe<sup>0</sup> = 20 g**

Time (hr)	pH	DO (mg/L)	ORP (mV)	Fe <sup>2+</sup> (mg/L)	NO <sub>3</sub> <sup>-</sup> (mg/L)	NO <sub>3</sub> <sup>-</sup> (mgN/L)	NH <sub>4</sub> <sup>+</sup> (mg/L)	NH <sub>4</sub> <sup>+</sup> (mgN/L)
0	6.50	7.42	260	0.00	100.78	22.76	0.00	0.00
0.16	4.79	0.27	-332	0.00	99.32	22.43	0.00	0.00
0.33	5.61	0.06	-573	0.00	100.33	22.66	0.00	0.00
0.5	5.70	0.04	-604	0.00	100.80	22.76	0.00	0.00
1	5.82	0.03	-638	0.00	100.87	22.78	0.00	0.00
1.5	5.83	0.03	-643	179.04	51.23	11.57	14.39	11.19
2	5.83	0.04	-647	308.82	23.60	5.33	22.41	17.43
2.5	5.85	0.05	-647	316.13	23.02	5.20	22.57	17.56
3	5.85	0.07	-653	323.45	23.07	5.21	22.56	17.55
5	5.83	0.07	-655	336.62	26.54	5.99	21.55	16.76
7	5.82	0.06	-646	333.21	30.51	6.89	20.40	15.87
9	5.82	0.05	-641	319.06	34.64	7.82	19.20	14.93
12	5.76	0.05	-625	297.11	39.69	8.96	17.74	13.79
15	5.59	0.21	-338	197.58	55.60	12.56	13.12	10.20
18	5.35	0.61	-173	139.53	71.19	16.08	8.59	6.68
21	4.99	0.55	-35	71.72	80.18	18.10	5.98	4.65
24	4.74	0.97	21	40.49	89.00	20.10	3.42	2.66

สถาบันวิทยบริการ  
จุฬาลงกรณ์มหาวิทยาลัย

**Table A-30 Effect of Fe<sup>0</sup> dosages on nitrate reduction (Continue)****(b). Fe<sup>0</sup> = 30 g**

Time (hr)	pH	DO (mg/L)	ORP (mV)	Fe <sup>2+</sup> (mg/L)	NO <sub>3</sub> <sup>-</sup> (mg/L)	NO <sub>3</sub> <sup>-</sup> (mgN/L)	NH <sub>4</sub> <sup>+</sup> (mg/L)	NH <sub>4</sub> <sup>+</sup> (mgN/L)
0	6.43	7.47	280	0.00	100.21	22.63	0.00	0.00
0.16	4.83	0.98	-480	0.00	99.64	22.50	0.00	0.00
0.33	5.71	0.29	-636	0.00	100.32	22.65	0.00	0.00
0.5	5.78	0.12	-682	0.00	102.56	23.16	0.00	0.00
1	5.83	0.03	-693	0.00	100.18	22.62	0.00	0.00
1.5	5.86	0.03	-693	255.15	38.13	8.61	18.02	14.02
2	5.86	0.03	-690	348.82	19.85	4.48	23.33	18.15
2.5	5.86	0.02	-688	355.16	20.53	4.64	23.13	17.99
3	5.85	0.01	-685	368.33	21.86	4.94	22.75	17.69
5	5.86	0.01	-675	380.04	24.22	5.47	22.06	17.16
7	5.83	0.01	-660	381.99	29.46	6.65	20.54	15.98
9	5.80	0.01	-650	378.58	32.38	7.31	19.69	15.32
12	5.76	0.01	-634	363.46	36.79	8.31	18.41	14.32
15	5.69	0.01	-622	340.04	43.35	9.79	16.51	12.84
18	5.64	0.02	-607	303.94	47.36	10.69	15.34	11.93
21	5.53	0.06	-440	252.22	55.44	12.52	13.00	10.11
24	5.25	0.77	-98	145.87	68.63	15.50	9.17	7.13

Table A-30 Effect of Fe<sup>0</sup> dosages on nitrate reduction (Continue)(c). Fe<sup>0</sup> = 40 g

Time (hr)	pH	DO (mg/L)	ORP (mV)	Fe <sup>2+</sup> (mg/L)	NO <sub>3</sub> <sup>-</sup> (mg/L)	NO <sub>3</sub> <sup>-</sup> (mgN/L)	NH <sub>4</sub> <sup>+</sup> (mg/L)	NH <sub>4</sub> <sup>+</sup> (mgN/L)
0	6.48	7.39	248	0.00	102.30	23.10	0.00	0.00
0.16	5.41	0.81	-644	0.00	103.54	23.38	0.00	0.00
0.33	5.90	0.69	-670	0.00	104.80	23.66	0.00	0.00
0.5	5.89	0.26	-689	0.00	104.61	23.62	0.00	0.00
1	5.89	0.10	-702	0.00	102.82	23.22	0.00	0.00
1.5	5.89	0.09	-699	300.62	20.22	4.57	23.83	18.53
2	5.88	0.08	-695	378.99	16.45	3.71	24.92	19.39
2.5	5.86	0.08	-696	390.78	16.56	3.74	24.89	19.36
3	5.86	0.08	-700	398.58	17.58	3.97	24.60	19.13
5	5.85	0.06	-690	417.12	22.20	5.01	23.25	18.09
7	5.82	0.07	-686	419.56	24.75	5.59	22.51	17.51
9	5.80	0.03	-687	419.56	28.10	6.35	21.54	16.75
12	5.76	0.03	-685	410.02	33.42	7.55	20.00	15.55
15	5.74	0.03	-683	384.92	39.51	8.92	18.23	14.18
18	5.72	0.03	-666	372.24	40.38	9.12	17.98	13.98
21	5.68	0.03	-638	348.33	43.71	9.87	17.01	13.23
24	5.65	0.05	-548	306.86	52.72	11.91	14.39	11.20

Table A-30 Effect of Fe<sup>0</sup> dosages on nitrate reduction (Continue)(d). Fe<sup>0</sup> = 60 g

Time (hr)	pH	DO (mg/L)	ORP (mV)	Fe <sup>2+</sup> (mg/L)	NO <sub>3</sub> <sup>-</sup> (mg/L)	NO <sub>3</sub> <sup>-</sup> (mgN/L)	NH <sub>4</sub> <sup>+</sup> (mg/L)	NH <sub>4</sub> <sup>+</sup> (mgN/L)
0	6.68	7.41	258	0.00	100.22	22.63	0.00	0.00
0.16	5.74	0.67	-623	0.00	99.94	22.57	0.00	0.00
0.33	5.90	0.33	-684	0.00	99.93	22.57	0.00	0.00
0.5	5.91	0.16	-690	0.00	100.32	22.65	0.00	0.00
1	5.91	0.06	-698	0.00	102.99	23.26	0.00	0.00
1.5	5.91	0.04	-698	301.25	29.84	6.74	20.44	15.89
2	5.92	0.03	-702	421.51	13.05	2.95	25.31	19.69
2.5	5.94	0.02	-708	431.76	12.96	2.93	25.33	19.70
3	6.04	0.02	-649	445.42	15.43	3.48	24.62	19.15
5	6.01	0.02	-646	475.66	16.86	3.81	24.20	18.82
7	6.01	0.01	-647	473.22	18.53	4.18	23.72	18.45
9	6.01	0.01	-645	469.81	19.25	4.35	23.51	18.28
12	6.01	0.01	-645	458.59	20.37	4.60	23.18	18.03
15	6.01	0.01	-646	446.39	23.40	5.28	22.30	17.35
18	5.98	0.01	-646	432.73	25.04	5.65	21.83	16.98
21	5.95	0.01	-647	408.83	27.51	6.21	21.11	16.42
24	5.93	0.01	-645	390.17	28.07	6.34	20.95	16.29

Table A-30 Effect of Fe<sup>0</sup> dosages on nitrate reduction (Continue)(e). Fe<sup>0</sup> = 80 g

Time (hr)	pH	DO (mg/L)	ORP (mV)	Fe <sup>2+</sup> (mg/L)	NO <sub>3</sub> <sup>-</sup> (mg/L)	NO <sub>3</sub> <sup>-</sup> (mgN/L)	NH <sub>4</sub> <sup>+</sup> (mg/L)	NH <sub>4</sub> <sup>+</sup> (mgN/L)
0	6.50	7.30	297	0.00	100.21	22.63	0.00	0.00
0.16	5.48	0.07	-665	0.00	99.64	22.50	0.00	0.00
0.33	5.96	0.04	-695	0.00	100.32	22.65	0.00	0.00
0.5	5.96	0.04	-705	0.00	102.56	23.16	0.00	0.00
1	5.97	0.02	-712	0.00	100.18	22.62	0.00	0.00
1.5	6.02	0.02	-713	319.06	25.90	5.85	21.57	16.78
2	6.04	0.01	-713	423.95	10.02	2.26	26.18	20.37
2.5	6.06	0.00	-714	455.66	10.20	2.30	26.13	20.33
3	6.06	0.00	-713	472.74	10.88	2.46	25.94	20.17
5	6.07	0.00	-713	501.03	13.65	3.08	25.13	19.55
7	6.06	0.00	-712	524.70	15.18	3.43	24.69	19.20
9	6.05	0.00	-708	535.67	17.04	3.85	24.15	18.78
12	5.99	0.00	-707	519.57	17.83	4.03	23.92	18.60
15	5.97	0.00	-701	510.16	18.54	4.19	23.71	18.44
18	5.96	0.00	-678	481.10	18.32	4.14	23.77	18.49
21	5.98	0.00	-678	467.37	18.83	4.25	23.63	18.38
24	5.98	0.00	-678	451.27	22.19	5.01	22.65	17.62



**Table A-31 Effect of feeding flow rate on nitrate reduction****(a). Feeding rate = 50 mL/min**

Time (hr)	pH	DO (mg/L)	ORP (mV)	Fe <sup>2+</sup> (mg/L)	NO <sub>3</sub> <sup>-</sup> (mg/L)	NO <sub>3</sub> <sup>-</sup> (mgN/L)	NH <sub>4</sub> <sup>+</sup> (mg/L)	NH <sub>4</sub> <sup>+</sup> (mgN/L)
0	6.48	7.39	248	0.00	102.30	23.10	0.00	0.00
0.16	5.41	0.81	-644	0.00	103.54	23.38	0.00	0.00
0.33	5.90	0.69	-670	0.00	104.80	23.66	0.00	0.00
0.5	5.89	0.26	-689	0.00	104.61	23.62	0.00	0.00
1	5.89	0.10	-702	0.00	102.82	23.22	0.00	0.00
1.5	5.89	0.09	-699	300.62	20.22	4.57	23.83	18.53
2	5.88	0.08	-695	378.99	16.45	3.71	24.92	19.39
2.5	5.86	0.08	-696	390.78	16.56	3.74	24.89	19.36
3	5.86	0.08	-700	398.58	17.58	3.97	24.60	19.13
5	5.85	0.06	-690	417.12	22.20	5.01	23.25	18.09
7	5.82	0.07	-686	419.56	24.75	5.59	22.51	17.51
9	5.80	0.03	-687	419.56	28.10	6.35	21.54	16.75
12	5.76	0.03	-685	410.02	33.42	7.55	20.00	15.55
15	5.74	0.03	-683	384.92	39.51	8.92	18.23	14.18
18	5.72	0.03	-666	372.24	40.38	9.12	17.98	13.98
21	5.68	0.03	-638	348.33	43.71	9.87	17.01	13.23
24	5.65	0.05	-548	306.86	52.72	11.91	14.39	11.20

สถาบันวิทยบริการ  
จุฬาลงกรณ์มหาวิทยาลัย

**Table A-31 Effect of feeding flow rate on nitrate reduction (Continue)****(b). Feeding rate = 100 mL/min**

Time (hr)	pH	DO (mg/L)	ORP (mV)	Fe <sup>2+</sup> (mg/L)	NO <sub>3</sub> <sup>-</sup> (mg/L)	NO <sub>3</sub> <sup>-</sup> (mgN/L)	NH <sub>4</sub> <sup>+</sup> (mg/L)	NH <sub>4</sub> <sup>+</sup> (mgN/L)
0	6.35	7.5	297	0.00	98.71	22.29	0.00	0.00
0.16	5.56	2.94	-632	0.00	98.27	22.19	0.00	0.00
0.33	5.88	1.05	-676	0.00	97.74	22.07	0.00	0.00
0.5	5.87	0.54	-697	0.00	98.91	22.33	0.00	0.00
1	5.85	0.08	-694	145.87	63.22	14.28	10.20	7.93
1.5	5.87	0.01	-691	253.2	37.18	8.39	18.64	14.50
2	5.87	0.01	-704	319.06	24.38	5.51	21.72	16.90
2.5	5.87	0.01	-694	365.9	19.05	4.3	22.95	17.85
3	5.88	0.01	-696	348.82	19.27	4.35	23.82	18.52
5	5.85	0.01	-690	343.45	22.05	4.98	22.22	17.28
7	5.81	0.02	-681	316.13	23.69	5.35	21.69	16.87
9	5.77	0.02	-672	318.57	25.55	5.77	21.08	16.39
12	5.74	0.03	-663	308.82	31.48	7.11	19.55	15.21
15	5.7	0.06	-653	294.18	41.07	9.27	17.43	13.55
18	5.64	0.06	-615	271.74	53.72	12.13	12.75	9.92
21	5.42	0.1	-460	196.12	67.67	15.28	9.52	7.40
24	4.97	0.48	0	79.52	87.79	19.82	3.44	2.68

**Table A-31 Effect of feeding flow rate on nitrate reduction (Continue)****(c). Feeding rate = 200 mL/min**

<b>Time (hr)</b>	<b>pH</b>	<b>DO (mg/L)</b>	<b>ORP (mV)</b>	<b>Fe<sup>2+</sup> (mg/L)</b>	<b>NO<sub>3</sub><sup>-</sup> (mg/L)</b>	<b>NO<sub>3</sub><sup>-</sup> (mgN/L)</b>	<b>NH<sub>4</sub><sup>+</sup> (mg/L)</b>	<b>NH<sub>4</sub><sup>+</sup> (mgN/L)</b>
0	6.68	7.5	276	0.00	98.08	22.15	0.00	0.00
0.16	5.63	0.38	-663	0.00	98.61	22.27	0.00	0.00
0.33	5.99	0.37	-688	1.95	60.52	13.67	13.02	10.13
0.5	5.94	0.12	-703	169.78	27.23	6.15	21.18	16.47
1	5.87	0.02	-707	308.82	26.84	6.06	20.53	15.97
1.5	5.84	0.01	-710	301.99	29.41	6.64	20.30	15.79
2	5.83	0.01	-710	299.06	30.96	6.99	19.46	15.13
2.5	5.8	0.01	-710	299.06	30.56	6.9	19.76	15.37
3	5.79	0.01	-709	295.16	30.29	6.84	20.15	15.67
5	5.75	0.01	-705	257.1	39.53	8.93	17.24	13.41
7	5.65	0.01	-694	225.39	43.59	9.84	16.09	12.51
9	5.57	0.02	-662	137.58	68.13	15.38	8.81	6.85
12	5.26	0.14	-375	85.38	92.99	21	1.92	1.49
15	4.71	2.05	-175	64.4	93.27	21.06	0.00	0.00
18	4.65	2.25	45	43.91	94.75	21.4	0.00	0.00
21	4.6	2.65	68	19.51	97.43	22	0.00	0.00
24	4.53	3.04	75	4.88	97.56	22.03	0.00	0.00

**Table A-32 Effect of initial nitrate concentration on nitrate reduction****(a).  $\text{NO}_3^- = 30 \text{ mg/L}$** 

Time (hr)	pH	DO (mg/L)	ORP (mV)	$\text{Fe}^{2+}$ (mg/L)	$\text{NO}_3^-$ (mg/L)	$\text{NO}_3^-$ (mgN/L)	$\text{NH}_4^+$ (mg/L)	$\text{NH}_4^+$ (mgN/L)
0	6.20	7.36	234	0.00	29.26	6.61	0.00	0.00
0.16	5.42	4.86	128	0.00	29.10	6.57	0.00	0.00
0.33	5.83	1.02	-728	0.00	29.00	6.55	0.00	0.00
0.5	5.78	0.54	-730	0.00	29.43	6.65	0.00	0.00
1	5.65	0.10	-724	0.00	29.35	6.63	0.00	0.00
1.5	5.64	0.07	-724	213.19	2.99	0.68	7.62	5.93
2	5.64	0.05	-722	241.49	2.94	0.66	7.64	5.94
2.5	5.63	0.05	-721	265.64	3.30	0.75	7.53	5.86
3	5.60	0.04	-720	287.59	3.27	0.74	7.55	5.87
5	5.54	0.02	-701	315.65	3.36	0.76	7.52	5.85
7	5.48	0.02	-699	321.28	3.36	0.76	7.52	5.85
9	5.45	0.02	-696	321.16	3.49	0.79	7.48	5.82
12	5.41	0.02	-688	320.04	3.46	0.78	7.49	5.83
15	5.38	0.01	-681	313.21	3.62	0.82	7.44	5.79
18	5.36	0.01	-673	298.57	3.73	0.84	7.41	5.76
21	5.32	0.01	-672	279.54	3.75	0.85	7.40	5.76
24	5.30	0.01	-670	262.13	3.72	0.84	7.41	5.77
27	5.28	0.01	-673	258.08	3.85	0.87	7.37	5.74
30	5.25	0.01	-671	250.76	4.05	0.91	7.32	5.69
33	5.25	0.01	-671	233.68	4.18	0.94	7.28	5.66
36	5.22	0.01	-668	223.19	4.18	0.94	7.28	5.66
39	5.19	0.01	-665	218.07	4.42	1.00	7.21	5.61
42	5.14	0.01	-625	184.41	4.74	1.07	7.12	5.53
45	5.1	0.01	-240	139.53	7.71	1.74	6.26	4.87
48	5.05	0.01	-69	104.89	13.05	2.95	4.70	3.66

จุฬาลงกรณ์มหาวิทยาลัย

**Table A-32 Effect of initial nitrate concentration on nitrate reduction (Continue)****(b).  $\text{NO}_3^- = 50 \text{ mg/L}$** 

Time (hr)	pH	DO (mg/L)	ORP (mV)	$\text{Fe}^{2+}$ (mg/L)	$\text{NO}_3^-$ (mg/L)	$\text{NO}_3^-$ (mgN/L)	$\text{NH}_4^+$ (mg/L)	$\text{NH}_4^+$ (mgN/L)
0	6.50	7.38	198	0.00	53.36	12.05	0.00	0.00
0.16	5.57	0.69	-487	0.00	54.28	12.26	0.00	0.00
0.33	5.62	0.20	-705	0.00	53.86	12.16	0.00	0.00
0.5	5.60	0.10	-705	0.00	53.86	12.16	0.00	0.00
1	5.66	0.04	-724	0.00	54.08	12.21	0.00	0.00
1.5	5.71	0.02	-727	265.88	5.00	1.13	14.04	10.92
2	5.72	0.01	-727	308.33	4.82	1.09	14.09	10.96
2.5	5.75	0.01	-729	328.82	5.08	1.15	14.02	10.90
3	5.76	0.01	-731	356.87	5.05	1.14	14.02	10.91
5	5.79	0.01	-732	379.80	5.09	1.15	14.01	10.90
7	5.76	0.01	-730	383.84	6.78	1.53	13.52	10.52
9	5.77	0.01	-723	385.40	7.31	1.65	13.37	10.40
12	5.74	0.00	-703	384.56	8.07	1.82	13.15	10.23
15	5.71	0.00	-673	382.40	7.22	1.63	13.39	10.42
18	5.68	0.00	-675	369.79	7.05	1.59	13.44	10.46
21	5.70	0.00	-678	349.91	8.07	1.82	13.15	10.23
24	5.69	0.00	-654	325.08	7.66	1.73	13.27	10.32
27	5.67	0.00	-652	308.72	8.31	1.88	13.08	10.17
30	5.66	0.01	-649	284.42	8.47	1.91	13.03	10.14
33	5.63	0.01	-648	272.96	9.37	2.11	12.77	9.93
36	5.61	0.01	-643	263.44	9.40	2.12	12.76	9.92
39	5.58	0.01	-620	247.35	9.29	2.10	12.79	9.95
42	5.47	0.03	-356	222.46	11.81	2.67	12.06	9.38
45	5.38	0.14	-150	175.63	20.44	4.62	9.56	7.43
48	5.12	0.03	-23	103.91	34.60	7.81	5.45	4.24

จุฬาลงกรณ์มหาวิทยาลัย

**Table A-32 Effect of initial nitrate concentration on nitrate reduction (Continue)****(c).  $\text{NO}_3^- = 100 \text{ mg/L}$** 

<b>Time (hr)</b>	<b>pH</b>	<b>DO (mg/L)</b>	<b>ORP (mV)</b>	<b>Fe<sup>2+</sup> (mg/L)</b>	<b>NO<sub>3</sub><sup>-</sup> (mg/L)</b>	<b>NO<sub>3</sub><sup>-</sup> (mgN/L)</b>	<b>NH<sub>4</sub><sup>+</sup> (mg/L)</b>	<b>NH<sub>4</sub><sup>+</sup> (mgN/L)</b>
0	6.68	7.41	258	0.00	100.22	22.63	0.00	0.00
0.16	5.74	0.67	-623	0.00	99.94	22.57	0.00	0.00
0.33	5.90	0.33	-684	0.00	99.93	22.57	0.00	0.00
0.5	5.91	0.16	-690	0.00	100.32	22.65	0.00	0.00
1	5.91	0.06	-698	0.00	102.99	23.26	0.00	0.00
1.5	5.91	0.04	-698	301.25	29.84	6.74	20.44	15.89
2	5.92	0.03	-702	421.51	13.05	2.95	25.31	19.69
2.5	5.94	0.02	-708	431.76	12.96	2.93	25.33	19.70
3	6.04	0.02	-649	445.42	15.43	3.48	24.62	19.15
5	6.01	0.02	-646	475.66	16.86	3.81	24.20	18.82
7	6.01	0.01	-647	473.22	18.53	4.18	23.72	18.45
9	6.01	0.01	-645	469.81	19.25	4.35	23.51	18.28
12	6.01	0.01	-645	458.59	20.37	4.60	23.18	18.03
15	6.01	0.01	-646	446.39	23.40	5.28	22.30	17.35
18	5.98	0.01	-646	432.73	25.04	5.65	21.83	16.98
21	5.95	0.01	-647	408.83	27.51	6.21	21.11	16.42
24	5.93	0.01	-645	390.17	28.07	6.34	20.95	16.29
27	5.92	0.02	-641	348.57	31.65	7.15	19.90	15.47
30	5.92	0.02	-638	303.94	41.25	9.31	17.11	13.31
33	5.9	0.02	-631	258.08	67.17	15.17	9.58	7.45
36	5.68	0.05	-117	186.36	85.81	19.38	4.17	3.24
39	5.38	0.63	-56	116.11	94.27	21.29	1.72	1.33
42	5.13	0.82	-3	64.88	98.00	22.13	0.63	0.49
45	4.94	0.88	38	47.32	100.80	22.76	0.00	0.00
48	4.8	0.99	66	22.68	100.81	22.76	0.00	0.00

จุฬาลงกรณ์มหาวิทยาลัย

Table A-32 Effect of initial nitrate concentration on nitrate reduction (Continue)

(d).  $\text{NO}_3^- = 150 \text{ mg/L}$ 

Time (hr)	pH	DO (mg/L)	ORP (mV)	$\text{Fe}^{2+}$ (mg/L)	$\text{NO}_3^-$ (mg/L)	$\text{NO}_3^-$ (mgN/L)	$\text{NH}_4^+$ (mg/L)	$\text{NH}_4^+$ (mgN/L)
0	6.52	7.67	236	0.00	148.14	33.45	0.00	0.00
0.16	5.57	0.00	-661	0.00	147.66	33.34	0.00	0.00
0.33	6.02	0.00	-679	0.00	148.57	33.55	0.00	0.00
0.5	6.10	0.00	-691	0.00	148.06	33.43	0.00	0.00
1	6.11	0.00	-713	0.00	147.84	33.38	0.00	0.00
1.5	6.09	0.00	-715	321.01	68.45	15.46	23.13	17.99
2	6.10	0.00	-714	438.10	41.59	9.39	30.94	24.06
2.5	6.11	0.00	-691	478.59	32.09	7.25	33.69	26.20
3	6.11	0.00	-712	492.57	31.02	7.01	34.00	26.45
5	6.12	0.00	-709	525.64	31.85	7.19	33.76	26.26
7	6.11	0.00	-704	521.25	32.72	7.39	33.51	26.06
9	6.10	0.00	-700	513.76	33.00	7.45	33.43	26.00
12	6.07	0.00	-690	490.01	34.40	7.77	33.02	25.68
15	6.06	0.00	-682	473.22	36.93	8.34	32.29	25.11
18	6.03	0.00	-676	439.56	39.66	8.96	31.49	24.50
21	6.01	0.02	-671	419.07	43.42	9.80	30.40	23.65
24	5.98	0.01	-652	388.61	48.59	10.97	28.90	22.48
27	5.9	0.04	-314	336.62	55.30	12.49	26.95	20.96
30	5.69	0.19	-158	232.71	71.77	16.21	22.17	17.24
33	5.42	0.48	-93	153.67	102.34	23.11	13.30	10.34
36	5.15	0.66	-31	81.47	125.59	28.36	6.55	5.09
39	4.94	0.76	22	38.54	137.37	31.02	3.13	2.43
42	4.81	0.83	50	23.91	144.72	32.68	0.99	0.77
45	4.72	0.88	69	14.15	148.14	33.45	0.00	0.00
48	4.66	0.96	78	7.81	148.53	33.54	0.00	0.00

จุฬาลงกรณ์มหาวิทยาลัย

**Table A-32 Effect of initial nitrate concentration on nitrate reduction (Continue)****(e).  $\text{NO}_3^- = 200 \text{ mg/L}$** 

<b>Time (hr)</b>	<b>pH</b>	<b>DO (mg/L)</b>	<b>ORP (mV)</b>	<b>Fe<sup>2+</sup> (mg/L)</b>	<b>NO<sub>3</sub><sup>-</sup> (mg/L)</b>	<b>NO<sub>3</sub><sup>-</sup> (mgN/L)</b>	<b>NH<sub>4</sub><sup>+</sup> (mg/L)</b>	<b>NH<sub>4</sub><sup>+</sup> (mgN/L)</b>
0	6.50	7.29	369	0.00	204.78	46.24	0.00	0.00
0.16	5.65	0.15	-511	0.00	205.20	46.34	0.00	0.00
0.33	6.03	0.09	-658	0.00	204.20	46.11	0.00	0.00
0.5	6.04	0.10	-691	0.00	204.63	46.21	0.00	0.00
1	6.04	0.07	-703	0.00	204.63	46.21	0.00	0.00
1.5	6.10	0.05	-683	322.96	121.37	27.41	24.22	18.84
2	6.11	0.04	-688	526.40	67.36	15.21	39.90	31.03
2.5	6.12	0.03	-691	568.36	60.10	13.57	42.00	32.67
3	6.12	0.03	-687	573.24	59.25	13.38	42.25	32.86
5	6.11	0.02	-676	577.38	60.57	13.68	41.87	32.56
7	6.08	0.01	-664	576.28	63.73	14.39	40.95	31.85
9	6.06	0.01	-656	568.97	65.10	14.70	40.55	31.54
12	6.05	0.01	-671	550.52	65.14	14.71	40.54	31.53
15	6.00	0.01	-656	533.60	67.22	15.18	39.94	31.06
18	5.99	0.01	-653	488.54	73.60	16.62	38.09	29.62
21	5.96	0.01	-638	459.20	83.69	18.90	35.16	27.34
24	5.84	0.03	-571	386.63	102.21	23.08	29.78	23.16
27	5.64	0.12	-273	248.81	138.93	31.37	19.12	14.87
30	5.4	0.37	-152	136.11	166.02	37.49	11.26	8.75
33	5.15	0.66	-85	79.03	190.01	42.61	11.25	8.75
36	4.88	0.53	-24	37.81	190.34	42.98	4.19	3.26
39	4.67	0.47	15	15.69	195.97	44.25	2.56	1.99
42	4.61	0.78	44	8.56	197.95	44.70	1.99	1.54
45	4.52	0.69	66	6.00	199.80	45.12	1.45	1.13
48	4.45	0.74	78	3.78	201.02	45.39	1.09	0.85

จุฬาลงกรณ์มหาวิทยาลัย



**Table A-33 Effect of Fe<sup>0</sup> supplement on nitrate reduction.****(a) 0g of Fe<sup>0</sup> supplement**

<b>Time (hr)</b>	<b>pH</b>	<b>DO (mg/L)</b>	<b>ORP (mV)</b>	<b>Fe<sup>2+</sup> (mg/L)</b>	<b>NO<sub>3</sub><sup>-</sup> (mg/L)</b>	<b>NO<sub>3</sub><sup>-</sup> (mgN/L)</b>	<b>NH<sub>4</sub><sup>+</sup> (mg/L)</b>	<b>NH<sub>4</sub><sup>+</sup> (mgN/L)</b>
0	6.50	7.29	369	0.00	204.78	46.24	0.00	0.00
0.16	5.65	0.15	-511	0.00	205.20	46.34	0.00	0.00
0.33	6.03	0.09	-658	0.00	204.20	46.11	0.00	0.00
0.5	6.04	0.10	-691	0.00	204.63	46.21	0.00	0.00
1	6.04	0.07	-703	0.00	204.63	46.21	0.00	0.00
1.5	6.10	0.05	-683	322.96	121.37	27.41	24.22	18.84
2	6.11	0.04	-688	526.40	67.36	15.21	39.90	31.03
2.5	6.12	0.03	-691	568.36	60.10	13.57	42.00	32.67
3	6.12	0.03	-687	573.24	59.25	13.38	42.25	32.86
5	6.11	0.02	-676	577.38	60.57	13.68	41.87	32.56
7	6.08	0.01	-664	576.28	63.73	14.39	40.95	31.85
9	6.06	0.01	-656	568.97	65.10	14.70	40.55	31.54
12	6.05	0.01	-671	550.52	65.14	14.71	40.54	31.53
15	6.00	0.01	-656	533.60	67.22	15.18	39.94	31.06
18	5.99	0.01	-653	488.54	73.60	16.62	38.09	29.62
21	5.96	0.01	-638	459.20	83.69	18.90	35.16	27.34
24	5.84	0.03	-571	386.63	102.21	23.08	29.78	23.16
27	5.64	0.12	-273	248.81	138.93	31.37	19.12	14.87
30	5.4	0.37	-152	136.11	166.02	37.49	11.26	8.75
33	5.15	0.66	-85	79.03	190.01	42.61	11.25	8.75
36	4.88	0.53	-24	37.81	190.34	42.98	4.19	3.26
39	4.67	0.47	15	15.69	195.97	44.25	2.56	1.99
42	4.61	0.78	44	8.56	197.95	44.70	1.99	1.54
45	4.52	0.69	66	6.00	199.80	45.12	1.45	1.13
48	4.45	0.74	78	3.78	201.02	45.39	1.09	0.85

จุฬาลงกรณ์มหาวิทยาลัย

**Table A-33 Effect of Fe<sup>0</sup> supplement on nitrate reduction (Continue)****(b) 30 g of Fe<sup>0</sup> supplement**

Time (hr)	pH	DO (mg/L)	ORP (mV)	Fe <sup>2+</sup> (mg/L)	NO <sub>3</sub> <sup>-</sup> (mg/L)	NO <sub>3</sub> <sup>-</sup> (mgN/L)	NH <sub>4</sub> <sup>+</sup> (mg/L)	NH <sub>4</sub> <sup>+</sup> (mgN/L)
0	6	6.7	210	0	98.16	22.17	0	0
0.16	4.98	0.8	-483	0	98.8	22.31	0	0
0.33	6.07	0.26	-696	0	99.05	22.37	0	0
0.5	6.13	0.1	-713	0	99.12	22.38	0	0
1	6.08	0.04	-722	0	96.74	21.85	0	0
1.5	6.05	0.02	-721	244.42	39.04	8.82	16.91	13.15
2	6.06	0.01	-722	347.84	16.18	3.65	23.41	18.21
2.5	6.06	0.01	-722	390.78	15.2	3.43	23.82	18.53
3	6.07	0.01	-722	391.75	15.17	3.43	24.18	18.81
5	6.08	0.01	-722	406.39	15.71	3.55	23.72	18.45
7	6.07	0	-721	407.36	16.48	3.72	23.45	18.24
9	6.05	0	-720	418.1	18.16	4.1	23.46	18.25
12	6.05	0	-716	404.44	19.36	4.37	22.55	17.54
15	6.03	0	-706	394.68	21.5	4.85	22.27	17.32
18	6.01	0	-697	385.41	24.49	5.53	21.38	16.63
21	5.98	0	-683	377.6	25.02	5.65	20.98	16.32
24	5.97	0	-674	357.11	24.86	5.61	20.87	16.23
27	5.98	0	-665	346.87	27.23	6.15	21.54	16.75
27.16	6.04	0	-682	349.31	30.48	6.88	21.41	16.65
27.33	6.06	0	-685	351.26	30.21	6.82	20.29	15.78
27.5	6.07	0	-685	355.16	29.76	6.72	20.26	15.76
28	6.08	0	-678	357.6	28.8	6.5	19.98	15.54
28.5	6.07	0	-680	398.09	25.79	5.82	20.25	15.75
29	6.07	0	-681	408.34	20.84	4.71	21.41	16.65
29.5	6.07	0.01	-680	415.66	19.57	4.42	22.82	17.75
30	6.07	0.01	-677	413.71	19.35	4.37	22.55	17.54
32	6.06	0.01	-678	413.22	19.24	4.35	22.67	17.63
34	6.06	0.01	-683	399.56	19.49	4.4	22.41	17.43
36	6.05	0.01	-680	399.56	24.13	5.45	22.94	17.84
39	6.02	0.01	-676	393.7	25.2	5.69	20.89	16.25
42	5.99	0.01	-672	371.75	29.33	6.62	18.63	14.49
45	5.96	0.02	-660	349.31	29.7	6.71	18.45	14.35
48	5.95	0.03	-658	330.28	33.4	7.54	18.31	14.24
51	5.88	0.06	-589	294.67	32.71	7.39	17.94	13.95
54	5.66	0.23	-154	191.73	67.27	15.19	10.48	8.15
54.16	5.92	0.03	-597	179.53	67.38	15.21	10.2	7.93

**Table A-33 Effect of Fe<sup>0</sup> supplement on nitrate reduction (Continue)****(b) 30 g of Fe<sup>0</sup> supplement (Continue)**

Time (hr)	pH	DO (mg/L)	ORP (mV)	Fe <sup>2+</sup> (mg/L)	NO <sub>3</sub> <sup>-</sup> (mg/L)	NO <sub>3</sub> <sup>-</sup> (mgN/L)	NH <sub>4</sub> <sup>+</sup> (mg/L)	NH <sub>4</sub> <sup>+</sup> (mgN/L)
54.33	5.96	0.03	-636	182.95	65.76	14.85	9.55	7.43
54.5	5.99	0.03	-643	183.44	65.16	14.71	10.05	7.82
55	6.01	0.02	-654	233.68	53.88	12.17	12.29	9.56
55.5	6.01	0.01	-657	339.55	23.75	5.36	16.98	13.21
56	6.04	0.01	-641	356.14	22.71	5.13	21.65	16.84
56.5	6.05	0.01	-637	370.29	22.17	5.01	21.54	16.75
57	6.04	0.01	-639	369.8	21.92	4.95	21.9	17.03
59	6.01	0.01	-651	375.16	25.51	5.76	20.84	16.21
61	6.01	0.01	-643	369.31	28.45	6.42	20.51	15.95
63	5.96	0.01	-653	359.55	32.54	7.35	19.56	15.21
66	5.94	0.03	-660	343.45	33.26	7.51	18.32	14.25
69	5.91	0.03	-653	328.82	33.34	7.53	17.97	13.98
72	5.89	0.05	-618	308.82	37.79	8.53	16.91	13.15
75	5.78	0.11	-278	236.61	53.78	12.14	11.64	9.05
78	5.53	0.46	-105	141.48	76.31	17.23	6.7	5.21
81	5.3	0.76	-52	80.98	91.02	20.55	2.89	2.25

Table A-33 Effect of Fe<sup>0</sup> supplement on nitrate reduction (Continue)(c) 40 g of Fe<sup>0</sup> supplement

Time (hr)	pH	DO (mg/L)	ORP (mV)	Fe <sup>2+</sup> (mg/L)	NO <sub>3</sub> <sup>-</sup> (mg/L)	NO <sub>3</sub> <sup>-</sup> (mgN/L)	NH <sub>4</sub> <sup>+</sup> (mg/L)	NH <sub>4</sub> <sup>+</sup> (mgN/L)
0	6	7.41	166	0	98.94	22.34	0	0
0.16	5.52	0.46	-564	0	99.41	22.45	0	0
0.33	6.07	0.33	-691	0	99.22	22.41	0	0
0.5	6.14	0.19	-705	0	99.13	22.38	0	0
1	6.07	0.05	-724	0	99.51	22.47	0	0
1.5	6.04	0.03	-724	265.88	34.04	7.69	19.41	15.09
2	6.05	0.03	-724	397.61	14.89	3.36	25.13	19.55
2.5	6.06	0.02	-724	407.36	14.44	3.26	25.27	19.65
3	6.07	0.02	-724	422.49	14.3	3.23	25.31	19.69
5	6.07	0.01	-724	432.24	17.64	3.98	24.31	18.91
7	6.05	0.01	-724	445.42	20.15	4.55	23.56	18.32
9	6.05	0.01	-724	450.78	20.67	4.67	23.41	18.21
12	6.02	0.01	-724	439.07	21.91	4.95	23.03	17.91
15	6.01	0.01	-723	429.32	23.35	5.27	22.82	17.75
18	5.98	0.01	-722	402.48	24.55	5.54	22.46	17.47
21	5.96	0.01	-719	390.29	26.07	5.89	22	17.11
24	5.95	0.01	-716	368.82	27.27	6.16	21.64	16.83
27	5.95	0.01	-715	352.72	29.11	6.57	21.08	16.4
27.16	6.04	0.01	-715	338.57	30.97	6.99	20.52	15.96
27.33	6.08	0.01	-716	336.62	31.34	7.08	20.41	15.87
27.5	6.09	0.01	-719	347.36	29.88	6.75	20.85	16.22
28	6.1	0.01	-720	341.01	28.65	6.47	21.22	16.51
28.5	6.11	0.01	-720	437.61	20.31	4.59	23.74	18.46
29	6.12	0.01	-720	433.22	18.83	4.25	24.19	18.81
29.5	6.11	0.01	-720	417.61	18.49	4.18	24.29	18.89
30	6.11	0.01	-719	454.69	18.69	4.22	24.23	18.85
32	6.1	0.01	-714	445.42	18.81	4.25	24.19	18.82
34	6.06	0.01	-713	440.05	19.57	4.42	23.96	18.64
36	6.05	0.01	-709	422	23.22	5.24	22.86	17.78
39	6.02	0.01	-699	391.26	25.15	5.68	22.28	17.33
42	5.99	0.01	-692	381.51	26.03	5.88	22.01	17.12
45	5.97	0.01	-686	379.56	28.2	6.37	21.36	16.61
48	5.97	0.01	-685	364.92	29.86	6.74	20.86	16.22
51	5.95	0.01	-680	344.92	32.79	7.4	19.97	15.54
54	5.9	0.01	-666	322.48	35.38	7.99	19.19	14.93
54.16	6.02	0.01	-695	315.65	35.74	8.07	19.08	14.84

**Table A-33 Effect of Fe<sup>0</sup> supplement on nitrate reduction (Continue)****(c) 40 g of Fe<sup>0</sup> supplement (Continue)**

Time (hr)	pH	DO (mg/L)	ORP (mV)	Fe <sup>2+</sup> (mg/L)	NO <sub>3</sub> <sup>-</sup> (mg/L)	NO <sub>3</sub> <sup>-</sup> (mgN/L)	NH <sub>4</sub> <sup>+</sup> (mg/L)	NH <sub>4</sub> <sup>+</sup> (mgN/L)
54.33	6.06	0.01	-699	314.67	35.74	8.07	19.08	14.84
54.5	6.07	0.01	-700	330.28	32.86	7.42	19.95	15.52
55	6.08	0.01	-705	365.9	28.82	6.51	21.17	16.47
55.5	6.07	0.01	-706	405.9	22.13	5	23.19	18.04
56	6.07	0.01	-705	404.44	20.39	4.61	23.72	18.45
56.5	6.07	0.01	-702	425.9	20.25	4.57	23.76	18.48
57	6.07	0.01	-702	408.83	20.12	4.54	23.8	18.51
59	6.04	0.01	-700	421.02	22.53	5.09	23.07	17.94
61	6.03	0.01	-696	425.9	22.87	5.17	22.97	17.86
63	6	0.01	-689	416.14	23.16	5.23	22.88	17.8
66	5.99	0.01	-673	396.63	24.15	5.45	22.58	17.56
69	5.97	0.01	-669	380.04	24.76	5.59	22.4	17.42
72	5.98	0.01	-664	368.82	26.87	6.07	21.76	16.92
75	5.96	0.01	-659	356.14	31.53	7.12	20.35	15.83
78	5.93	0.01	-644	332.72	32.59	7.36	20.03	15.58
81	5.85	0.01	-588	299.06	36.21	8.18	18.94	14.73

**Table A-33 Effect of Fe<sup>0</sup> supplement on nitrate reduction (Continue)****(d) 50 g of Fe<sup>0</sup> supplement**

Time (hr)	pH	DO (mg/L)	ORP (mV)	Fe <sup>2+</sup> (mg/L)	NO <sub>3</sub> <sup>-</sup> (mg/L)	NO <sub>3</sub> <sup>-</sup> (mgN/L)	NH <sub>4</sub> <sup>+</sup> (mg/L)	NH <sub>4</sub> <sup>+</sup> (mgN/L)
0	6.21	6.8	230	0	99.4	22.44	0	0
0.16	5.32	0.43	-653	0	99	22.36	0	0
0.33	6.08	0.21	-692	0	98.44	22.23	0	0
0.5	6.19	0.08	-708	0	98.84	22.32	0	0
1	6.11	0.03	-722	0	96.42	21.77	0	0
1.5	6.09	0.05	-722	292.72	33.23	7.5	19	14.78
2	6.09	0.01	-722	347.84	15.83	3.57	24.7	19.21
2.5	6.09	0.01	-720	375.65	13.76	3.11	25.14	19.55
3	6.11	0.01	-720	386.87	13.24	2.99	25.43	19.78
5	6.12	0.01	-720	415.17	15.32	3.46	24.7	19.21
7	6.12	0.01	-719	420.54	17.46	3.94	23.55	18.32
9	6.11	0.01	-716	421.02	19.37	4.37	23.86	18.56
12	6.07	0.01	-715	412.24	20.92	4.72	22.98	17.87
15	6.06	0.01	-712	407.36	22.15	5	22.55	17.54
18	6.04	0.01	-709	388.82	22.83	5.16	22.55	17.54
21	6.05	0.01	-704	383.46	25.69	5.8	22.72	17.67
24	6.04	0.01	-699	363.46	28.75	6.49	20.98	16.32
27	6.01	0.01	-690	358.09	32.09	7.25	20.51	15.95
27.16	6.11	0	-705	343.94	31.8	7.18	20.25	15.75
27.33	6.14	0	-710	347.84	31.02	7	20.15	15.67
27.5	6.15	0	-717	351.26	29.22	6.6	21.83	16.98
28	6.16	0	-718	365.41	18.35	4.14	22.86	17.78
28.5	6.16	0	-720	436.15	17.17	3.88	23.49	18.27
29	6.16	0	-722	446.88	16.81	3.79	23.72	18.45
29.5	6.16	0	-722	455.66	17.42	3.93	23.46	18.25
30	6.16	0	-723	459.56	18.8	4.24	23.34	18.15
32	6.15	0	-723	457.12	20.42	4.61	23.34	18.15
34	6.15	0	-723	450.29	22.53	5.09	23.55	18.32
36	6.15	0	-723	449.32	25.75	5.81	22.27	17.32
39	6.12	0	-723	436.63	27.56	6.22	22.44	17.45
42	6.11	0	-716	424.44	28.94	6.53	22.13	17.21
45	6.11	0	-709	408.83	30.1	6.8	21.15	16.45
48	6.11	0	-703	384.43	30.72	6.94	20.51	15.95
51	6.08	0	-698	393.22	31.5	7.11	19.56	15.21
54	6.05	0	-692	359.06	32.65	7.37	19.22	14.95
54.16	6.14	0	-699	362.97	30.83	6.96	20.25	15.75

**Table A-33 Effect of Fe<sup>0</sup> supplement on nitrate reduction (Continue)****(d) 50 g of Fe<sup>0</sup> supplement (Continue)**

Time (hr)	pH	DO (mg/L)	ORP (mV)	Fe <sup>2+</sup> (mg/L)	NO <sub>3</sub> <sup>-</sup> (mg/L)	NO <sub>3</sub> <sup>-</sup> (mgN/L)	NH <sub>4</sub> <sup>+</sup> (mg/L)	NH <sub>4</sub> <sup>+</sup> (mgN/L)
54.33	6.17	0	-702	370.29	29.83	6.74	20.25	15.75
54.5	6.18	0	-702	376.63	23.9	5.4	22.44	17.45
55	6.18	0	-700	410.78	19.41	4.38	22.82	17.75
55.5	6.19	0	-699	429.32	17.2	3.88	23.73	18.46
56	6.2	0	-699	458.59	17.36	3.92	23.95	18.63
56.5	6.2	0	-722	464.93	17.07	3.85	23.85	18.55
57	6.19	0	-722	462.49	18.79	4.24	23.46	18.25
59	6.17	0	-721	470.78	20.17	4.55	23.41	18.21
61	6.15	0	-722	459.08	21.36	4.82	22.86	17.78
63	6.14	0	-721	448.34	22.73	5.13	22.44	17.45
66	6.12	0	-722	429.32	22.88	5.17	22.31	17.35
69	6.1	0	-718	395.17	23.72	5.36	22.15	17.23
72	6.09	0	-713	388.34	27.42	6.19	21.54	16.75
75	6.05	0	-708	374.68	28.12	6.35	21.02	16.35
78	6.04	0	-702	370.29	30.99	7	20.84	16.21
81	6.01	0	-692	349.31	32.23	7.28	20.25	15.75

## Continuous mode study of ferrous removal by iron precipitation process

**Table A-34 Effect of sand dosage on ferrous removal**

**(a). sand with size of 0.42-0.59 mm = 10 kg**

Time (hr)	pH	DO (mg/L)	ORP (mV)	Total iron (mg/L)
0	6.18	6.62	192	0
1	7.07	7.32	109	1.8
3	6.68	6.75	-68	3.34
5	6.1	6.92	-68	4.23
7	6.21	7.74	-55	3.51
9	6.19	7.86	-58	3.1
12	6.19	7.09	-55	5.31
15	6.33	8.49	-66	5.82
18	6.39	8.23	-66	5.62
21	6.48	9.12	-46	12.67
24	6.43	9.32	-43	9.96
27	6.41	9.35	-60	9.61
30	6.42	9.02	-60	9.78
33	6.38	8.32	-63	14.88
36	6.37	9.35	-55	23.81
39	6.5	8.02	-50	22.19
42	6.49	8.22	-43	33.83
45	6.51	8.09	-22	32.54
48	6.47	9.3	-34	40.71
51	6.52	8.76	-24	50.34

สถาบันวิทยบริการ  
จุฬาลงกรณ์มหาวิทยาลัย



**Table A-34 Effect of sand dosage on ferrous removal (Continue)****(b). sand with size of 0.42-0.59 mm = 15 kg**

<b>Time (hr)</b>	<b>pH</b>	<b>DO (mg/L)</b>	<b>ORP (mV)</b>	<b>Total iron (mg/L)</b>
0	6.02	6.02	220	0.00
1	6.52	7.32	153	0.76
3	6.75	8.12	83	1.93
5	6.7	9.13	-43	2.14
7	6.74	9.12	-44	2.52
9	6.69	9.06	-40	2.69
12	6.43	9.1	-39	2.76
15	6.3	9.49	-30	5.21
18	6.93	9.36	-22	3.86
21	7.07	9.41	-9	2.92
24	7.02	9.36	-12	4.29
27	6.87	9.33	-11	5.00
30	6.93	9.36	-8	4.49
33	6.99	9.11	-3	11.05
36	6.98	9.25	23	9.94
39	7.1	8.95	42	8.82
42	7.09	9.94	18	12.81
45	6.36	9.93	25	16.84
48	6.42	9.12	29	15.44
51	7.39	9.63	30	24.24
54	6.45	8.53	34	31.67
57	6.32	9.43	65	36.29
60	6.28	9.21	43	39.4
63	6.85	9.15	23	43.57
66	6.53	8.43	10	49.93

**Table A-34 Effect of sand dosage on ferrous removal (Continue)****(c). sand with size of 0.42-0.59 mm = 20 kg**

<b>Time (hr)</b>	<b>pH</b>	<b>DO (mg/L)</b>	<b>ORP (mV)</b>	<b>Total iron (mg/L)</b>
0	6.32	6.05	210	0
1	6.45	7.85	121	0.64
3	6.48	8.03	24	1.54
5	6.8	8.22	67	1.92
7	6.83	9.29	32	3.2
9	6.82	8.73	-26	3.16
12	6.71	8.58	-30	2.9
15	6.69	9.71	-20	3.14
18	6.75	9.78	18	3.26
21	6.98	9.78	25	3.34
24	6.63	9.6	29	4.34
27	6.52	9.62	30	1.68
30	6.44	9.5	34	3.15
33	6.98	9.1	65	3.87
36	7.06	9.48	-9	5.66
39	6.78	9.45	3	6.88
42	6.78	9.43	5	8.33
45	6.84	9.39	2	13.57
48	7	9.4	8	13.94
51	6.37	9.66	5	17.27
54	6.45	9.52	6	23.4
57	7	9.98	8	22.93
60	6.27	9.54	8	25.54
63	6.32	8.15	8	31.01
66	6.81	8.24	3	34.14

**Table A-34 Effect of sand dosage on ferrous removal (Continue)****(d). sand with no size classification = 25 kg**

<b>Time (hr)</b>	<b>pH</b>	<b>DO (mg/L)</b>	<b>ORP (mV)</b>	<b>Total iron (mg/L)</b>
0	7.3	8.48	235	0
1	7.24	9.73	116	2.47
3	7.04	9.03	100	4.33
5	7.07	9.26	56	5.56
7	7.1	9.27	21	6.1
9	7.09	9.25	34	5.94
12	6.87	9.4	22	5.31
15	6.52	9.34	34	7.58
18	6.51	10.43	15	9.14
21	7.1	9.39	8	12.64
24	7.2	9.56	5	13.12
27	7.2	9.5	-5	15.03
30	7.15	9.23	-24	15.17
33	7.08	9.28	-13	17.13
36	6.97	9.21	-21	18.63
39	7.05	9.76	-18	20.83
42	7.15	10.21	-15	22.49
45	6.98	9.92	-13	24.49
48	7.15	9.95	-8	25.57
51	7.29	9.84	-19	32.97
54	7.14	10	-7	33.56
57	7.12	10	-5	36.07
60	6.98	9.86	-17	34.26
63	6.98	10.24	-16	38.04
66	6.98	10.36	-15	40.23

## Continuous mode study of ammonia removal by air stripping process

**Table A-35 Effect of air flow rate on ammonia removal**

**(a). air = 150 L/min**

Time (hr)	pH	NH <sub>4</sub> <sup>+</sup> (mg N/L)
0	6.54	0
1	6.56	0
3	6.85	0.78
5	6.85	1.60
7	6.92	2.94
9	6.8	3.46
11	6.89	3.71
13	6.78	3.67
15	6.84	3.55
18	6.98	3.68
21	6.83	3.81
24	6.8	3.73

Tray	NH <sub>4</sub> <sup>+</sup> (mg N/L)
1	17.56
2	13.60
3	9.08
4	6.58
5	4.15
6	3.71

สถาบันวิทยบริการ  
จุฬาลงกรณ์มหาวิทยาลัย

**Table A-35 Effect of air flow rate on ammonia removal (Continue)****(b). air = 180 L/min**

Time (hr)	pH	NH <sub>4</sub> <sup>+</sup> (mg N/L)
0	6.71	0
1	6.92	0
3	7.03	0.68
5	7.12	1.27
7	7.03	1.92
9	6.86	2.07
11	6.9	2.30
13	6.89	2.35
15	6.91	2.45
18	6.93	2.32
21	6.94	2.36
24	6.93	2.35

Tray	NH <sub>4</sub> <sup>+</sup> (mg N/L)
1	15.27
2	10.96
3	6.44
4	3.97
5	2.61
6	2.35

สถาบันวิทยบริการ  
จุฬาลงกรณ์มหาวิทยาลัย

## Field testing study of nitrate reduction by Fe<sup>0</sup>/CO<sub>2</sub> process

**Table A-36 Comparison performance of integrated system**

**(a) NO<sub>3</sub><sup>-</sup> spiked in groundwater**

Time (hr)	pH	DO (mg/L)	ORP (mV)	Fe <sup>2+</sup> (mg/L)	NO <sub>3</sub> <sup>-</sup> (mg/L)	NO <sub>3</sub> <sup>-</sup> (mgN/L)	NH <sub>4</sub> <sup>+</sup> (mg/L)	NH <sub>4</sub> <sup>+</sup> (mgN/L)
0	7.52	5.81	247	0	97.77	22.08	0	0
0.16	6.25	7.4	213	0	97.78	22.08	0	0
0.33	6.06	6.35	162	0	97.16	21.94	0	0
0.5	5.94	4.33	100	0	96.3	21.75	0	0
1	6.03	0.22	-402	0	94.97	21.44	1.02	0.8
1.5	6.16	0.07	-723	28.3	92.82	20.96	1.69	1.32
2	6.12	0.19	-728	127.82	43.97	9.93	15.23	11.85
2.5	6.12	0.16	-710	232.22	35.76	8.07	17.69	13.76
3	6.11	0.13	-710	301.01	27.67	6.25	19.22	14.95
5	6.01	0.12	-711	349.8	30.12	6.8	19.42	15.11
7	6.03	0.12	-710	361.02	31.54	7.12	19.35	15.05
9	6.03	0.15	-712	372.73	28.9	6.53	19.90	15.48
12	6	0.18	-712	379.56	27.68	6.25	20.28	15.78
15	5.95	0.16	-711	373.21	28.27	6.38	20.12	15.65
18	5.84	0.19	-710	368.33	28.94	6.53	19.55	15.21
21	5.98	0.15	-709	364.43	30.9	6.98	19.10	14.86
24	6.04	0.13	-704	358.09	35.5	8.02	18.60	14.47
27	5.84	0.11	-708	338.09	38.72	8.74	18.27	14.21
30	5.88	0.1	-704	371.26	31.66	7.15	19.00	14.78
33	5.92	0.07	-718	374.19	30.59	6.91	19.23	14.96
36	5.9	0.06	-718	390.29	30.75	6.94	19.26	14.98
39	5.9	0.06	-718	384.43	33.37	7.54	19.73	15.35
42	5.95	0.05	-717	369.31	33.89	7.65	18.93	14.73
45	6.04	0.05	-716	356.14	34.16	7.71	19.22	14.95
48	6.02	0.04	-714	322.96	34.47	7.78	19.10	14.86
51	5.95	0.04	-711	301.99	36.07	8.14	18.16	14.13
54	5.82	0.04	-705	291.25	37.69	8.51	17.82	13.86
57	5.89	0.03	-717	366.38	31.44	7.1	18.59	14.46
60	5.92	0.03	-717	372.73	34.02	7.68	18.02	14.02
63	5.94	0.02	-715	381.02	34.07	7.69	18.16	14.13
66	5.94	0.02	-715	375.65	34.61	7.82	17.16	13.35
69	6.05	0.02	-713	358.58	35.62	8.04	16.98	13.21
72	6.09	0.02	-708	342.48	36.6	8.26	16.74	13.02

**Table A-36 Comparison performance of integrated system (Continue)****(b) NO<sub>3</sub><sup>-</sup> spiked in RO water**

<b>Time (hr)</b>	<b>pH</b>	<b>DO (mg/L)</b>	<b>ORP (mV)</b>	<b>Fe<sup>2+</sup> (mg/L)</b>	<b>NO<sub>3</sub><sup>-</sup> (mg/L)</b>	<b>NO<sub>3</sub><sup>-</sup> (mgN/L)</b>	<b>NH<sub>4</sub><sup>+</sup> (mg/L)</b>	<b>NH<sub>4</sub><sup>+</sup> (mgN/L)</b>
0	7.21	6.76	245	0	97.81	22.09	0	0
0.16	5.42	0.96	-498	0	98.41	22.22	0	0
0.33	6.07	0.57	-688	0	98.02	22.13	0	0
0.5	6.31	0.25	-685	0	97.7	22.06	0	0
1	6.19	0.1	-719	0	97.73	22.07	0	0
1.5	6.07	0.1	-719	250.27	35.83	8.09	16.61	12.92
2	6.02	0.1	-718	340.53	22.47	5.07	22.49	17.49
2.5	6.02	0.08	-720	396.14	14.81	3.34	22.62	17.59
3	6.01	0.08	-721	418.58	16.09	3.63	23.04	17.92
5	6.01	0.05	-722	446.39	17.35	3.92	22.88	17.8
7	5.98	0.05	-722	441.51	18.09	4.09	22.54	17.53
9	5.98	0.03	-720	433.71	18.97	4.28	22.33	17.37
12	5.95	0.03	-721	430.78	19.79	4.47	22.21	17.28
15	5.96	0.03	-718	424.44	21.61	4.88	21.77	16.93
18	5.94	0.03	-714	398.58	24.54	5.54	21.32	16.58
21	5.92	0.03	-713	385.41	24.86	5.61	21.27	16.54
24	5.92	0.03	-713	380.04	29.47	6.65	21.03	16.36
27	5.92	0.02	-710	375.65	31.29	7.07	20.41	15.88
30	6.05	0.02	-717	446.88	16.33	3.69	22.25	17.31
33	6.03	0.02	-714	444.93	17.63	3.98	22.38	17.41
36	5.98	0.02	-712	436.63	20.31	4.59	22.03	17.13
39	5.98	0.02	-710	428.34	23.16	5.23	21.65	16.84
42	5.96	0.02	-708	419.07	23.55	5.32	20.77	16.16
45	5.95	0.02	-710	402	24.65	5.57	21.08	16.4
48	5.96	0.02	-704	382.48	27.08	6.11	20.75	16.14
51	5.93	0.02	-698	361.5	29.32	6.62	20.34	15.82
54	5.9	0.02	-691	347.36	31.65	7.15	20.93	16.28
57	6.04	0.01	-700	412.24	18.71	4.22	22.03	17.13
60	6.01	0.01	-699	420.05	20.55	4.64	21.81	16.96
63	5.98	0.01	-698	435.17	21.53	4.86	22.48	17.49
66	5.96	0.01	-690	433.22	23.86	5.39	21.68	16.86
69	5.95	0.01	-684	408.34	24.07	5.44	22.17	17.24
72	5.95	0.01	-673	397.12	25.23	5.7	20.15	15.67

## Field testing study of iron removal by iron precipitation process

**Table A-37 Comparison performance of integrated system.**

**(a) NO<sub>3</sub><sup>-</sup> spiked in groundwater**

Time (hr)	pH	DO (mg/L)	ORP (mV)	Fe <sup>2+</sup> (mg/L)	NO <sub>3</sub> <sup>-</sup> (mg/L)	NO <sub>3</sub> <sup>-</sup> (mgN/L)	NH <sub>4</sub> <sup>+</sup> (mg/L)	NH <sub>4</sub> <sup>+</sup> (mgN/L)
0	6.79	7.12	212	0	0	0	0	0
1	7.28	11.12	100	2.62	25.24	5.7	0.55	0.42
1.5	7.29	10.99	87	4	18.18	4.1	0.83	0.65
2	7.3	10.72	21	6.17	19.38	4.38	1	0.78
2.5	7.15	10.57	-39	6.52	18.84	4.25	1.66	1.29
3	7.29	10.37	-44	7.09	20.55	4.64	2.53	1.97
5	7.36	10.32	-60	10.76	25.86	5.84	6.7	5.21
7	7.48	9.82	-36	15.89	25.12	5.67	9.39	7.3
9	7.52	9.56	-21	15.39	27.97	6.32	13.04	10.14
12	7.55	9.66	-13	21.53	31.1	7.02	15.7	12.21
15	7.56	10.08	-35	28.13	31.01	7	17.09	13.29
18	7.56	9.97	-45	29.77	30.6	6.91	17.31	13.46
21	7.66	9.92	-7	31.24	32.37	7.31	17.26	13.43
24	7.66	9.84	-4	39.27	33.63	7.59	16.31	12.68
27	7.65	10.00	-9	40.79	33.05	7.46	16.93	13.17
30	7.63	10.00	-5	42.93	31.79	7.18	17.34	13.49
33	7.55	9.87	-55	42.09	31.05	7.01	16.89	13.14
36	7.52	10.14	-58	39.21	29.09	6.57	18.22	14.17
39	7.61	10.5	-32	47.97	31.29	7.07	18.77	14.6
42	7.58	10.53	-32	54.99	31.5	7.11	19.32	15.02
45	7.61	10.33	-19	64.5	32.35	7.3	18.7	14.55
48	7.63	9.91	-2	64.8	34.42	7.77	19.1	14.85
51	7.63	10.03	-1	60.9	31.07	7.02	18.64	14.5
54	7.64	9.91	-5	75.66	31.01	7.00	19.27	14.99
57	7.53	10.09	-28	69.51	27.97	6.32	19.34	15.04
60	7.52	10.1	-34	75.84	31.37	7.08	19.27	14.99
63	7.49	10.24	-60	71.6	28.66	6.47	19.29	15.01
66	7.49	10.36	-49	76.83	29.15	6.58	18.92	14.72
69	7.54	10.18	-18	87.41	30.26	6.83	19.56	15.21
72	7.56	9.86	5	91.61	31.18	7.04	19.32	15.02



**Table A-37 Comparison performance of integrated system (Continue)****(b) NO<sub>3</sub><sup>-</sup> spiked in RO water**

Time (hr)	pH	DO (mg/L)	ORP (mV)	Fe <sup>2+</sup> (mg/L)	NO <sub>3</sub> <sup>-</sup> (mg/L)	NO <sub>3</sub> <sup>-</sup> (mgN/L)	NH <sub>4</sub> <sup>+</sup> (mg/L)	NH <sub>4</sub> <sup>+</sup> (mgN/L)
0	7.02	6.52	149	0	0	0	0	0
1	7.05	10.5	115	2.18	18.37	4.15	1.93	1.5
1.5	6.81	10.41	92	3.76	17.98	4.06	2.65	2.06
2	6.48	11.23	5	5.07	12.66	2.86	7.64	5.94
2.5	6.52	11.32	-51	6.67	12.76	2.88	9.01	7.01
3	6.46	10.34	-68	5.08	14.1	3.18	9.28	7.22
5	6.67	10.54	-71	6.74	13.94	3.15	10.15	7.89
7	6.52	10.57	-74	6.44	15.53	3.51	12.57	9.77
9	6.66	10.75	-70	9.85	16.1	3.64	14.77	11.49
12	6.74	10.91	-51	8.36	16.96	3.83	17.78	13.83
15	6.8	10.87	-35	11.69	17.03	3.85	18.6	14.47
18	6.76	11.03	-16	13.6	19.29	4.35	19.58	15.23
21	6.73	11.17	-37	17.36	18.75	4.23	20.37	15.84
24	6.71	11.28	-27	17.2	20.06	4.53	20.46	15.91
27	6.77	10.96	-35	14.34	17.77	4.01	21.07	16.39
30	6.75	11.42	-33	18.77	18.2	4.11	21.01	16.34
33	6.77	11.94	-36	21.91	16.47	3.72	21.68	16.86
36	6.74	12.24	-19	19.57	15.21	3.43	21.56	16.77
39	6.71	12.04	-29	23.83	16.22	3.66	21.95	17.07
42	6.72	11.94	-38	33.56	16.67	3.76	21.93	17.06
45	6.69	12.04	-34	31.07	17.78	4.01	22.25	17.3
48	6.67	11.79	-25	34.98	18.69	4.22	21.27	16.55
51	6.68	11.61	-21	30.04	19.07	4.31	20.96	16.3
54	6.64	11.7	-30	39.37	18.93	4.28	21.24	16.52
57	6.59	11.76	-22	36.47	19.72	4.45	20.77	16.16
60	6.73	12.26	-25	31.71	17.59	3.97	21.87	17.01
63	6.68	12.38	-26	44.5	16.52	3.73	21.65	16.84
66	6.66	12.6	-26	50.64	17.35	3.92	22.32	17.36
69	6.62	12.3	-31	55.24	16.91	3.82	21.53	16.74
72	6.69	12.24	-30	51.43	17.81	4.02	22	17.11

## Field testing study of ammonia removal by ammonia stripping process

**Table A-38 Comparison performance of integrated system**

**(a) NO<sub>3</sub><sup>-</sup> spiked in groundwater**

Time (hr)	pH	DO (mg/L)	ORP (mV)	Fe <sup>2+</sup> (mg/L)	NO <sub>3</sub> <sup>-</sup> (mg/L)	NO <sub>3</sub> <sup>-</sup> (mgN/L)	NH <sub>4</sub> <sup>+</sup> (mg/L)	NH <sub>4</sub> <sup>+</sup> (mgN/L)
0	7.79	6.88	182	0	0	0	0	0
1	6.77	1.94	158	0	0	0	0	0
1.5	6.75	2.33	156	0	0	0	0	0
2	6.73	1.99	148	0	0	0	0	0
2.5	6.72	2.54	141	0	0	0	0	0
3	7.03	2.67	116	0	0	0	0	0
5	7.19	2.3	74	0.05	1.18	0.27	0.72	0.56
7	7.17	1.92	85	0.08	4.21	0.95	1.65	1.28
9	7.03	1.76	74	0.52	10.75	2.43	2.43	1.89
12	7.04	1.75	95	1.3	15.99	3.61	2.84	2.21
15	7	1.81	85	5.7	21.73	4.91	2.96	2.3
18	7.01	1.93	101	4.34	22.38	5.05	3.18	2.48
21	7.05	1.89	110	7.26	23.18	5.24	3.49	2.72
24	7.02	2.02	120	9.15	24.34	5.5	3.13	2.43
27	7.05	2.05	133	12.44	25.62	5.79	2.9	2.25
30	7.07	1.85	135	12.37	29.1	6.57	3.26	2.54
33	7.02	1.72	135	14.94	31.01	7	3.27	2.55
36	7.01	1.23	138	17.44	31.86	7.19	3.53	2.75
39	6.91	1.31	151	18.23	31.69	7.16	3.64	2.83
42	6.91	1.31	152	22.46	31.77	7.17	3.08	2.39
45	6.91	1.53	150	24.99	31.33	7.07	3.42	2.66
48	6.92	1.36	153	29.23	31.86	7.2	3.55	2.76
51	6.92	1.28	152	24.44	31.44	7.1	3.14	2.45
54	6.9	1.2	153	27.11	31.61	7.14	3.14	2.44
57	6.88	1.23	152	29.37	29.66	6.7	3.57	2.78
60	6.95	1.25	145	27.81	29.78	6.72	3.07	2.38
63	6.92	1.23	135	30.3	28.85	6.51	3.5	2.72
66	6.93	1.23	132	27.77	28.45	6.42	3.24	2.52
69	6.95	1.23	136	32.54	28.74	6.49	3.39	2.64
72	6.96	1.33	148	33.57	29.11	6.57	3.25	2.53

**Table A-38 Comparison performance of integrated system (Continue)****(b) NO<sub>3</sub><sup>-</sup> spiked in RO water**

<b>Time (hr)</b>	<b>pH</b>	<b>DO (mg/L)</b>	<b>ORP (mV)</b>	<b>Fe<sup>2+</sup> (mg/L)</b>	<b>NO<sub>3</sub><sup>-</sup> (mg/L)</b>	<b>NO<sub>3</sub><sup>-</sup> (mgN/L)</b>	<b>NH<sub>4</sub><sup>+</sup> (mg/L)</b>	<b>NH<sub>4</sub><sup>+</sup> (mgN/L)</b>
0	7.53	8.99	155	0	0	0	0	0
1	6.52	4.67	81	0	0	0	0	0
1.5	6.55	4.32	92	0	0	0	0	0
2	6.45	4.52	192	0	0	0	0	0
2.5	6.49	4.82	185	0	0	0	0	0
3	6.55	5.07	188	0	0	0	0	0
5	6.58	4.6	180	0.03	2.52	0.57	0.48	0.37
7	6.69	4.72	119	0.1	6.99	1.58	2.11	1.64
9	6.81	3.84	125	0.26	8.97	2.03	2.82	2.19
12	6.81	3.63	113	0.28	11.97	2.7	3.9	3.04
15	6.87	3.16	149	0.22	12.39	2.8	3.75	2.92
18	6.86	3.03	135	0.82	12.79	2.89	4.02	3.12
21	6.88	3.35	125	1.34	13.86	3.13	4.47	3.48
24	6.89	3.45	109	1.41	13.79	3.11	4.73	3.68
27	6.89	3.39	112	0.93	14.72	3.32	4.53	3.52
30	6.88	3.65	104	1.49	15.55	3.51	4.92	3.83
33	6.86	3.43	92	2.42	16.9	3.82	4.33	3.36
36	6.81	3.56	104	2.25	17.56	3.97	4.79	3.73
39	6.79	3.68	96	1.52	17.25	3.89	4.93	3.83
42	6.77	4.21	106	1.83	16.72	3.78	4.83	3.75
45	6.75	3.81	113	3.76	16.99	3.84	5.14	4.00
48	6.78	3.05	103	2.87	18.49	4.17	4.83	3.76
51	6.82	3.33	105	4.65	17.04	3.85	4.86	3.78
54	6.85	3.53	108	5.4	17.99	4.06	5.25	4.09
57	6.81	3.69	103	6.39	18.14	4.1	5.54	4.31
60	6.94	3.23	109	5.66	19.42	4.39	4.97	3.86
63	6.96	3.32	127	5.59	19.39	4.38	5.13	3.99
66	6.85	3.15	131	4.89	17.64	3.98	4.91	3.82
69	6.86	3.05	113	6.62	17.97	4.06	5.01	3.90
72	6.81	2.95	98	5.78	17.45	3.94	4.79	3.73

## APPENDIX B

### **Ferrous ion ( $\text{Fe}^{2+}$ ) analysis** (Standard Method, 1995)

#### **1. General Discussion**

The 1,10-phenanthroline complex with iron (II) was first discovered by Blau. A spectrophotometric determination of iron dependent on the formation of the iron(II)-1,10-phenanthroline complex was developed by Fortune Mellon. The iron(II)-1,10-phenanthroline complex was reddish orange in color.

#### **2. Apparatus**

##### **2.1 Colorimetric Equipment**

**2.1.1 Spectrophotometer** (Shimadzu UV-1201): The absorbance used for ferrous ( $\text{Fe}^{2+}$ ) analysis was 510 nm.

**2.1.2 Acid- washed Glassware:** All glass wares were washed with conc. HCl and rinsed with DI water to remove deposit of iron oxide.

**2.1.3 Membrane Filter:** a 0.45  $\mu\text{m}$  membrane filter was used to filter the sample to remove precipitation particle on solution.

##### **2.2 Reagents**

All reagents were prepared by distilled water. Reagents were stored in glass bottles. The hydrochloric acid and ammonium acetate solutions were stable indefinitely if they were tightly closed the bottles. The standard ferrous ion ( $\text{Fe}^{2+}$ ) solutions were not stable, it was prepared daily.

**2.2.1 Hydrochloric Acid, HCl:** 20 ml of concentrated hydrochloric acid was diluted to 1000 ml with DI water.

**2.2.2 Ammonium Acetate Buffer Solution:** 500 g of  $\text{NH}_4\text{C}_2\text{H}_3\text{O}_2$  was dissolved in 300 ml of DI water. Then, 1400 ml of concentrated acetic acid was filled up to the mark of 2000 ml.

**2.2.3 Phenanthroline Solution:** 5 g of 1,10-phenanthroline monohydrate,  $C_{12}H_8N_2 \cdot H_2O$ , was dissolved and 1 ml of concentrated hydrochloric acid was added. Then, DI water was used to make the mark of 1000 ml.

**2.2.4 Stock Ferrous Ion Solution:** 20 ml of concentrated  $H_2SO_4$  was slowly added to 50 ml DI water and 0.25g of ferrous sulfate ( $FeSO_4 \cdot 7H_2O$ ) was added. Then DI water was used to make the mark of 1000 ml. The stock solution was 500 mg/l as  $Fe^{2+}$ .

**2.2.5 Standard Solution:** 1 ml of concentrated  $H_2SO_4$  was slowly added to 25 ml DI water. Then 5 ml of stock ferrous ion solution was diluted to 50 ml with DI water. The standard solution was 50 mg/l as  $Fe^{2+}$ .

### 3. Procedure

**3.1 Sample Preparation for Calibration Curves:** The standard ferrous ( $Fe^{2+}$ ) solutions were prepared in the range 0 to 10 mg/L as  $Fe^{2+}$ . 25 ml of HCl from stock solution was prepared in six 50 ml volumetric flasks. Then, 10 ml of phenanthroline solution and 5 ml of ammonium acetate solution were added with vigorous stirring. 1, 2, 3, 4, 5 and 10 ml of 50 mg/L as  $Fe^{2+}$  standard solution were pipetted, respectively. After that, the samples were diluted to 50 ml with DI water, mixed thoroughly.

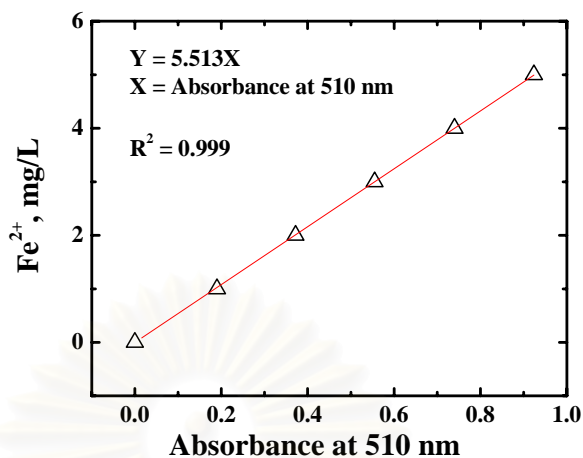
**3.2 Ferrous Ion Analysis:** To determine ferrous ion, 25 ml of HCl from stock solution was prepared in 50 ml volumetric flask. Then, 10 ml of phenanthroline solution and 5 ml of ammonium acetate solution were added with vigorous stirring. 2 ml of sample was filled and diluted to 50 ml with DI water. After that, it had to stand for 10 min. Do not expose to sunlight. (Color development was rapid in the presence of excess phenanthroline).

### 4. Calculation

$$Y = 5.513x$$

Where  $Y = Fe^{2+}$ , mg/L

$X =$  absorbance at 510 nm



**Ammonia ion (NH<sub>4</sub><sup>+</sup>) analysis by Phenate Method** (Standard Method, 1995)

## 1. General Discussion

**1.1 Principle:** An intensely blue compound, indophenol, is formed by the reaction of ammonia, hypochlorite, and phenol catalyzed by sodium nitroprusside.

**1.2 Interferences:** Complexing magnesium and calcium with citrate eliminates interference produced by precipitation of these ions at high pH. There is no interference from other trivalent forms of nitrogen. Remove interfering turbidity by distillation or filtration. If hydrogen sulfide is present, remove by acidifying samples to pH 3 with dilute HCl and aerating vigorously until sulfide odor no longer can be detected.

## 2. Apparatus

### 2.1 Colorimetric Equipment

**2.1.1 Spectrophotometer** (Shimadzu UV-1201): The absorbance used for ammonia analysis was 640 nm.

**2.1.2 Acid- washed Glassware:** All glass wares were washed with conc. HCl.

**2.1.3 Membrane Filter:** a 0.45 μm membrane filter was used to filter the sample to remove precipitation particle on solution.

## 2.2 Reagents

**2.2.1 Phenol solution:** Mix 11.1 mL liquified phenol ( $\geq 89\%$ ) with 95% v/v ethyl alcohol to a final volume of 100 mL. Prepare weekly. CAUTION: Wear gloves and eye protection when handling phenol; use good ventilation to minimize all personnel exposure to this toxic volatile substance.

**2.2.2 Sodium nitroprusside, 0.5% w/v:** Dissolve 0.5 g sodium nitroprusside in 100 mL deionized water. Store in amber bottle for up to 1 month.

**2.2.3 Alkaline citrate:** Dissolve 200 g trisodium citrate and 10 g sodium hydroxide in deionized water. Dilute to 1000 mL.

**2.2.4 Sodium hypochlorite, commercial solution, about 5%:** This solution slowly decomposes once the seal on the bottle cap is broken. Replace about every 2 months.

**2.2.5 Oxidizing solution:** Mix 100 mL alkaline citrate solution with 25 mL sodium hypochlorite. Prepare fresh daily.

**2.2.6 Stock ammonium solution:** Dissolve 3.819g anhydrous  $\text{NH}_4\text{Cl}$  (dried at  $100^\circ\text{C}$ ) in DI water, and Dilute to 1000 mL;  $1.00\text{mL} = 1\text{ mg N} = 1.22\text{ mg NH}_3$ .

**2.2.7 Standard ammonium solution:** Use stock ammonium solution and water to prepare a calibration curve in a range appropriate for the concentrations of the samples.

## 3. Procedure

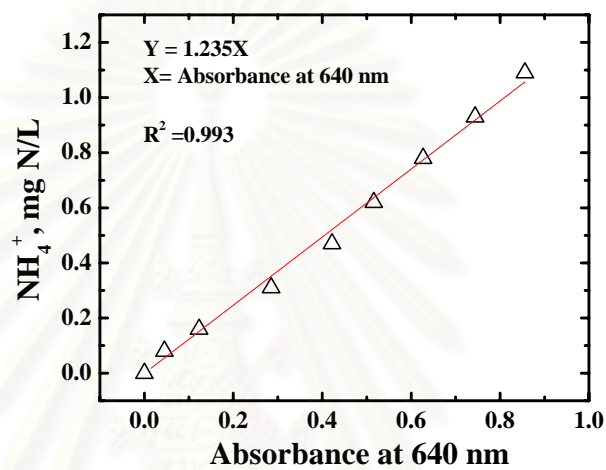
To a 25-mL sample in a 50-mL erlenmeyer flask, add, with thorough mixing after each addition, 1 mL phenol solution, 1 mL sodium nitroprusside solution, and 2.5 mL oxidizing solution. Cover samples with plastic wrap or paraffin wrapper film. Let color develop at room temperature ( $22$  to  $27^\circ\text{C}$ ) in subdued light for at least 1 h. Color is stable for 24 h. Measure absorbance at 640 nm. Prepare a blank and at least two other standards by diluting stock ammonia solution into the sample concentration range. Treat standards the same as samples.

#### 4. Calculation

$$Y = 1.235x$$

Where  $Y = \text{NH}_4^+$ , mg N/L

$X =$  absorbance at 640 nm



สถาบันวิทยบริการ  
จุฬาลงกรณ์มหาวิทยาลัย



### Nitrate ( $\text{NO}_3^-$ ), nitrite ( $\text{NO}_2^-$ ) and ammonium ( $\text{NH}_4^+$ ) analysis

Nitrate ( $\text{NO}_3^-$ ), nitrite ( $\text{NO}_2^-$ ) and ammonia ( $\text{NH}_4^+$ ) was analyzed by Ion Chromatography (IC). The IC condition for  $\text{NO}_3^-$  and  $\text{NO}_2^-$  was shown in Table B-1. The IC condition for  $\text{NH}_4^+$  was shown in Table B-2.

**Table B-1 IC condition for  $\text{NO}_3^-$  and  $\text{NO}_2^-$**

IC Model	DIONEX-120
flow rate	1.20 mL/min
Mobile phase	3.5 mM $\text{Na}_2\text{CO}_3$ and 1.0 mM $\text{NaHCO}_3$
Operating pressure	$P > 1200$ psi
Injection volume	50 $\mu\text{L}$
ASRS Model	10 $\mu\text{SFS}$ of ASRS-ULTRA, 4mm, P/N 53946
Column	Ion Pac $\text{\textcircled{R}}$ AS14, 4 $\times$ 250 mm, Analytical Column
Guard	Ion Pac $\text{\textcircled{R}}$ AG14, 4 $\times$ 50 mm, Guard

**Table B-2 IC condition for  $\text{NH}_4^+$**

IC Model	DIONEX-120
Flow rate	1.00 mL/min
Mobile phase	20 mN Methanesulfonic acid
Operating pressure	$P > 1200$ psi
Injection volume	50 $\mu\text{L}$
ASRS Model	ASRS- ULTRA CS12A, 4mm, P/N 53948
Column	Ion Pac $\text{\textcircled{R}}$ CS12A, 4 $\times$ 250 mm, Analytical Column,
Guard	Ion Pac $\text{\textcircled{R}}$ CS12A, 4 $\times$ 50 mm, Guard

## Hydrogen Peroxide analysis using Potassium (IV) Oxalate (Seller, 1980)

### 1. General Discussion

A specific spectrophotometric test was based on formation of a formation of a complex, as  $TiO_2^+$ , between hydrogen peroxide and titanium (IV) ion. This method was developed for the determination of hydrogen peroxide using potassium titanium (IV) oxalate.

### 2. Apparatus

#### 2.1 Colorimetric Equipment:

**2.1.1 Spectrophotometer (Shimadsu UV-1201).** The absorbance used for titanium(IV)-peroxide complex analysis was 400 nm.

**2.1.2 Membrane Filter:** a 0.45  $\mu m$  membrane filter was used to filter the sample to remove precipitation particle on solution.

#### 2.2 Reagent

Reagent was prepared by DI water. Reagents were Stored in glass bottles.

**2.2.1 Titanium Reagent:** 272 ml of concentrated sulphuric acid ( $H_2SO_4$ ) was mixed with 300 ml of DI water. 35.4 g of Potassiumtitanium(IV) oxalate,  $[K_2TiO(C_2O_4)_2 \cdot 2H_2O]$ , was dissolved. Then, DI water was used to make the mark of 1000 ml.

### 3. Procedure

5 ml of titanium reagent and 5ml of sample were added into 25 ml calibrated flask. Then, solution was made up to the mark. The absorbance measured the solution was 400 nm. A blank, consisting of 5 ml of the titanium reagent and 5 ml of sample without the hydrogen present made up to 25 ml, should be measured.

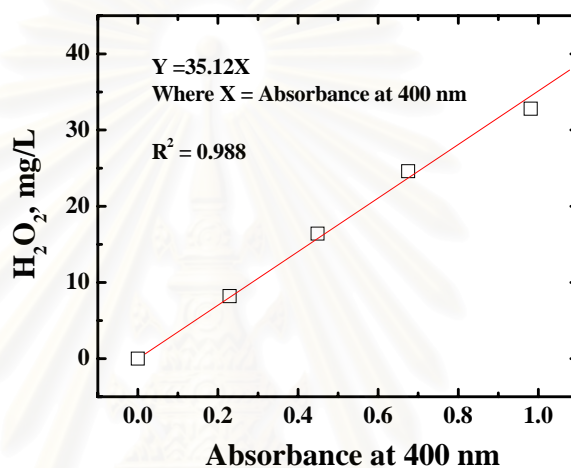
#### 4. Calculation

$$Y = 36.735X$$

$$R^2 = 0.9966$$

Where X = H<sub>2</sub>O<sub>2</sub>, mg/L

Y = absorbance at 400 nm



### Hydrogen Peroxide analysis using Permanganate titration method

([www.H2O2.com](http://www.H2O2.com))

#### 1. General Discussion

This method utilizes the reduction of potassium permanganate (KMnO<sub>4</sub>) by hydrogen peroxide in sulfuric acid.

#### 2. Apparatus

##### 2.1 Buret

##### 2.2 Pipette

##### 2.3 Glassware

##### 2.4 Reagent

**2.4.1 H<sub>2</sub>O<sub>2</sub> stock solution:** 10 ml 35% H<sub>2</sub>O<sub>2</sub> is added in 1 L volumetric flask. Then, DI water is used to make up to 1000 ml.

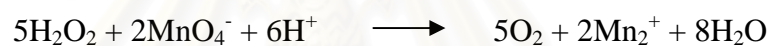
**2.4.2 H<sub>2</sub>SO<sub>4</sub> (1:4) solution:** H<sub>2</sub>SO<sub>4</sub> (1:4) is prepared by adding 98% H<sub>2</sub>SO<sub>4</sub> 10 ml in 50 ml volumetric flask. Then, DI water is used to make up to 50 ml.

**2.4.3 Potassium permanganate solution:** 0.1 N KMnO<sub>4</sub> is prepared by adding 3.1608gKMnO<sub>4</sub> in 1 L volumetric flask. Then, DI water is used to make up to 1 Liter.

### 3. Procedure

20 ml of H<sub>2</sub>O<sub>2</sub> stock solution is poured in 250 ml flask. Then, 20 ml of 1:4 H<sub>2</sub>SO<sub>4</sub> solution is added in the same flask. Potassium permanganate solution is used as titration solution. Lastly, The sample is titrated until changing the color.

### 4. Calculation



$$\text{H}_2\text{O}_2 \text{ ppm} = \frac{(5/2 \times 0.02) \times V_{\text{KMnO}_4} \times 10^{-3} \times 34 \times 10^{-3}}{20 \times 10^{-3}}$$

สถาบันวิทยบริการ  
จุฬาลงกรณ์มหาวิทยาลัย

## APPENDIX C

### Journal publication list

1. **Ruangchainikom C., Liao C.H., Anotai J., Lee M.T. (2006)** Characteristics of nitrate reduction by zero-valent iron powder in the recirculated and CO<sub>2</sub>-bubbled system. *Water Research*, 40, 195-204.
2. **Ruangchainikom C., Liao C.H., Anotai J., Lee M.T. (2005)** Effects of water characteristics on nitrate reduction by the Fe<sup>0</sup>/CO<sub>2</sub> process. *Chemosphere*. In press.
3. **Ruangchainikom C., Liao C.H., Anotai J., Lee M.T. (2005)** Innovated Process of Fe<sup>0</sup>/CO<sub>2</sub> for the Removal of Nitrate from Groundwater. *Water Science and Technology: Water Supply* 5(5), 49-56.

### International book

1. **Liao C. H., Kang S. F., Anotai J. and Ruangchainikom C. (2006)** Aqueous Nitrate Reduction by Zero-valent Iron Powder. To be published in the Book of “*Engineering Application of Zero-valent Iron for Water and Groundwater Pollution Control*”, Chapter 6, American Society of Civil Engineers (ASCE). Rao Surampalli, Irene M. C. Lo, Keith C. K. Lai (Eds).

### Conference paper publication list

1. **Ruangchainikom C., Liao C.H., Anotai J., Lee M.T. (2004)** Corrosion Behavior of Zero-Valent Iron in CO<sub>2</sub>-Bubbled Reactor. 2004 *Asian Regional Conference on Environmental Pollution Control Technologies*, Chia Nan University of Pharmacy and Science, Tainan, TAIWAN. August 16, 2004
2. **Ruangchainikom C., Liao C.H., Anotai J., Lee M.T. (2004)** Nitrate Removal by Fe<sup>0</sup>/CO<sub>2</sub> Process with Various Water Qualities. *Taiwan-Japan*

*Conference on GW and Soil Pollution Investigation and Remediation*, National Kaohsiung University, Kaohsiung, TAIWAN. October 8, 2004.

3. **Ruangchainikom C., Liao C.H., Anotai J., Lee M.T. (2004)** Zero-valent Iron Reduction of Nitrate-contaminated Water in the Presence of CO<sub>2</sub> Bubbling. *Environmental Engineering Annual Conference*, National Cheng-Kung University, Tainan, TAIWAN. November 26-27, 2004.
4. **Ruangchainikom C., Liao C.H., Anotai J., Lee M.T. (2005)** Characteristics of Nitrate reduction by zero-valent iron powder in the recirculated and CO<sub>2</sub>-bubbled system. 2005 *The First International Students Workshop on Environmental Quality Concern, Control and Conservation*, Tainan, TAIWAN. April 14, 2005.
5. **Ruangchainikom C., Liao C.H., Anotai J., Lee M.T. (2005)** Nitrate Removal by Fe<sup>0</sup>/CO<sub>2</sub> Process with Various Water Qualities. *The 1st IWA-ASPIRE Conference & Exhibition*, SINGAPORE. July 10-15, 2005.
6. **Ruangchainikom C., Liao C.H., Anotai J., Lee M.T. (2005)** Innovated Process of Fe<sup>0</sup>/CO<sub>2</sub> for the Removal of Nitrate from Groundwater. *The 3rd IWA Leading-Edge Conference on Water and Wastewater Treatment Technologies*, Sapporo, JAPAN. June 6 – 8, 2005.
7. **Ruangchainikom C., Anotai J., Liao C.H. (2005)** Innovative Purification Technology of Fe<sup>0</sup>/CO<sub>2</sub> for Removing Highly Nitrate-Contaminated Saline Groundwater in Northeastern Thailand. *GEOINDO 2005*, Khonkaen, THAILAND. November 28-30, 2005.
8. **Ruangchainikom C., Liao C.H., Lin C.J., Anotai J., Homanee S. (2005)** Innovative Chemical Process of Fe<sup>0</sup>/CO<sub>2</sub> for the Treatment of Nitrate-contaminated Groundwater. *Regional Symposium on Chemical Engineering 2005*, Hanoi, VIETNAM. November 30- December 2, 2005.
9. **Ruangchainikom C., Anotai J., Liao C.H. (2006)** Innovative Reactor Design for Treating Nitrate-Contaminated Groundwater by Fe<sup>0</sup>/CO<sub>2</sub>. *International Conference Hazardous Waste Management for a Sustainable Future*, Bangkok, THAILAND. January 10-12, 2006.

## BIOGRAPHY

Mr. Chalermchai Ruangchainikom was born on September 16, 1980 in Bangkok, Thailand. He received his Bachelor's degree in Degree with honor in Department of Environmental Engineering form Faculty of Engineering, King Mongkut's University of Technology Thonburi in 2001. He received his Master's degree in the International Postgraduate Program in Environmental Management (Hazardous Waste Management), Inter-Department of Environmental Management Chulalongkorn University, Bangkok, Thailand in 2003. He pursued his Philosophy of Doctoral Degree studies in the International Postgraduate Program in Environmental Management (Hazardous Waste Management), Inter-Department of Environmental Management Chulalongkorn University, Bangkok, Thailand on May, 2003. He finished his Philosophy of Doctoral Degree in May 2006.



สถาบันวิทยบริการ  
จุฬาลงกรณ์มหาวิทยาลัย